High-Affinity Alkynyl Bisubstrate Inhibitors of Nicotinamide N-Methyltransferase (NNMT)

High-Affinity Alkynyl Bisubstrate Inhibitors of Nicotinamide N-Methyltransferase (NNMT)

A DISSERTATION PRESENTED
BY
ROCCO L. POLICARPO
TO
THE DEPARTMENT OF CHEMISTRY & CHEMICAL BIOLOGY

IN PARTIAL FULFILLMENT OF THE REQUIREMENTS
FOR THE DEGREE OF
DOCTOR OF PHILOSOPHY
IN THE SUBJECT OF
CHEMISTRY

HARVARD UNIVERSITY
CAMBRIDGE, MASSACHUSETTS
MAY 2019

Thesis advisor: Matthew D. Shair Rocco L. Policarpo

High-Affinity Alkynyl Bisubstrate Inhibitors of Nicotinamide N-Methyltransferase (NNMT)

Abstract

Nicotinamide N-methyltransferase (NNMT) is a metabolic enzyme responsible for the methylation of nicotinamide (NAM) using cofactor S-adenosylmethionine (SAM). NNMT overexpression has been linked to diabetes, obesity, and a variety of cancers. Successful development of potent and selective NNMT inhibitors could further reveal the role of NNMT in various diseases, potentially enabling new treatments for metabolic disorders and several cancers. In this work, structure-based rational design led to the development of potent and selective alkynyl bisubstrate inhibitors of NNMT. The reported nicotinamide-SAM conjugate (named **NS1**) features an alkyne as a key design element that closely mimics the linear, 180° transition state geometry found in the NNMT-catalyzed SAM → NAM methyl transfer reaction. NS1 was synthesized as a single enantiomer and diastereomer in 14 steps and found to be a high-affinity, subnanomolar NNMT inhibitor. An X-ray co-crystal structure and structure-activity relationship (SAR) study revealed the unique ability of an alkynyl linker to span the methyl transfer tunnel of NNMT with ideal shape complementarity. The compounds reported in this work represent the most potent and selective NNMT inhibitors reported to date. The rational design principle described herein could potentially be extended to other methyltransferase enzymes.

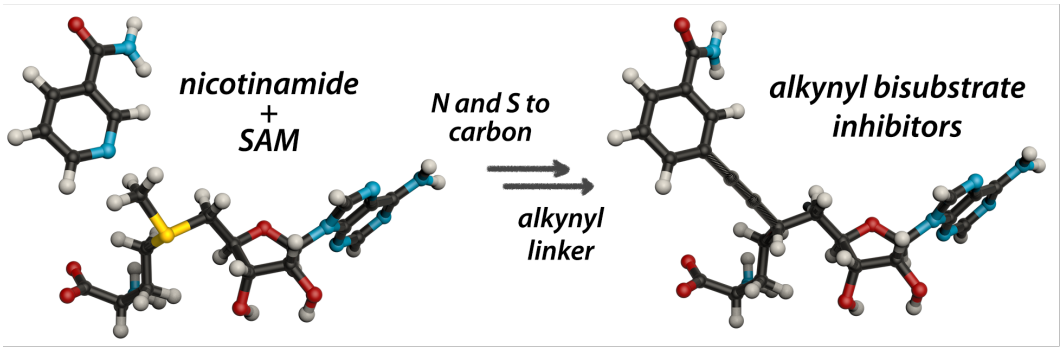

Table of Contents

Acknowledgments

THANK YOU to Professor Matthew D. Shair for the guidance and support provided throughout my graduate studies. Thank you to Professors Stuart Schreiber and Daniel Kahn for serving on my thesis defense committee and to Professor Brian Liau for helpful guidance and mentorship. Thank you to Professor Bradley Pentelute for mentorship during my undergraduate training. Thank you to Tatiana Policarpo, Mom, Dad, and Rachael for your love and support. Thank you to the Shair Lab members that have made this journey possible, including Dr. Ludovic Decultot and James Tucker.

Thank you to Elizabeth May and Professor Rachelle Gaudet for assistance with protein crystallography. Thank you to Dr. Petr Kuzmič for assistance with enzyme kinetics. Thank you to Dr. Shao-Liang Zheng for assistance with small molecule X-ray crystallography and to Cheryl Arrowsmith for supplying the NNMT and INMT plasmids used in this work (via Addgene). I thank the National Science Foundation for funding me with a Graduate Research Fellowship. I thank the Harvard Blavatnik Biomedical Accelerator for funding portions of this project. Thank you to Grace Kenney for assistance with sequence similarity network generation and Kevin Dalton for assistance with crystallographic data processing and refinement. I gratefully acknowledge the beamline staff of NE-CAT at the Advanced Photon Source (Argonne, IL, USA) for help with crystallographic data collection.

List of Abbreviations

Å	angstrom
E	*Ger.*, entgegen
Z	*Ger.*, zusammen
1MQ	1-methylquinolinium
Ac	acetate
Bn	benzyl
BPE	bis(phospholano)ethane
BSA	*N,O*-bis(trimethylsilyl)acetamide
Bz	benzoyl
Cbz	benzyloxycarbonyl
DMAP	4-(dimethylamino)pyridine
DMEAD	di-2-methoxyethyl azodicarboxylate
DMF	*N,N*-dimethylformamide
DMP	Dess-Martin periodinane
DMPU	*N,N'*-dimethylpropylene urea
DMSO	dimethyl sulfoxide
DTBMP-OTf	2,6-di-*tert*-butyl-4-methylpyridinium triflate
equiv.	equivalent
Fmoc	9-fluorenylmethoxycarbonyl
HMPA	hexamethylphosphoramide
HRMS	high-resolution mass spectrometry

ITC	isothermal titration calorimetry
LDA	lithium diisopropylamide
M.S.	molecular sieves
MTBE	methyl *tert*-Butyl ether
NAM	nicotinamide
Ns	2-nitrobenzenesulfonyl
ODE	ordinary differential equation
PG	protecting group
PhH	benzene
PhMe	toluene
PMHS	(poly)methylhydrosiloxane
Pyr	pyridine
quant.	quantitative
rbf	round-bottom flask
rfu	relative fluorescence units
RT	room temperature
SAH	S-adenosylhomocysteine
SAM	S-adenosylmethionine
SAR	structure-activity relationship
TASF	tris(dimethylamino)sulfonium difluorotrimethylsilicate
TBAF	tetra-*n*-butylammonium fluoride
TBAI	tetra-*n*-butylammonium iodide
TBDPS	*tert*-Butyldiphenylsilyl
TBS	*tert*-Butyldimethylsilyl
Tf_2O	trifluoromethanesulfonic (triflic) anhydride
TFA	trifluoroacetic acid / trifluoroacetyl

Tf	trifluoromethanesulfonyl
THF	tetrahydrofuran
TIPS	triisopropylsilyl
TMS	trimethylsilyl
Ts	*p*-toluenesulfonyl

1

Introduction

1.1 Nicotinamide N-Methyltransferase (NNMT)

Nicotinamide N-methyltransferase (NNMT) is a metabolic enzyme responsible for the methylation of nicotinamide (NAM) using the cofactor S-adenosylmethionine (SAM), resulting in the production of 1-methylnicotinamide (MNAM) and S-adenosylhomocysteine (SAH) (Figure 1.1.1).[1] While initially established as a vitamin B3 clearance enzyme, recent work has shown NNMT to be an important regulator of several intracellular pathways in fat, liver, and cancer cells.[2] NNMT can regulate methyl donor metabolism by direct interaction with proteins of the methionine cycle[3] and can regulate hepatic nutrient metabolism through

---

[1] Currently, there are many abbreviations used for nicotinamide and 1-methylnicotinamide in the literature, leading to inconsistency and confusion. We use the standardized nomenclature proposed by Pissios in a 2017 review article on NNMT (see following citation).

[2] Pissios, P. *Trends Endocrinol. Metab.* **2017**, *28*, 340–353.

[3] Hong, S; Zhai, B; Pissios, P *Biochemistry* **2018**, *57*, 5775–5779.

Sirt1 stabilization. By decreasing cellular SAM levels, NNMT can modulate the epigenetic landscape of cancer cells[4] and embryonic-stem cells[5].

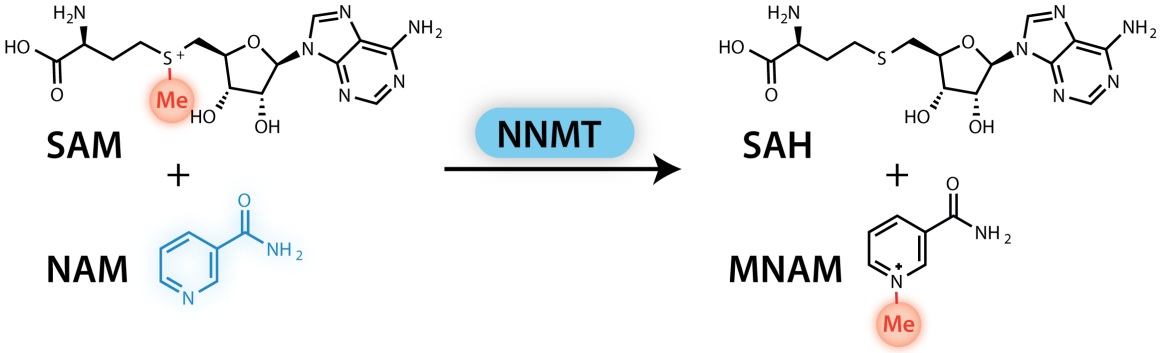

Figure 1.1.1: NNMT catalyzes the SAM-dependent methylation of nicotinamide (NAM), generating 1-methylnicotinamide (MNAM) and S-adenosylhomocysteine (SAH).

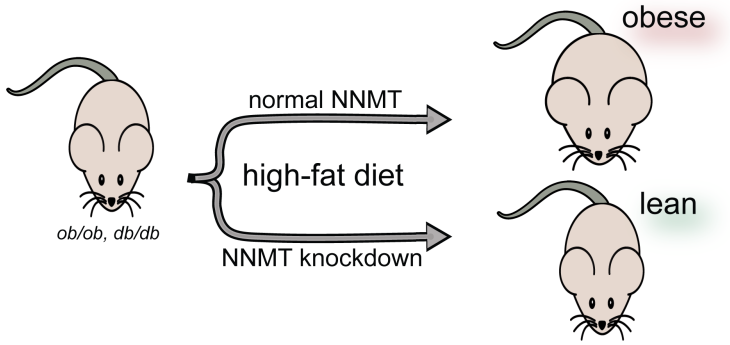

Figure 1.1.2: NNMT knockdown has a preventative effect in mice, keeping them from gaining weight even when fed a high-fat diet.

Accordingly, NNMT has emerged as a disease-relevant enzyme and a possible point of therapeutic intervention. Abnormal NNMT expression is implicated in several diseases, including diabetes[6,7], obesity[6,8],

---

[4] Ulanovskaya, O. A.; Zuhl, A. M.; Cravatt, B. F. *Nat. Chem. Biol.* **2013**, *9*, 300–306.

[5] Sperber, H. et al. *Nat. Cell Biol.* **2015**, *17*, 1523–1535.

[6] Kraus, D. et al. *Nature* **2014**, *508*, 258–262.

[7] Brachs, S et al. *Diabetes* **2019**, *68*, 527–542.

[8] Liu, M et al. *J. Clin. Endocrinol. Metab.* **2015**, *100*, 3112–3117.

and a variety of cancers[9,10,11]. In a seminal study establishing the role of NNMT in metabolism, Kahn et al. showed that NNMT knockdown via RNAi had a protective effect in mice, keeping them lean when fed a high-fat diet (Figure 1.1.2). This study further showed that NNMT inhibition increases polyamine metabolism, leading to increased energy expenditure (Figure 1.1.3).

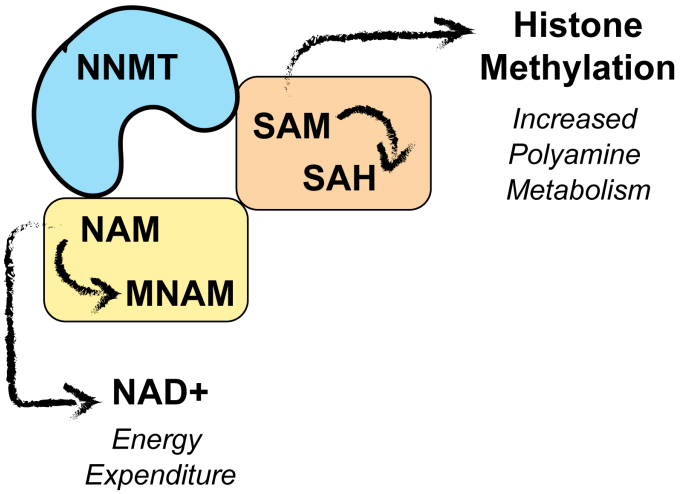

Figure 1.1.3: Role of NNMT in metabolism presented by Kahn et al., 2014.

Increased NNMT protein expression was observed in adipose and liver tissue of obese and diabetic mice[12], while increased NNMT mRNA expression was observed in humans[13]. NNMT is overexpressed in glioblastoma, leading to cellular SAM depletion, DNA hypomethylation, and accelerated tumor growth (Figure 1.1.4).[14] The successful development of potent and selective NNMT inhibitors would aid efforts to elucidate the role of NNMT in disease, potentially enabling new strategies to treat a variety of metabolic disorders, cancers, and other pathologies.

---

[9] Pissios, P. *Trends Endocrinol. Metab.* **2017**, *28*, 340–353.

[10] Ulanovskaya, O. A.; Zuhl, A. M.; Cravatt, B. F. *Nat. Chem. Biol.* **2013**, *9*, 300–306.

[11] You, Z; Liu, Y; Liu, X *Oncol. Lett.* **2018**, *15*, 9195–9201.

[12] Kraus, D. et al. *Nature* **2014**, *508*, 258–262.

[13] Kannt, A. et al. *Sci. Rep.* **2018**, *8*, 3660–3660.

[14] Jung, J. et al. *JCI Insight* **2017**, *2*.

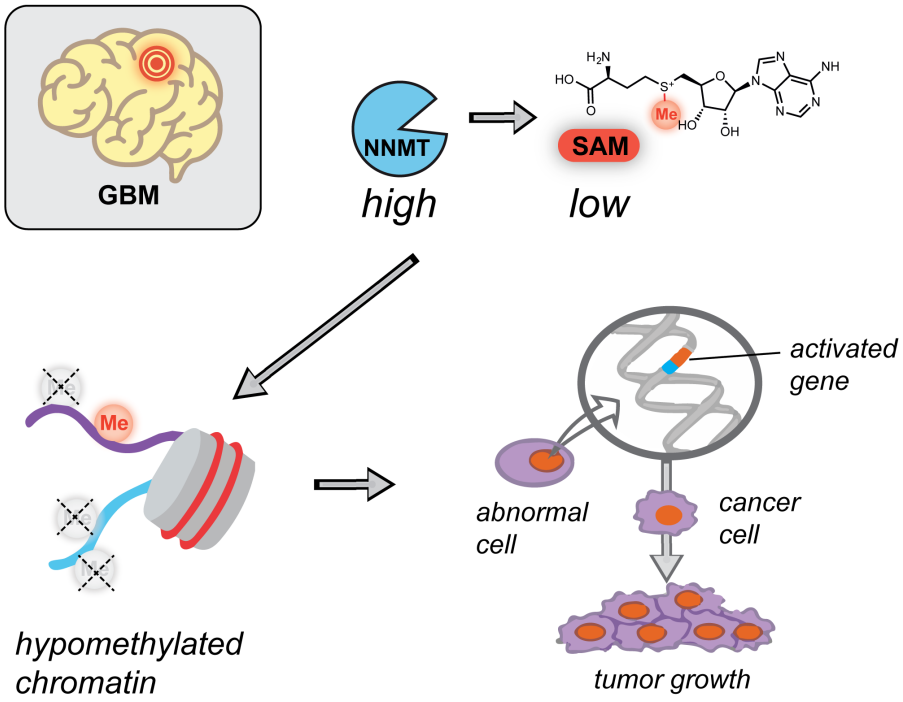

Figure 1.1.4: Overactive NNMT leads to hypomethylated chromatin, driving tumor cell proliferation in glioblastoma.

1.2 NNMT Inhibition & Bisubstrate Inhibitors

Over the past two years several NNMT inhibitors have been reported, including methylated quinolines[15], nicotinamide analogues[16,17], covalent inhibitors[18,19], and amino-adenosine derived bisubstrate inhibitors[20,21]. Bisubstrate inhibitors are compounds that bind both the substrate and cofactor binding pockets within an

---

[15] Neelakantan, H.; Vance, V.; Wang, H.-Y. L.; McHardy, S. F.; Watowich, S. J. *Biochemistry* **2017**, *56*, 824–832.

[16] Kannt, A. et al. *Sci. Rep.* **2018**, *8*, 3660.

[17] Ruf, S. et al. *Bioorg. Med. Chem. Lett.* **2018**, *28*, 922 –925.

[18] Horning, B. D.; Suciu, R. M.; Ghadiri, D. A.; Ulanovskaya, O. A.; Matthews, M. L.; Lum, K. M.; Backus, K. M.; Brown, S. J.; Rosen, H; Cravatt, B. F. *J. Am. Chem. Soc.* **2016**, *138*, 13335–13343.

[19] Lee, H.-Y.; Suciu, R. M.; Horning, B. D.; Vinogradova, E. V.; Ulanovskaya, O. A.; Cravatt, B. F. *Bioorg. Med. Chem. Lett.* **2018**, *28*, 2682–2687.

[20] Van Haren, M. J.; Taig, R.; Kuppens, J.; Sastre Toraño, J.; Moret, E. E.; Parsons, R. B.; Sartini, D.; Emanuelli, M.; Martin, N. I. *Org. Biomol. Chem.* **2017**, *15*, 6656–6667.

[21] Babault, N.; Allali-Hassani, A.; Li, F.; Fan, J.; Yue, A.; Ju, K.; Liu, F.; Vedadi, M.; Liu, J.; Jin, J. *J. Med. Chem.* **2018**, *61*, 1541–1551.

enzyme active site. The bisubstrate strategy has been previously applied to several methyltransferases, including catechol O-methyltransferase (COMT)[22,23] (Figure 1.2.2) and protein N-terminal methyltransferase 1 (NTMT1)[24].

The design of bisubstrate inhibitors relates closely to two well-established ligand design strategies: transition-state mimicry and fragment-based design.[25] Importantly, if two weak inhibitors that bind a protein at distinct sites are linked in an optimal manner, the resulting bisubstrate inhibitors can obtain several orders of magnitude increase in binding affinity.[26,27]. As a result, linker identity is crucial to properly position the key interacting groups of the two component molecules and minimize unfavorable interactions between the linker and the protein. This work outlines the conception and development of alkynes as linkers in potent, subnanomolar NNMT inhibitors. Linking together a SAM-like fragment with a NAM-like fragment *via* an alkyne linker led to the development of "***N***icotinamide-***S***AM conjugate ***1***" **NS1**. The following Chapter of this Dissertation recounts the design, synthesis, and study of **NS1**.

---

[22] Paulini, R.; Trindler, C.; Lerner, C.; Brändli, L.; Schweizer, W. B.; Jakob-Roetne, R.; Zürcher, G.; Borroni, E.; Diederich, F. *ChemMedChem* **2006**, *1*, 340–357.

[23] Paulini, R.; Lerner, C.; Jakob-Roetne, R.; Zürcher, G.; Borroni, E.; Diederich, F. *ChemBioChem* **2004**, *5*, 1270–1274.

[24] Chen, D.; Dong, G.; Noinaj, N.; Huang, R. *J. Med. Chem.* **2019**, *62*, 3773–3779.

[25] Lavogina, D.; Enkvist, E.; Uri, A. *ChemMedChem* **2010**, *5*, 23–34.

[26] Lechtenberg, B. C.; Mace, P. D.; Sessions, E. H.; Williamson, R; Stalder, R; Wallez, Y; Roth, G. P.; Riedl, S. J.; Pasquale, E. B. *ACS Med. Chem. Lett.* **2017**, *8*, 726–731.

[27] Copeland, R. A., *Evaluation of Enzyme Inhibitors in Drug Discovery*, 2005, pp 1–294.

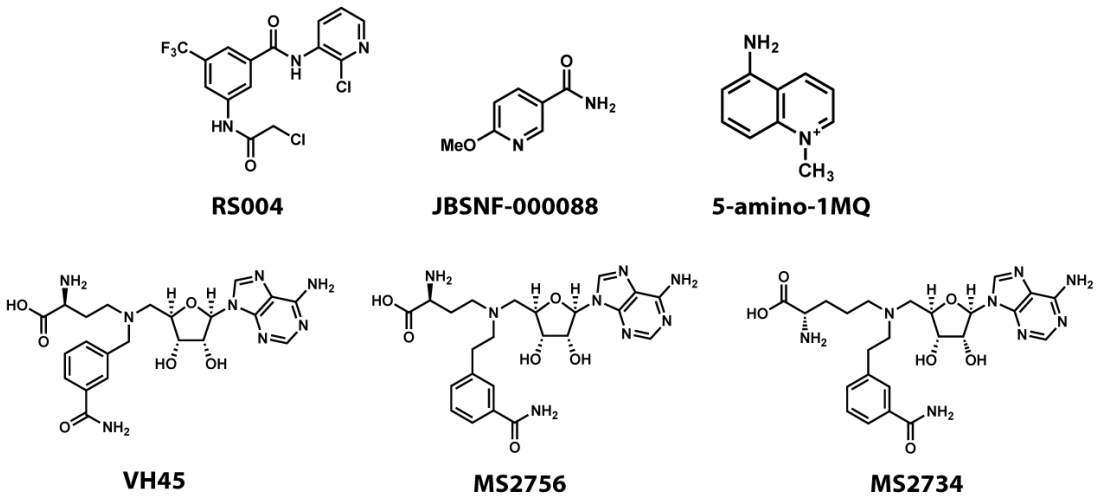

Figure 1.2.1: Previously published NNMT inhibitors.

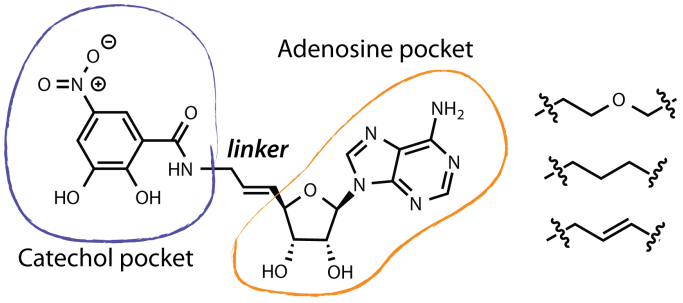

Figure 1.2.2: Example of bisubstrate methyltransferase inhibitors designed to target COMT.

2

NS1

2.1 Design of NS1

In this work a combination of structure-based design and molecular docking was used to develop high-affinity alkynyl bisubstrate inhibitors of NNMT. To begin, I examined the substrate-bound NNMT co-crystal structure (PDB ID 3ROD) and noted that the NAM nitrogen and SAH sulfur atoms are positioned 4 Å apart and reside in a small tunnel that facilitates the S_N2-type methyl transfer reaction (Figure 2.1.1a,b).[1] I envisioned an alkyne as the optimal linker between a NAM-like and a SAM-like fragment, as an alkyne linker resembles the linear, 180° transition state geometry found in the SAM → NAM methyl transfer reaction (Figure 2.1.1c,d).

[1] Peng, Y.; Sartini, D.; Pozzi, V.; Wilk, D.; Emanuelli, M.; Yee, V. C. *Biochemistry* **2011**, *50*, 7800–7808.

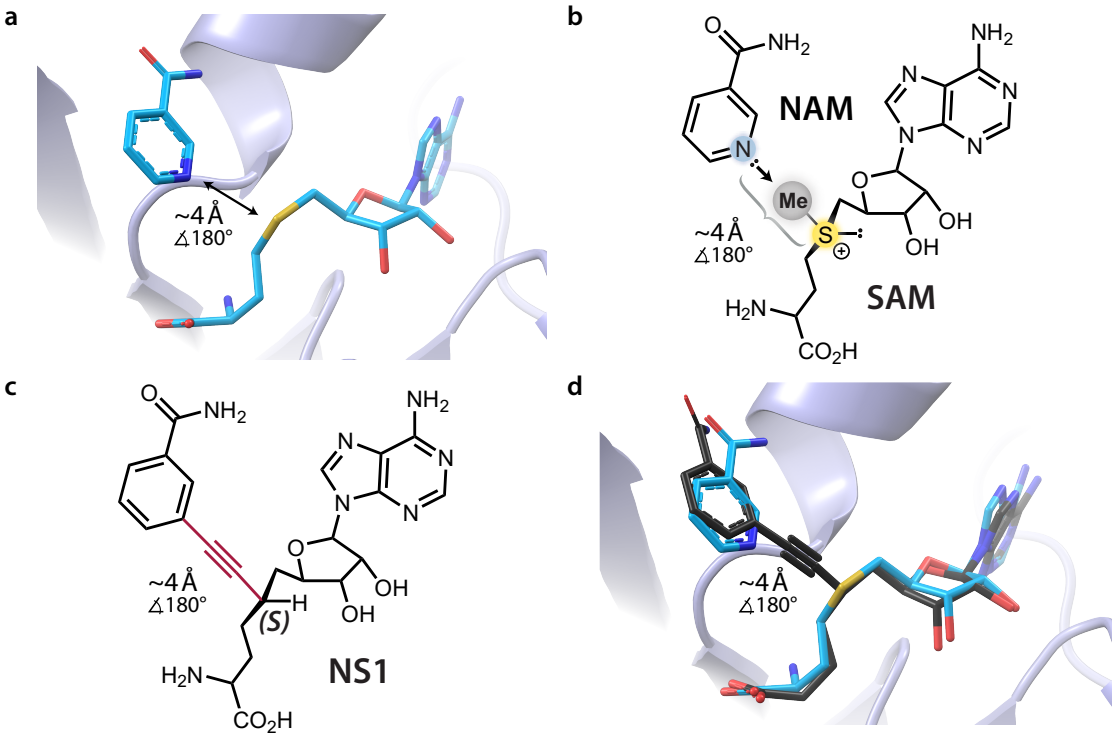

Figure 2.1.1: Overview of the alkynyl bisubstrate strategy. (a) Binding pose of ligands SAH and NAM (teal) based on previously published co-crystal structure (PDB ID 3ROD). (b) Graphical representation of the SAM → NAM methyl transfer reaction catalyzed by NNMT. (c) Graphical representation of alkynyl bisubstrate inhibitor NS1 posed to mimic the binding geometry of SAH/NAM. (d) Molecular docking output pose of alkynyl bisubstrate inhibitor NS1 (black) overlaid with native substrates SAH and NAM (teal).

This analysis led to the rational design of alkynyl nicotinamide-SAM conjugate 1 (named **NS1**). Molecular docking with Glide[2] predicted NS1 to be a better binder than SAM by >3 kcal/mol. The docked pose of NS1 (Figure 2.1.1d) overlays well with NAM and SAH in the previously published substrate-bound crystal structure; the alkyne linker fits well into the methyl transfer tunnel. With molecular docking suggesting NS1 as a potential NNMT inhibitor, I aimed to synthesize and test NS1 in an NNMT inhibition assay. The remainder of this Chapter outlines the development of a strategy for the synthesis of NS1 and other alkynyl nucleosides as single enantiomers and diastereomers.

[2] Friesner, R. A. et al. *J. Med. Chem.* **2004**, *47*, 1739–1749.

2.2 Precedent for Synthesis of 6'-Alkynyl Nucleosides

A survey of the literature revealed that 6'-alkynyl nucleosides were first proposed and synthesized in 1990 as mixtures of alkynyl and amino acid diastereomers.[3] Initial synthetic efforts toward 6'-alkynl nucleosides began with known adenosine-derived aldehyde **1** (Figure 2.2.1).[4] Wittig olefination of **1** with γ-butyrolactone-derived ylide **2** and subsequent hydrogenation yielded lactone **3**. DIBAL reduction followed by TBDPS-protection yielded aldehyde **5**, containing an aldehyde at the C6'-position amenable to further functionalization. Accordingly, reaction of **5** with dimethyl(diazomethyl)phosphosnate **6**[5] followed by ammonolysis generated alkyne **7**. Alkyne **7** was then coupled to aryl iodide **8** via Sonogashira cross-coupling (Figure 2.2.2). Side-chain silyl deprotection, iodination, and alkylation with N-benzylidene glycinate methyl ester followed by deprotection yielded compound **13**. Unfortunately, the designed alkynyl nucleoside **13** was a poor inhibitor when tested against catechol O-methyltransferase (COMT, the intended target of **13**).[6] After reading these prior syntheses of alkynyl nucleosides I hypothesized that one reason for the poor activity of **13** as observed by Coward and colleagues was due to compound **13** (and analogues) being prepared as mixtures of alkynyl and amino acid diastereomers. Thus, I aimed to develop a platform for alkynyl nucleoside synthesis that would allow for the preparation of single enantiomers and diastereomers.

2.3 Early Strategies Toward NS1

With Coward's syntheses starting from protected adenosine derivatives such as aldehyde **1**, early NS1 synthetic strategies also started with protected adenosine derivatives (Figure 2.3.1). Iodide **14** and pseudoephedrine amide **15** were attempted partners in an asymmetric alkylation reaction[7], but β-branched iodide **14** suffered from poor reactivity. Triflation of 5'-alcohol **17** (to allow for nucleophilic displacement of the 5'-triflate with Li-TMS-acetylide) yielded intramolecular cyclization product **18**. Homologation of aldehyde **19** to generate α,β-unsaturated aldehyde **20** was considered, as **20** was a potential substrate for an asymmetric alkyny-

---

[3] Yau, E. K.; Coward, J. K. *J. Org. Chem.* **1990**, *55*, 3147–3158.

[4] Ranganathan, R.; Jones, G. H.; Moffatt, J. G. *J. Org. Chem.* **1974**, *39*, 290–298.

[5] Gilbert, J. C.; Weerasooriya, U. *J. Org. Chem.* **1982**, *47*, 1837–1845.

[6] Burns, M. R.; Coward, J. K. *Bioorg. Med. Chem.* **1996**, *4*, 1455–1470.

[7] Myers, A. G.; Yang, B. H.; Chen, H.; Gleason, J. L. *J. Am. Chem. Soc.* **1994**, *116*, 9361–9362.

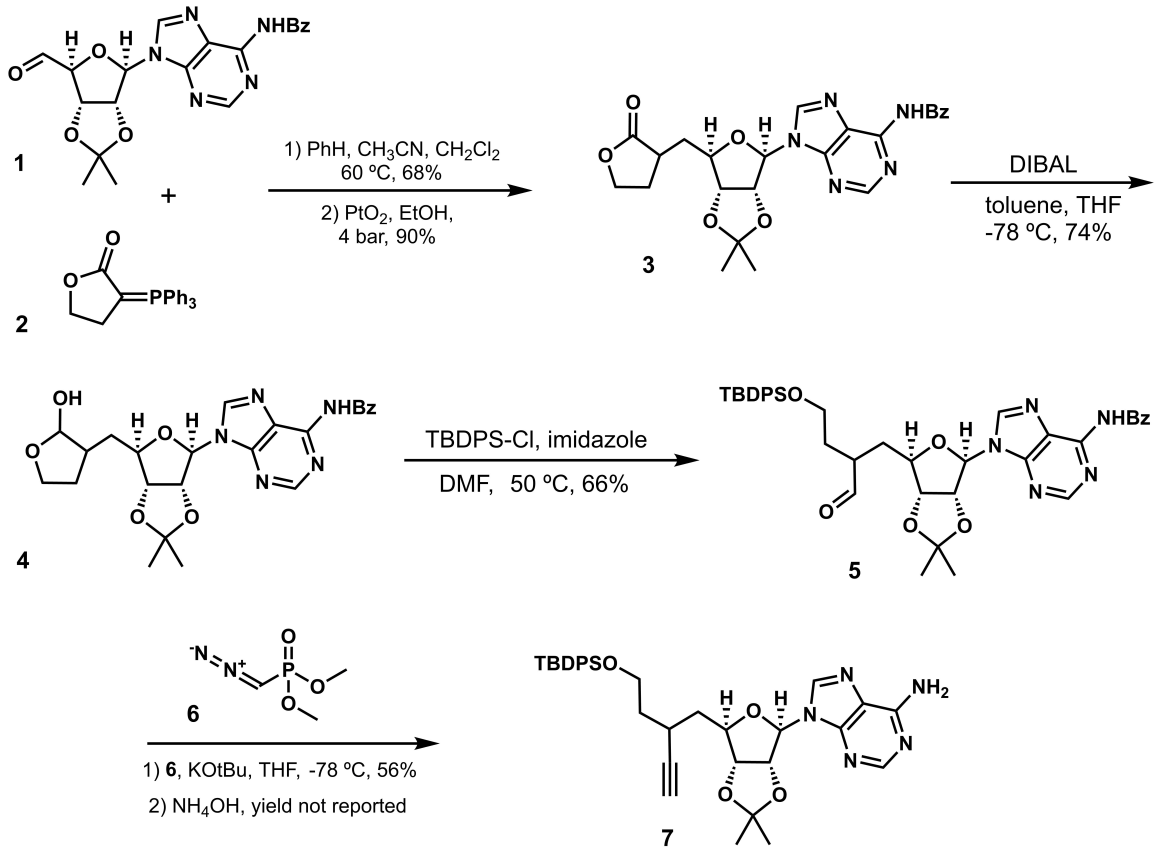

Figure 2.2.1: Coward synthesis of 6'-alkynyl nucleosides (Part 1).

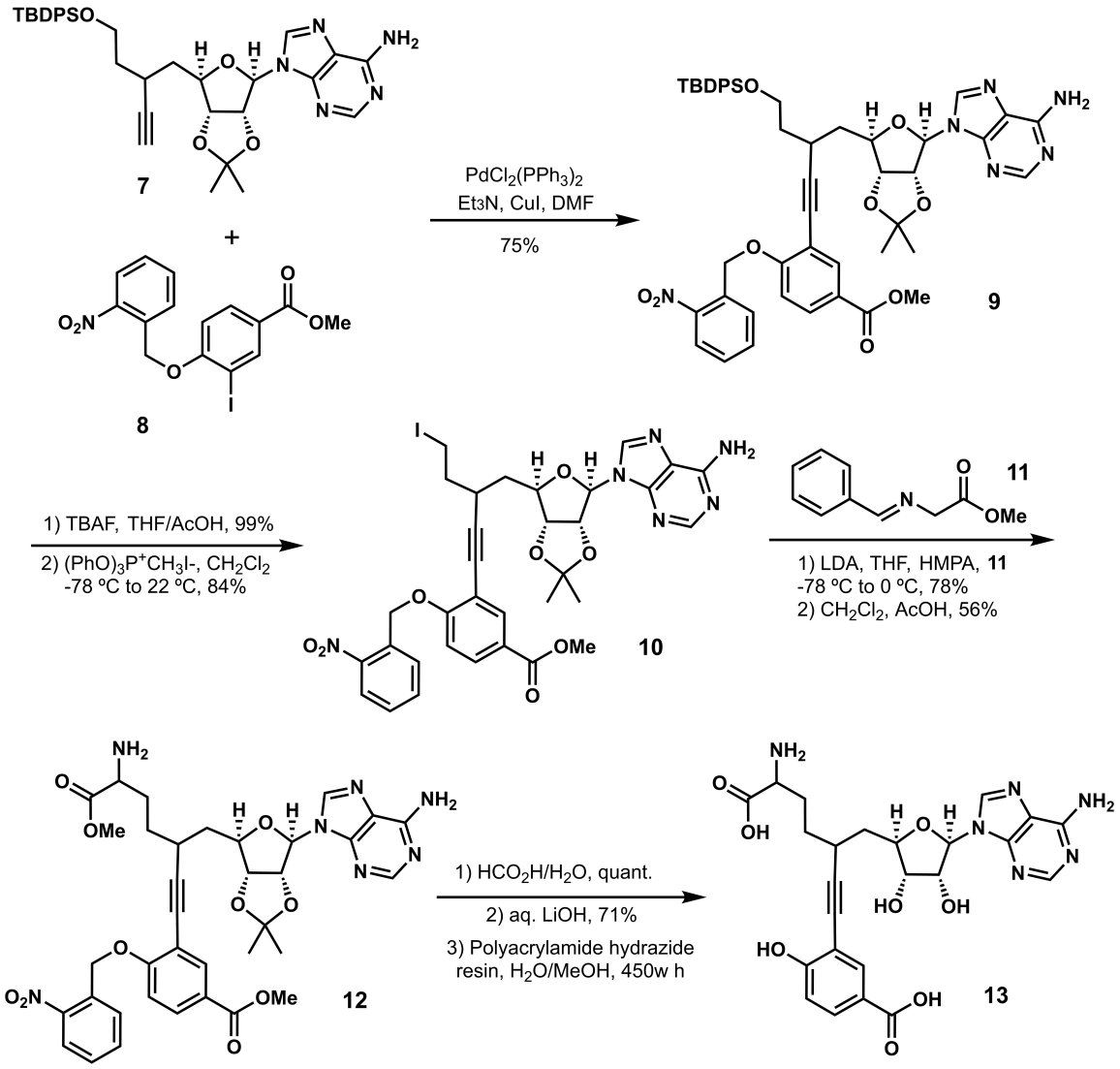

Figure 2.2.2: Coward synthesis of 6'-alkynyl nucleosides (Part 2).

lation reaction. At this point, however, I decided that routes starting from adenosine would be disadvantageous from a practical perspective. Specifically, the proposed nucleosides (and intermediates) are highly polar compounds, often requiring purification by reverse-phase HPLC. Thus, I redirected my efforts toward the synthesis of NS1 starting from commercially available D-ribose acetonide **21** (Figure 2.4.1). Intermediates en route to NS1 (starting from **21**) are suitable for large-scale synthesis and purification by traditional (normal-phase) chromatography. Switching to **21** as a starting material proved advantageous, enabling the first-generation synthesis of NS1 outlined in Figure 2.4.1.

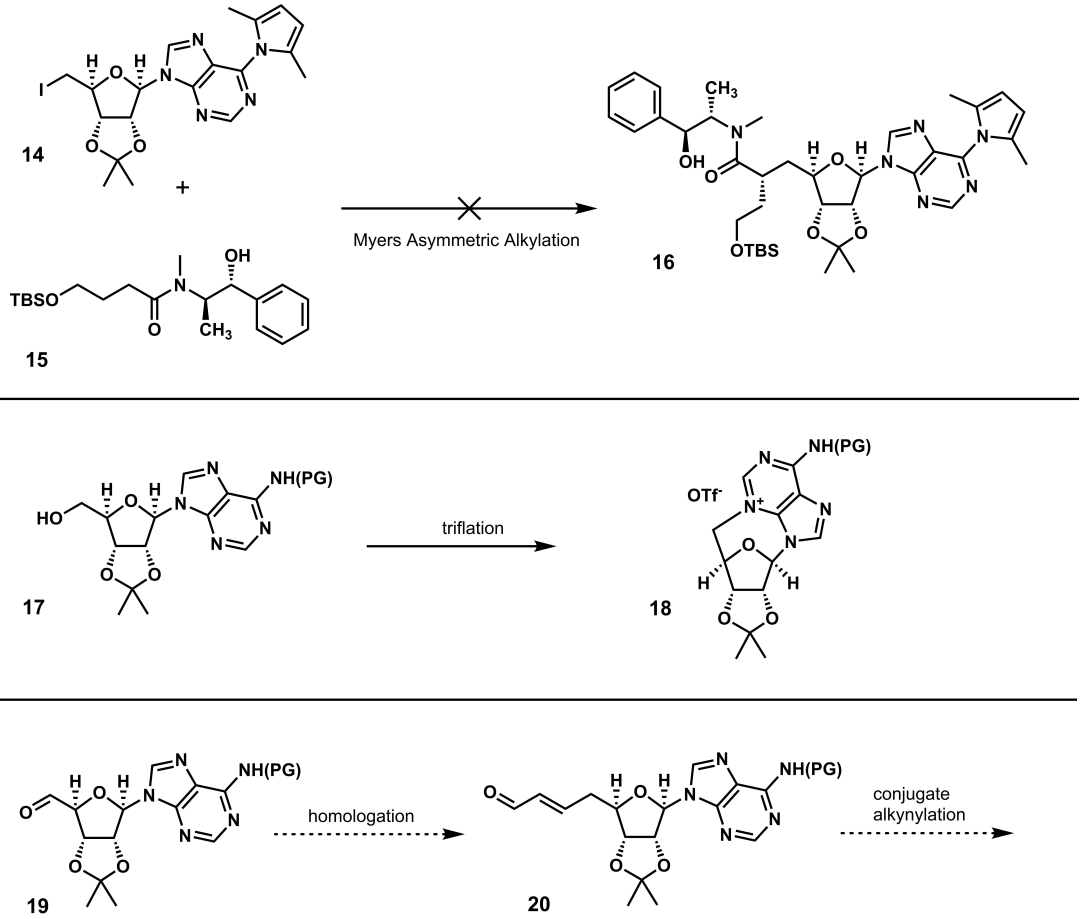

Figure 2.3.1: Early strategies toward NS1

2.4 First-Generation Synthesis of NS1

A first-generation synthesis of NS1 started from commcercially available D-ribose acetonide **21** (Figure 2.4.1). Parikh-doering oxidation followed by Wittig olefination yielded intermediate **22**. Hydroboration-

oxidation was performed according to previously reported procedures[8],[9] generating known homologated 6' alcohol (**S1**) to be used as starting material for the DMP oxidation which yields **23**. Subsequent Wittig olefination yielded key intermediate **24**. Access to **24** enabled a key step in the sequence: asymmetric alkynylation with TIPS-acetylene under conditions reported by Hayashi et al.[10] Fortunately, the reaction of **24** with TIPS-acetylene under Hayashi's conditons generated the desired alkynylation product (**25**) as a single diastereomer by ^{1}H NMR. With the key C6'-alkynyl stereocenter set, I aimed to install the amino acid side chain. Alkylation of iodide **26** via the Schöllkopf method generated **28** as a 2:1 mixture of desired:undesired diastereomers. Desilylation, cleavage of the Schöllkopf auxiliary, and protection with Fmoc-Cl generated alkynyl amino acid **29**. Compound **29** was readily converted to triacetate **30**, which was smoothly glycosylated under conditions reported by Jamison and coworkers[11] to yield nucleoside **31**. Compound **31** reacted with 3-iodobenzamide in a Sonogashira reaction to generate fully protected NS1 (**32**). Global deprotection yielded NS1 (**33**) as a single enantiomer and diastereomer as the trifluoroacetate salt after purification by reverse-phase HPLC. This first-generation route provided sufficient material for proof-of-concept studies, but I sought to redesign the NS1 synthesis to remove early oxidation/homologation steps, eliminate the use of a chiral auxiliary (Schöllkopf reagent), minimize protecting group cycling, and generate a shorter, scalable route that would enable the synthesis of a variety of NS1 analogues for a full structure-activity relationship (SAR) study.

2.5 Second-Generation Synthesis of NS1.

The optimized, second-generation synthesis of NS1 (**33**) also began with commercially available D-ribose acetonide **21** (Figure 2.5.1). Alkylation of the corresponding triflate with lithium TMS-acetylide followed by silyl deprotection generated alkyne **34**. Copper-catalyzed semi-reduction[12] of **34** rendered terminal alkene **35**, which was converted to enal **24** by cross-metathesis with crotonaldehyde. Solvent and catalyst screening (Table 2.5.1, Figure 2.5.2) revealed methyl tert-butyl ether (MTBE) and the commercially

---

[8] Alfaro, J. F.; Zhang, T.; Wynn, D. P.; Karschner, E. L.; Zhou, Z. S. *Org. Lett.* **2004**, *6*, 3043–3046.

[9] Yang, M.; Schneller, S. W. *Bioorganic Medicinal Chemistry Letters* **2005**, *15*, 149 –151.

[10] Nishimura, T.; Sawano, T.; Hayashi, T. *Angew. Chem. Int. Ed. 48*, 8057–8059.

[11] Sniady, A.; Bedore, M. W.; Jamison, T. F. *Angew. Chem. Int. Ed. 50*, 2155–2158.

[12] Cox, N.; Dang, H.; Whittaker, A. M.; Lalic, G. *Org. Synth.* **2016**, *93*, 385–400.

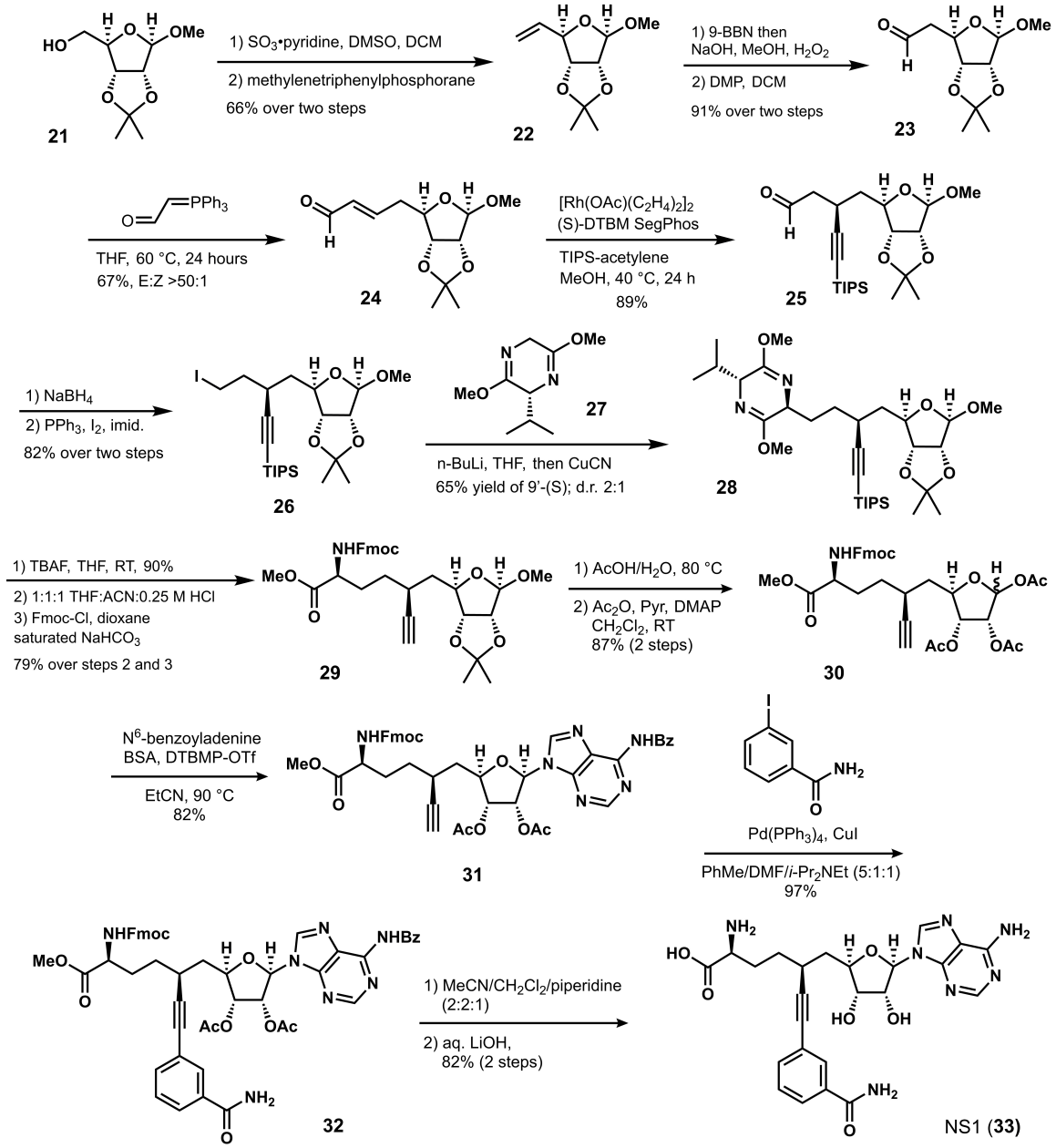

Figure 2.4.1: First-generation synthesis of NS1.

available Nitro-Grela olefin metathesis catalyst[13] as an optimal solvent/catalyst system to effect this transformation.

Table 2.5.1: Catalyst/solvent pairs screened in this work. All metathesis catalysts below were purchased from Strem, with the exception of Grubbs Catalyst C571, which was purchased from Millipore Sigma.

Catalyst/Solvent Pair in Figure 2.5.2	Catalyst	Solvent	Catalyst CAS #	Catalyst Structure
1	nitro-Grela	MTBE	502964-52-5	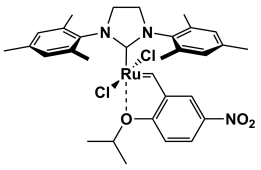
2	Grubbs Catalyst C571	CH_2Cl_2	927429-61-6	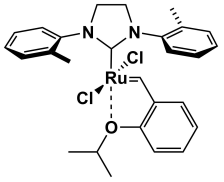
3	StickyCat Cl	CH_2Cl_2	1452227-72-3	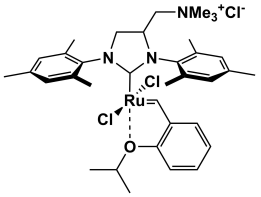
4	GreenCat	CH_2Cl_2	1448663-06-6	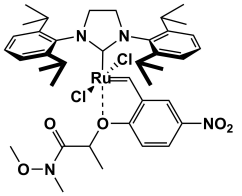
5	M71-S1Pr	CH_2Cl_2	1212008-99-5	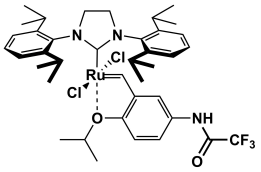
6	nitro-Grela	fluorobenzene	502964-52-5	see entry 1
7	nitro-Grela	CH_2Cl_2	502964-52-5	see entry 1

[13] Michrowska, A; Bujok, R; Harutyunyan, S; Sashuk, V; Dolgonos, G; Grela, K *J. Am. Chem. Soc.* **2004**, *126*, 9318–9325.

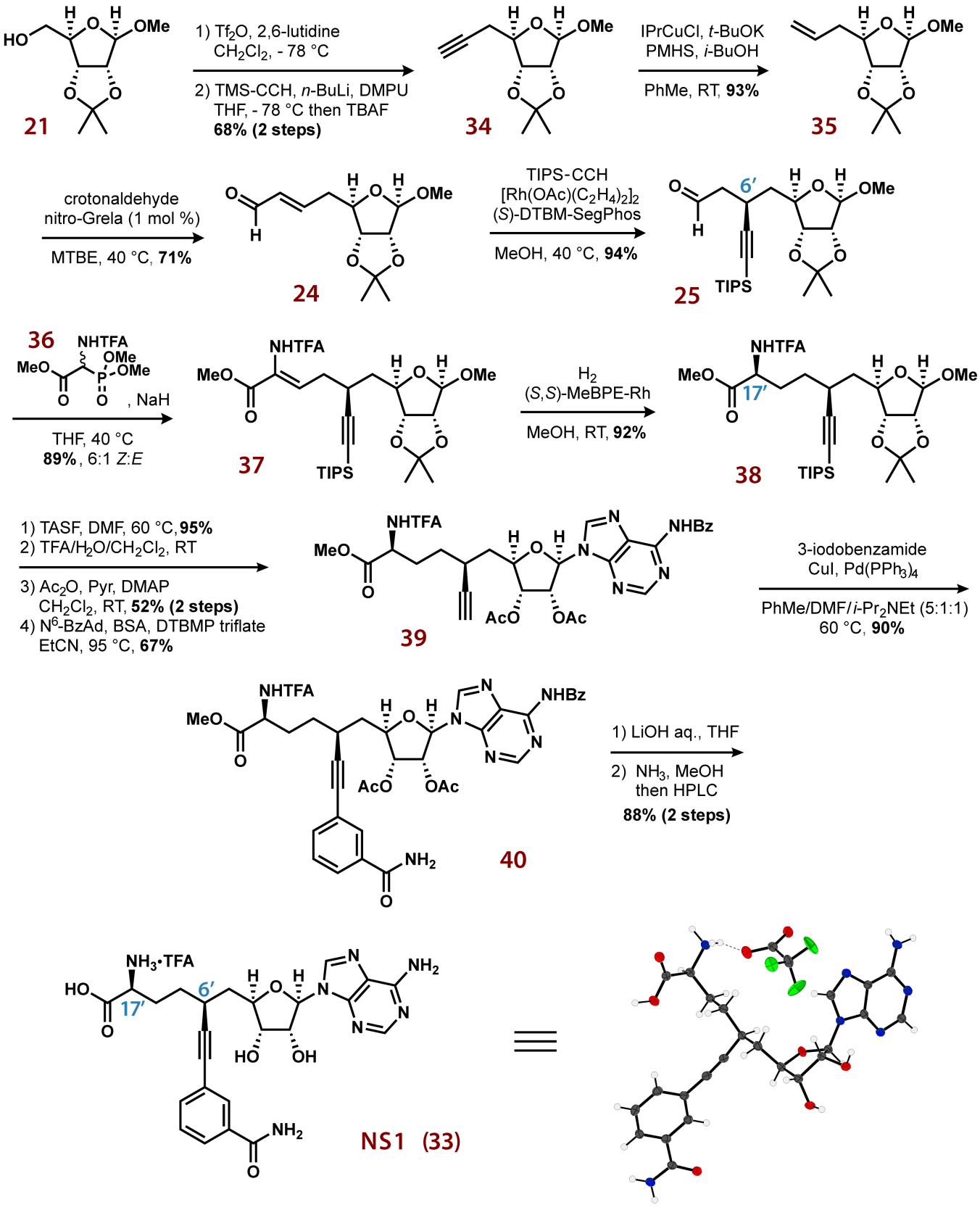

Figure 2.5.1: Second-generation synthesis of NS1

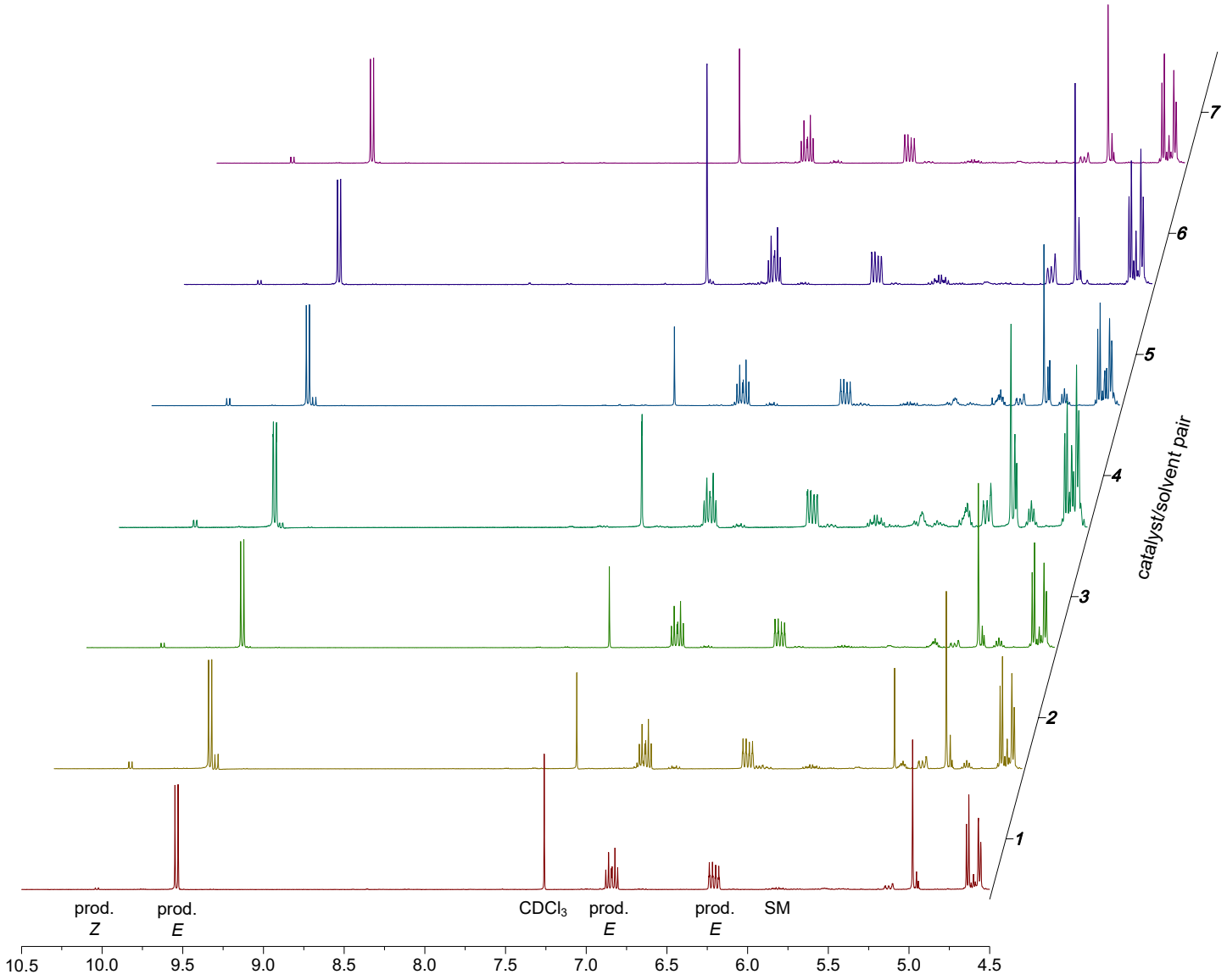

Figure 2.5.2: Crude ^{1}H NMR traces of alkene/aldehyde regions for solvent/catalyst pairs screened and shown in Table 2.5.1. All reactions were performed on 1 mmol of alkene **35** with 1 mol % catalyst loading and 5 mmol of crotonaldehyde (5 equiv.). Crotonaldehyde (predominantly *trans*) was used as received from Millipore Sigma (catalog #: 262668, CAS: 123-73-9).

The key C6' stereocenter was installed by the same rhodium-catalyzed asymmetric alkynylation[14] reaction used in the First-generation route, affording aldehyde **25** as a single diastereomer. A Horner-Wadsworth-Emmons olefination with phosphonoglycine derivative **36** yielded enamide **37**. The C17' stereocenter was set via rhodium-catalyzed asymmetric hydrogenation with a Burk-type 1,2-bis(phospholano)ethane (BPE) ligand[15], providing (*S*)-trifluoroacetamide **38** as a single diastereomer. The observed high diastereoselectivity of this transformation can be rationalized on the basis of a preferred orientation of eneamide chelation to the rhodium center (to minimize steric interactions, Figure 2.5.3).

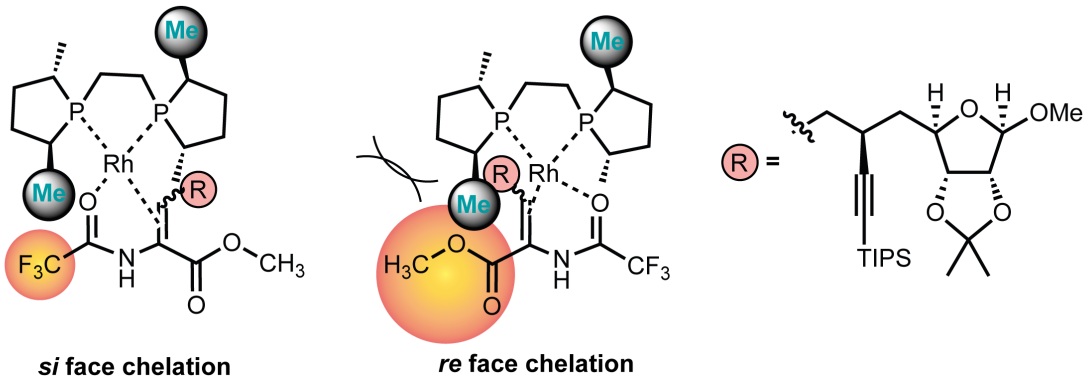

Figure 2.5.3: Mechanistic rationale for asymmetric hydrogenation of trifluoroacetyl eneamide with Burk-type ligands.

Subsequent acylation and Vorbrüggen glycosylation promoted by a 2,6-di-*tert*-butyl-4-methylpyridinium triflate salt[16] delivered nucleoside **39**. Introduction of the benzamide moiety by a Sonogashira cross-coupling and a global deprotection sequence completed the synthesis of NS1 (**33**) in a total of 14 steps with an overall yield of 9.1%. The small-molecule X-ray crystal structure of NS1•TFA was obtained, confirming the regiochemistry of the adenine nucleobase (N9-linkage) as well as the configuration of the C6' and C17' stereocenters (Figure 2.5.1, bottom right. See section 2.9.9 for full crystallographic details). Importantly, this second-generation route enabled the large-scale synthesis of NS1 and analogues.

---

[14] Nishimura, T.; Sawano, T.; Hayashi, T. *Angew. Chem. Int. Ed.* **2009**, *48*, 8057–8059.

[15] Burk, M. J. *Acc. Chem. Res.* **2000**, *33*, 363–372.

[16] Sniady, A.; Bedore, M. W.; Jamison, T. F. *Angew. Chem. Int. Ed. 50*, 2155–2158.

2.6 Biochemical Evaluation of NS1 and Analogues

A fluorescence-based NNMT inhibition assay[17] (Figure 2.6.1) revealed NS1 to be a highly potent, sub-nanomolar (500 pM) NNMT inhibitor. In the assay, NNMT converts quinoline to the fluorescent 1-methylquinolinium (1MQ), allowing reaction progress to be monitored continuously in real time (Figure 2.6.2).

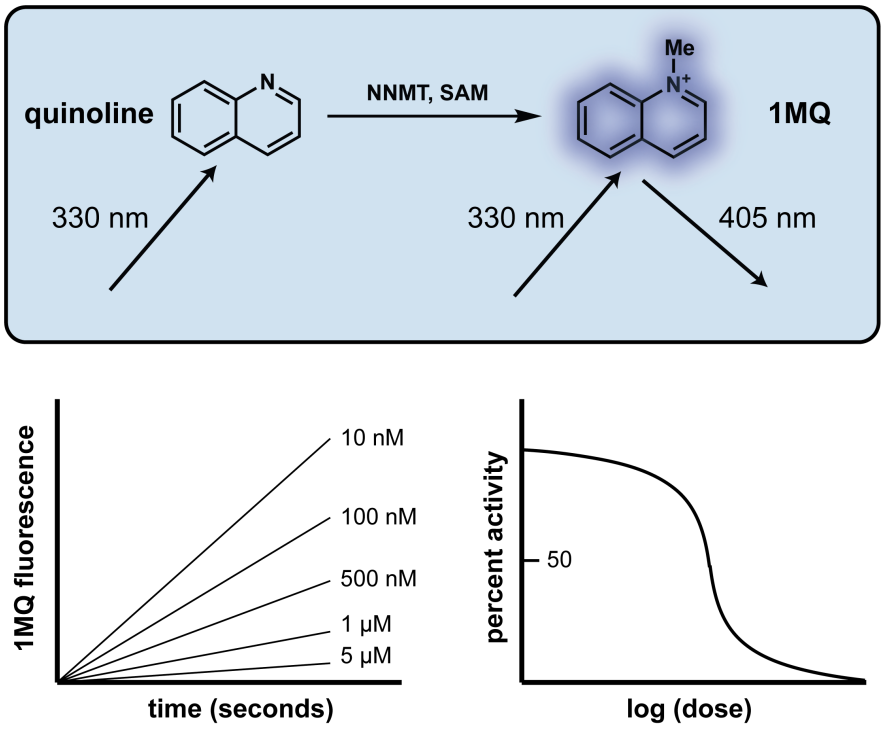

Figure 2.6.1: NNMT assay outlined by Neelakantan et al.

The reaction progress curves were prominently nonlinear, both in the presence and in the absence of inhibitors. Therefore, we analyzed the full reaction time-course using the software package DynaFit[18,19]

[17] Neelakantan, H.; Wang, H.-Y.; Vance, V.; Hommel, J. D.; McHardy, S. F.; Watowich, S. J. *J. Med. Chem.* **2017**, *60*, 5015–5028.

[18] Kuzmič, P. *Anal. Biochem.* **1996**, *237*, 260–273.

[19] Kuzmič, P. In *Methods in Enzymology*, 2009, pp 247–280.

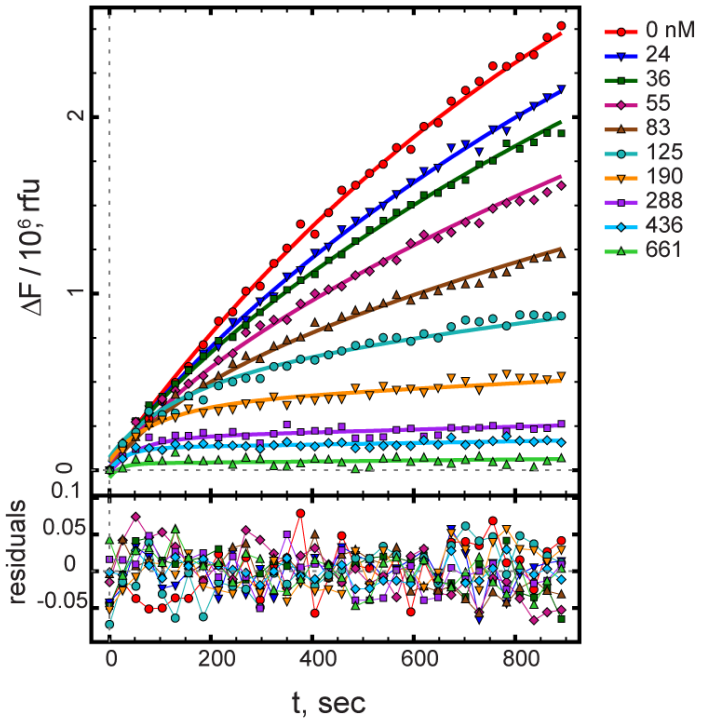

Figure 2.6.2: Time-course of NNMT kinetic assay in the absence (red circles) or in the presence (remaining symbols) of NS1. Inhibitor concentrations are shown at top right. ΔF are scaled fluorescence changes in relative fluorescence units ("rfu"). The smooth curves represent the best least-squares fit to a system of first-order differential equations automatically generated by the DynaFit software package.

instead of employing initial-rate methods to evaluate the biochemical potency of each inhibitor[20,21,22,23].

The mathematical models for each of several postulated kinetic mechanisms were systems of first-order Ordinary Differential Equations (ODEs) automatically derived by the DynaFit software. Inhibition constants were computed as the ratio $K_i = k_{off}/k_{on}$, where k_{off} is the microscopic rate constant for the dissociation of the enzyme-inhibitor complex and k_{on} is the corresponding microscopic association rate constant. The full kinetic treatment of NNMT inhibitors reported in this work has been published online at the ChemRxiv under *Supporting Information, Part 3*. Because K_i values reported in this work span six orders of magnitude, they are presented and discussed as pK_i.

---

[20] Copeland, R. A., *Evaluation of Enzyme Inhibitors in Drug Discovery*, 2005, pp 1–294.

[21] Segel, I. H., *Enzyme Kinetics*; John Wiley & Sons: New York, 1975.

[22] Greco, W. R.; Hakala, M. T. *J. Biol. Chem.* **1979**, *254*, 12104–12109.

[23] Work with the DynaFit software package was performed in collaboration with Dr. Petr Kuzmič of BioKin Ltd. (Watertown, MA).

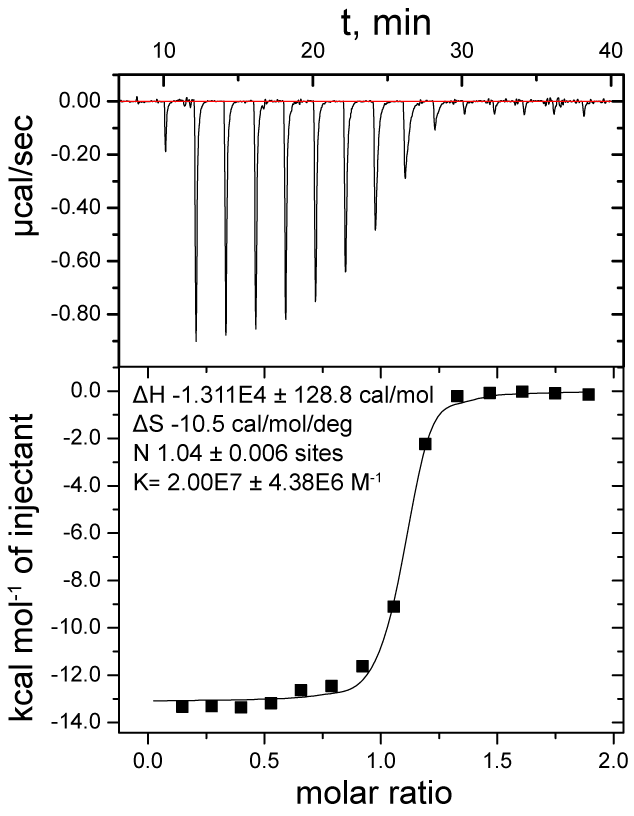

Figure 2.7.1: Isothermal titration calorimetry experiment of NS1 binding to NNMT.

2.7 Thermodynamics of Binding

After biochemical characterization of NS1, isothermal titration calorimetry (ITC) showed NS1 to be a high-affinity ligand for NNMT (Figure 2.7.1).[24] NS1 bound to NNMT in a 1:1 molar stoichiometry with a K_d of 49.5 nM. The binding curve demonstrated that NS1-NNMT binding was enthalpically favorable yet entropically unfavorable. The K_d value obtained in the thermodynamic (ITC) study was higher than the corresponding inhibition constant (K_i) obtained during the kinetic modeling of NNMT inhibition. This difference was also observed when comparing the K_d values (via ITC) of previously reported[25] NNMT inhibitors to K_i values obtained in this study. The observed differences between K_d and K_i underscore the challenge of comparing thermodynamic and kinetic measurements.

Kinetic inhibition experiments reflect the highly dynamic nature of enzymatic reactions, but in an ITC

[24] ITC experiments were performed in collaboration with Samuel Carlson of the Harvard University Department of Molecular and Cellular Biology (MCB).

[25] Babault, N.; Allali-Hassani, A.; Li, F.; Fan, J.; Yue, A.; Ju, K.; Liu, F.; Vedadi, M.; Liu, J.; Jin, J. *J. Med. Chem.* **2018**, *61*, 1541–1551.

experiment a small-molecule ligand is often titrated into an apo-structure containing no bound ligands. This apo-structure may not be physiologically relevant; in the case of NNMT-mediated quinoline methylation, both SAM and quinoline have ~20-fold improved affinity for their complementary binary enzyme complex than for apo-NNMT[26]. Thus, binding affinity (K_d) obtained from thermodynamic experiments is fundamentally different from the inhibition constant (K_i), which measures the ability of a small molecule to inhibit a dynamic, active enzymatic process.

2.8 X-Ray Co-Crystal Structure of NS1 Bound to hNNMT

We determined the co-crystal structure of NS1-bound NNMT (PDB ID to be assigned, Table 2.8.1) and observed an NS1-shaped density in the NAM/SAM binding pocket in the electron density map (Figure 2.8.1a).[27] Fitting NS1 into the density decreased the R_{free} value and improved the map quality, revealing that NS1 occupies both the NAM and SAM binding sites in the same orientation as the native substrates, with the alkynyl linker occupying the methyl transfer tunnel. The NS1 alkyne is an optimal surrogate for the SAM-dependent methyl transfer reaction of NNMT and effectively positions both structural components of NS1 properly in space, allowing NS1 to capture similar binding interactions as the native substrates (Figure 2.8.1b).

Table 2.8.1: Data collection and refinement statistics. Statistics for the highest-resolution shell are shown in parentheses.

Wavelength (Å)	0.97910
Resolution range (Å)	42.6–2.25 (2.33–2.25)
Space group	P 1
Unit cell (a, b, c (Å); α, β, γ (°))	46.07 62.20 108.20 82.52 81.84 68.35
Total reflections	80875 (8176)
Unique reflections	46037 (4664)
Multiplicity	1.8 (1.8)
Completeness (%)	87.23 (86.28)
Mean I/σ(I)	3.15 (1.34)
Wilson B-factor	28.87
R_{merge}	0.1752 (1.151)

[26] Neelakantan, H.; Vance, V.; Wang, H.-Y. L.; McHardy, S. F.; Watowich, S. J. *Biochemistry* **2017**, *56*, 824–832.

[27] Solution of the NNMT/NS1 co-crystal structure was done in collaboration with Elizabeth May and Prof. Rachelle Gaudet of Harvard MCB.

Table 2.8.1 continued from previous page.

R_{meas}	0.2478 (1.628)
R_{pim}	0.1752 (1.151)
$CC_{1/2}$	0.919 (0.182)
CC*	0.979 (0.555)
Reflections used in refinement	45689 (4534)
Reflections used for R_{free}	2293 (220)
R_{work}	0.2273 (0.3135)
R_{free}	0.2686 (0.3373)
CC(work)	0.921 (0.664)
CC(free)	0.876 (0.660)
Number of non-hydrogen atoms	8562
macromolecules	8211
ligands	178
solvent	173
Protein residues	1058
RMS(bonds) (Å)	0.003
RMS(angles) (	0.52
Ramachandran favored (%)	99.05
Ramachandran allowed (%)	0.76
Ramachandran outliers (%)	0.19
Rotamer outliers (%)	0.89
Clashscore	3.72
Average B-factor	35.48
macromolecules	35.57
ligands	28.32
solvent	38.61
Number of TLS groups	24

NS1 exploits the same amino acids that contact the native substrates to bind NNMT. To stabilize the adenosine portion of NS1, D142 forms a hydrogen bond with the primary amine on the adenine nucleobase, while the hydroxyl groups of ribose hydrogen-bond extensively with the backbone nitrogen atom of S87 and the side chains of D85 and N90 (Figure 2.8.2a). The carboxylic acid of the NS1 amino acid accepts four hydrogen bonds from Y20, Y25, Y69, and T163, while the amino group hydrogen-bonds with the backbone carbonyl of G63 (Figure 2.8.2b). A hydrophobic clamp positions the aromatic ring of the benzamide moiety between Y204 and L164, with S201 and S213 stabilizing the amide group through hydrogen bonds (Figure 2.8.2c).

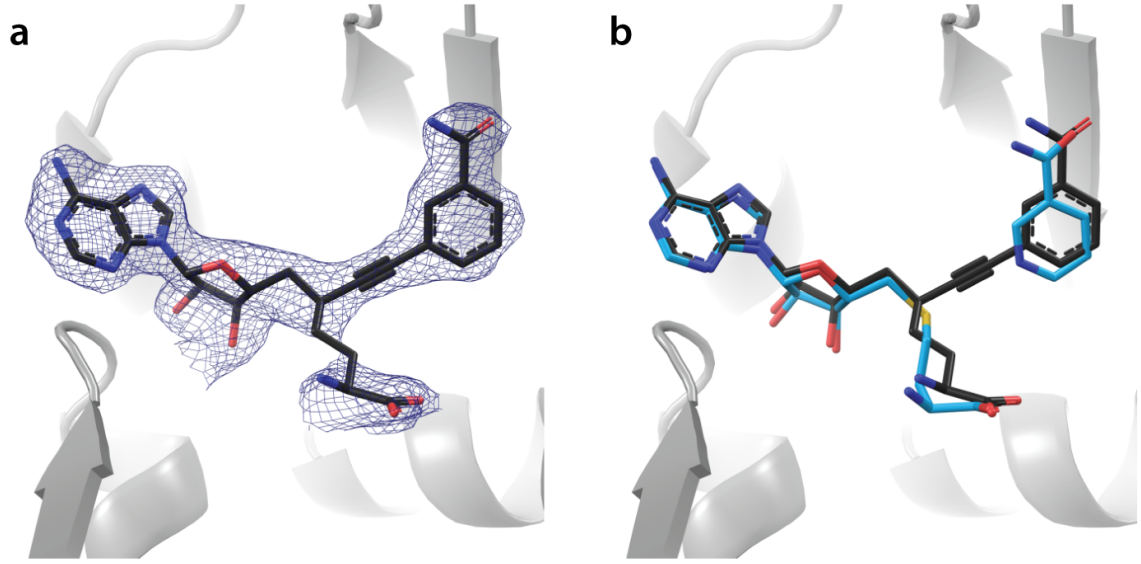

Figure 2.8.1: (a) A $2F_o$-F_c omit map contoured at 1σ reveals NS1-shaped electron density in the binding pocket of NNMT. (b) NS1 (black) binds NNMT in an orientation that closely resembles that of the native substrates SAM and NAM (cyan; PDB ID 3ROD).

2.9 Experimental Details

2.9.1 Molecular Docking with Schrödinger Glide

The molecular docking workflow presented below was performed in Schrödinger Maestro Version 11.8.012, MMshare Version 4.4.012, Release 2018-4, Platform Windows-x64. A detailed tutorial (Structure-Based Virtual Screening Using Glide Workshop Tutorial, 2018-4) published by Schrödinger can be found at https://www.schrodinger.com/training/tutorials.

Protein Preparation

Glide docking began with the Protein Preparation Wizard. The PDB entry 3ROD[28] (NAM and SAH bound to NNMT) was imported into the workspace. Preprocessing parameters in the *Import and Process* tab were set as presented in Figure 6.1.1. The imported structure was preprocessed. Parameters in the *Review and Modify* tab were set as presented in Figure 6.1.2. All chains, waters, and hets not belonging to chain C were deleted. Parameters in the *Refine* tab were set as presented in Figure 6.1.3. H-bond assignment was optimized, waters were removed, and restrained minimization was performed.

[28] Peng, Y.; Sartini, D.; Pozzi, V.; Wilk, D.; Emanuelli, M.; Yee, V. C. *Biochemistry* **2011**, *50*, 7800–7808.

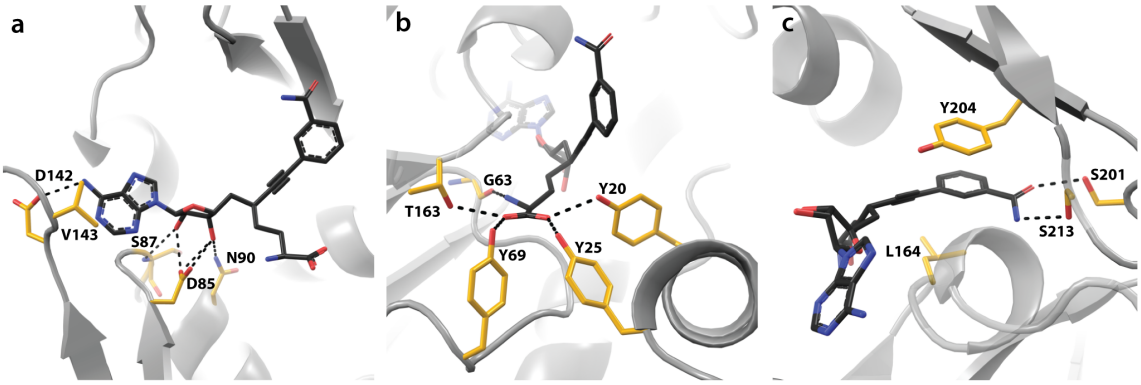

Figure 2.8.2: NS1 also exploits the same protein interactions that NNMT uses to bind its native substrates. Ligand-interacting residues from NNMT are shown in yellow; black dotted lines represent hydrogen bonds.

Receptor Grid Generation

Receptor grid generation was performed according to the parameters outlined in Figure 6.1.4. No other tabs (*Site, Constraints, Rotatable Groups, Excluded Volumes*) were edited. Nicotinamide (NCA, NAM) was deleted from the workspace prior to choosing the workspace ligand SAH for grid generation.

Ligand Preparation

NS1 was drawn in ChemDraw and saved as an MDL Molfile (.mol). The .mol file was opened in the LigPrep wizard and was prepared using the parameters outlined in Figure 6.1.5.

Glide Docking

The Ligand Docking panel was opened and the output file from LigPrep was loaded with the parameters shown in Figure 6.1.6 and Figure 6.1.7. Docking calculations were run locally and NS1 was determined to have a Glide Score of –15.991. A table of output values is presented below in Table 2.9.1. An image of the NS1 output pose is presented in Figure 2.9.1. Reference ligand S-adenosylmethionine (SAM) was docked using this same protocol, having a Glide score of –12.741. An image of the SAM output pose is presented in Figure 2.9.2.

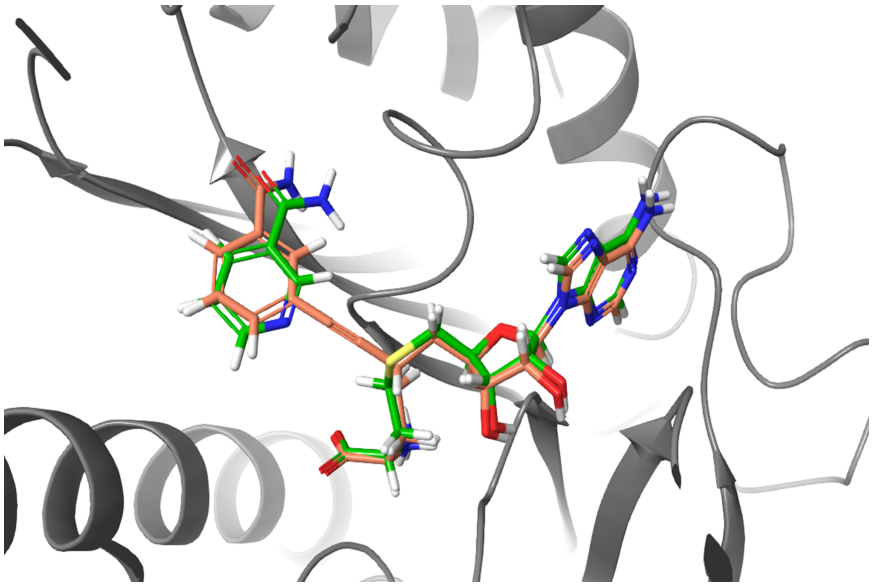

Figure 2.9.1: Output image of docked NS1 (orange), taken directly from the Maestro workspace, overlaid with substrates SAH and NAM (green).

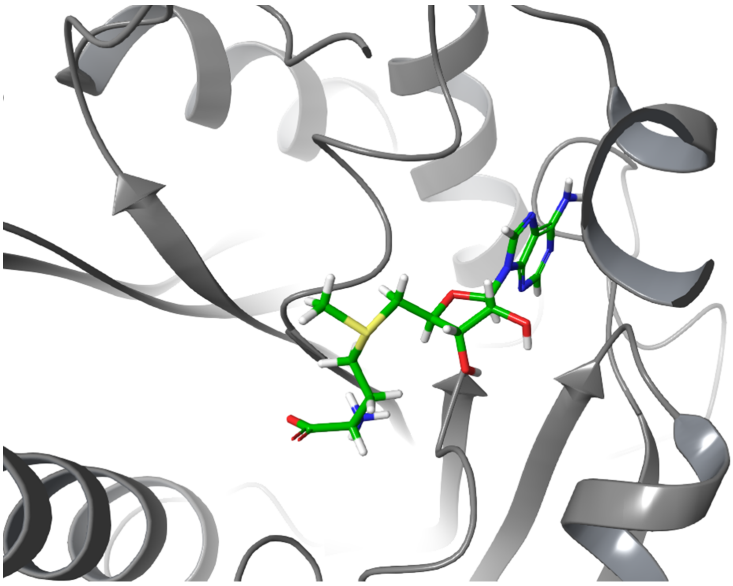

Figure 2.9.2: Output image of docked reference ligand SAM, taken directly from the Maestro workspace.

Table 2.9.1: Docking output values from the Maestro docking table.

parameter	NS1	SAM
glide rotatable bonds	12	9
docking score	-15.991	-12.741
glide ligand efficiency	-0.432	-0.472
glide ligand efficiency sa	-1.44	-1.416
glide ligand efficiency ln	-3.468	-2.966
glide gscore	-15.991	-12.741
glide lipo	-4.095	-2.187
glide hbond	-1.584	-0.986
glide metal	0	0
glide rewards	-3.069	-3.744
glide evdw	-72.943	-49.357
glide ecoul	-30.436	-29.203
glide erotb	0.631	0.737
glide esite	-0.227	-0.093
glide emodel	-213.421	-157.523
glide energy	-103.378	-78.56
glide einternal	9.997	8.134

2.9.2 General Chemistry Procedures

Air and/or moisture sensitive reactions were performed under an atmosphere of nitrogen in a flame dried apparatus. Reactions were monitored by thin layer chromatography (TLC) using Merck 0.25 mm silica gel 60 covered glass backed plates F_{254}. TLC plates were visualized under UV light and/or exposure to an acidic solution of *p*-anisaldehyde (Anis), an aqueous solution of ceric ammonium molybdate (CAM) or an aqueous solution of potassium permanganate ($KMnO_4$), followed by heating on a hot plate. Reactions were also monitored by analytical LCMS using an Agilent 6120 Quadrupole LC/MS and an Agilent 1260 Infinity II LC system equipped with (1) a Kinetex® F5 column (2.6 μm, 100 Å, 100 × 3.0 mm), (2) a Kinetex® Biphenyl column (2.6 μm, 100 Å, 100 × 3.0 mm) or (3) a Thermo Scientific™ Accucore™ aQ C18 column (2.6 μm, 100 × 2.1 mm). Two methods were used: method A for columns 1, 2, 3: solvent A: 0.1% (v/v) formic acid in water, solvent B: 0.1% (v/v) formic acid in CH_3CN, gradient elution: 5% B for 1 min then 5% → 95% B over 8 min followed by 95% B for 2 min and reequilibration for 2 min, flow rate: 0.55 mL/min (1), 0.95 mL/min (2), 0.70 mL/min (3), column temperature: 50 °C, UV detection: 254 nm, and method B for columns 2, 3: solvent A: 0.1% (v/v) formic acid in water, solvent B: 0.1% (v/v) formic acid in CH_3CN, gradient elution: 0% B for 1 min, 0% → 40% B over 8 min, 40% → 95% B over 2 min followed by 95% B for 2 min and reequilibration for 2 min, flow rate: 0.95 mL/min (2), 0.70 mL/min (3), column temperature: 50 °C, UV detection: 254 nm. When appropriate, the purity of compounds was determined by analytical LCMS using the columns and method outlined. Flash column chromatography was performed using an In-

terchim PuriFlash® 215 system on prepacked silica gel cartridges. Prepacked silica gel cartridges used in this work included Büchi FlashPure (35 to 45 μm), Büchi Reveleris HP (16 to 24 μm), Teledyne Isco RediSep® Rf (35 to 70 μm) and Teledyne Isco RediSep Rf Gold® (20 to 40 μm).

2.9.3 Materials

Commercial reagents and solvents were used as received unless specified otherwise. The molarity of *n*-butyllithium solutions was determined by titration using *N*-benzylbenzamide[3] or *N*-pivaloyl-o-toluidine[4] with similar results (average of three determinations).

2.9.4 Instrumentation

^{1}H NMR spectra were recorded on Varian INOVA-600 or Varian INOVA-500 spectrometers at ambient temperature. Chemical shifts are reported in ppm (δ scale) relative to residual undeuterated solvent ($CDCl_3$: 7.26 ($CHCl_3$), CD_3OD: 3.31 (CD_2HOD), CD_3CN: 1.94 (CD_2HCN), D_2O: 4.79 (HOD)). Data are reported as follows: chemical shift (δ ppm) (integration, multiplicity (s = singlet, d = doublet, t = triplet, q = quartet, m = multiplet, br = broad, app = apparent, or a combination of these), coupling constant(s) *J* (Hz)). When a mixture of deuterated solvents is employed, the residual undeuterated solvent used for reference is indicated in bold. ^{13}C NMR spectra were recorded on Varian INOVA-500, Varian MERCURY-400 and JEOL J400 spectrometers at ambient temperature. Data are reported as follows: chemical shifts (δ scale, ppm) relative to the carbon resonances of the solvent ($CDCl_3$: 77.16, CD_3OD: 49.00, CD_3CN: 1.32). When a mixture of deuterated solvents is employed, the solvent used for reference is indicated in bold. ^{19}F NMR spectra were recorded on Varian INOVA-500 and Varian MERCURY-400 spectrometers at ambient temperature. Data are reported as follows: chemical shifts (δ scale, ppm) relative to $CFCl_3$ and referenced to benzotrifluoride (BTF), hexafluorobenzene (HFB), or trifluoroacetic acid (TFA) as internal standards (BTF IStd: δ –63.7, HFB IStd: δ –164.9, TFA IStd: δ –76.6). ^{31}P NMR spectra were recorded on a Varian MERCURY-400 spectrometer at ambient temperature. Data are reported as follows: chemical shifts (δ scale, ppm), calibrated to an external standard of triphenyl phosphate in $CDCl_3$ (0.0485 M, δ –17.6 relative to H_3PO_4 at δ 0). Infrared (FTIR) spectra were recorded on a Bruker Alpha FT-IR spectropho-

---

[3] Burchat, A. F.; Chong, J.; Nielsen, N. *J. Organomet. Chem.* **1997**, *542*, 281–283.

[4] Suffert, J. *J. Org. Chem.* **1989**, *54*, 509–510.

tometer. Data is reported in frequency of absorption (cm^{-1}). The IR spectrum of each compound (solid or liquid) was acquired directly on a thin layer at ambient temperature. High resolution mass spectra (HRMS) were recorded using electrospray ionization (ESI+) on a Bruker micrOTOF-Q II mass spectrometer or on an Agilent 6220 LC-TOF instrument. The structures of Desilylated **26**, NS1•TFA (**33**), NS1-Cyclopropyl Alkyne **S24** and NS1-Urea Alkynyl Alcohol **S30** were obtained with the assistance of Dr. Shao-Liang Zheng at the X-ray diffraction facility of the Department of Chemistry & Chemical Biology at Harvard University.

2.9.5 Positional Numbering System

The following figure features representative examples of the positional numbering system used in this work. Several compound names directly derive from it, such as NS1-12'F for the analog where a fluorine substituent was added at the 12' position.

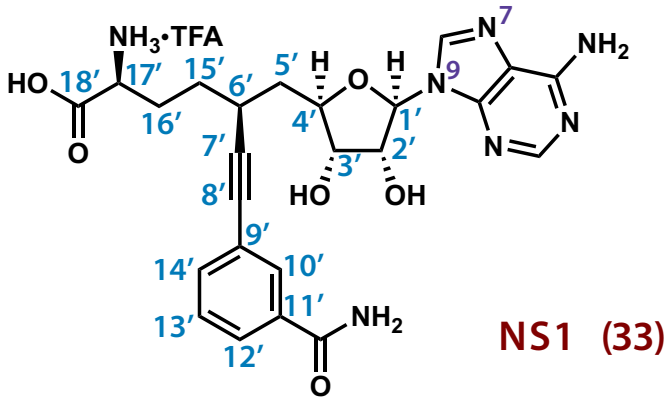

*(Intermediates that have not been assigned numbering in main Chapter figures are numbered sequentially in the experimental section starting with **S1**).*

2.9.6 **NS1**, First-Generation Route

Aldehyde **23**

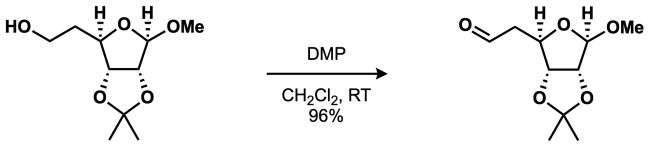

S1 **23**

To a stirred solution of compound **S1**[5,6] (13.12 g, 60.12 mmol, 1.0 equiv) in CH_2Cl_2 (200 mL) at 0 °C under N_2 was carefully added Dess-Martin periodinane (31.87 g, 75.15 mmol, 1.25 equiv) portionwise over 30 min. The mixture was stirred at room tempterature for 2 h before being partially concentrated in vacuo. Diethyl ether (400 mL) was added to the residue and the mixture was washed sequentially with 1:1 10% sodium thiosulfate:sat. aq. $NaHCO_3$ (2 x 200 mL) and brine (200 mL). The aqueous layers were extracted with diethyl ether (2 x 200 mL) and the resulting organic layer was washed with brine (200 mL). The combined organic layers were dried with $MgSO_4$, filtered, and concentrated in vacuo to yield the product **23** as a clear oil (12.5 g, 57.8 mmol, 96%) of suitable purity to be used in the next transformation. Workup of the aldehyde (briefly described above) was performed using protocols reported by Meyer and Schreiber.[7]

$\mathbf{R_f}$ = 0.41 (hexanes/EtOAc, 50:50);

FTIR (neat), cm^{-1}: ν_{max} 2989, 2936, 2834, 2731, 1724, 1456, 1379, 1375, 1275, 1240, 1210, 1209, 1195, 1161, 1106, 1093, 1050, 1008;

^{1}H NMR (500 MHz, $CDCl_3$): δ 9.79 (dd, J = 2.3, 1.3 Hz, 1H), 4.96 (s, 1H), 4.72 (ddd, J = 8.6, 6.3, 1.0 Hz, 1H), 4.62 (d, J = 5.9 Hz, 1H), 4.58 (dd, J = 5.9, 1.0 Hz, 1H), 3.31 (s, 3H), 2.81 (ddd, J = 16.9, 8.6, 2.3 Hz, 1H), 2.68 (dddd, J = 16.9, 6.3, 1.4, 0.4 Hz, 1H), 1.49 (d, J = 0.7 Hz, 3H), 1.31 (d, J = 0.7 Hz, 3H);

---

[5] Yang, M.; Schneller, S. W. *Bioorganic Medicinal Chemistry Letters* **2005**, *15*, 149 –151.

[6] Alfaro, J. F.; Zhang, T.; Wynn, D. P.; Karschner, E. L.; Zhou, Z. S. *Org. Lett.* **2004**, *6*, 3043–3046.

[7] Meyer, S. D.; Schreiber, S. L. *J. Org. Chem.* **1994**, *59*, 7549–7552.

^{13}C NMR (126 MHz, $CDCl_3$): δ 199.83, 112.61, 109.71, 85.26, 83.90, 81.48, 54.87, 48.80, 26.38, 24.90;

Enal **24**

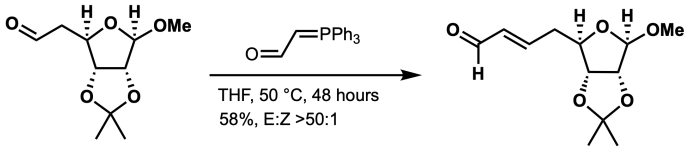

23 **24**

To a stirring solution of compound **23** (14.17 g, 65.6 mmol, 1.0 equiv) in THF (anhydrous, 30 mL) was added (triphenylphosphorylidine)acetaldehyde (29.92 g, 98.32 mmol, 1.5 equiv) and an additional 25 mL of THF. The mixture was stirred at 50 °C for 48 h. The reaction was monitored carefully by ^{1}H NMR to prevent epimerization at C4'. NMR samples for reaction monitoring were prepared by removing a small aliquot of the reaction mixture, diluting it with 1:1 pentane:Et_2O, and filtering through a silica plug. When ^{1}H NMR indicated full conversion of SM, The mixture was diluted with 1:1 pentane:Et_2O (500 mL), filtered through a silica plug, and concentrated *in vacuo* to yield the crude product as a yellow-orange oil. The crude product was further purified by silica gel chromatography (hexanes/EtOAc, 0 $\rightarrow$ 60%) to yield 9.21 g of **24** (38.0 mmol, 58%) as a yellow oil.

R_f = 0.41 (hexanes/EtOAc, 50:50);

FTIR (neat), cm^{-1}: ν_{max} 2990, 2936, 2832, 2735, 1688, 1641, 1453, 1382, 1377, 1298, 1269, 1263, 1242, 1210, 1194, 1161, 1140, 1104, 1089, 1058, 1026;

^{1}H NMR (600 MHz, $CDCl_3$): δ 9.54 (d, J = 7.8 Hz, 1H), 6.84 (dt, J = 15.7, 6.8 Hz, 1H), 6.21 (ddt, J = 15.7, 7.8, 1.5 Hz, 1H), 4.98 (s, 1H), 4.64 (d, J = 5.9 Hz, 1H), 4.56 (dd, J = 6.0, 1.1 Hz, 1H), 4.35 (ddd, J = 8.8, 6.4, 1.0 Hz, 1H), 3.34 (s, 3H), 2.68 (dddd, J = 15.4, 8.5, 6.6, 1.6 Hz, 1H), 2.58 (dtd, J = 15.2, 6.7, 1.5 Hz, 1H), 1.48 (s, 3H), 1.32 (s, 3H);

^{13}C NMR (151 MHz, $CDCl_3$): δ 193.6, 153.5, 134.8, 112.6, 109.8, 85.4, 85.3, 83.7, 54.7, 38.4, 26.5, 25.0;

HRMS (ESI+): calcd. for $[C_{12}H_{18}O_5Na]^+$ 265.1046, meas. 265.1062, Δ 6.0 ppm.

ALDEHYDE **5**

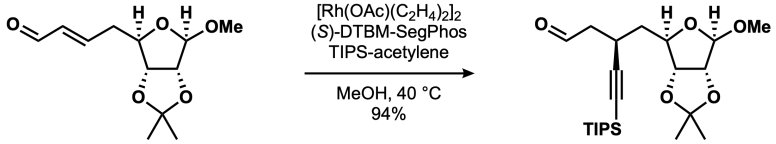

24 **25**

Aldehyde **25** was prepared using previously reported protocols.[8] A 250 mL flask was charged with $[Rh(OAc)(C_2H_4)_2]_2$ catalyst[9,10] (126 mg, 0.290 mmol, 2.5 mol %), (*S*)-DTBM-SegPhos (821 mg, 0.696 mmol, 6.0 mol %) and a large stir bar. The flask headspace was evacuated and backfilled with nitrogen (3 ×) and methanol was added (22 mL). The resulting orange suspension was stirred vigorously at RT until a red-orange solution was obtained (30 min). At this time, a solution of enal **24** (2.80 g, 11.6 mmol) in MeOH (10 mL) and TIPS-acetylene (5.18 mL, 23.1 mmol, 2.0 equiv.) were added sequentially to the reaction mixture. The resulting red mixture was stirred at 40 °C for 15 h and volatiles were removed *in vacuo*. Crude material was purified by silica gel chromatography (hexanes/EtOAc, 0 → 50%) to afford aldehyde **25** (4.60 g, 10.8 mmol, 94%) as a single diastereomer, as a light yellow oil.

R_f = 0.42 (cyclohexane/EtOAc, 75:25);

FTIR (thin-film), cm^{-1}: ν_{max} 2941, 2865, 2722, 2167, 1728, 1463, 1381, 1371, 1271, 1241, 1210, 1193, 1160, 1093, 1058, 1018;

---

[8] Nishimura, T.; Sawano, T.; Hayashi, T. *Angew. Chem. Int. Ed.* **2009**, *48*, 8057–8059.

[9] Werner, H.; Poelsma, S.; Schneider, M. E.; Windmüller, B.; Barth, D. *Chem. Ber.* **1996**, *129*, 647–652.

[10] $[RhCl(C_2H_4)_2]_2$, CAS: 12081-16-2, was obtained from Strem Chemicals, Inc. (catalog #: 45-0270).

^{1}H NMR (600 MHz, $CDCl_3$): δ 9.82 (t, J = 2.1 Hz, 1H), 4.95 (s, 1H), 4.61 (dd, J = 5.9, 1.2 Hz, 1H), 4.58 (d, J = 5.9 Hz, 1H), 4.49 (ddd, J = 10.6, 4.2, 1.2 Hz, 1H), 3.35 (s, 3H), 3.16 (dtd, J = 11.2, 6.9, 3.9 Hz, 1H), 2.60 (ddd, J = 16.5, 7.5, 2.2 Hz, 1H), 2.55 (ddd, J = 16.5, 6.4, 2.1 Hz, 1H), 1.74 (ddd, J = 13.3, 10.6, 4.0 Hz, 1H), 1.64 (ddd, J = 13.2, 11.1, 4.2 Hz, 1H), 1.47 (s, 3H), 1.31 (s, 3H), 1.11 – 0.97 (m, 21H);

^{13}C NMR (151 MHz, $CDCl_3$): δ 200.7, 112.6, 109.9, 108.6, 85.5, 85.3, 84.5, 84.2, 55.4, 49.0, 40.7, 26.7, 25.4, 25.1, 18.7, 11.3;

HRMS (ESI+): calcd. for $[C_{23}H_{40}O_5SiNa]^+$ 447.2537, meas. 447.2527, Δ 2.3 ppm.

Iodide **26**

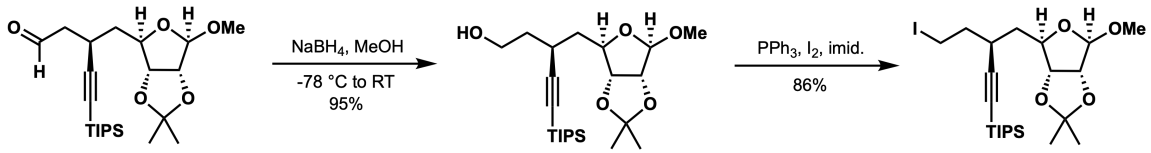

25 **S2** **26**

Part 1: To a solution of aldehyde **25** (5.50 g, 12.9 mmol) in MeOH (100 mL) at –78 °C was added $NaBH_4$ (588 mg, 15.5 mmol, 1.2 equiv.) portionwise. The reaction mixture was allowed to warm to 0 °C over 1 h, then was warmed to RT and stirred for 1 h. Volatiles were removed *in vacuo*. The residue was partitioned between CH_2Cl_2 (30 mL) and a NH_4Cl sat. aq. solution (25 mL). The layers were separated and the aqueous phase was extracted with CH_2Cl_2 (3 × 25 mL). The combined organic extracts were dried over $MgSO_4$ and filtered over a silica plug to yield crude alcohol **S2** as a yellow oil (5.29 g, 12.4 mmol, 95%) which was of suitable purity to be used in the next step without further purification.[11]

---

[11] While the protocol reported here was performed on purified starting material, it was found that direct treatment of the rhodium-catalyzed conjugate alkynylation reaction mixture with $NaBH_4$ at 0 °C reliably generated alcohol **S2** in > 90% yield over two steps (alkynylation/reduction).

R_f = 0.28 (hexanes/EtOAc, 67:33);

FTIR (thin-film), cm^{-1}: ν_{max} 3424, 2936, 2891, 2864, 2163, 1463, 1377, 1372, 1347, 1272, 1242, 1211, 1193, 1161, 1104, 1092, 1057, 1019;

^{1}H NMR (600 MHz MHz, $CDCl_3$): δ 4.95 (s, 1H), 4.63 (dd, *J* = 6.0, 1.2 Hz, 1H), 4.59 (d, *J* = 5.9 Hz, 1H), 4.48 (ddd, *J* = 10.3, 4.6, 1.2 Hz, 1H), 3.88–3.80 (m, 2H), 3.33 (s, 3H), 2.83 (dddd, *J* = 10.9, 9.3, 5.2, 4.0 Hz, 1H), 1.80–1.62 (m, 5H), 1.47 (s, 3H), 1.31 (s, 3H), 1.10–1.00 (m, 21H);

^{13}C NMR (151 MHz MHz, $CDCl_3$): δ 112.5, 110.6, 109.7, 85.6, 84.5, 83.3, 61.2, 55.2, 41.2, 38.5, 27.4, 26.7, 25.4, 18.8, 11.3;

HRMS (ESI+): calcd. for $[C_{23}H_{43}O_5Si_1]^+$ 427.2874, meas. 427.2870, Δ 0.9 ppm.

Part 2: To a stirred solution of imidazole (5.172 g, 76.0 mmol, 6.10 equiv.) in CH_2Cl_2 (100 mL) at RT under N_2 was added triphenylphosphine (8.97 g, 34.2 mmol, 2.75 equiv) followed by I_2 (9.64 g, 38.0 mmol, 3.10 equiv). Next, a solution of alcohol **S2** (5.287 g, 12.4 mmol, 1.00 equiv) in CH_2Cl_2 (50 mL) was added by syringe. The mixture was stirred for 3 h. Saturated sodium bisulfite (100 mL) and sat. NaHCO3 (50 mL) were added to the mixture, the aqueous layers were extracted with DCM (3 x 100 mL), and the resulting organic layers were washed sequentially with sat. $NaHCO_3$ (70 mL) and sat. NaCl (50 mL). The combined organic layers were dried with $MgSO_4$, filtered, concentrated *in vacuo*, and purified by silica gel chromatography (hexanes/EtOAc, 0 → 20%) to yield the iodide **26** as a colorless oil (5.624 g, 10.48 mmol, 86 %). A small amount of **26** was desilyated with TBAF/THF to yield desilylated **26**. This compound (data not shown) was found to crystallize when stored as a neat oil at -20 °C for several weeks. Crystals of desilylated **26** were of suitable quality for X-ray crystallographic analysis. The crystal structure of desilylated **26** presented in section 2.9.8 confirmed the absolute stereochemistry of the 6'-alkynyl stereocenter.

R_f = 0.46 (hexanes/EtOAc, 85:15);

FTIR (neat), cm^{-1}: ν_{max} 2936, 2891, 2863, 2164, 1462, 1438, 1381, 1372, 1271, 1240, 1227, 1212, 1192,

1161, 1141, 1099, 1060, 1037, 1016;

^{1}H NMR (600 MHz, $CDCl_3$): δ 4.96 (s, 1H), 4.63 (dd, J = 5.9, 1.1 Hz, 1H), 4.59 (d, J = 5.9 Hz, 1H), 4.48 (ddd, J = 10.0, 5.3, 1.1 Hz, 1H), 3.42 – 3.37 (m, 1H), 3.36 (s, 4H), 2.86 (tt, J = 9.5, 5.4 Hz, 1H), 1.97 – 1.91 (m, 2H), 1.71 – 1.62 (m, 2H), 1.47 (s, 3H), 1.34 – 1.30 (m, 3H), 1.12 – 0.99 (m, 21H);

^{13}C NMR (151 MHz, $CDCl_3$): δ 114.99, 112.33, 111.35, 88.12, 88.01, 87.04, 86.35, 57.94, 43.18, 41.99, 34.05, 29.20, 27.96, 21.31, 13.84, 6.41;

Schöllkopf Product **28**

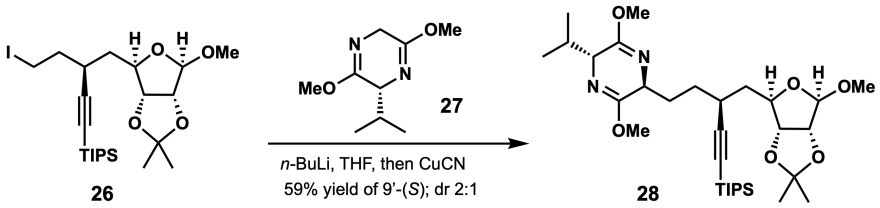

To a stirring solution of Schöllkopf reagent **27** ((*R*)-2-isopropyl-3,6-dimethoxy-2,5-dihydropyrazine, 2.288 g, 12.42 mmol, 3.0 equiv) in 10 mL THF at -78 °C under N_2 was added a solution of *n*-butyllithium (4.65 mL, 12.00 mmol, 2.9 equiv, 2.58 M in hexanes) dropwise and the resulting yellow solution was allowed to stir for 10 min. Copper (I) cyanide (556 mg, 6.21 mmol, 1.5 equiv) was added at once via solid addition tube and stirred for 5 min at 0 °C to form the cyanocuprate as a tan colored solution before being cooled back down to -78 °C. A solution of iodide **26** was added dropwise as a solution in 5 mL THF. The reaction mixture was stirred for 20 h at -78 °C under N_2. The reaction was quenched with a 1:9 mixture of NH_4OH/sat. NH_4Cl (20 mL), the layers were separated, and the aqueous phase was further extracted with MTBE (3 x 30 mL). The organic layers were combined and washed with the 1:9 mixture of NH_4OH/sat. NH_4Cl (20 mL), brine (30 ml), and then dried with $MgSO_4$, filtered, and concentrated in vacuo. ^{1}H analysis of the crude product revealed a 2:1 mixture of the desired *S*:undesired *R* isomers at the amino acid stereocenter. Crude material was purified by silica gel chromatography (hexanes/EtOAc, 0 $\rightarrow$ 30%) to yield the desired

28 *S* isomer (which elutes first) as a light-yellow oil (1.45 g, 2.44 mmol, 59%).

$\mathbf{R_f}$ = 0.56 (hexanes/EtOAc, 75:25);

^{1}H NMR (600 MHz, $CDCl_3$): δ 4.94 (s, 1H), 4.66 – 4.63 (m, 1H), 4.58 (d, J = 6.0 Hz, 1H), 4.45 (dd, J = 10.1, 4.9 Hz, 1H), 4.04 (dt, J = 7.4, 3.9 Hz, 1H), 3.92 (t, J = 3.5 Hz, 1H), 3.67 (s, 3H), 3.65 (s, 3H), 3.31 (s, 3H), 2.67 – 2.57 (m, 1H), 2.30 – 2.20 (m, 1H), 2.03 – 1.88 (m, 1H), 1.69 – 1.57 (m, 2H), 1.52 – 1.47 (m, 1H), 1.46 (s, 3H), 1.43 – 1.34 (m, 1H), 1.31 (s, 3H), 1.09 – 1.00 (m, 21H);

^{13}C NMR (151 MHz, $CDCl_3$): δ 163.81, 163.45, 112.24, 110.77, 109.52, 109.49, 85.71, 85.50, 84.38, 82.28, 77.25, 77.20, 77.00, 76.75, 60.70, 54.89, 52.27, 52.25, 41.19, 31.97, 31.72, 30.75, 29.89, 26.55, 25.27, 19.04, 18.65, 16.55, 11.25;

Fmoc Intermediate **29**

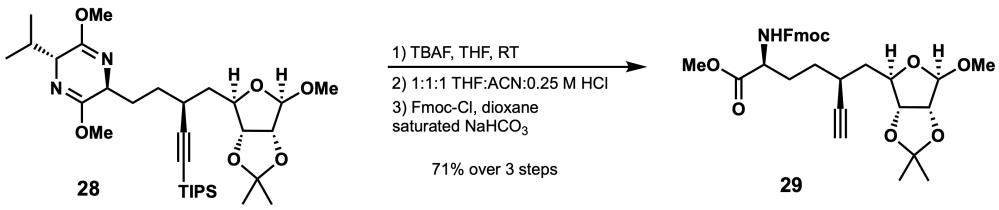

To a vial containing 156 mg compound **28** (0.263 mmol) in THF (1 mL) was added TBAF solution (1 M in THF, 0.526 mmol, 2.0 equiv.) and the reaction mixture was stirred at RT for 3 hours until TLC showed complete disappearance of starting material and clean conversion to a lower R_f spot. The reaction was then quenched by addition of saturated NH_4Cl (3 mL) and extracted with Et_2O (4 X 4 mL). Combined organic layers were dried over $MgSO_4$ and concentrated *in vacuo*. The crude material was used immediately in the next step without further purification.

To the crude material from Step 1 was added 1 mL 0.25 M HCl, 1 mL THF, and 1 ml MeCN. The solution was stirred rapidly at RT for 4.5 h, after which time TLC indicated complete disappearance of starting

material (indicating cleavage of the Schollkopf auxiliary). At this time, volatiles were removed *in vacuo* and the crude residue was dried once by azeotropic distillation with benzene (5 mL). To the crude mixture was added 2 mL dioxane followed by 2 mL saturated $NaHCO_3$ and the mixture cooled to 0 °C. A solution of Fmoc-Cl in dioxane (180 mg in 0.7 mL, 0.70 mmol, 2.65 equiv.) was added dropwise by syringe over 5 min. The mixture was set to stir for 30 min and then 2 mL H2O was added and the mixture was warmed to RT and extracted with 50/50 Et_2O/EtOAc (4 X 5 mL). Combined organic layers were dried over $MgSO_4$, solvent was removed *in vacuo*, and the crude reaction product purified by silica gel chromatography (2,2,4-trimethylpentane/EtOAc, 0 → 100%) to afford Fmoc-protected amino acid compound **29** (105 mg, 0.187 mmol, 71% over 3 steps) as an amorphous white solid.

R_f = 0.56 (cyclohexane/EtOAc, 50:50);

FTIR (thin film), cm^{-1}: ν_{max} 3300, 2987, 2947, 1723, 1526, 1447, 1377, 1341, 1212, 1163, 1099, 1061;

^{1}H NMR (500 MHz, $CDCl_3$): δ 7.77 (dq, *J* = 7.5, 1.0 Hz, 2H), 7.60 (t, *J* = 6.8 Hz, 2H), 7.40 (tq, *J* = 7.4, 1.0 Hz, 2H), 7.32 (tt, *J* = 7.5, 1.4 Hz, 2H), 5.31 (d, *J* = 8.5 Hz, 1H), 4.94 (s, 1H), 4.58 (q, *J* = 6.0 Hz, 2H), 4.48 (dd, *J* = 11.1, 4.0 Hz, 1H), 4.46–4.33 (m, 3H), 4.23 (t, *J* = 7.1 Hz, 1H), 3.77 (s, 3H), 3.31 (s, 3H), 2.66–2.60 (m, 1H), 2.14 (d, *J* = 2.3 Hz, 1H), 2.06–1.95 (m, 1H), 1.95–1.85 (m, 1H), 1.69 (ddd, *J* = 14.8, 11.2, 4.0 Hz, 1H), 1.58 (ddd, *J* = 16.3, 12.3, 4.7 Hz, 2H), 1.52fz (m, 1H), 1.49 (s, 3H), 1.31 (s, 3H);

^{13}C NMR (126 MHz, $CDCl_3$): δ 172.9, 156.1, 144.0, 143.8, 141.4, 127.8, 127.2, 125.2, 125.1, 120.1, 112.4, 110.1, 110.1, 85.6, 85.1, 84.5, 71.4, 67.2, 55.3, 53.8, 52.6, 47.3, 40.4, 31.1, 30.5, 28.7, 26.6, 25.1;

HRMS (ESI+): calcd. for $[C_{32}H_{37}N_1O_8Na]^+$ 586.2411, meas. 586.2407, Δ 0.8 ppm.

Triacetate **30**

29 **30**

To a vial charged with acetonide **29** (43 mg, 76 μmol) was added a 4:1 mixture of acetic acid and water (3.5 mL) at RT. The resulting mixture was stirred at 80 °C for 10 h. Volatiles were removed *in vacuo* and the residue was dried by azeotropic distillation with benzene (2 × 1.0 mL). Crude material was used directly in the next step without further purification.

To a solution of the crude triol in CH_2Cl_2 (3.5 mL) at RT, were added pyridine (60 μL, 0.76 mmol, 10 equiv.), Ac_2O (70 μL, 0.76 mmol, 10 equiv.) and DMAP (7 mg, 53 μmol, 0.70 equiv.) sequentially. The resulting mixture was stirred at RT for 2 h and volatiles were removed *in vacuo*. Crude material was purified by silica gel chromatography (2,2,4-trimethylpentane/EtOAc, 5 → 60%) to afford triacetate **30** (42 mg, 66 μmol, 87% over 2 steps) as a 1:1 mixture of diastereomers, as a colorless oil.

R_f = 0.30/0.38 (hexanes/EtOAc, 50:50);

FTIR (thin film), cm^{-1}: ν_{max} 3355, 3294, 2954, 2924, 2853, 1744, 1722, 1526, 1451, 1372, 1218, 1107, 1050, 1012;

^{1}H NMR (500 MHz, $CDCl_3$): δ 7.78–7.75 (m, 4H), 7.63–7.58 (m, 4H), 7.42–7.38 (m, 4H), 7.34–7.29 (m, 4H), 6.36 (d, J = 4.6 Hz, 1H), 6.14 (d, J = 1.0 Hz, 1H), 5.38 (br d, J = 8.5 Hz, 1H), 5.34 (br d, J = 8.4 Hz, 1H), 5.32 (dd, J = 4.8, 1.0 Hz, 1H), 5.23 (dd, J = 6.8, 4.6 Hz, 1H), 5.18 (dd, J = 7.1, 4.8 Hz, 1H), 5.07 (dd, J = 6.8, 3.6 Hz, 1H), 4.46 (app dt, J = 10.2, 3.6 Hz, 1H), 4.42–4.36 (m, 7H), 4.23 (app t, J = 7.0 Hz, 2H), 3.76 (s, 6H), 2.69–2.57 (m, 2H), 2.13 (d, J = 2.4 Hz, 1H), 2.12 (d, J = 2.4 Hz, 1H), 2.12 (s, 3H), 2.11 (s, 3H), 2.10 (s, 3H), 2.07 (s, 6H), 2.06 (s, 3H), 2.00–1.75 (m, 6H), 1.70–1.43 (m, 6H);

^{13}C NMR (126 MHz, $CDCl_3$): δ 172.9, 172.8, 170.2, 170.0, 169.8, 169.6, 169.5, 169.3, 156.1, 156.0, 144.0,

144.0, 143.9, 143.8, 141.4, 141.4, 127.8, 127.2, 125.2, 120.1, 120.1, 98.5, 93.9, 85.3, 85.1, 81.4, 79.9, 74.6, 73.9, 72.6, 71.5, 71.3, 69.9, 67.1, 53.8, 53.7, 52.6, 47.3, 40.1, 39.2, 31.0, 30.4, 30.3, 28.6, 28.2, 21.2, 21.2, 20.8, 20.7, 20.7, 20.4;

HRMS (ESI+): calcd. for $[C_{34}H_{37}N_1O_{11}Na]^+$ 658.2259, meas. 658.2248, Δ 1.7 ppm.

Nucleoside **31**

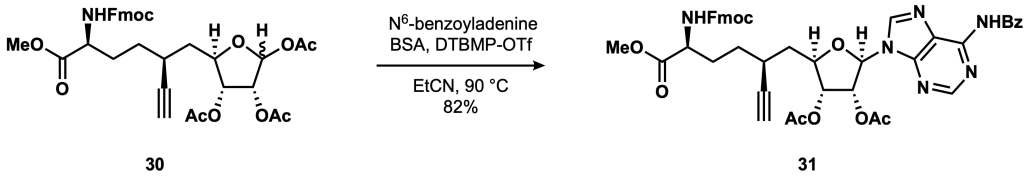

30 **31**

To a suspension of N^6-benzoyladenine (63 mg, 0.26 mmol, 4.0 equiv.) in propionitrile (dried over 4 Å M.S., 1.5 mL) at RT, was added *N*,*O*-bis(trimethylsilyl)acetamide (80 μL, 0.33 mmol, 5.0 equiv.). The resulting mixture was stirred at 80 °C for 10 min, upon which complete solubilization of N^6-benzoyladenine was observed. To a separate flask charged with triacetate **30** (dried by azeotropic distillation with benzene (4 ×), 42 mg, 66 μmol) and 2,6-di-*tert*-butyl-4-methylpyridinium triflate (12 mg, 33 μmol, 50 mol %) was added propionitrile (1.5 mL). The resulting mixture was stirred at RT for 5 min, until a clear solution was obtained, and the solution of silylated N^6-benzoyladenine was added. The reaction mixture was stirred at 90 °C for 4 h, cooled to RT and the volatiles were removed *in vacuo*. Crude material was purified by silica gel chromatography (2,2,4-trimethylpentane/EtOAc, 30 → 100%) to afford nucleoside **31** (44 mg, 54 μmol, 82%) as a colorless oil.

$\mathbf{R_f}$ = 0.49 (EtOAc);

FTIR (thin film), cm^{-1}: ν_{max} 3300, 2953, 2926, 2854, 1745, 1704, 1610, 1582, 1510, 1452, 1241, 1217, 1098, 1073, 1047;

^{1}H NMR (500 MHz, $CDCl_3$): δ 8.79 (s, 1H), 8.13 (s, 1H), 8.02–7.97 (m, 2H), 7.76–7.72 (m, 2H), 7.62–7.57 (m, 3H), 7.53–7.49 (m, 2H), 7.40–7.35 (m, 2H), 7.31–7.27 (m, 2H), 6.13 (br d, J = 5.5 Hz, 1H), 6.05 (br t, J = 5.5 Hz, 1H), 5.55 (br t, J = 5.0 Hz, 1H), 5.35 (br d, J = 8.4 Hz, 1H), 4.54–4.48 (m, 1H), 4.46–4.35 (m, 3H), 4.23 (br t, J = 7.1 Hz, 1H), 3.74 (s, 3H), 2.67–2.58 (m, 1H), 2.16 (s, 3H), 2.15 (d, J = 2.4 Hz, 1H), 2.12–2.05 (m, 1H), 2.07 (s, 3H), 2.00–1.92 (m, 1H), 1.92–1.80 (m, 2H), 1.64–1.45 (m, 2H);

^{13}C NMR (126 MHz, $CDCl_3$): δ 172.8, 169.8, 169.6, 164.8, 156.1, 152.8, 151.7, 149.8, 144.0, 143.8, 142.3, 141.4, 133.5, 133.0, 129.0, 128.0, 127.8, 127.2, 125.2, 123.9, 120.1, 87.1, 85.1, 80.9, 73.7, 73.0, 71.6, 67.1, 53.6, 52.6, 47.3, 38.5, 31.0, 30.5, 28.0, 20.8, 20.5;

HRMS (ESI+): calcd. for $[C_{44}H_{43}N_6O_{10}]^+$ 815.3035, meas. 815.3028, Δ 0.9 ppm.

Benzamide **32**

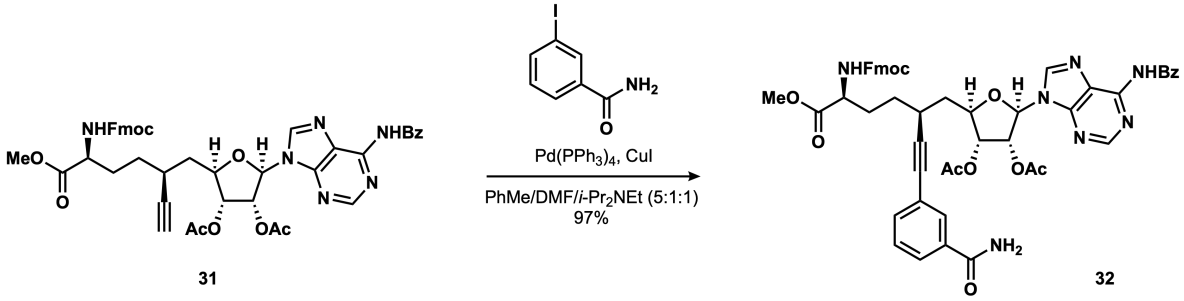

To a vial charged with nucleoside **31** (61 mg, 75 μmol) were added 2-iodobenzamide (46 mg, 0.19 mmol, 2.5 equiv.), CuI (4 mg, 0.02 mmol, 25 mol %) and $Pd(PPh_3)_4$ (4 mg, 4 μmol, 5 mol %). The vial headspace was purged with nitrogen for 10 min and a 5:1:1 mixture of toluene, DMF and *i*-Pr_2NEt (degassed by sparging with nitrogen for 15 min, 2.5 mL) was added at RT. The resulting mixture was stirred at 60 °C for 2 h. The solution was allowed to cool to RT and volatiles were removed *in vacuo*. Crude material was purified by silica gel chromatography (EtOAc/*i*-PrOH, 0 → 25%) to afford benzamide **32** (68 mg, 73 μmol, 97%) as a light yellow oil.

FTIR (thin film), cm^{-1}: ν_{max} 3357, 3070, 2951, 2928, 1746, 1703, 1669, 1613, 1582, 1520, 1452, 1376, 1245, 1219, 1103, 1080, 1050;

^{1}H NMR (500 MHz, $CDCl_3$): δ 8.78 (s, 1H), 8.36 (s, 1H), 8.01 (br d, J = 7.7 Hz, 2H), 7.90–7.86 (m, 1H), 7.77 (dt, J = 7.9, 1.5 Hz, 1H), 7.74–7.69 (m, 2H), 7.63–7.58 (m, 1H), 7.57–7.52 (m, 3H), 7.52–7.48 (m, 2H), 7.39–7.33 (m, 3H), 7.28–7.24 (m, 2H), 6.92 (br s, 1H), 6.82 (br s, 1H), 6.17 (br d, J = 5.8 Hz, 1H), 6.10 (br t, J = 5.8 Hz, 1H), 5.71–5.65 (m, 1H), 5.51 (br d, J = 8.3 Hz, 1H), 4.56–4.50 (m, 1H), 4.49–4.41 (m, 1H), 4.41–4.32 (m, 2H), 4.18 (br t, J = 7.0 Hz, 1H), 3.75 (s, 3H), 2.89–2.80 (m, 1H), 2.16 (s, 3H), 2.19–2.12 (m, 1H), 2.06 (s, 3H), 2.12–2.02 (m, 2H), 1.99–1.89 (m, 1H), 1.74–1.64 (m, 1H), 1.64–1.54 (m, 1H);

^{13}C NMR (126 MHz, $CDCl_3$): δ 172.8, 170.3, 170.2, 169.8, 165.6, 156.2, 152.0, 151.8, 149.4, 143.9, 143.7, 143.3, 141.4, 135.2, 133.5, 132.6, 131.1, 129.0, 128.9, 128.4, 127.9, 127.9, 127.4, 127.2, 127.2, 125.1, 123.9, 123.3, 120.1, 92.0, 87.1, 82.9, 81.7, 73.8, 72.9, 67.2, 53.6, 52.8, 47.2, 38.6, 31.1, 30.5, 28.8, 20.8, 20.5;

HRMS (ESI+): calcd. for $[C_{51}H_{47}N_7O_{11}Na]^+$ 956.3226, meas. 956.3214, Δ 1.2 ppm.

NS1 (**33**)

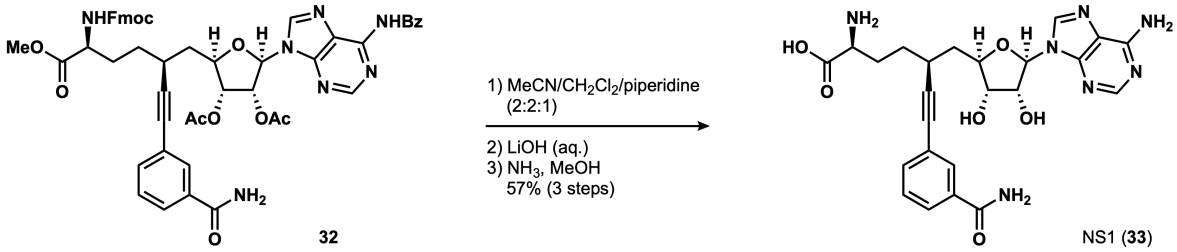

To a solution of fully protected Fmoc NS1 **32** (32 mg, 34 μmol) in a 1:1 mixture of MeCN and CH_2Cl_2 (2.0 mL) at RT, was added piperidine (0.50 mL). The resulting mixture was stirred for 20 min and volatiles were removed *in vacuo*. The residue was dissolved in THF (1.0 mL) and 1 mL of a 0.5 M LiOH aq. solution was added. The resulting mixture was stirred for 2.5 h, cooled to 0 °C and a 10% AcOH aq. solution was added dropwise until pH 7 was reached. Volatiles were removed *in vacuo*. The residue was dissolved in a solution

of ammonia in methanol (7 N, 3 mL) at RT. The resulting mixture was stirred for 18 h and the volatiles were removed *in vacuo*. Crude material was purified by preparative HPLC using a Kromasil® C18 column (gradient elution: 5→45 %B over 40 min, 45→95 %B over 20 min, flow rate 10 mL/min, UV detection at 254 nm) to afford NS1 (**33**, 12 mg, 19 μmol, 57%) as the TFA salt.

^{1}H NMR (600 MHz, **CD_3CN** (350 μL)/D_2O (350 μL)/*d*-TFA (40 μL)): δ 8.37 (s, 1H), 8.34 (s, 1H), 7.78 (td, *J* = 1.8, 0.6 Hz, 1H), 7.72 (ddd, *J* = 7.8, 1.9, 1.2 Hz, 1H), 7.52 (dt, *J* = 7.8, 1.4 Hz, 1H), 7.40 (td, *J* = 7.8, 0.6 Hz, 1H), 6.01 (d, *J* = 5.1 Hz, 1H), 4.74 (t, *J* = 5.1 Hz, 1H), 4.38 (ddd, *J* = 10.3, 4.4, 3.2 Hz, 1H), 4.23 (t, *J* = 4.8 Hz, 1H), 4.02 (dd, *J* = 6.6, 5.8 Hz, 1H), 2.81 (ddt, *J* = 10.6, 9.1, 4.5 Hz, 1H), 2.17 (dddd, *J* = 14.4, 11.5, 6.7, 4.5 Hz, 1H), 2.10–1.97 (m, 2H), 1.95–1.89 (m, 1H), 1.81–1.72 (m, 1H), 1.61–1.52 (m, 1H);

^{13}C NMR (101 MHz, **CD_3CN** (350 μL)/D_2O (350 μL)/*d*-TFA (40 μL)): δ 172.1, 171.3, 151.0, 149.4, 145.2, 144.1, 135.8, 134.4, 131.6, 129.9, 128.1, 124.5, 120.1, 92.8, 90.0, 83.9, 83.4, 74.8, 74.5, 53.5, 38.9, 30.9, 29.6, 28.7;

HRMS (ESI+): calcd. for $[C_{24}H_{28}N_7O_6]^+$ 510.2096, meas. 510.2082, Δ 2.6 ppm.

2.9.7 **NS1**, Second-Generation Route

Alkyne **34**

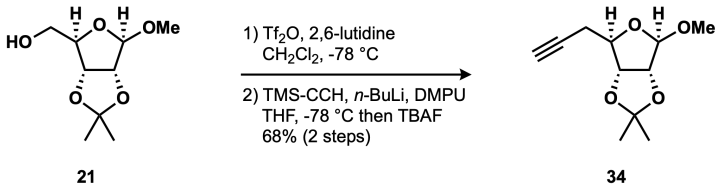

21 **34**

To a stirred solution of 2,6-lutidine in dry CH_2Cl_2 (130 mL) at –78 °C was added Tf_2O (13.7 mL, 81.4 mmol, 1.06 equiv.) over 5 min (flask A, 1 L rbf), followed by the addition of a solution of alcohol **21** (15.7 g, 76.9 mmol) in dry CH_2Cl_2 (33 mL) over 10 min. The mixture was stirred at –78 °C for 2 h and warmed to 0 °C. Meanwhile, to a separate flask (flask B, 500 mL rbf) containing a solution of TMS-acetylene (32.9

mL, 231 mmol, 3.00 equiv.) in dry THF (130 mL) at –78 °C was added *n*-BuLi (2.56 M in hexanes, 93.7 mL, 240 mmol, 3.12 equiv.) at a rate of 5 mL/min *via* syringe. The resulting mixture was stirred at –78 °C for 1.5 h and warmed to 0 °C. While the contents of flask B remained at 0 °C, flask A was removed from the ice/water bath, volatiles were removed *in vacuo* (bath temperature set to 20 °C) and a brief subjection to high vacuum yielded a red-orange paste. The crude triflate in flask A was resuspended in dry THF (65 mL) and DMPU (35 mL) was added. The contents were stirred vigorously for 10 min until complete solubilization was noted and cooled to –78 °C. The contents of flask B were cooled to –78 °C and transferred to flask A *via* cannula. The resulting mixture was stirred at –78 °C for 1 h and at –12 °C for 3 h (NaCl/ice bath), before the slow addition of TBAF (⚠ **Caution, gas evolution** ⚠, 1.0 M in THF, 250 mL, 250 mmol, 3.25 equiv.) *via* cannula. The mixture was allowed to warm to RT and was stirred for another 30 min before removing the volatiles *in vacuo*. The reddish-brown residue was resuspended in MTBE (350 mL) and a NH_4Cl sat. aq. solution (300 mL) was added. The layers were roughly separated and the organic phase, largely emulsified, was filtered through a pad of $CaCO_3$/celite to give two clear layers in the filtrate. The layers were separated and the combined aqueous phases were extracted with MTBE (2 × 200 mL) and EtOAc (200 mL). The combined organic extracts were washed with a 5% LiCl aq. solution (800 mL) and then with brine (800 mL), dried over $MgSO_4$, filtered and concentrated. The crude residue was purified by dry column vacuum chromatography[12] (cyclohexane/EtOAc, 0 → 30%) to yield pure material as well as semi-pure residue which was repurified by silica gel chromatography (hexanes/EtOAc, 0 → 30%). Alkyne **34** (11.1 g, 52.3 mmol, 68%) was obtained as a light yellow oil.

R_f = 0.60 (hexanes/EtOAc, 67:33);

FTIR (neat), cm^{-1}: ν_{max} 3286, 2989, 2938, 2835, 1438, 1209, 1090, 1053, 1041;

^{1}H NMR (600 MHz, $CDCl_3$): δ 4.95 (s, 1H), 4.69 (d, J = 5.9 Hz, 1H), 4.60 (d, J = 5.9 Hz, 1H), 4.30 (dd, J = 9.3, 6.6 Hz, 1H), 3.32 (s, 3H), 2.52 (ddd, J = 16.7, 6.6, 2.7 Hz, 1H), 2.42 (ddd, J = 16.6, 9.4, 2.7 Hz, 1H), 2.04 (t, J = 2.7 Hz, 1H), 1.46 (s, 3H), 1.31 (s, 3H);

[12] Pedersen, D. S.; Rosenbohm, C. *Synthesis* **2001**, 2431–2434.

^{13}C NMR (126 MHz, $CDCl_3$): δ 112.33, 109.56, 85.17, 85.09, 83.28, 80.17, 70.38, 54.69, 26.35, 24.93, 24.62;

HRMS (ESI+): calcd. for $[C_{11}H_{16}O_4Na]^+$ 235.0941, meas. 235.0938, Δ 1.0 ppm.

Alkene **3**

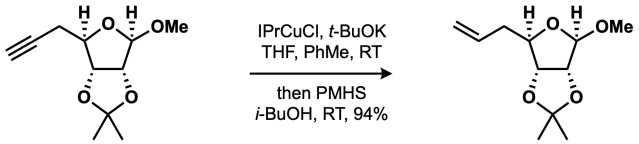

34 **35**

Terminal alkyne **34** (10.6 g, 50 mmol) was reduced according to previously reported protocols.[13] Crude material was purified by silica gel chromatography (hexanes/EtOAc, 0 $\rightarrow$ 30%) to afford alkene **35** (9.97 g, 46.5 mmol, 94%) as a clear, viscous oil. The flash column chromatography removed ca. 98% of PHMS, yielding material that was suitable for use in subsequent reactions. An analytically pure sample was prepared by subjecting 2.0 g of the post-column material to short path distillation (Kugelrohr) at 130 and 200 mTorr.

R_f = 0.50 (hexanes/EtOAc, 80:20);

FTIR (neat), cm^{-1}: ν_{max} 3078, 2987, 2938, 2833, 1643, 1381, 1372, 1209, 1193, 1105, 1090, 1059, 1031;

^{1}H NMR (600 MHz, $CDCl_3$): δ 5.82 (dddd, J = 16.7, 10.3, 7.4, 6.2 Hz, 1H), 5.15–5.09 (m, 2H), 4.96 (s, 1H), 4.61 (d, J = 5.9 Hz, 1H), 4.57 (dd, J = 6.0, 1.0 Hz, 1H), 4.23 (td, J = 7.8, 1.0 Hz, 1H), 3.34 (s, 3H), 2.46–2.38 (m, 1H), 2.32–2.24 (m, 1H), 1.48 (s, 3H), 1.31 (s, 3H);

^{13}C NMR (126 MHz, $CDCl_3$): δ 134.5, 117.7, 112.4, 109.6, 86.6, 85.7, 83.6, 55.0, 39.6, 26.6, 25.2;

---

[13] Cox, N.; Dang, H.; Whittaker, A. M.; Lalic, G. *Org. Synth.* **2016**, *93*, 385–400.

HRMS (ESI+): calcd. for $[C_{11}H_{18}O_4Na]^+$ 237.1095, meas. 237.1097, Δ 1.0 ppm.

Enal **24**

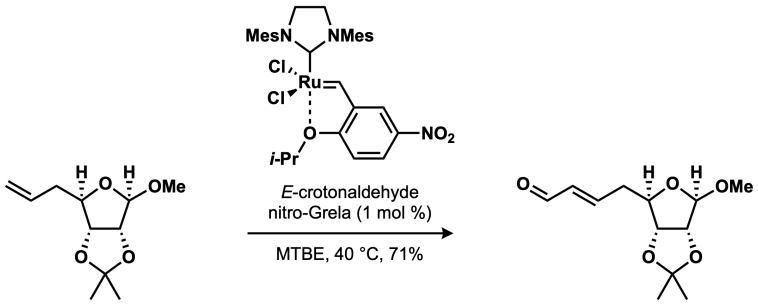

35 **24**

To a solution of alkene **35** (2.0 g, 9.3 mmol) in degassed MTBE (28 mL) at RT, were added *E*-crotonaldehyde (3.9 mL, 47 mmol, 5.0 equiv.) and nitro-Grela metathesis catalyst[14] (63 mg, 93 μmol, 1 mol %) sequentially. The flask headspace was purged with nitrogen for 10 min and the mixture was stirred at 40 °C for 48 h, at which point TLC analysis indicated *ca.* 50% conversion. More nitro-Grela catalyst (63 mg, 93 μmol, 1 mol %) and *E*-crotonaldehyde (3.9 mL, 47 mmol, 5.0 equiv.) were added and the reaction mixture was stirred at 40 for another 24 h, at which point complete conversion was indicated by TLC analysis. Volatiles were removed *in vacuo* and crude material was purified by silica gel chromatography (hexanes/EtOAc, 2 → 50%) to afford enal **24** (1.60 g, 6.60 mmol, 71%) as a yellow oil. Characterization data were identical to those reported for this same compound in the First-Generation NS1 Synthesis.

---

[14] Nitro-Grela catalyst, [1,3-bis(2,4,6-trimethylphenylimidazolidin-2-ylidene)]-(2-*i*-propoxy-5-nitrobenzylidene)ruthenium(II) dichloride, CAS: 502964-52-5, was obtained from Strem Chemicals, Inc. (Catalog #: 44-0758).

PHOSPHONATE **36**[15]

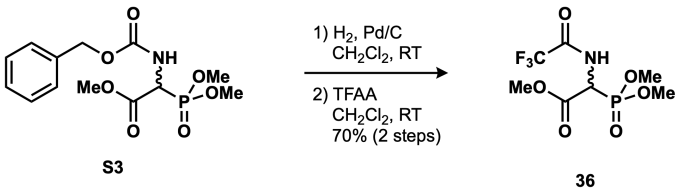

To a solution of (±)-Z-α-phosphonoglycine trimethyl ester[16] (**S3**) (3.31 g, 9.99 mmol) in CH_2Cl_2 (50 mL) at RT, was added Pd/C (10%, 0.53 g, 0.50 mmol, 5 mol %). The flask headspace was evacuated and refilled with hydrogen (3 ×) and the reaction mixture was stirred vigorously under a hydrogen atmosphere (balloon) for 24 h. The flask headspace was evacuated and refilled with nitrogen, and the contents were filtered through a pad of celite. The filtrate was cooled to 0 °C and TFAA (3.47 mL, 25.0 mmol, 2.5 equiv.) was added dropwise. The reaction mixture was stirred at RT for 12 h and the solution was concentrated to yield an orange residue. Crude material was purified by silica gel chromatography (hexanes/EtOAc, 0 → 100%) to afford TFA protected phosphonate **36** (2.05 g, 6.99 mmol, 70% over 2 steps).

R_f = 0.41 (EtOAc);

FTIR (thin film), cm^{-1}: ν_{max} 3197, 3046, 2964, 2861, 1757, 1722, 1559, 1433, 1360, 1307, 1257, 1212, 1180, 1150, 1035;

^{1}H NMR (600 MHz, $CDCl_3$): δ 7.23 (br s, 1H), 5.14 (dd, $^2J_{H\text{-}P}$ = 21.3, J = 8.7 Hz, 1H), 3.89 (s, 3H), 3.87 (d, $^3J_{H\text{-}P}$, J = 11.2 Hz, 3H), 3.83 (d, $^3J_{H\text{-}P}$, J = 11.1 Hz, 3H);

^{13}C NMR (126 MHz, $CDCl_3$): δ 165.5, 157.2 (qd, $^2J_{C\text{-}F}$ = 38 Hz, $^3J_{C\text{-}P}$ = 5.9 Hz), 115.7 (q, $^1J_{C\text{-}F}$ = 287 Hz), 54.5 (d, $^2J_{C\text{-}P}$ = 6.6 Hz), 54.1 (d, $^2J_{C\text{-}P}$ = 6.9 Hz), 53.3, 50.3 (d, $^1J_{C\text{-}P}$ = 152 Hz);

---

[15] Becerra-Figueroa, L.; Movilla, S.; Prunet, J.; Miscione, G. P.; Gamba-Sánchez, D. *Org. Biomol. Chem.* **2018**, *16*, 1277–1286.

[16] (±)-Z-α-phosphonoglycine trimethyl ester, CAS: 88568-95-0, was obtained from Chem-Impex International, (Catalog #: 14125).

^{19}F NMR (471 MHz, $CDCl_3$, BTF IStd): δ –76.5;

^{31}P NMR (162 MHz, $CDCl_3$): δ 16.1;

HRMS (ESI+): calcd. for $[C_7H_{12}F_3N_1O_6P_1]^+$ 294.0360, meas. 294.0349, Δ 3.7 ppm.

Enamide **37**

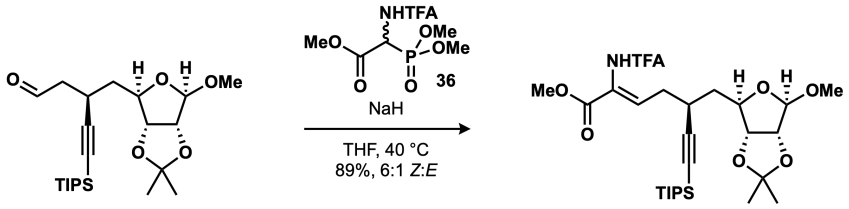

A solution of phosphonate **36** (3.10 g, 10.6 mmol, 1.5 equiv.) in THF (21 mL) was added dropwise over 20 min to a stirred suspension of NaH (95%, 254 mg, 10.6 mmol, 1.5 equiv.) in THF (10 mL) at 0 °C. The resulting cloudy mixture was stirred at 0 °C for 30 min and a solution of aldehyde **25** (3.00 g, 7.06 mmol) in THF (7.1 mL) was added over 5 min. The resulting mixture was allowed to warm gradually to RT and was stirred for 2 h, at which point the reaction mixture was heated to 40 °C and stirred for another 6 h. The mixture was allowed to cool to RT and volatiles were removed *in vacuo*. The residue was partitioned between MTBE (25 mL) and 1X PBS (15 mL). The mixture was stirred vigorously for 10 min and the layers were separated. The aqueous phase was extracted with MTBE (3 × 25 mL). The combined organic extracts were washed with brine (80 mL), dried over $MgSO_4$, filtered and concentrated. Crude material was purified by silica gel chromatography (hexanes/EtOAc, 0 → 30%) to yield enamide **37** (3.74 g, 6.32 mmol, 89%) as a 6:1 mixture of *Z* and *E* isomers as a light yellow oil.

R_f = 0.48 (hexanes/EtOAc, 67:33);

FTIR (neat), cm^{-1}: ν_{max} 3297, 2943, 2866, 1720, 1664, 1528, 1463, 1439, 1382, 1373, 1335, 1283, 1210,

1160, 1106, 1092, 1062, 1043, 1016;

^{1}H NMR (600 MHz, $CDCl_3$): δ *Z* isomer: 7.73 (s, 1H), 7.07 (t, *J* = 7.2 Hz, 1H), 4.94 (s, 1H), 4.61 (dd, *J* = 6.0, 1.1 Hz, 1H), 4.58 (d, *J* = 5.9 Hz, 1H), 4.44 (ddd, *J* = 10.4, 4.4, 1.1 Hz, 1H), 3.81 (s, 3H), 3.32 (s, 3H), 2.87 (ddd, *J* = 8.3, 5.5, 3.7 Hz, 1H), 2.40 (ddd, *J* = 15.8, 7.2, 5.1 Hz, 1H), 2.26 (ddd, *J* = 15.8, 8.7, 7.2 Hz, 1H), 1.71 (ddd, *J* = 13.3, 10.4, 4.2 Hz, 1H), 1.65 (ddd, *J* = 13.4, 10.8, 4.5 Hz, 1H), 1.46 (s, 3H), 1.30 (s, 3H), 1.06–1.02 (m, 21H);

^{13}C NMR (126 MHz, $CDCl_3$): δ *Z* isomer: 163.3, 155.1 (q, $^{2}J_{C\text{-}F}$ = 38 Hz), 138.3, 133.3, 123.8, 115.6 (q, $^{1}J_{C\text{-}F}$ = 288 Hz), 112.0, 109.4, 109.1, 85.2, 84.2, 83.7, 54.5, 52.2, 40.6, 34.4, 29.2, 26.2, 24.8, 18.3, 11.0;

^{19}F NMR (471 MHz, $CDCl_3$, BTF IStd): δ *Z* isomer: –76.4;

HRMS (ESI+): calcd. for $[C_{28}H_{44}F_3N_1O_7Si_1K]^+$ 630.2471, meas. 630.2462, Δ 1.4 ppm.

Protected Amino Acid **38**

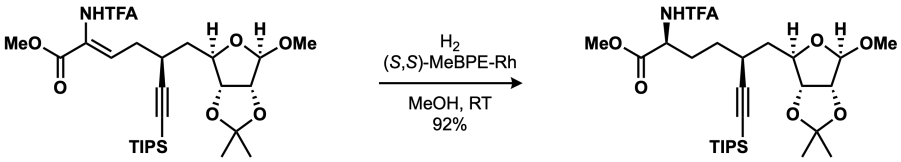

37 **38**

To a flask containing olefin **37** (300 mg, 0.507 mmol), as a 6:1 mixture of *Z* and *E* isomers, was added MeOH (20 mL) at RT under a nitrogen atmosphere. The contents were stirred until full dissolution was noted. Separately, (*S*,*S*)-MeBPE-Rh[17,18] (28 mg, 0.051 mmol, 10 mol %) was weighed out into a vial in a glove box.

---

[17] (*S*,*S*)-MeBPE-Rh catalyst, (-)-1,2-bis((2*S*,5*S*)-2,5-dimethylphospholano)ethane(1,5-cyclooctadiene)rhodium(I) tetrafluoroborate, CAS: 213343-65-8, was obtained from Strem Chemicals, Inc. (catalog #: 45-0169).

[18] The authors note that at times better results were obtained when the asymmetric hydrogenation catalyst was prepared freshly before use from $[Rh(nbd)_2]BF_4$ (CAS: 36620-11-8, obtained from Strem Chemicals, Inc. (catalog #: 45-0230)) and (*S*,*S*)-MeBPE ligand (CAS: 136779-26-5, obtained from Strem Chemicals, Inc. (catalog #: 15-0105)).

The vial was removed from the glove box, placed under a nitrogen atmosphere, and MeOH (10 mL) was added. The methanolic solution of (*S*,*S*)-MeBPE-Rh was transferred *via* syringe to the methanolic solution of olefin **37**. The flask headspace was purged with hydrogen (balloon), the outlet needle was removed and the balloon was refilled with hydrogen. The contents were stirred vigorously at RT under a hydrogen atmosphere (balloon) for 4 h and volatiles were removed *in vacuo*. Crude material was purified by silica gel chromatography (hexanes/EtOAc, 0 → 50%) to afford protected amino acid **38** (276 mg, 0.465 mmol, 92%) as a single diastereomer, as a clear viscous oil.

$\mathbf{R_f}$ = 0.45 (hexanes/EtOAc, 67:33);

FTIR (neat), cm^{-1}: ν_{max} 3321, 2942, 2865, 2165, 1750, 1719, 1549, 1462, 1440, 1382, 1372, 1208, 1160, 1095, 1060, 1017;

^{1}H NMR (600 MHz, $CDCl_3$): δ 6.84 (d, J = 7.8 Hz, 1H), 4.93 (s, 1H), 4.66 (td, J = 7.7, 4.6 Hz, 1H), 4.61 (dd, J = 5.9, 1.2 Hz, 1H), 4.57 (d, J = 5.9 Hz, 1H), 4.43 (ddd, J = 10.1, 4.8, 1.2 Hz, 1H), 3.79 (s, 3H), 3.30 (s, 3H), 2.70–2.62 (m, 1H), 2.14 (dddd, J = 14.0, 10.8, 5.8, 4.6 Hz, 1H), 2.08–1.99 (m, 1H), 1.68–1.57 (m, 2H), 1.54 (dddd, J = 13.1, 10.7, 5.9, 4.5 Hz, 1H), 1.46 (s, 3H), 1.36 (dddd, J = 13.1, 11.2, 9.7, 4.4 Hz, 1H), 1.30 (s, 3H), 1.08–1.03 (m, 21H);

^{13}C NMR (126 MHz, $CDCl_3$): δ 171.4, 156.9 (q, $^2J_{C\text{-}F}$ = 38 Hz), 115.7 (q, $^1J_{C\text{-}F}$ = 288 Hz), 112.5, 109.8, 109.5, 85.6, 85.5, 84.5, 83.7, 55.1, 53.0, 52.3, 41.1, 31.1, 30.1, 29.8, 26.7, 25.4, 18.7, 11.3;

^{19}F NMR (471 MHz, $CDCl_3$, BTF IStd): δ –76.8;

HRMS (ESI+): calcd. for $[C_{28}H_{46}F_3N_1O_7Si_1Na]^+$ 616.2888, meas. 616.2890, Δ 0.4 ppm.

Alkyne **S4**

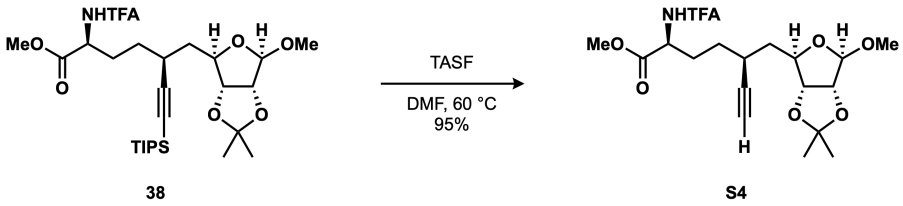

38 **S4**

To a vial charged with TIPS alkyne **38** (182 mg, 0.307 mmol) was added DMF (3 mL) at RT under a nitrogen atmosphere. A separate vial was charged with TASF (253 mg, 0.920 mmol, 3.0 equiv.) in a glovebox, put under a nitrogen atmosphere, and DMF (2 mL) was added at RT. The resulting solution was added to the vial containing alkyne **7** and the reaction mixture was stirred at 60 °C for 2 h. Volatiles were removed *in vacuo*. The residue was partitioned between Et_2O (40 mL) and a 1:1 mixture of brine and 5% LiCl aq. solution (40 mL). The layers were separated and the aqueous phase was extracted with Et_2O (3 × 30 mL). The combined organic extracts were dried over $MgSO_4$, filtered and concentrated. Crude material was purified by silica gel chromatography (hexanes/EtOAc, 5 → 50%) to yield alkyne **S4** (128 mg, 0.293 mmol, 95%) as a colorless oil.

R_f = 0.35 (hexanes/EtOAc, 60:40);

FTIR (neat), cm^{-1}: ν_{max} 3292, 3089, 2990, 2954, 2938, 2836, 1747, 1719, 1553, 1455, 1440, 1383, 1275, 1209, 1160, 1104, 1060;

^{1}H NMR (600 MHz, $CDCl_3$): δ 6.94 (d, J = 7.9 Hz, 1H), 4.93 (s, 1H), 4.64 (td, J = 7.8, 4.9 Hz, 1H), 4.59 (d, J = 6.0 Hz, 1H), 4.55 (dd, J = 6.0, 1.0 Hz, 1H), 4.45 (ddd, J = 11.2, 3.9, 0.9 Hz, 1H), 3.80 (s, 3H), 3.31 (s, 3H), 2.66–2.58 (m, 1H), 2.14 (d, J = 2.4 Hz, 1H), 2.10 (ddq, J = 14.0, 10.8, 5.2 Hz, 1H), 2.05–1.94 (m, 1H), 1.67 (ddd, J = 13.3, 11.2, 4.0 Hz, 1H), 1.55 (dddd, J = 21.7, 13.2, 10.9, 4.6 Hz, 2H), 1.47 (s, 3H), 1.40 (dddd, J = 16.5, 14.4, 8.7, 3.9 Hz, 1H), 1.30 (s, 3H);

^{13}C NMR (126 MHz, $CDCl_3$): δ 171.3, 157.0 (q, $^2J_{C\text{-}F}$ = 38 Hz), 115.1 (q, $^1J_{C\text{-}F}$ = 287 Hz), 112.5, 110.1, 85.6, 85.1, 85.0, 84.5, 71.6, 55.3, 53.1, 52.6, 52.5, 40.4, 30.7, 29.8, 28.6, 26.6, 25.1;

HRMS (ESI+): calcd. for $[C_{19}H_{26}F_3N_1O_7Na]^+$ 460.1554, meas. 460.1569, Δ 3.3 ppm.

Triacetate **S5**

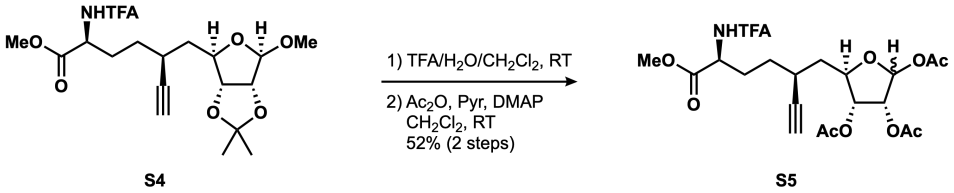

To a solution of acetonide **S4** (1.21 g, 2.77 mmol) in CH_2Cl_2 (16.5 mL) at RT, was added a 2:1 mixture of TFA and water (51 mL). The reaction mixture was stirred at RT for 21 h and volatiles were removed *in vacuo*.

The residue was resuspended in Ac_2O (6.0 mL, 64 mmol, 23 equiv.) and pyridine (12.0 mL, 149 mmol, 54 equiv.). The resulting mixture was stirred at RT for 22 h and volatiles were removed *in vacuo*. Crude material was purified by silica gel chromatography (hexanes/EtOAc, 0 → 40%) to afford triacetate **S5** (735 mg, 1.44 mmol, 52% over 2 steps) as a 1:1.7 mixture of α and β anomers, as a light yellow oil.

$\mathbf{R_f}$ = 0.37 (α-anomer) / 0.46 (β-anomer) (hexanes/EtOAc, 50:50);

FTIR (thin-film), cm^{-1}: ν_{max} 3290, 2956, 1748, 1724, 1553, 1438, 1373, 1219, 1178, 1112, 1049, 1013;

^{1}H NMR (600 MHz, $CDCl_3$): δ α-anomer: 6.92 (d, J = 7.8 Hz, 1H), 6.36 (d, J = 4.6 Hz, 1H), 5.22 (dd, J = 6.8, 4.6 Hz, 1H), 5.05 (dd, J = 6.8, 3.7 Hz, 1H), 4.63 (td, J = 7.6, 5.1 Hz, 1H), 4.43 (dt, J = 10.2, 3.6 Hz, 1H), 3.80 (s, 3H), 2.62 (dqd, J = 13.8, 4.6, 2.4 Hz, 1H), 2.13 (d, J = 2.4 Hz, 1H), 2.12 (s, 3H), 2.08 (s, 3H), 2.08–2.04 (m, 1H), 2.07 (s, 3H), 2.01 (dddd, J = 18.5, 9.1, 5.3, 2.9 Hz, 1H), 1.84 (ddd, J = 14.1, 10.8, 3.5 Hz, 1H), 1.65–1.59 (m, 1H), 1.59–1.53 (m, 1H), 1.40 (dddd, J = 13.1, 11.0, 9.5, 4.8 Hz, 1H); β-anomer: 7.02 (d, J = 8.1 Hz, 1H), 6.10 (s, 1H), 5.31 (dd, J = 4.9, 0.9 Hz, 1H), 5.16 (dd, J = 7.2, 4.7 Hz, 1H), 4.64 (td, J = 8.2, 4.6 Hz, 1H), 4.33 (ddd, J = 10.1, 7.1, 2.7 Hz, 1H), 3.81 (s, 3H), 2.66 (ttd, J = 9.6, 4.9, 2.4 Hz, 1H), 2.13 (d, J =

2.4 Hz, 1H), 2.12 (s, 3H), 2.10 (s, 3H), 2.08–2.04 (m, 1H), 2.06 (s, 3H), 2.05–1.97 (m, 1H), 1.84 (ddd, J = 13.1, 9.9, 2.8 Hz, 1H), 1.69–1.61 (m, 1H), 1.60–1.55 (m, 1H), 1.47 (dddd, J = 13.2, 11.3, 8.9, 4.5 Hz, 1H);

^{13}C NMR (126 MHz, $CDCl_3$): δ *a*-anomer: 171.1, 169.9, 169.5, 169.3, 156.9 (q, $^2J_{C\text{-}F}$ = 38 Hz), 115.7 (q, $^1J_{C\text{-}F}$ = 288 Hz), 93.7, 84.6, 81.2, 72.5, 71.5, 69.7, 52.9, 52.3, 38.9, 30.4, 29.1, 28.4, 21.0, 20.5, 20.2; β-anomer: 171.1, 170.1, 169.7, 169.4, 156.9 (q, $^2J_{C\text{-}F}$ = 38 Hz), 115.6 (q, $^1J_{C\text{-}F}$ = 288 Hz), 98.3, 84.9, 79.8, 74.3, 73.8, 71.3, 52.9, 52.3, 39.6, 30.6, 29.5, 28.0, 21.0, 20.6, 20.2;

^{19}F NMR (471 MHz, $CDCl_3$, BTF IStd): δ –75.8;

HRMS (ESI+): calcd. for $[C_{21}H_{26}F_3N_1O_{10}Na]^+$ 532.1401, meas. 532.1407, Δ 1.2 ppm.

Nucleoside **39**

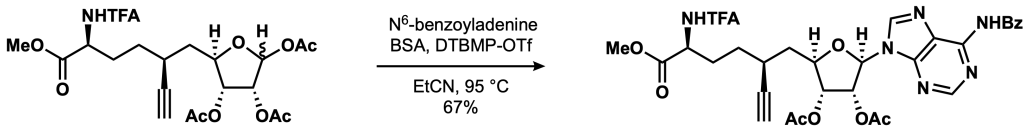

S5 **39**

To a suspension of N^6-benzoyladenine (742 mg, 3.10 mmol, 2.15 equiv.) in propionitrile (dried over 4 Å M.S., 10 mL) at RT, was added *N,O*-bis(trimethylsilyl)acetamide (0.97 mL, 4.0 mmol, 2.75 equiv.). The resulting mixture was stirred at 80 °C for 10 min, upon which complete solubilization of N^6-benzoyladenine was observed. To a separate flask charged with triacetate **S5** (dried by azeotropic distillation with benzene (4 ×), 735 mg, 1.44 mmol) and 2,6-di-*tert*-butyl-4-methylpyridinium triflate[19] (50 mg, 0.14 mmol, 10 mol %) was added propionitrile (10 mL). The resulting mixture was stirred at RT for 5 min until a clear solution was obtained and the solution of silylated N^6-benzoyladenine was added. The reaction mixture was stirred at 95 °C for 3 h, cooled to RT and the volatiles were removed *in vacuo*. Crude material was purified by silica gel chromatography (PhMe/MeCN, 0 → 50%) to afford nucleoside **39** (663 mg, 0.963 mmol, 67%) as a

[19] Sniady, A.; Bedore, M. W.; Jamison, T. F. *Angew. Chem. Int. Ed. 50*, 2155–2158.

white amorphous solid.

R_f = 0.48 (PhMe/MeCN, 50:50);

FTIR (thin-film), cm^{-1}: ν_{max} 3273, 3086, 2928, 1748, 1720, 1611, 1582, 1511, 1487, 1456, 1374, 1329, 1243, 1217, 1182, 1160, 1099, 1074, 1047, 1029;

^{1}H NMR (500 MHz, $CDCl_3$): δ 9.09 (s, 1H), 8.77 (s, 1H), 8.09 (s, 1H), 8.03–7.99 (m, 2H), 7.62–7.57 (m, 1H), 7.53–7.48 (m, 2H), 7.06 (d, *J* = 7.9 Hz, 1H), 6.12 (d, *J* = 5.4 Hz, 1H), 6.07 (t, *J* = 5.4 Hz, 1H), 5.55 (dd, *J* = 5.5, 4.5 Hz, 1H), 4.61 (td, *J* = 7.8, 5.0 Hz, 1H), 4.48 (ddd, *J* = 10.9, 4.5, 2.9 Hz, 1H), 3.77 (s, 3H), 2.59 (ddtd, *J* = 11.4, 9.1, 4.4, 2.5 Hz, 1H), 2.16 (d, *J* = 2.4 Hz, 1H), 2.15 (s, 3H), 2.11–2.00 (m, 2H), 2.06 (s, 3H), 1.95 (dddd, *J* = 13.9, 10.9, 7.7, 4.6 Hz, 1H), 1.86 (ddd, *J* = 13.8, 11.2, 2.9 Hz, 1H), 1.61–1.54 (m, 1H), 1.45 (dddd, *J* = 13.6, 10.9, 9.3, 4.6 Hz, 1H);

^{13}C NMR (126 MHz, $CDCl_3$): δ 171.2, 169.8, 169.6, 165.2, 157.0 (q, $^2J_{C\text{-}F}$ = 37.6 Hz), 152.6, 151.6, 149.9, 142.4, 133.5, 132.8, 128.8, 128.1, 123.9, 115.7 (q, $^1J_{C\text{-}F}$ = 287.7 Hz), 87.0, 84.7, 80.7, 73.5, 72.9, 71.7, 53.0, 52.3, 38.2, 30.8, 29.6, 27.9, 20.6, 20.4;

^{19}F NMR (471 MHz, $CDCl_3$, BTF IStd): δ –76.7;

HRMS (ESI+): calcd. for $[C_{31}H_{31}F_3N_6O_9Na]^+$ 711.1988, meas. 711.1997, Δ 1.2 ppm.

Benzamide **40**

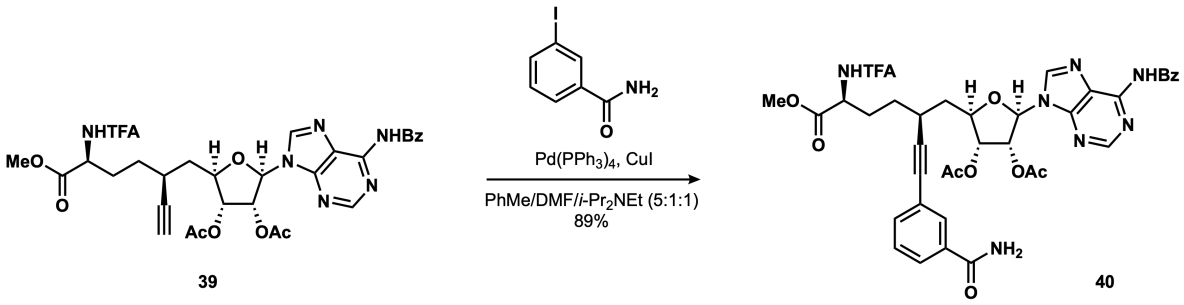

To a vial charged with alkyne **39** (79 mg, 0.11 mmol) were added 3-iodobenzamide (57 mg, 0.23 mmol, 2.0 equiv.), CuI (4 mg, 0.02 mmol, 20 mol %) and $Pd(PPh_3)_4$ (7 mg, 6 μmol, 5 mol %). The vial headspace was purged with nitrogen for 5 min and a 5:1:1 mixture of toluene, DMF and *i*-Pr_2NEt (degassed by sparging with nitrogen for 15 min, 3.5 mL) was added at RT. The resulting mixture was stirred at 70 °C for 3 h. The solution was allowed to cool to RT and volatiles were removed *in vacuo*. Crude material was purified by silica gel chromatography (PhMe/MeCN, 0 → 100% over 40 min then 100% for 10 min) to afford alkyne **40** (83 mg, 0.10 mmol, 89%) as a white amorphous solid.

R_f = 0.17 (EtOAc/*i*-PrOH, 90:10);

FTIR (neat), cm^{-1}: ν_{max} 3255, 3064, 2929, 1744, 1717, 1666, 1610, 1578, 1511, 1486, 1455, 1374, 1329, 1240, 1212, 1180, 1158, 1096, 1073, 1046, 1029;

^{1}H NMR (600 MHz, CD_2Cl_2): δ 9.03 (br s, 1H), 8.75 (s, 1H), 8.14 (s, 1H), 8.00 (t, *J* = 1.3 Hz, 1H), 7.99 (d, *J* = 1.5 Hz, 1H), 7.87 (td, *J* = 1.8, 0.6 Hz, 1H), 7.77 (ddd, *J* = 7.8, 1.9, 1.1 Hz, 1H), 7.64 (ddt, *J* = 8.0, 7.0, 1.3 Hz, 1H), 7.57–7.54 (m, 2H), 7.53 (dd, *J* = 1.6, 1.0 Hz, 1H), 7.40 (td, *J* = 7.8, 0.6 Hz, 1H), 7.15 (d, *J* = 7.7 Hz, 1H), 6.53 (br s, 1H), 6.18 (d, *J* = 5.8 Hz, 1H), 6.15 (t, *J* = 5.5 Hz, 1H), 5.70 (br s, 1H), 5.65 (dd, *J* = 5.3, 4.0 Hz, 1H), 4.65 (td, *J* = 7.5, 5.5 Hz, 1H), 4.54 (dt, *J* = 10.1, 3.9 Hz, 1H), 3.77 (s, 3H), 2.83 (ddt, *J* = 11.0, 9.0, 4.4 Hz, 1H), 2.19 (ddd, *J* = 13.8, 10.1, 4.0 Hz, 1H), 2.15 (s, 3H), 2.11 (dt, *J* = 10.5, 5.1 Hz, 1H), 2.11–1.99 (m, 2H), 2.04 (s, 3H), 1.68 (ddt, *J* = 13.0, 10.7, 5.6 Hz, 1H), 1.57 (dddd, *J* = 13.5, 10.8, 9.3, 4.8 Hz, 1H);

^{13}C NMR (101 MHz, CD_2Cl_2): δ 171.6, 170.4, 170.1, 168.8, 165.4, 157.4 (q, $^2J_{C\text{-}F}$ = 37 Hz), 152.8, 152.1,

150.3, 142.9, 134.8, 134.1, 134.0, 133.1, 131.1, 129.1, 128.9, 128.3, 127.4, 124.6, 123.9, 116.1 (q, $^{1}J_{C\text{-}F}$ = 287 Hz), 91.9, 87.3, 83.1, 81.5, 74.1, 73.0, 53.3, 53.0, 38.8, 31.4, 29.8, 29.1, 20.8, 20.6;

^{19}F NMR (471 MHz, $CDCl_3$, BTF IStd): δ –76.7;

HRMS (ESI+): calcd. for $[C_{38}H_{37}F_3N_7O_{10}]^+$ 808.2549, meas. 808.2538, Δ 1.3 ppm.

NS1 (**33**)

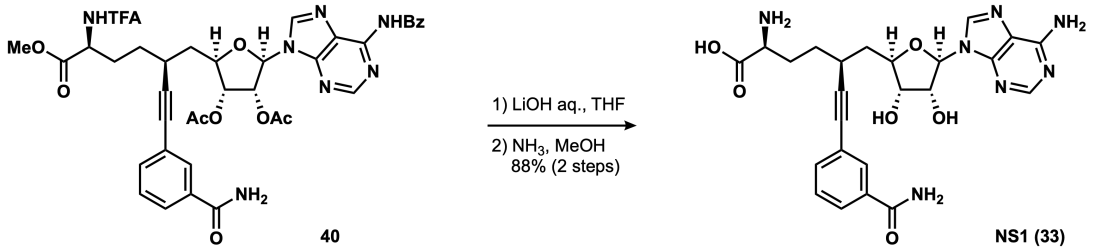

To a solution of alkyne **40** (158 mg, 196 μmol) in THF (2.0 mL) at RT, was added a 0.5 M LiOH aq. solution (2.0 mL). The resulting mixture was stirred for 2.5 h, cooled to 0 °C and a 10% AcOH aq. solution was added dropwise until pH 7 was reached. Volatiles were removed *in vacuo*. The residue was dissolved in a solution of ammonia in methanol (7 N, 8 mL) at RT. The resulting mixture was stirred for 18 h and the volatiles were removed *in vacuo*. Crude material was purified by preparative HPLC using a Kromasil® C18 column (10 μm particle size, 21.2 × 250 mm, room temperature, injection volume: 3.0 mL (water/CH_3CN, 90:10), solvent A: 0.1% (v/v) TFA in water, solvent B: 0.1% (v/v) TFA in CH_3CN, gradient elution: 5% B with flow rate: 0 → 10 mL/min over 5 min then 5% → 55% B over 45 min followed by 55% → 95% B over 5 min with flow rate: 10 mL/min, UV detection at 254 nm) to afford NS1 (**33**) (107 mg, 172 μmol, 88% over 2 steps) as the TFA salt. Compound characterization data matched those reported for this same compound in the First-Generation NS1 Synthesis. Single crystals suitable for X-ray diffraction studies were grown from a 4:1:1 volumetric mixture of 10 mM aq. NS1-TFA:*n*-BuOH:*i*-PrOH *via* slow evaporation at 4 °C over two weeks. X-ray crystallographic data are reported in section 2.9.9.

2.9.8 *X-Ray Crystal Structure,* **26** *after TIPS removal*

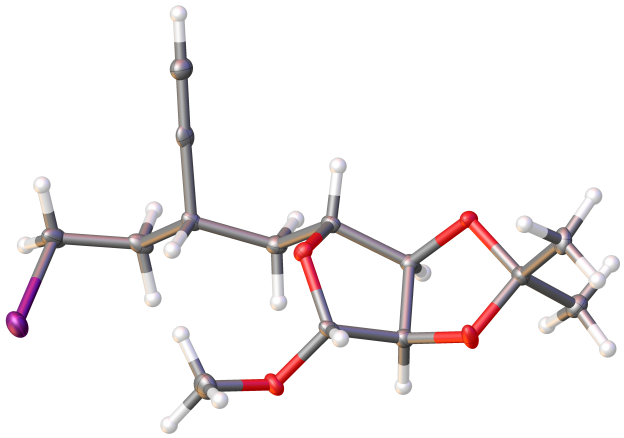

A crystal mounted on a diffractometer was collected data at 100 K. The intensities of the reflections were collected by means of a Bruker APEX II CCD diffractometer ($Mo_{K\alpha}$ radiation, λ=0.71073 Å), and equipped with an Oxford Cryosystems nitrogen flow apparatus. The collection method involved 0.5° scans in ω at 28°in 2θ. Data integration down to 0.78 Å resolution was carried out using SAINT V8.37 A[20] with reflection spot size optimization. Absorption corrections were made with the program SADABS[26]. The structure was solved by the Intrinsic Phasing methods and refined by least-squares methods again F^2 using SHELXT-2014[21] and SHELXL-2014[22] with OLEX 2 interface[23]. Non-hydrogen atoms were refined anisotropically, and hydrogen atoms were allowed to ride on the respective atoms. Crystal data as well as details of data

[20] Bruker AXS APEX3, Bruker AXS, Madison, Wisconsin, 2015.

[21] Sheldrick, G. M. *Acta Crystallogr., Sect. A* **2015**, *71*, 3–8.

[22] Sheldrick, G. M. *Acta Crystallogr., Sect. C* **2015**, *71*, 3–8.

[23] Dolomanov, O. V.; Bourhis, L. J.; Gildea, R. J.; Howard, J. A. K.; Puschmann, H. *J. Appl. Cryst.* **2009**, *42*, 339–341.

collection and refinement are summarized in Table 2.9.2. Geometric parameters are shown in Table 2.9.3. The Ortep plots were produced with SHELXL-2014, and the other images were produced with Accelrys DS Visualizer 2.0[24].

Table 2.9.2: Experimental Details

Crystal Data	
Chemical Formula	$C_{14}H_{21}I_{04}$
M_r	380.21
Crystal system, space group	Orthorhombic, $P2_12_12_1$
Temperature (K)	100
a, b, c (Å)	5.6630 (2), 9.8581 (4), 28.2938 (11)
V(Å^3)	1579.54 (10)
Z	4
Radiation type	Mo $K\alpha$
μ (mm^{-1})	2.04
Crystal size (mm)	$0.12 \times 0.04 \times 0.02$
Data Collection	
Diffractometer	Bruker D8 goniometer with CCD area detector
Multi-scan *SADABS*	
T_{min}, T_{max}	0.567, 0.694
No. of measured, independent and observed $[I > 2\sigma(I)]$ reflections	24468, 3497, 3284
R_{int}	0.031
$(\sin\theta/\lambda)_{max}$(Å^{-1})	0.642
Refinement	
$R[F^2 > 2\sigma(F^2)], wR(F^2), S$	0.018, 0.035, 1.04
No. of reflections	3497
No. of parameters	176
H-atom treatment	H atom parameters constrained
$\Delta\rho_{max}, \Delta\rho_{min}$ (eÅ^{-3})	0.35, -0.33
Absolute structure	Flack x determined using 1305 quotients [(I+)-(I-)]/[(I+)+(I-)][25]
Absolute structure parameter	-0.038 (6)

Computer programs: APEX3 v2016.9-0 (Bruker-AXS, 2016), SAINT 8.37A (Bruker-AXS, 2015), SHELXT2014 (Sheldrick, 2015), SHELXL2014 (Sheldrick, 2015), Bruker SHELXTL (Sheldrick, 2015).

[24] Accelrys DS Visualizer v2.0.1, Accelrys Software Inc., 2007.

[25] Parsons, S.; Flack, H. D.; Wagner, T. *Acta Crystallogr., Sect. B* **2013**, *69*, 249–259.

Table 2.9.3: Geometric parameters (Å, °)

O1–C1	1.427 (4)	C7–C13	1.476 (4)
O1–C2	1.433 (3)	C7–C8	1.538 (4)
O2–C3	1.424 (3)	C7–H7	1.0000
O2–C1	1.436 (3)	C8–C9	1.506 (4)
O3–C4	1.418 (3)	C8–H8A	0.9900
O3–C5	1.444 (3)	C8–H8B	0.9900
O4–C4	1.419 (3)	C9–H9A	0.9900
O4–C12	1.428 (3)	C9–H9B	0.9900
C1–C11	1.506 (4)	C10–H10A	0.9800
C1–C10	1.513 (4)	C10–H10B	0.9800
C2–C5	1.513 (4)	C10–H10C	0.9800
C2–C3	1.538 (3)	C11–H11A	0.9800
C2–H2	1.0000	C11–H11B	0.9800
C3–C4	1.524 (4)	C11–H11C	0.9800
C3–H3	1.0000	C12–H12A	0.9800
C4–H4	1.0000	C12–H12B	0.9800
C5–C6	1.529 (4)	C12–H12C	0.9800
C5–H5	1.0000	C13–C14	1.180 (4)
C6–C7	1.530 (4)	C14–H14	0.9500
C6–H6A	0.9900		
C1–O1–C2	105.82 (18)	H6A–C6–H6B	107.7
C3–O2–C1	107.7 (2)	C13–C7–C6	111.4 (2)
C4–O3–C5	108.61 (19)	C13–C7–C8	110.7 (2)
C4–O4–C12	112.0 (2)	C6–C7–C8	110.8 (2)
O1–C1–O2	103.8 (2)	C13–C7–H7	107.9
O1–C1–C11	109.4 (2)	C6–C7–H7	107.9
O2–C1–C11	109.0 (2)	C8–C7–H7	107.9
O1–C1–C10	110.9 (3)	C9–C8–C7	114.2 (2)
O2–C1–C10	111.0 (2)	C9–C8–H8A	108.7
C11–C1–C10	112.5 (3)	C7–C8–H8A	108.7
O1–C2–C5	110.5 (2)	C9–C8–H8B	108.7
O1–C2–C3	103.24 (19)	C7–C8–H8B	108.7
C5–C2–C3	104.7 (2)	H8A–C8–H8B	107.6
O1–C2–H2	112.6	C8–C9–I1	110.65 (18)
C5–C2–H2	112.6	C8–C9–H9A	109.5
C3–C2–H2	112.6	I1–C9–H9A	109.5
O2–C3–C4	110.2 (2)	C8–C9–H9B	109.5
O2–C3–C2	105.03 (19)	I1–C9–H9B	109.5
C4–C3–C2	104.6 (2)	H9A–C9–H9B	108.1
O2–C3–H3	112.2	C1–C10–H10A	109.5
C4–C3–H3	112.2	C1–C10–H10B	109.5
C2–C3–H3	112.2	H10A–C10–H10B	109.5
O3–C4–O4	111.6 (2)	C1–C10–H10C	109.5

Table 2.9.3 continued from previous page.

O3–C4–C3	106.98 (19)	H10A–C10–H10C	109.5
O4–C4–C3	108.5 (2)	H10B–C10–H10C	109.5
O3–C4–H4	109.9	C1–C11–H11A	109.5
O4–C4–H4	109.9	C1–C11–H11B	109.5
C3–C4–H4	109.9	H11A–C11–H11B	109.5
O3–C5–C2	104.6 (2)	C1–C11–H11C	109.5
O3–C5–C6	112.8 (2)	H11A–C11–H11C	109.5
C2–C5–C6	111.1 (2)	H11B–C11–H11C	109.5
O3–C5–H5	109.4	O4–C12–H12A	109.5
C2–C5–H5	109.4	O4–C12–H12B	109.5
C6–C5–H5	109.4	H12A–C12–H12B	109.5
C5–C6–C7	113.9 (2)	O4–C12–H12C	109.5
C5–C6–H6A	108.8	H12A–C12–H12C	109.5
C7–C6–H6A	108.8	H12B–C12–H12C	109.5
C5–C6–H6B	108.8	C14–C13–C7	177.8 (3)
C7–C6–H6B	108.8	C13–C14–H14	180.0
C2–O1–C1–O2	-39.2 (2)	O2–C3–C4–O3	103.8 (2)
C2–O1–C1–C11	-155.4 (2)	C2–C3–C4–O3	-8.6 (3)
C2–O1–C1–C10	80.0 (3)	O2–C3–C4–O4	-135.5 (2)
C3–O2–C1–O1	31.4 (3)	C2–C3–C4–O4	112.0 (2)
C3–O2–C1–C11	147.9 (2)	C4–O3–C5–C2	-33.9 (2)
C3–O2–C1–C10	-87.8 (3)	C4–O3–C5–C6	86.9 (2)
C1–O1–C2–C5	142.6 (2)	O1–C2–C5–O3	-83.6 (2)
C1–O1–C2–C3	31.1 (3)	C3–C2–C5–O3	26.9 (2)
C1–O2–C3–C4	-124.1 (2)	O1–C2–C5–C6	154.4 (2)
C1–O2–C3–C2	-11.9 (3)	C3–C2–C5–C6	-95.1 (2)
O1–C2–C3–O2	-11.6 (3)	O3–C5–C6–C7	51.9 (3)
C5–C2–C3–O2	-127.4 (2)	C2–C5–C6–C7	169.0 (2)
O1–C2–C3–C4	104.4 (2)	C5–C6–C7–C13	56.3 (3)
C5–C2–C3–C4	-11.3 (3)	C5–C6–C7–C8	-179.9 (2)
C5–O3–C4–O4	-91.9 (2)	C13–C7–C8–C9	-67.8 (3)
C5–O3–C4–C3	26.7 (3)	C6–C7–C8–C9	168.1 (2)
C12–O4–C4–O3	-69.3 (3)	C7–C8–C9–I1	-68.2 (2)
C12–O4–C4–C3	173.0 (2)		

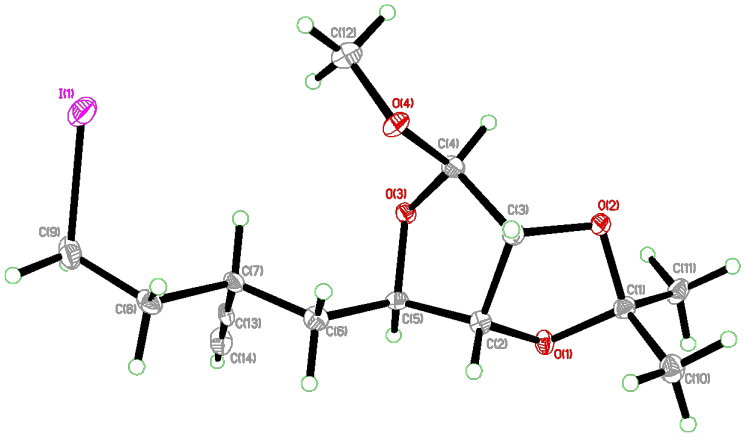

Figure 2.9.3: Perspective views showing 50% probability displacement.

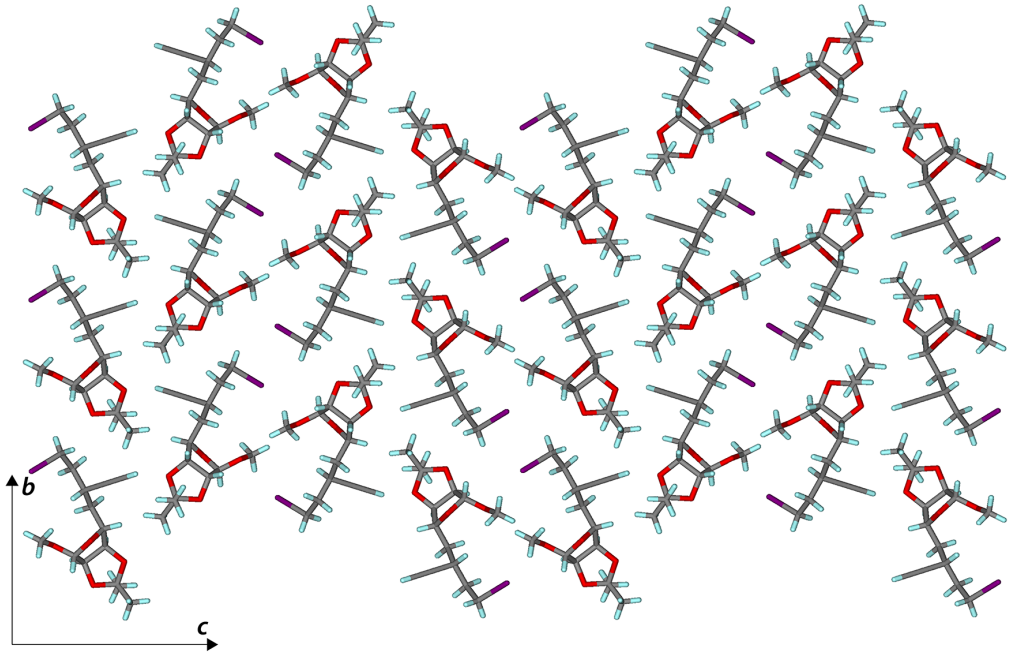

Figure 2.9.4: Three-dimensional supramolecular architecture viewed along the *a*-axis direction.

2.9.9 *X-Ray Crystal Structure*, NS1•TFA (**33**)

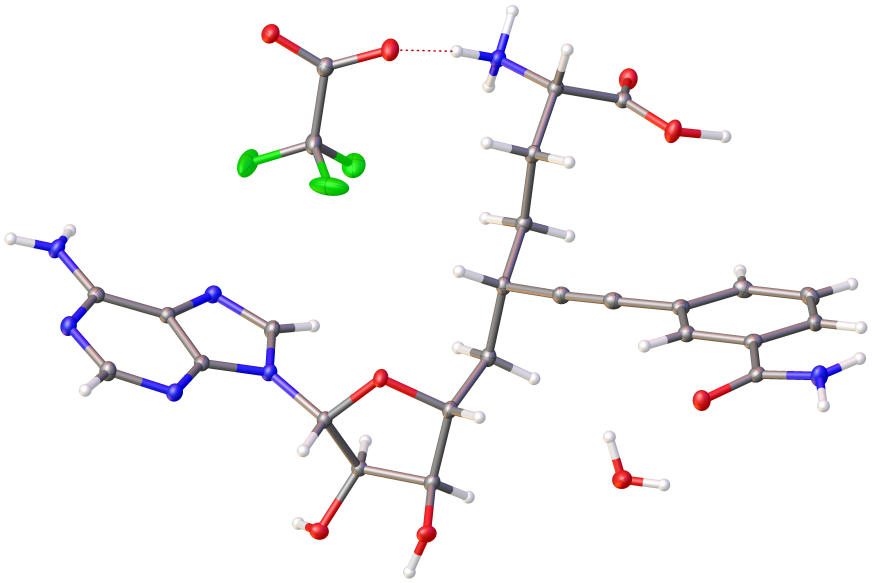

A crystal mounted on a diffractometer was collected data at 100 K. The intensities of the reflections were collected by means of a Bruker APEX DUO CCD diffractometer ($Cu_{K\alpha}$ radiation, λ=1.54178 Å), and equipped with an Oxford Cryosystems nitrogen flow apparatus. The collection method involved 1.0° scans in ω at –30°, –55°, –80°, 30°, 55°, 80° and 115° in 2θ. Data integration down to 0.84 Å resolution was carried out using SAINT V8.37 A[26] with reflection spot size optimization. Absorption corrections were made with the program SADABS[26]. The structure was solved by the Intrinsic Phasing methods and refined by least-squares methods again F^2 using SHELXT-2014[27] and SHELXL-2014[28] with OLEX 2 interface[29]. Non-hydrogen atoms were refined anisotropically, and hydrogen atoms were allowed to ride on the respective atoms. Crystal data as well as details of data collection and refinement are summarized in Tables 2.9.4, 3.5.1, and 3.5.3, for NS1 (**33**), **S24**, and **S30**, respectively. Geometric parameters are shown in Tables 2.9.5, 3.5.4, 3.5.2 and hydrogen-bond parameters are listed in Tables 2.9.6 and 3.5.5. The Ortep plots were produced with

---

[26] Bruker AXS APEX3, Bruker AXS, Madison, Wisconsin, 2015.

[27] Sheldrick, G. M. *Acta Crystallogr., Sect. A* **2015**, *71*, 3–8.

[28] Sheldrick, G. M. *Acta Crystallogr., Sect. C* **2015**, *71*, 3–8.

[29] Dolomanov, O. V.; Bourhis, L. J.; Gildea, R. J.; Howard, J. A. K.; Puschmann, H. *J. Appl. Cryst.* **2009**, *42*, 339–341.

SHELXL-2014, and the other images were produced with Accelrys DS Visualizer 2.0[30].

Table 2.9.4: Experimental Details

Crystal Data	
Chemical Formula	$C_{26}H_{30}F_3N_7O_9$
M_r	641.57
Crystal system, space group	Triclinic, $P\bar{1}$
Temperature (K)	100
a, b, c (Å)	5.0591 (1), 10.9615 (2), 13.2000 (7)
α, β, γ (°)	103.0375 (11), 90.8460 (9), 90.3108 (10)
V(Å^3)	713.03 (2)
Z	1
Radiation type	Cu $K\alpha$
μ (mm^{-1})	1.09
Crystal size (mm)	$0.18 \times 0.08 \times 0.06$
Data Collection	
Diffractometer	Bruker D8 goniometer with CCD area detector
Absorption correction	Multi-scan *SADABS*
T_{min}, T_{max}	0.738, 0.806
No. of measured, independent and observed $[I > 2\sigma(I)]$ reflections	17748, 4335, 4280
R_{int}	0.027
$(\sin\theta/\lambda)_{max}$(Å^{-1})	0.596
Refinement	
$R[F^2 > 2\sigma(F^2)], wR(F^2), S$	0.027, 0.073, 1.02
No. of reflections	4335
No. of parameters	464
No. of restraints	9
H-atom treatment	H atom parameters constrained
$\Delta\rho_{max}, \Delta\rho_{min}$ (eÅ^{-3})	0.53, -0.17
Absolute structure	Flack x determined using 1012 quotients [(I+)-(I-)]/[(I+)+(I-)][31]
Absolute structure parameter	-0.06 (8)

Computer programs: SAINT 8.37A (Bruker-AXS, 2015), SHELXT2014 (Sheldrick, 2015), SHELXL2014 (Sheldrick, 2015), Bruker SHELXTL (Sheldrick, 2015).

[30] Accelrys DS Visualizer v2.0.1, Accelrys Software Inc., 2007.

[31] Parsons, S.; Flack, H. D.; Wagner, T. *Acta Crystallogr., Sect. B* **2013**, *69*, 249–259.

Table 2.9.5: Geometric parameters (Å, °)

O1–C6	1.417 (3)	C9–H9	1
O1–C9	1.466 (3)	C10–C11	1.537 (3)
O2–C7	1.409 (3)	C10–H10A	0.99
O2–H2	0.86 (4)	C10–H10B	0.99
O3–C8	1.421 (3)	C11–C16	1.474 (4)
O3–H3	0.88 (4)	C11–C12	1.549 (3)
O4–C15	1.220 (3)	C11–H11	1
O5–C15	1.301 (3)	C12–C13	1.524 (3)
O5–H5	1.14 (6)	C12–H12A	0.99
O6–C24	1.252 (3)	C12–H12B	0.99
N1–C1	1.370 (3)	C13–C14	1.528 (3)
N1–C5	1.380 (3)	C13–H13A	0.99
N1–C6	1.462 (3)	C13–H13B	0.99
N2–C2	1.319 (3)	C14–C15	1.516 (3)
N2–C1	1.346 (3)	C14–H14	1
N3–C2	1.339 (3)	C16–C17	1.195 (4)
N3–C3	1.359 (3)	C17–C18	1.442 (4)
N4–C3	1.322 (3)	C18–C23	1.394 (3)
N4–H4A	0.92 (4)	C18–C19	1.401 (4)
N4–H4B	0.88 (4)	C19–C20	1.381 (4)
N5–C5	1.303 (3)	C19–H19	0.95
N5–C4	1.386 (3)	C20–C21	1.393 (4)
N6–C14	1.492 (3)	C20–H20	0.95
N6–H6A	0.93 (4)	C21–C22	1.402 (4)
N6–H6B	0.92 (4)	C21–H21	0.95
N6–H6C	0.97 (3)	C22–C23	1.389 (4)
N7–C24	1.319 (4)	C22–C24	1.499 (3)
N7–H7A	0.90 (4)	C23–H23	0.95
N7–H7B	0.88 (4)	O11–C31	1.232 (3)
C1–C4	1.391 (3)	O12–C31	1.253 (3)
C2–H2A	0.95	C31–C32A	1.540 (3)
C3–C4	1.417 (3)	C31–C32	1.540 (3)
C5–H5A	0.95	C32–F1	1.335 (9)
C6–C7	1.531 (3)	C32–F2	1.338 (9)
C6–H6	1	C32–F3	1.374 (6)
C7–C8	1.516 (4)	C32A–F3A	1.283 (12)
C7–H7	1	C32A–F1A	1.311 (18)
C8–C9	1.527 (3)	C32A–F2A	1.378 (18)
C8–H8	1	O1W–H1WA	0.85 (6)
C9–C10	1.522 (3)	O1W–H1WB	0.79 (5)
C6–O1–C9	109.24 (17)	C16–C11–C12	109.25 (19)
C7–O2–H2	104 (2)	C10–C11–C12	113.13 (19)
C8–O3–H3	103 (3)	C16–C11–H11	108

Table 2.9.5 continued from previous page.

C15–O5–H5	112 (3)	C10–C11–H11	108
C1–N1–C5	105.4 (2)	C12–C11–H11	108
C1–N1–C6	126.1 (2)	C13–C12–C11	110.10 (19)
C5–N1–C6	128.5 (2)	C13–C12–H12A	109.6
C2–N2–C1	111.4 (2)	C11–C12–H12A	109.6
C2–N3–C3	120.7 (2)	C13–C12–H12B	109.6
C3–N4–H4A	120 (2)	C11–C12–H12B	109.6
C3–N4–H4B	123 (2)	H12A–C12–H12B	108.2
H4A–N4–H4B	116 (3)	C12–C13–C14	116.8 (2)
C5–N5–C4	104.1 (2)	C12–C13–H13A	108.1
C14–N6–H6A	109 (2)	C14–C13–H13A	108.1
C14–N6–H6B	114 (2)	C12–C13–H13B	108.1
H6A–N6–H6B	111 (3)	C14–C13–H13B	108.1
C14–N6–H6C	108.9 (19)	H13A–C13–H13B	107.3
H6A–N6–H6C	106 (3)	N6–C14–C15	109.3 (2)
H6B–N6–H6C	108 (3)	N6–C14–C13	113.8 (2)
C24–N7–H7A	117 (2)	C15–C14–C13	113.6 (2)
C24–N7–H7B	125 (2)	N6–C14–H14	106.5
H7A–N7–H7B	116 (3)	C15–C14–H14	106.5
N2–C1–N1	127.3 (2)	C13–C14–H14	106.5
N2–C1–C4	126.6 (2)	O4–C15–O5	125.5 (2)
N1–C1–C4	106.1 (2)	O4–C15–C14	122.5 (2)
N2–C2–N3	128.2 (2)	O5–C15–C14	112.0 (2)
N2–C2–H2A	115.9	C17–C16–C11	173.0 (3)
N3–C2–H2A	115.9	C16–C17–C18	172.7 (3)
N4–C3–N3	119.1 (2)	C23–C18–C19	119.1 (2)
N4–C3–C4	125.3 (2)	C23–C18–C17	122.6 (2)
N3–C3–C4	115.6 (2)	C19–C18–C17	118.3 (2)
N5–C4–C1	110.4 (2)	C20–C19–C18	120.6 (2)
N5–C4–C3	132.1 (2)	C20–C19–H19	119.7
C1–C4–C3	117.5 (2)	C18–C19–H19	119.7
N5–C5–N1	114.1 (2)	C19–C20–C21	120.2 (2)
N5–C5–H5A	122.9	C19–C20–H20	119.9
N1–C5–H5A	122.9	C21–C20–H20	119.9
O1–C6–N1	109.56 (19)	C20–C21–C22	119.8 (2)
O1–C6–C7	106.44 (19)	C20–C21–H21	120.1
N1–C6–C7	113.56 (19)	C22–C21–H21	120.1
O1–C6–H6	109.1	C23–C22–C21	119.6 (2)
N1–C6–H6	109.1	C23–C22–C24	118.8 (2)
C7–C6–H6	109.1	C21–C22–C24	121.5 (2)
O2–C7–C8	113.55 (19)	C22–C23–C18	120.7 (2)
O2–C7–C6	112.21 (19)	C22–C23–H23	119.7
C8–C7–C6	101.34 (19)	C18–C23–H23	119.7
O2–C7–H7	109.8	O6–C24–N7	121.6 (2)
C8–C7–H7	109.8	O6–C24–C22	120.0 (2)

Table 2.9.5 continued from previous page.

C6–C7–H7	109.8	N7–C24–C22	118.4 (2)
O3–C8–C7	110.95 (19)	O11–C31–O12	130.5 (2)
O3–C8–C9	108.27 (19)	O11–C31–C32A	115.1 (2)
C7–C8–C9	101.94 (18)	O12–C31–C32A	114.3 (2)
O3–C8–H8	111.7	O11–C31–C32	115.1 (2)
C7–C8–H8	111.7	O12–C31–C32	114.3 (2)
C9–C8–H8	111.7	F1–C32–F2	104.1 (11)
O1–C9–C10	107.96 (18)	F1–C32–F3	105.6 (7)
O1–C9–C8	105.45 (18)	F2–C32–F3	110.3 (7)
C10–C9–C8	115.4 (2)	F1–C32–C31	112.2 (9)
O1–C9–H9	109.3	F2–C32–C31	113.1 (7)
C10–C9–H9	109.3	F3–C32–C31	111.1 (3)
C8–C9–H9	109.3	F3A–C32A–F1A	112.6 (16)
C9–C10–C11	111.14 (19)	F3A–C32A–F2A	96.4 (15)
C9–C10–H10A	109.4	F1A–C32A–F2A	108 (2)
C11–C10–H10A	109.4	F3A–C32A–C31	115.7 (6)
C9–C10–H10B	109.4	F1A–C32A–C31	118 (2)
C11–C10–H10B	109.4	F2A–C32A–C31	103.0 (14)
H10A–C10–H10B	108	H1WA–O1W–H1WB	113 (5)
C16–C11–C10	110.3 (2)		
C2–N2–C1–N1	179.2 (2)	O3–C8–C9–C10	154.9 (2)
C2–N2–C1–C4	0.9 (3)	C7–C8–C9–C10	-88.1 (2)
C5–N1–C1–N2	-178.1 (2)	O1–C9–C10–C11	62.3 (2)
C6–N1–C1–N2	3.3 (4)	C8–C9–C10–C11	179.94 (19)
C5–N1–C1–C4	0.5 (2)	C9–C10–C11–C16	72.6 (2)
C6–N1–C1–C4	-178.1 (2)	C9–C10–C11–C12	-164.7 (2)
C1–N2–C2–N3	-0.5 (4)	C16–C11–C12–C13	-60.6 (3)
C3–N3–C2–N2	-0.9 (4)	C10–C11–C12–C13	176.03 (19)
C2–N3–C3–N4	-177.5 (2)	C11–C12–C13–C14	177.8 (2)
C2–N3–C3–C4	1.7 (3)	C12–C13–C14–N6	72.3 (3)
C5–N5–C4–C1	0.6 (3)	C12–C13–C14–C15	-53.6 (3)
C5–N5–C4–C3	178.2 (2)	N6–C14–C15–O4	7.7 (3)
N2–C1–C4–N5	177.9 (2)	C13–C14–C15–O4	136.0 (2)
N1–C1–C4–N5	-0.7 (2)	N6–C14–C15–O5	-174.33 (19)
N2–C1–C4–C3	-0.1 (3)	C13–C14–C15–O5	-46.0 (3)
N1–C1–C4–C3	-178.70 (19)	C23–C18–C19–C20	0.1 (4)
N4–C3–C4–N5	0.5 (4)	C17–C18–C19–C20	-177.7 (2)
N3–C3–C4–N5	-178.6 (2)	C18–C19–C20–C21	-0.2 (4)
N4–C3–C4–C1	177.9 (2)	C19–C20–C21–C22	0.5 (3)
N3–C3–C4–C1	-1.2 (3)	C20–C21–C22–C23	-0.6 (3)
C4–N5–C5–N1	-0.3 (3)	C20–C21–C22–C24	175.8 (2)
C1–N1–C5–N5	-0.2 (3)	C21–C22–C23–C18	0.4 (3)
C6–N1–C5–N5	178.5 (2)	C24–C22–C23–C18	-176.1 (2)
C9–O1–C6–N1	-138.04 (18)	C19–C18–C23–C22	-0.2 (3)

Table 2.9.5 continued from previous page.

C9–O1–C6–C7	-14.9 (2)	C17–C18–C23–C22	177.5 (2)
C1–N1–C6–O1	-110.1 (2)	C23–C22–C24–O6	7.0 (3)
C5–N1–C6–O1	71.5 (3)	C21–C22–C24–O6	-169.5 (2)
C1–N1–C6–C7	131.0 (2)	C23–C22–C24–N7	-173.9 (2)
C5–N1–C6–C7	-47.3 (3)	C21–C22–C24–N7	9.7 (3)
O1–C6–C7–O2	155.32 (19)	O11–C31–C32–F1	148.7 (9)
N1–C6–C7–O2	-84.1 (2)	O12–C31–C32–F1	-33.4 (9)
O1–C6–C7–C8	33.9 (2)	O11–C31–C32–F2	-93.9 (9)
N1–C6–C7–C8	154.47 (19)	O12–C31–C32–F2	84.0 (9)
O2–C7–C8–O3	-44.0 (3)	O11–C31–C32–F3	30.7 (6)
C6–C7–C8–O3	76.6 (2)	O12–C31–C32–F3	-151.4 (5)
O2–C7–C8–C9	-159.06 (19)	O11–C31–C32A–F3A	1.0 (9)
C6–C7–C8–C9	-38.5 (2)	O12–C31–C32A–F3A	178.9 (9)
C6–O1–C9–C10	113.7 (2)	O11–C31–C32A–F1A	139 (2)
C6–O1–C9–C8	-10.2 (2)	O12–C31–C32A–F1A	-43 (2)
O3–C8–C9–O1	-86.1 (2)	O11–C31–C32A–F2A	-102.8 (17)
C7–C8–C9–O1	30.9 (2)	O12–C31–C32A–F2A	75.1 (17)

Table 2.9.6: Hydrogen-bond parameters

D – H ··· A	D – H (Å)	H ··· A (Å)	D ··· A (Å)	D – H ··· A (°)
O2–H2···N2^{i}	0.86 (4)	1.92 (4)	2.757 (3)	163 (3)
O3–H3···O11^{ii}	0.88 (4)	1.94 (4)	2.784 (2)	162 (4)
O3–H3···O2	0.88 (4)	2.38 (4)	2.766 (3)	107 (3)
O5–H5···N3^{iii}	1.14 (6)	1.41 (6)	2.542 (3)	172 (5)
N4–H4A···O4^{iv}	0.92 (4)	2.19 (4)	3.070 (3)	159 (3)
N4–H4B···O6^{v}	0.88 (4)	2.01 (4)	2.876 (3)	166 (3)
N6–H6B···O12^{i}	0.92 (4)	1.95 (4)	2.861 (3)	174 (3)
N6–H6A···O12	0.93 (4)	2.11 (4)	2.991 (3)	158 (3)
N6–H6A···O3^{vi}	0.93 (4)	2.64 (3)	2.948 (3)	100 (2)
N6–H6C···O1W^{vi}	0.97 (3)	1.91 (3)	2.830 (3)	156 (3)
N7–H7B···O11^{vii}	0.88 (4)	2.18 (4)	3.005 (3)	157 (3)
N7–H7A···N5^{viii}	0.90 (4)	2.10 (4)	2.975 (3)	165 (3)
O1W–H1WB···O6i	0.79 (5)	2.09 (5)	2.870 (3)	173 (5)
N4–H4A···O6^{ix}	0.92 (4)	2.85 (4)	3.310 (3)	112 (3)
O1W–H1WB···O4^{x}	0.79 (5)	2.79 (5)	3.052 (3)	102 (4)

Symmetry code(s): (i) x-1, y, z; (ii) x-1, y+1, z; (iii) x-1, y, z+1; (iv) x+1, y, z-1; (v) x-1, y-1, z-1; (vi) x, y-1, z; (vii) x, y+1, z+1; (viii) x+1, y+1, z+1; (ix) x, y-1, z-1; (x) x, y+1, z.

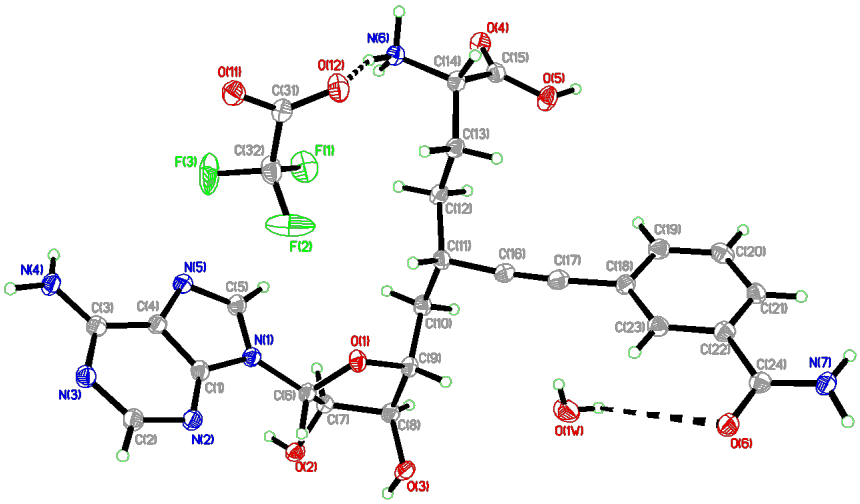

Figure 2.9.5: Perspective views showing 50% probability displacement.

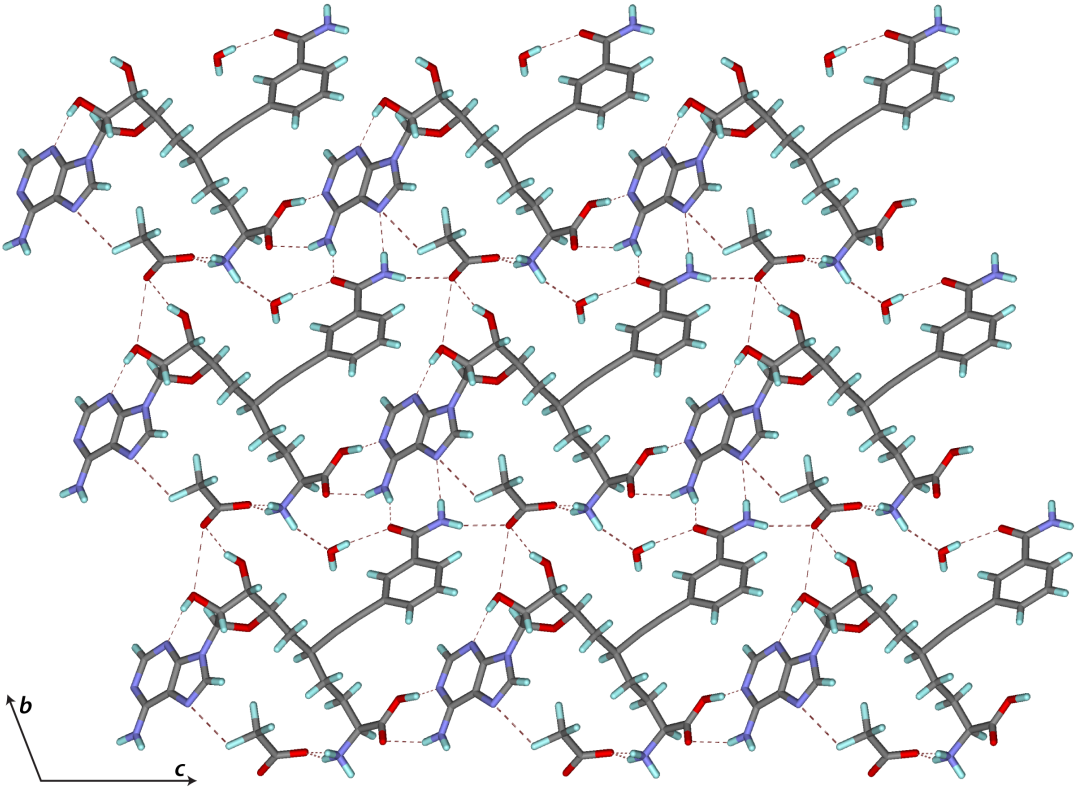

Figure 2.9.6: Three-dimensional supramolecular architecture viewed along the *a*-axis direction.

2.9.10 NNMT Inhibition Assay

wt-hNNMT Preparation

Cloning

The tm-hNNMT plasmid obtained from Addgene (40734; http://n2t.net/addgene:40734; RRID:Addgene_40734) and used in protein crystallography experiments was supplied as a K100A:E101A:E103A mutant. In order to study the wild-type enzyme, we performed site-directed mutagenesis using Agilent's QuikChange Lightning Kit (P/N 210515) to generate a wt-hNNMT plasmid. The following primers were used:

forward: 5'-ggaccagtcaaaggcctctggctctttcttcagccacttctcc-3'

reverse: 5'-ggagaagtggctgaagaaagagccagaggcctttgactggtcc-3'

The wt-hNNMT protein sequence is as follows:

MGSSHHHHHHSSGLVPRGSMESGFTSKDTYLSHFNPRDYLEKYYKFGSRHSAESQILKHLLKNLF
KIFCLDGVKGDLLIDIGSGPTIYQLLSACESFKEIVVTDYSDQNLQELEKWLKKEPEAFDWSPVV
TYVCDLEGNRVKGPEKEEKLRQAVKQVLKCDVTQSQPLGAVPLPPADCVLSTLCLDAACPDLPTY
CRALRNLGSLLKPGGFLVIMDALKSSYYMIGEQKFSSLPLGREAVEAAVKEAGYTIEWFEVISQS
YSSTMANNEGLFSLVARKLSRPL

Protein Expression and Purification

The plasmid containing N-terminally His_6-tagged wt-hNNMT (generated via cloning above) was transformed into NiCo21(DE3) Competent E. coli (New England BioLabs Catalog # C2529H) according to the manufacturer's protocol. Bacteria were subsequently grown up in 1L LB (containing 50 μg/mL kanamycin sulfate and supplemented with 0.5 mM $MgCl_2$ and 0.5 mM $CaCl_2$) at 37 °C, induced with IPTG (1 mM) when they reached an OD_{600} of ~0.8, and incubated overnight at 37 °C.

The following day the cell pellet was harvested by centrifugation and then suspended in 25 mL lysis buffer (*50 mL prepared*: 20 mM Tris-HCl pH 8.0, 0.5 M NaCl, 40 mM imidazole, 1 mM DTT, 20% glycerol, and 1 tablet of Roche cOmplete™ EDTA-containing protease inhibitor cocktail in 50 mL V_{tot}). To the pellet/lysis buffer containing tube were added 10 mg lysozyme and 1 mL DNase and the contents were vortexed briefly

to suspend the cells. The cell suspension was incubated on ice for 30 minutes and then sonicated on ice for 7 minutes (total sonication time) employing a duty cycle of 10/50 sec on/off at 20% power. The crude lysate was clarified by centrifugation and $MgCl_2$ was added to a final concentration of 2 mM (to chelate EDTA and prevent interference Ni-NTA affinity chromatography).

The clarified lysate was purified by automated affinity chromatography using a GE Healthcare ÄKTA chromatography system and a 5 mL GE FF HisTrap Crude Ni-NTA affinity chromatography column. The column was equilibrated with buffer A (40 mM imidazole, 500 mM NaCl, 20 mM Tris-HCl pH 8.0, 1.0 mM DTT, 10% glycerol) and the clarified lysate was loaded via sample application pump. The column was washed with 30 CV (column volumes) buffer A and then a gradient of $0 \rightarrow 100$ % buffer B (500 mM imidazole, 500 mM NaCl, 20 mM Tris-HCl pH 8.0, 1.0 mM DTT, 10% glycerol) was delivered over 20 CV. Eluted fractions corresponding to UV detector peaks were checked by SDS-PAGE analysis and showed clean elution of a single protein at the appropriate MW. Fractions were combined, concentrated, and desalted into storage buffer (20 mM Tris-HCl pH 8.0, 50 mM NaCl, 1 mM DTT, 5% glycerol) via GE HiTrap Desalting column. Fractions were combined, concentrated to 11.4 mg/mL, flash-frozen in liquid nitrogen and stored at –80 °C for future use.

Detailed NNMT Inhibition Assay Protocol

Molecular biology grade water and Tris-HCl buffer (pH 8.0 ± 0.1, 1 M) were obtained from Corning (Manassas, VA). DL-dithiothreitol (DTT, for molecular biology, $\geq$ 98% (HPLC)) and quinoline (reagent grade, 98%) were purchased from Sigma-Aldrich (St. Louis, MO). DTT was used as received, while quinoline was distilled under reduced pressure before use and stored in the dark. *S*-adenosyl-L-methionine was obtained from New England BioLabs (Ipswich, MA) as a 32 mM solution in 0.005 M H_2SO_4 and 10% EtOH and used as received (NEB catalog #: B9003S).

The protocol described below was adapted from those outlined in Neelakantan et al.[32] Enzymatic reactions were performed at room temperature in 96-well plates (costar® black, flat bottom, non-treated, polystyrene, 14.3 mm height). To minimize potential small differences in initial reaction concentrations due to pipetting errors, a master stock consisting of 5 mM Tris-HCl (pH 8.0), 1 mM DTT and 109 μM quinoline was prepared by adding to a 50 mL falcon tube water (50 mL), Tris-HCl pH 8.0 ± 0.1 buffer (1 M, 250.0 μL), DTT (7.7

[32] Neelakantan, H.; Vance, V.; Wang, H.-Y. L.; McHardy, S. F.; Watowich, S. J. *Biochemistry* **2017**, *56*, 824–832.

mg, 50 μmol) and a solution of quinoline in water (20 mM, 272.5 μL). This 50 mL stock was then split into 4 mL stocks.

Using ten PCR tubes of a twelve 0.2 mL tube strip, a dilution series of inhibitor concentrations was prepared. With a multichannel pipette, 10 µL of each of these solutions of inhibitor in water were transferred to the first ten PCR tubes of another twelve 0.2 mL tube strip. The two remaining tubes were charged with 10 µL of water (controls). To each of these tubes was then added 10 µL of a 250 μM solution of SAM in water (prepared by mixing 15.6 µL of a freshly thawed 32 mM SAM solution in 2 mL of water). The reactions were initiated by adding to each tube 230 μL of a 109 nM solution of NNMT in master stock (prepared by adding 1.2 μL of a 362 μM freshly thawed NNMT aliquot in 4 mL of master stock), bringing the final composition of each reaction to 4.6 mM Tris-HCl (pH 8.0), 0.92 mM DTT, 100 μM quinoline, 10 μM SAM and 100 nM NNMT.

Immediately after initiation, the progress of each reaction was monitored using a SpectraMax® i3x multi-mode microplate reader and data were collected approximately every 27 seconds for 5.5 minutes (13 reads, 100 flashes/read, 1.00 mm read height). The production of 1-MQ in each well was monitored by recording fluorescence emission intensities at 400 nm (excitation wavelength at 310 nm) with the detector bandwidths set up at 9 nm for the excitation and at 15 nm for the emission.

2.9.11 Isothermal Titration Calorimetry (ITC)

Rocco L. Policarpo and Samuel Carlson of Harvard MCB performed this experiment jointly. ITC was performed at 25 °C using a MicroCal iTC200 instrument (Malvern). hNNMT was buffer exchanged (via GE HiTrap Desalting column, 5 mL, P/N 29048684) into ITC buffer (50mM $NaPO_4$ pH 8.0, 100 mM NaCl, 0.5 mM TCEP) and diluted to 25 µM. Compound NS1 was also prepared in ITC buffer and diluted to 250 µM. Titration series consisted of a single 0.5 µL injection followed by 14 2.5 µL injections and were conducted in triplicate. A titration of NS1 (**33**) into ITC buffer was also conducted as a control to obtain heats of dilution, which were subtracted from titrations prior to analysis. Binding constants were calculated by fitting the data using the ITC data analysis module in Origin 7 SR4 (OriginLab Corp).

2.9.12 Protein Crystallography

Protein crystallography experiments were performed in collaboration between Rocco L. Policarpo and Elizabeth May of the Gaudet lab of Harvard MCB. The results are published here with permission. Rocco L.

Policarpo provided NS1, expressed and purified NNMT, and helped set crystallization trays. Elizabeth May expressed and purified NNMT, fished crystals, supervised data acquisition, and solved/refined the NS1/NNMT cocrystal structure.

The tm-hNNMT plasmid obtained from Addgene (40734) and used in protein crystallography experiments was supplied as a K100A:E101A:E103A mutant (see Section 2.9.10). These mutations reduce the entropy of surface residues and facilitate crystallization.

The tm-hNNMT protein sequence is as follows:

```
MGSSHHHHHHSSGLVPRGSMESGFTSKDTYLSHFNPRDYLEKYYKFGSRHSAESQILKHLLKNLF
KIFCLDGVKGDLLIDIGSGPTIYQLLSACESFKEIVVTDYSDQNLQELEKWLKAAPAAFDWSPVV
TYVCDLEGNRVKGPEKEEKLRQAVKQVLKCDVTQSQPLGAVPLPPADCVLSTLCLDAACPDLPTY
CRALRNLGSLLKPGGFLVIMDALKSSYYMIGEQKFSSLPLGREAVEAAVKEAGYTIEWFEVISQS
YSSTMANNEGLFSLVARKLSRPL
```

tm-hNNMT Preparation

The pET-28a plasmid containing N-terminally His_6-tagged tm-hNNMT (Addgene) was transformed into BL21(DE3) cells, which were subsequently grown in terrific broth at 37 °C. The cultures were induced with 1 mM IPTG when they reached an OD_{600} of ~1.1 and incubated overnight at 25 °C. Cell pellets were harvested by centrifugation and solubilized in lysis buffer (50 mM Tris-HCl pH 8.0, 0.5 M NaCl, 5 mM imidazole, 2 mM β-mercaptoethanol, 5% glycerol) supplemented with 1 mM PMSF and 1 μg/mL lysozyme. Solubilized cell pellets were centrifuged and the supernatant was loaded onto Ni-NTA Agarose resin (Qiagen), washed with wash buffer (50 mM Tris-HCl pH 8.0, 0.5 M NaCl, 25 mM imidazole, 5% glycerol), and the tm-hNNMT protein was eluted with 50 mM Tris-HCl pH 8.0, 0.5 M NaCl, 250 mM imidazole, and 5% glycerol. Eluted fractions were concentrated and buffer exchanged using a PD-10 desalting column (GE) into NNMT storage buffer (20 mM Tris-HCl pH 8.0, 50 mM NaCl, 1 mM DTT). The final purified protein was concentrated to 18 mg/mL, flash-frozen in liquid nitrogen and stored at –80 °C for future use.

Crystallization and Data Collection

The purified tm-hNNMT was diluted by adding NNMT storage buffer and NS1 formulated in water to final concentrations of 10 mg/mL protein and 1 mM NS1. Co-crystals of tm-hNNMT and NS1 were obtained by sitting drop vapor diffusion at 20 °C with a protein:precipitant volume ratio of 1:1 in 2 µL total volume drops. Crystals appeared after about one week in a precipitant condition containing 100 mM HEPES pH 6.8 and 2 M ammonium sulfate and were harvested about six weeks after setting the drops. Crystals were cryoprotected by briefly soaking in artificial mother liquor to which 16-20% glycerol had been added before flash-freezing in liquid nitrogen. Diffraction data were collected at Beamline ID-24C of the Northeastern Collaborative Access Team (NE-CAT) at the Advanced Photon Source in Argonne, Illinois.

Data Processing and Refinement

The crystals grew in clusters, and our diffraction data had multiple lattices. Images were indexed and integrated with the Diffraction Integration for Advanced Light Sources (DIALS)[33] package using the multi-lattice search functionality within *dials.index*[34]. We searched for three lattices, providing initial unit cell parameters from the published NNMT structure 3ROD[35]. We chose the lattice accounting for the largest number of indexed spots for integration. Data were scaled and merged using the CCP4 suite programs POINTLESS and AIMLESS[36,37,38]. The NS1-bound NNMT structure was determined by molecular replacement with a previous NNMT structure (PDB ID 3ROD; chain A with all ligands removed)[50] as a search model in PHASER as implemented in PHENIX[39]. Subsequent model building and refinement were done in Coot[40] and PHENIX[54]. The asymmetric unit contains four protein chains (A-D) each bound to an NS1 inhibitor molecule. For all analyses and figures, chain A was used. Figures were prepared using PyMOL (Schrödinger)[41]. The diffraction images are available at the SBGrid Data Bank (ID **to be assigned**). The structure factors and refined coordinates are deposited in the Protein Data Bank (PDB ID **to be assigned**).

---

[33] Winter, G. et al. *Acta Crystallogr., Sect. D* **2018**, *74*, 85–97.

[34] Gildea, R. J.; Waterman, D. G.; Parkhurst, J. M.; Axford, D.; Sutton, G.; Stuart, D. I.; Sauter, N. K.; Evans, G.; Winter, G. *Acta Crystallogr., Sect. D* **2014**, *70*, 2652–2666.

[35] Peng, Y.; Sartini, D.; Pozzi, V.; Wilk, D.; Emanuelli, M.; Yee, V. C. *Biochemistry* **2011**, *50*, 7800–7808.

[36] Winn, M. D. et al. *Acta Crystallogr., Sect. D* **2011**, *67*, 235–242.

[37] Evans, P. R. *Acta Crystallogr., Sect. D* **2011**, *67*, 282–292.

[38] Evans, P. R.; Murshudov, G. N. *Acta Crystallogr., Sect. D* **2013**, *69*, 1204–1214.

[39] Adams, P. D. et al. *Acta Crystallogr., Sect. D* **2010**, *66*, 213–221.

[40] Emsley, P.; Lohkamp, B.; Scott, W. G.; Cowtan, K. *Acta Crystallogr., Sect. D* **2010**, *66*, 486–501.

[41] Schrödinger, LLC. The PyMOL Molecular Graphics System, Version 1.8., 2015.

3

SAR and NS1 analogues

3.1 Validation of the Alkynyl Bisubstrate Approach to NNMT Inhibition

The synthesis of NS1 was designed to be highly modular to facilitate a systematic structure-activity analysis of our bisubstrate approach (Figures 3.1.1, 3.2.1, 3.3.1). SAR analysis began with the minimal motif desthia-SAH (**41**) and built up to the full NS1 structure incrementally (Figure 3.1.1). Desthia-SAH, completely lacking an alkynyl-benzamide side chain, was a poor NNMT inhibitor. Addition of an acetylene (**42**) or a phenyl-acetylene (**43**) side chain yielded equally poor NNMT inhibitors. The potency of the parent compound NS1 (**33**) highlights the importance of the benzamide functionality in driving compound potency.

A fundamental aspect of the NS1 design strategy relied on the C6' stereocenter to properly direct the NS1 alkyne toward the NAM binding pocket. Analysis of the NNMT crystal structure (3ROD) suggested that the *S* stereochemistry would best capture the transition state geometry modeled in Figure 2.1.1. Ac-

cordingly, NS1 was a better inhibitor than the NS1-C6' epimer (**44**) by >200-fold in terms of the inhibition constant K_i. The linear vector maintained by the alkynyl linker of NS1 proved optimal; aliphatic NS1 (**45**) was almost 10-fold less potent than NS1 itself (in terms of K_i). The aliphatic NS1 epimer (**46**) and alkynyl epimer **44** had similar pK_i values (6.97 vs. 6.91, respectively). These results may be explained by the shape of the NNMT binding pocket; the narrow width of the methyl transfer tunnel may accommodate linear alkynyl geometry better than a staggered aliphatic chain. Furthermore, the rigidity of the alkynyl linker could lower the entropic cost of binding relative to alkane containing analogues.

More drastic structural modifications to the NS1 scaffold included excision of the entire amino acid side chain (**47**) or the entire adenine nucleobase (**49**). Compound **47**, a simplified bisubstrate inhibitor designed to target the adenosine and NAM binding pockets of NNMT, was a weaker inhibitor than NS1 by ~500-fold in terms of K_i. Attempts to improve the inhibitory activity of **47** by conformational restriction (via the installation of a cyclopropyl group; **48**) proved detrimental. Removal of the adenine nucleobase (**49**) completely abrogated NNMT inhibition.

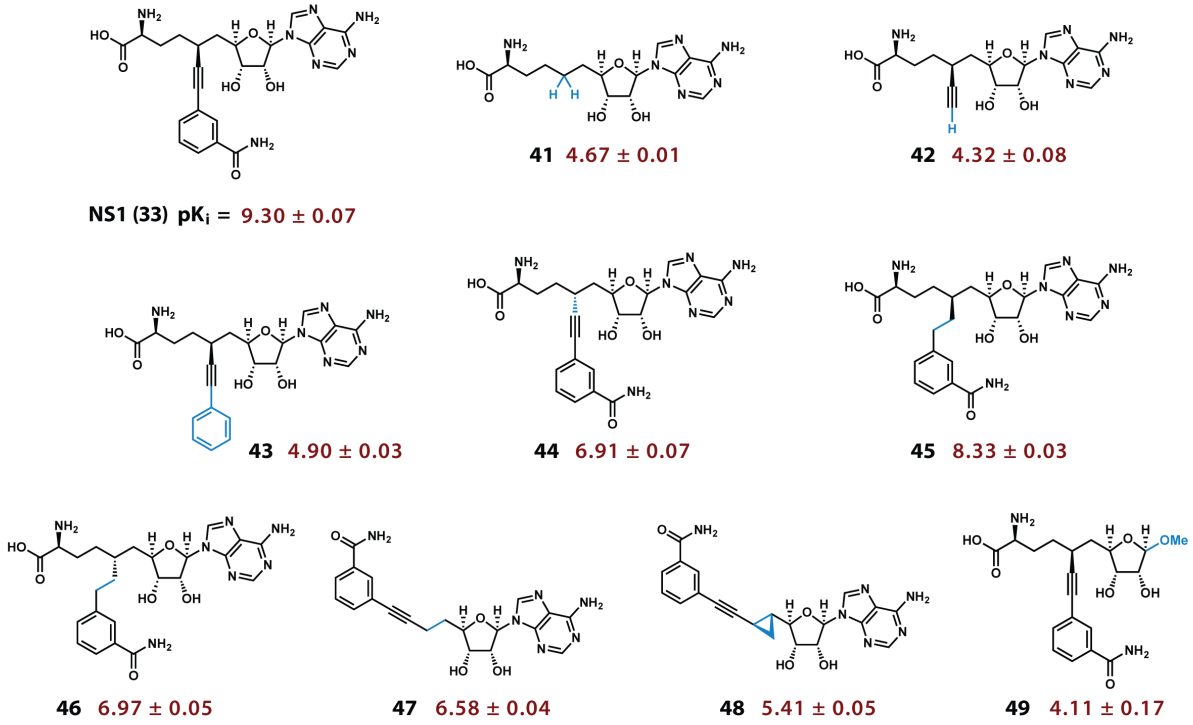

Figure 3.1.1: Structure-activity relationship (SAR) studies of bisubstrate NNMT inhibitors: Exploration of the alkynyl bisubstrate approach to NNMT inhibition. K_i values are presented as pK_i ($-\log_{10}K_i$) to facilitate comparison between inhibitors of widely varying potency.

3.2 Amino Acid Modification

Alteration of the NS1 amino acid (Figure 3.2.1) revealed the C17' (refer to Section 2.9.5 for numbering scheme) amino group of NS1 to be critical for inhibition, as compound **50** (lacking the C17' amine) was a poor NNMT inhibitor. Removal of the carboxylic acid was better tolerated, as compound **51** (which retains the C17' amine) had a pK_i of 7.24 ± 0.02. Amide- (**52**) and methyl ester-containing (**53**) analogues were poor NNMT inhibitors (5.98 ± 0.01 and 6.36 ± 0.08, respectively), while amino-amide- (**54**) or urea-containing (**55**) analogues were slightly better (7.77 ± 0.02 and 7.12 ± 0.05, respectively). These results are consistent with the structural features of **54** and **55**, as both contain the same number of potential hydrogen-bonding groups as NS1 and native substrate SAH (although differing slightly in their donor/acceptor capacities and positions). Compound **52** has one fewer hydrogen-bonding atom than NS1. In **53**, the methyl ester likely adds too much bulk to fit in the amino acid pocket while also decreasing the hydrogen bonding ability of the amino acid carboxylate.

Only one side chain modification yielded a more potent compound than NS1: the addition of a single methylene unit in the NS1 backbone (**56**, homo-NS1). Homo-NS1 had a pK_i of 9.62 ± 0.05 (compared to NS1 with pK_i = 9.30 ± 0.07), indicating a ∼2-fold increase in inhibitory activity in terms of K_i. This finding is consistent with prior reports showing that the addition of a methylene unit in amino-bisubstrate NNMT inhibitors can improve potency.[1] We also synthesized and tested previously reported compounds MS2734 and MS2756 (Figure 3.4.1). In our hands, MS2734–a one-carbon chain-extended homologue of MS2756–was a 10-fold better inhibitor than MS2756 in terms of K_i (pK_i of 7.05 ± 0.01 vs. 6.04 ± 0.06). The benefit of an extra methylene group in bisubstrate inhibitors could arise because an added methylene better mimics the longer C–S bonds of the native substrates. The trimethylene linker of homo-NS1 (**56**) would also be more flexible than the dimethylene linker of NS1 (**33**), which may allow the molecule more room to optimally satisfy hydrogen bonds between the amino acid, benzamide, ribose and adenine moieties to the NNMT binding pocket.

[1] Babault, N.; Allali-Hassani, A.; Li, F.; Fan, J.; Yue, A.; Ju, K.; Liu, F.; Vedadi, M.; Liu, J.; Jin, J. *J. Med. Chem.* **2018**, *61*, 1541–1551.

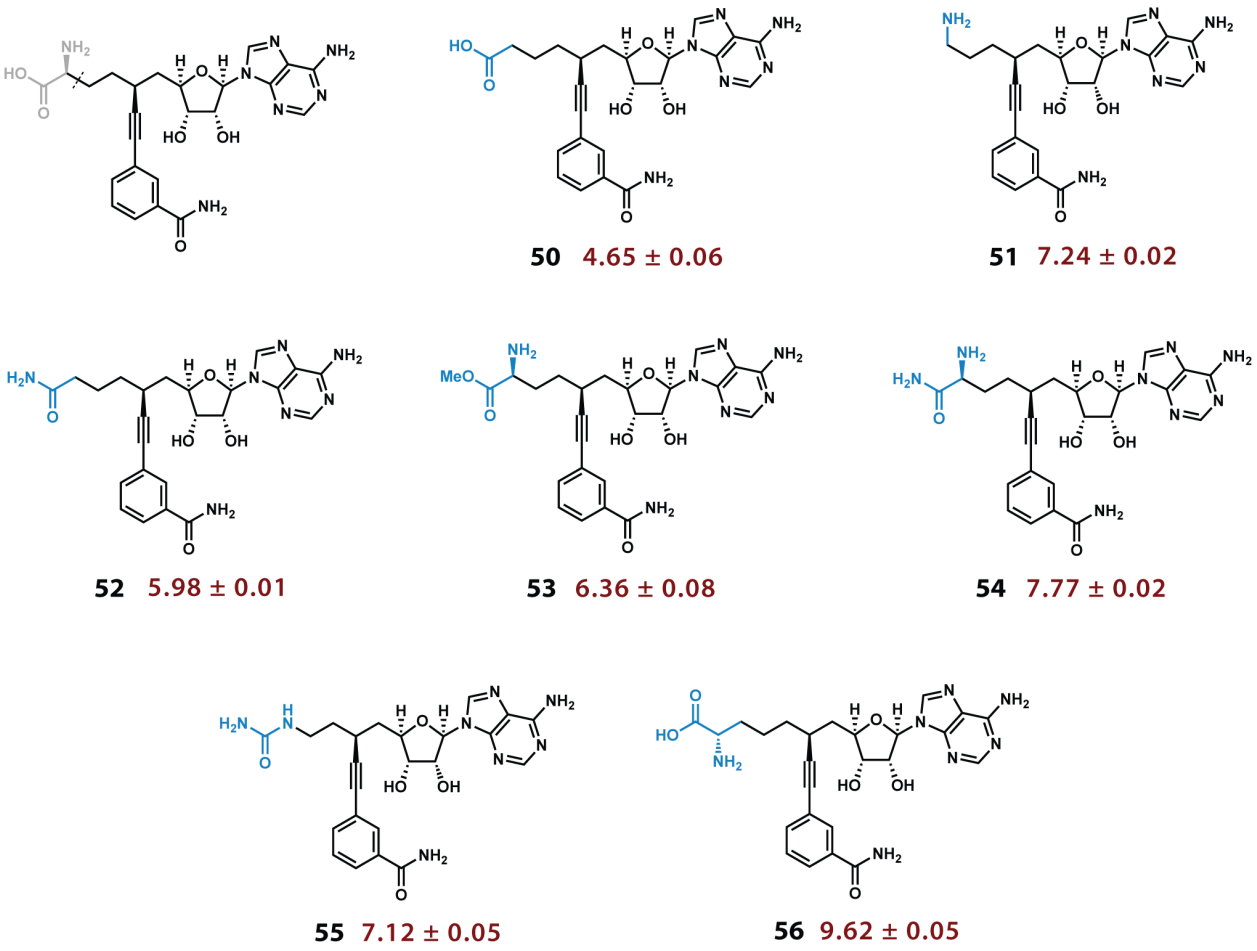

Figure 3.2.1: Structure-activity relationship (SAR) studies of bisubstrate NNMT inhibitors: Amino acid modifications. K_i values are presented as pK_i ($-\log_{10}K_i$) to facilitate comparison between inhibitors of widely varying potency.

3.3 Aryl Modification

After examining the impact of side chain modifications on inhibitor potency, we tested the effects of aryl group modification. We purposely designed the NS1 synthesis to accommodate a late-stage Sonogashira cross-coupling reaction to allow for easy introduction of a desired aryl moiety late in our synthesis. Leveraging this capability, we prepared gram quantities of intermediate **39** (Figure 2.5.1) and synthesized a variety of aryl substituted NS1 analogues (Figure 3.3.1).

These studies revealed that proper positioning of an amide group on NS1 is essential for NNMT binding, as para-benzamide (**57**), ortho-benzamide (**58**), and sulfonamide (**59**) substituted NS1 analogues were much less potent than NS1. We designed fluorine (**60**), methyl (**61**), trifluoromethyl (**62**), and chlorine (**63**) containing analogues to 1) bind a small hydrophobic pocket in the nicotinamide binding site, 2) mod-

ulate the pK_a of the NS1 benzamide group through inductive effects, and 3) potentially alter the rotation of the NS1 amide relative to the NS1 benzamide phenyl ring. While **60**, **61**, and **62** were potent NNMT inhibitors (pK_i > 8.0), only chloro-substitution (**63**) yielded a more potent NNMT inhibitor than NS1 (pK_i = 9.72 ± 0.15). As shown in Figure 3.4.3a, there is a small hydrophobic region in the NAM binding pocket para to the alkyne of the NS1 scaffold. The small, hydrophobic chlorine atom of **63** likely makes Van der Waals contacts with this region, providing additional binding affinity. It is also well poised to engage in halogen-bonding[2],[3] with a nearby tyrosine residue (T242).

After interrogating ring substitution at the para-position, we attempted to restrict rotation of the NS1 amide by converting the benzamide moiety to a benzolactam (Figure 3.3.1, **64** and **65**). Benzolactams **64** and **65** were moderate NNMT inhibitors, with a six-membered ring (**64**) better tolerated than a five-membered ring (**65**). We also examined C13'/C14' substitution with methylenedioxy analogue **66** (pK_i = 7.49 ± 0.05) or introduced a heterocyclic nitrogen atom (to better mimic NAM, **67**, **68**, **69**, **70**). Compounds **66**-**70** all had pK_i values below that of NS1, demonstrating that C13'/C14' substitution or inclusion of a nitrogen atom are not beneficial in these cases. Lastly, we designed and synthesized amino naphthalene derivative **71** (a bisubstrate analogue of the previously reported NNMT inhibitor 5-amino-1-methylquinolinium[4]), but **71** was also a poor inhibitor (pK_i = 5.43 ± 0.07).

---

[2] Wilcken, R; Zimmermann, M. O.; Lange, A; Joerger, A. C.; Boeckler, F. M. *Journal of Medicinal Chemistry* **2013**, *56*, 1363–1388.

[3] Matter, H; Nazare, M; Gussregen, S; Will, D. W.; Schreuder, H; Bauer, A; Urmann, M; Ritter, K; Wagner, M; Wehner, V *Angew. Chem. Int. Ed.* **2009**, *48*, 2911–2916.

[4] Neelakantan, H.; Vance, V.; Wetzel, M. D.; Wang, H.-Y. L.; McHardy, S. F.; Finnerty, C. C.; Hommel, J. D.; Watowich, S. J. *Biochemical Pharmacology* **2018**, *147*, 141–152.

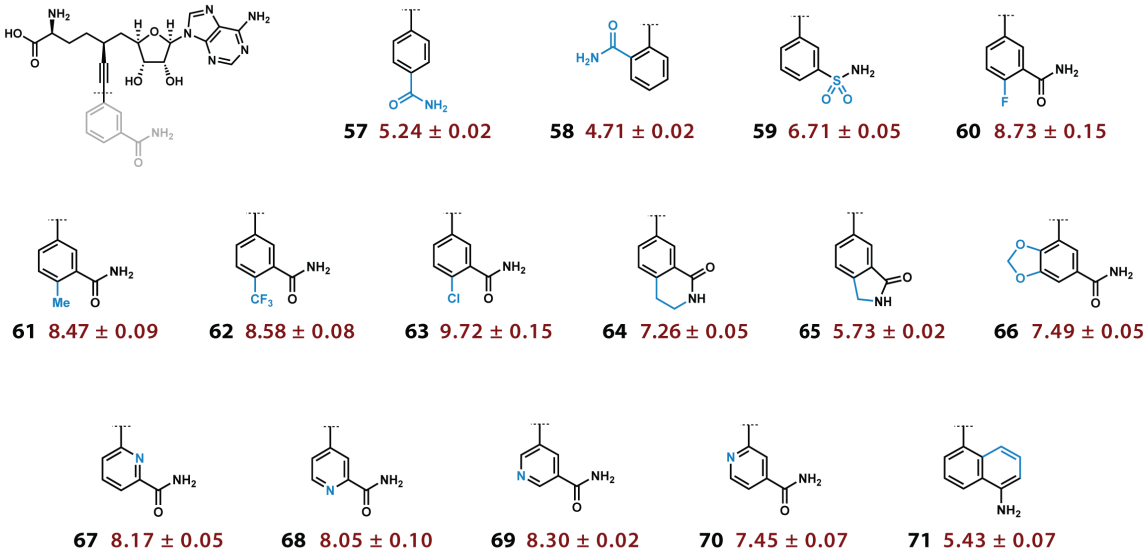

Figure 3.3.1: SAR studies of NNMT inhibitors: Modification of the benzamide moiety of NS1.

3.4 Aliphatic-NS1 vs. Amino-Bisubstrate Inhibitor MS2756

In the final stage of our SAR analysis we compared our inhibitors with previously reported amino bisubstrate NNMT inhibitors (Figure 3.4.1). Previously reported compounds VH45[5] , MS2756, and MS2734[6] use a tertiary amine core and an alkyl tether to link a SAM-like fragment to a NAM-like fragment. An alignment of NS1-bound NNMT with MS2756-bound NNMT shows the similar binding modes of the two compounds (Figure 3.4.2). We synthesized and tested all three of these compounds alongside aliphatic-NS1 (**45**, Figure 3.1.1) using the same assay protocols and kinetic analyses to determine K_i values. We compared MS2756 and aliphatic-NS1 *directly* because they are close structural analogues in which the tertiary amine core of MS2756 has been replaced with an sp^3 hybridized carbon stereocenter. These studies revealed that aliphatic-NS1 was approximately 200-fold more potent than MS2756 in terms of K_i.

[5] Van Haren, M. J.; Taig, R.; Kuppens, J.; Sastre Toraño, J.; Moret, E. E.; Parsons, R. B.; Sartini, D.; Emanuelli, M.; Martin, N. I. *Org. Biomol. Chem.* **2017**, *15*, 6656–6667.

[6] Babault, N.; Allali-Hassani, A.; Li, F.; Fan, J.; Yue, A.; Ju, K.; Liu, F.; Vedadi, M.; Liu, J.; Jin, J. *J. Med. Chem.* **2018**, *61*, 1541–1551.

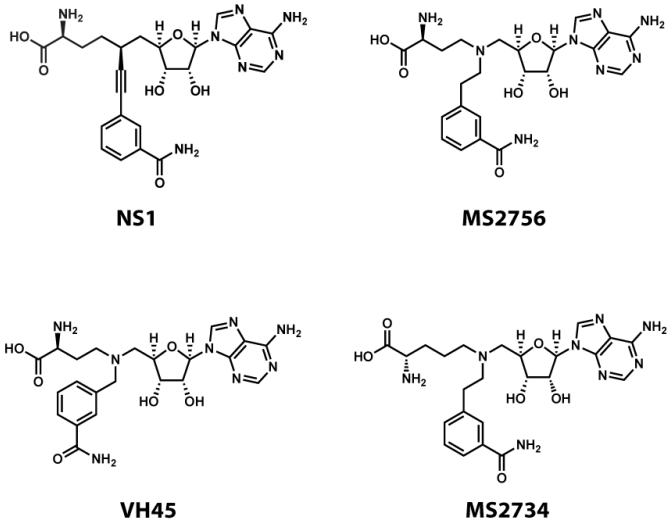

Figure 3.4.1: Comparison of alkynyl bisubstrate inhibitor NS1 to previously published inhibitors MS2756, VH45, and MS2734.

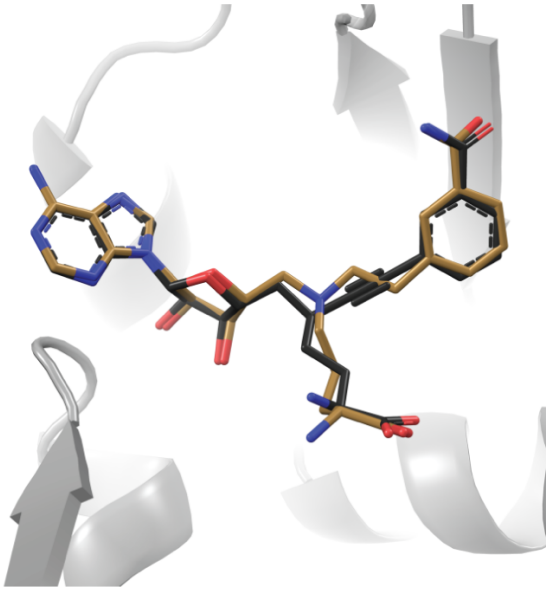

Figure 3.4.2: MS2756-bound NNMT (brown; PDB ID 6B1A) superimposed on NS1-bound NNMT.

The contrast between the observed activity of MS2756 and aliphatic-NS1 is noteworthy; changing a single non-hydrogen atom (tertiary nitrogen to sp^3 carbon stereocenter) substantially alters compound potency. We hypothesize that a variety of factors could be responsible for this observation. It is evident that the stereochemical definition at the C6' stereocenter of aliphatic-NS1 is beneficial as evidenced by the ~20-fold difference in K_i between aliphatic-NS1 and its C6' epimer (**46**). A much larger difference (~250-fold) in

K_i between NS1 and its C6' epimer (**44**) was also observed, demonstrating that as linker rigidity increases, C6' stereodefinition becomes more important.

While aliphatic-NS1 and NS1 both show large differences in K_i values between their C6' stereoisomers, the tertiary nitrogen atom in MS2756 maintains sp^3 tetrahedral geometry but is free to invert rapidly at room temperature. In solution, we imagine that aliphatic-NS1 and NS1 assume the optimal tetrahedral geometry at C6' necessary for binding, whereas MS2756 is free to occupy conformations that are unproductive for binding because of nitrogen inversion. It is also likely that the hydrophobic, carbon-based scaffolds of aliphatic-NS1 and NS1 are preferred over the polar, tertiary amine core of MS2756. Aliphatic-NS1 and NS1 likely form favorable Van der Waals contacts with the NNMT active site, as the closest residue to the aliphatic-NS1/NS1 C6' carbon stereocenter is F15 (~4 Å away). This phenylalanine residue presents a large hydrophobic[7] surface in the NNMT ligand binding pocket (Figure 3.4.3), near the aliphatic-NS1/NS1 C6' stereocenter.

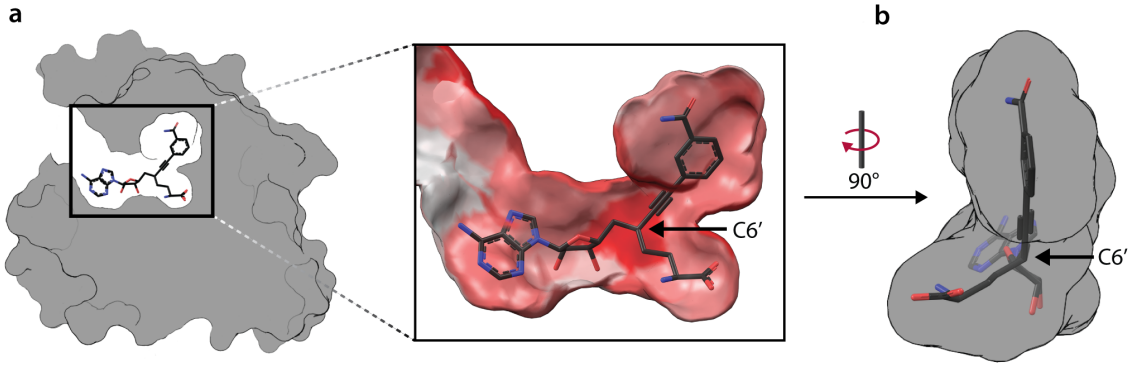

Figure 3.4.3: The chemical properties and geometry of NS1 closely match the hydrophobic profile and shape of the NNMT binding pocket. (a) The binding pocket is buried in the hydrophobic core of the protein (gray). (Inset) A solvent-accessible surface representation of the binding pocket colored by the Eisenberg hydrophobicity scale reveals a hydrophobic patch (dark red) that contacts the C6' carbon atom of NS1. (b) A side-on view shows that the binding pocket has shape complementarity specific to the *S* diastereomer of NS1 at the C6' carbon.

Finally, the transition state structure of PNMT, the second closest homologue of NNMT, involves even

[7] Eisenberg, D; Schwarz, E; Komaromy, M; Wall, R *Journal of Molecular Biology* **1984**, *179*, 125–142.

distribution of positive charge along the entire axis of methyl transfer.[8] If NNMT has a transition state structure similar to that of PNMT, analogues like MS2756, which localize positive charge on a single nitrogen atom, do not accurately capture the transient electrostatics of the methyl transfer transition state. While not positively charged, carbon-based linkers avoid the localized positive charge of MS2756 and other amino-bisubstrate inhibitors.

3.5 Experimental Details

General procedures, materials, instrumentation, and positional numbering system are identical to those presented in Chapter 2. General experimental protocols for small molecule X-ray crystallography of **S24** and **S30** are identical to protocols used for NS1 (**33**). Work on the Structure-Activity Relationships (SAR) of NNMT inhibitors was done in collaboration with Dr. Ludovic Decultot of Harvard University CCB. Several compounds synthesized by Dr. Decultot are presented in Figures 3.1.1, 3.2.1, and 3.3.1 and are included in this work with permission. Dr. Decultot prepared compounds 44-46, 50-54, 56-58, 61, 63-65, and 67-71. Full characterization data and synthetic schemes for these compounds are not included in this Dissertation, but have been published online in the ChemRxiv under *Supporting Information Part 1*. All other compounds were prepared by the author Rocco L. Policarpo unless otherwise noted.

[8] Stratton, C. F.; Poulin, M. B.; Du, Q.; Schramm, V. L. *ACS Chem. Biol* **2017**, *12*, 13.

3.5.1 (**41**) Desthia-SAH

Synthetic Scheme

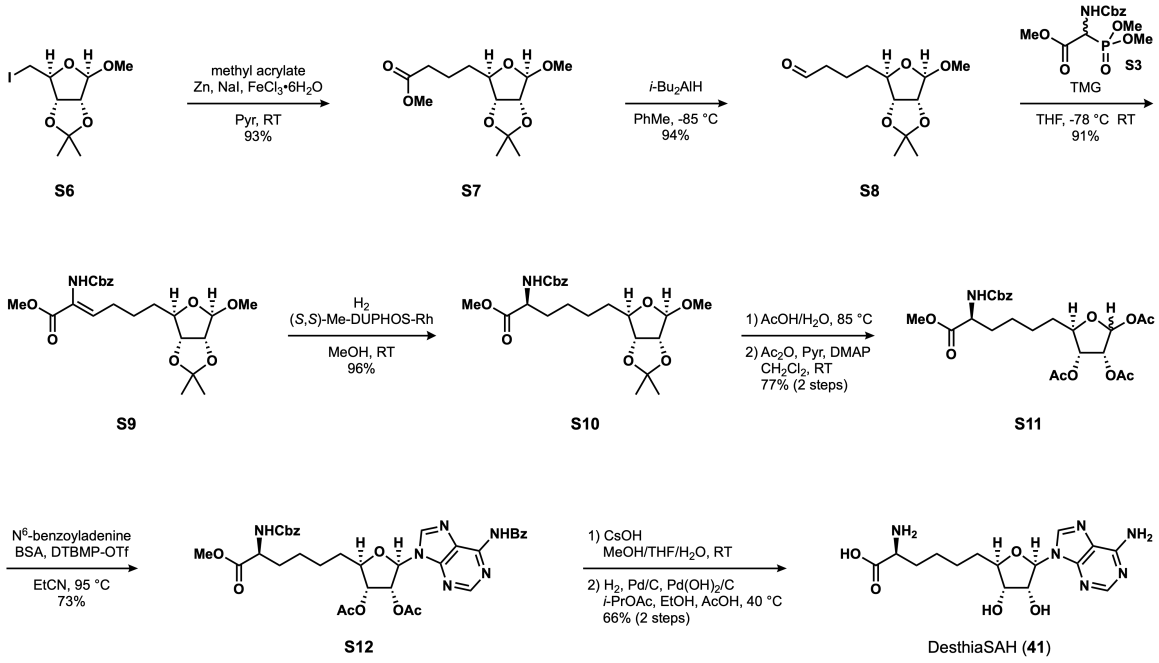

Methyl Ester **S7**[9]

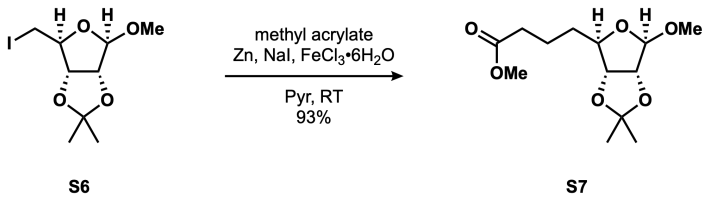

To a 3-necked flask charged with pyridine (10 mL) were added NaI (1.49 g, 10.0 mmol, 1.0 equiv.) and $FeCl_3 \cdot 6H_2O$ (1.35 g, 5.00 mmol, 50 mol %) sequentially, both in one portion. Zinc powder (3.92 g, 60.0 mmol, 6.0 equiv.) was added portionwise to the reaction mixture (⚠ **Caution, exothermic** ⚠), monitoring the temperature so that it remains below 40 °C. Upon complete addition of the zinc powder, the resulting

[9] Blanchard, P.; Da Silva, A. D.; El Kortbi, M. S.; Fourrey, J. L.; Robert-Gero, M. *J. Org. Chem.* **1993**, *58*, 6517–6519.

mixture was allowed to cool gradually to RT and a solution of riboside **S6**[10] (3.14 g, 10.0 mmol) in methyl acrylate (6.0 mL) was added over 10 min *via* syringe. The reaction mixture was stirred at RT for 2 h, before the addition of toluene (100 mL) and filtration over celite. Volatiles were removed *in vacuo* to give methyl ester **S7** (2.52 g, 9.25 mmol, 93%) which was of suitable purity to be used in the next step without further purification.

R_f = 0.42 (cyclohexane/EtOAc, 67:33);

FTIR (thin film), cm^{-1}: ν_{max} 2989, 2940, 1735, 1437, 1372, 1270, 1239, 1208, 1194, 1159, 1090, 1057, 1011;

^{1}H NMR (600 MHz, $CDCl_3$): δ 4.94 (s, 1H), 4.59 (d, J = 5.9 Hz, 1H), 4.52 (dd, J = 5.9, 1.1 Hz, 1H), 4.13 (ddd, J = 8.9, 6.4, 1.1 Hz, 1H), 3.67 (s, 3H), 3.34 (s, 2H), 2.35 (td, J = 7.4, 1.4 Hz, 2H), 1.86 – 1.76 (m, 1H), 1.71 (ddtd, J = 13.2, 10.1, 7.3, 5.7 Hz, 1H), 1.62 (dddd, J = 14.1, 10.1, 8.9, 5.1 Hz, 1H), 1.53 (ddt, J = 13.4, 10.4, 6.0 Hz, 1H), 1.47 (s, 3H), 1.31 (s, 3H);

^{13}C NMR (151 MHz, $CDCl_3$): δ 173.5, 112.1, 109.5, 86.7, 85.5, 84.1, 54.9, 51.4, 34.4, 33.5, 26.4, 24.9, 21.7;

HRMS (ESI+): calcd. for $[C_{13}H_{22}O_6Na]^+$ 297.1309, meas. 297.1307, Δ 0.7 ppm.

ALDEHYDE **S8**

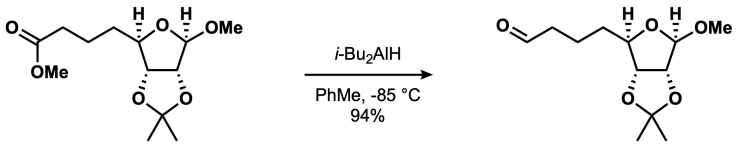

S7 **S8**

---

[10] Li, W.; Niu, Y.; Xiong, D.-C.; Cao, X.; Ye, X.-S. *J. Med. Chem.* **2015**, *58*, 7972–7990.

To an oversized flask (250 mL) containing a solution of methyl ester **S7** (2.15 g, 7.83 mmol) in toluene (20 mL) at –85 °C (*i*-PrOH/liquid nitrogen bath) was added *i*-Bu_2AlH (1.0 M in hexanes, 8.0 mL, 8.0 mmol, 1.02 equiv.) over 40 minutes *via* syringe pump, down the side-wall of the flask. Upon complete addition of *i*-Bu_2AlH, the reaction mixture was stirred at –85 °C for 1 h, before the slow addition of MeOH (4 mL) over 20 min down the side-wall of the flask, followed by a potassium sodium tartrate sat. aq. solution (40 mL) and EtOAc (50 mL). The reaction mixture was removed from the cooling bath and allowed to warm gradually to RT. Water (10 mL) and brine (10 mL) were added, and the biphasic mixture was stirred for another 10 min. The layers were separated and the aqueous phase was extracted with EtOAc (3 × 50 mL). The combined organic extracts were washed with brine (200 mL), dried over $MgSO_4$, filtered and concentrated to give aldehyde **S8** (1.80 g, 7.37 mmol, 94%) as a light yellow oil which was of suitable purity to be used in the next step without further purification.

R_f = 0.31 (cyclohexane/EtOAc, 67:33);

FTIR (thin film), cm^{-1}: ν_{max} 2988, 2938, 2832, 2723, 1724, 1457, 1412, 1381, 1372, 1273, 1240, 1209, 1193, 1160, 1087, 1058, 1018;

^{1}H NMR (600 MHz, $CDCl_3$): δ 9.73 (t, J = 1.6 Hz, 1H), 4.89 (s, 1H), 4.55 (d, J = 6.0 Hz, 1H), 4.48 (dd, J = 6.0, 1.1 Hz, 1H), 4.09 (ddd, J = 9.0, 6.3, 1.1 Hz, 1H), 3.30 (s, 3H), 2.45 (dddd, J = 8.7, 7.1, 3.4, 1.6 Hz, 2H), 1.81–1.71 (m, 1H), 1.72–1.63 (m, 1H), 1.59 (dtd, J = 13.6, 9.2, 5.2 Hz, 1H), 1.49 (ddt, J = 13.5, 10.1, 6.1 Hz, 1H), 1.43 (s, 3H), 1.27 (s, 3H);

^{13}C NMR (151 MHz, $CDCl_3$): δ 202.0, 112.3, 109.6, 86.8, 85.5, 84.1, 55.1, 43.4, 34.4, 26.6, 25.0, 18.9;

ENAMIDE **S9**

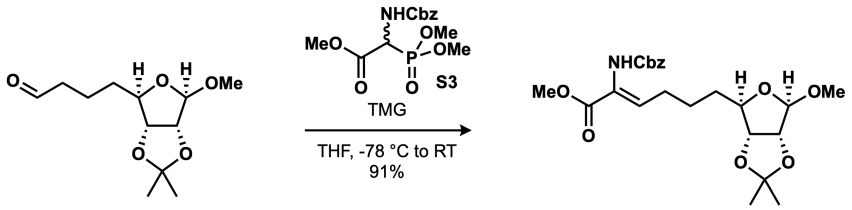

S8 **S9**

To a stirred suspension of (±)-Cbz-*α*-phosphonoglycine trimethyl ester[11] (**S3**) (343 mg, 1.04 mmol, 1.2 equiv.) in THF (3.0 mL) at –78 °C was added 1,1,3,3-tetramethylguanidine (0.12 mL, 0.95 mmol, 1.1 equiv.). The resulting mixture was stirred at –78 °C for 15 min, before the addition of a solution of aldehyde **S8** (211 mg, 0.864 mmol) in THF (2.0 mL). The reaction mixture was stirred at –78 °C for 30 min and then placed in an ice/water bath and stirred for 1 h. The reaction was quenched by the addition of a 10% AcOH aq. solution (2 mL) and water (10 mL) was added. The layers were separated and the aqueous phase was extracted with CH_2Cl_2 (3 × 15 mL). The combined organic extracts were washed with water (10 mL) and brine (10 mL), dried over $MgSO_4$, filtered and concentrated. ^{1}H NMR analysis of the crude revealed a 15:1 mixture of *Z* and *E* isomers. Crude material was purified by silica gel chromatography (2,2,4-trimethylpentane/EtOAc, 0 → 50%). *Z* and *E* isomers separated and only fractions containing *Z* isomers were collected to afford enamide **S9** (353 mg, 0.785 mmol, 91 %) as a clear viscous oil.

R$_f$ = 0.44 (cyclohexane/EtOAc, 50:50);

FTIR (thin film), cm^{-1}: ν_{max} 3316, 2988, 2942, 1716, 1657, 1500, 1455, 1437, 1381, 1373, 1270, 1213, 1160, 1105, 1089, 1047;

^{1}H NMR (600 MHz, $CDCl_3$): δ 7.41–7.30 (m, 5H), 6.61 (t, *J* = 7.2 Hz, 1H), 5.14 (s, 2H), 4.93 (s, 1H), 4.58 (d, *J* = 5.9 Hz, 1H), 4.49 (d, *J* = 5.9 Hz, 1H), 4.12 (dd, *J* = 8.3, 6.3 Hz, 1H), 3.75 (s, 3H), 3.33 (s, 3H), 2.31–2.18 (m, 2H), 1.68–1.48 (m, 4H), 1.47 (s, 3H), 1.30 (s, 3H);

[11] (±)-Cbz-*α*-phosphonoglycine trimethyl ester, CAS: 88568-95-0, was purchased from Chem-Impex International, Inc. (catalog #: 14125).

^{13}C NMR (151 MHz, $CDCl_3$): δ 165.1, 137.5, 136.1, 128.6, 128.3, 128.2, 112.3, 109.6, 86.9, 85.6, 84.2, 67.4, 55.0, 52.5, 34.7, 28.1, 26.6, 25.1;

HRMS (ESI+): calcd. for $[C_{23}H_{32}NO_8]^+$ 450.2122, meas. 450.2124, Δ 0.3 ppm.

Protected Amino Acid **S10**

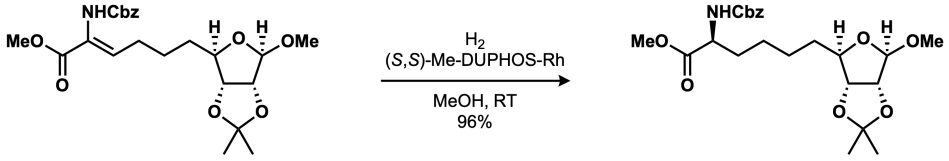

S9 **S10**

To a flask charged with enamide **S9** (179 mg, 0.398 mmol, exclusively *Z* isomer) was added MeOH (5 mL) at RT under a nitrogen atmosphere. The contents were stirred until full dissolution was noted. Separately, $[Rh(nbd)_2]BF_4$[12] (49 mg, 0.12 mmol, 30 mol %) and (*S*,*S*)-Me-DUPHOS[13] (43 mg, 0.14 mmol, 35 mol %) were weighed out into the same vial in a glove box. The vial was removed from the glove box, placed under a nitrogen atmosphere and MeOH (10 mL) was added. The flask headspace was evacuated and backfilled with hydrogen (3 ×). The methanolic solution of enamide **S9** was transferred to the vial containing the catalyst (2 mL of MeOH used for vial rinse) and the contents were stirred vigorously at RT under a hydrogen atmosphere (balloon) for 1 h. Volatiles were removed *in vacuo* and crude material was purified by silica gel chromatography (2,2,4-trimethylpentane/EtOAc, 0 → 50%) to afford protected amino acid **S10** (172 mg, 0.381 mmol, 96%) as a clear viscous oil and as a single diastereomer.

R_f = 0.32 (cyclohexane/EtOAc, 67:33);

---

[12] $[Rh(nbd)_2]BF_4$, CAS: 36620-11-8, was obtained from Strem Chemicals, Inc. (catalog #: 45-0230).

[13] (+)-1,2-Bis((2*S*,5*S*)-2,5-dimethylphospholano)benzene, CAS: 136735-95-0, was obtained from Strem Chemicals, Inc. (catalog #: 15-0092).

FTIR (thin film), cm^{-1}: ν_{max} 3338, 2988, 2939, 2862, 1720, 1523, 1455, 1439, 1381, 1373, 1348, 1259, 1239, 1209, 1161, 1106, 1087, 1056, 1026;

^{1}H NMR (600 MHz, $CDCl_3$): δ 7.38–7.28 (m, 5H), 5.31 (d, J = 8.4 Hz, 1H), 5.09 (s, 2H), 4.92 (s, 1H), 4.57 (d, J = 5.9 Hz, 1H), 4.48 (d, J = 6.0 Hz, 1H), 4.37 (td, J = 8.0, 5.1 Hz, 1H), 4.10 (dd, J = 8.9, 5.8 Hz, 1H), 3.73 (s, 3H), 3.31 (s, 3H), 1.88–1.79 (m, 1H), 1.64 (app. h, J = 8.1 Hz, 1H), 1.58 (app. q, J = 8.8 Hz, 1H), 1.49–1.43 (m, 2H), 1.46 (s, 3H), 1.40–1.32 (m, 3H), 1.30 (s, 3H);

^{13}C NMR (151 MHz, $CDCl_3$): δ 173.0, 155.9, 136.3, 128.5, 128.2, 128.1, 112.2, 109.4, 87.0, 85.6, 84.1, 67.0, 54.9, 53.8, 52.3, 34.8, 32.6, 26.5, 25.8, 25.0;

HRMS (ESI+): calcd. for $[C_{23}H_{34}NO_8]^+$ 452.2280, meas. 452.2285, Δ 1.1 ppm.

Triacetate **S11**

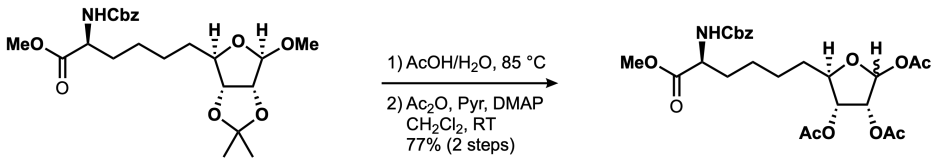

S10 **S11**

To a vial charged with acetonide **S10** (171 mg, 0.378 mmol) was added a 4:1 mixture of acetic acid and water (7.5 mL) at RT. The resulting mixture was stirred at 85 °C for 8 h. Volatiles were removed *in vacuo* and the residue was dried by azeotropic distillation with benzene (1 × 10 mL). Crude material was used directly in the next step without further purification.

To a solution of the crude triol in CH_2Cl_2 (4.0 mL) at RT, were added pyridine (0.50 mL, 6.2 mmol, 16 equiv.), Ac_2O (0.50 mL, 5.3 mmol, 14 equiv.) and DMAP (5 mg, 0.04 mmol, 0.11 equiv.) sequentially. The resulting mixture was stirred at RT for 2 h and the volatiles were removed *in vacuo*. Crude material was purified by silica gel chromatography (2,2,4-trimethylpentane/EtOAc, 0 → 100%) to afford triacetate **S11**

(152 mg, 0.290 mmol, 77% over 2 steps) as a *ca.* 1:1 mixture of α and β anomers as a colorless oil.

$\mathbf{R_f}$ = 0.28 (α-anomer)/0.37 (β-anomer) (EtOAc);

FTIR (thin film), cm^{-1}: ν_{max} 3359, 2950, 1743, 1721, 1523, 1455, 1437, 1371, 1216, 1110, 1047, 1010;

^{1}H NMR (600 MHz, $CDCl_3$): δ α-anomer: 7.38–7.27 (m, 5H), 6.34 (d, J = 4.6 Hz, 1H), 5.29 (d, J = 8.2 Hz, 1H), 5.18 (dd, J = 6.8, 4.6 Hz, 1H), 5.09 (s, 2H), 5.01 (dd, J = 6.8, 3.6 Hz, 1H), 4.35 (td, J = 7.8, 5.1 Hz, 1H), 4.20–4.15 (m, 1H), 3.73 (s, 3H), 2.10 (s, 3H), 2.09 (s, 3H), 2.05 (s, 3H), 1.83–1.77 (m, 1H), 1.69–1.54 (m, 3H), 1.47–1.42 (m, 1H), 1.39–1.28 (m, 3H); β-anomer: 7.38–7.28 (m, 5H), 6.10 (d, J = 1.1 Hz, 1H), 5.31 (d, J = 8.1 Hz, 1H), 5.29 (dd, J = 4.8, 1.2 Hz, 1H), 5.14 (dd, J = 6.9, 4.8 Hz, 1H), 5.10 (s, 2H), 4.36 (td, J = 7.8, 5.0 Hz, 1H), 4.12 (td, J = 7.4, 5.2 Hz, 1H), 3.73 (s, 3H), 2.10 (s, 3H), 2.07 (s, 3H), 2.05 (s, 3H), 1.85–1.78 (m, 1H), 1.68–1.55 (m, 2H), 1.51–1.42 (m, 1H), 1.40–1.29 (m, 4H);

^{13}C NMR (126 MHz, $CDCl_3$): δ mixture of α and β-anomers: 172.9, 170.2, 169.8, 169.4, 155.9, 136.3, 128.6, 128.2, 128.2, 98.3, 94.0, 83.3, 81.4, 74.6, 73.6, 72.3, 69.9, 67.0, 53.8, 52.4, 33.8, 33.1, 32.5, 25.0, 25.0, 24.9, 24.8, 21.1, 21.1, 20.7, 20.6, 20.6, 20.4;

HRMS (ESI+): calcd. for $[C_{25}H_{34}NO_{11}]^+$ 524.2126, meas. 524.2134, Δ 1.5 ppm.

Nucleoside **S12**

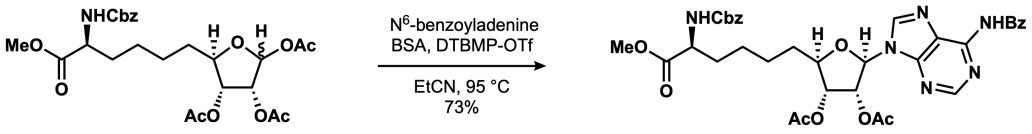

S11 **S12**

To a suspension of N^6-benzoyladenine (149 mg, 0.624 mmol, 2.15 equiv.) in propionitrile (dried over 4 Å M.S., 6.0 mL) at RT, was added *N,O*-bis(trimethylsilyl)acetamide (0.21 mL, 0.87 mmol, 3.00 equiv.). The

resulting mixture was stirred at 95 °C for 10 min, upon which complete solubilization of N^6-benzoyladenine was observed. To a separate flask charged with triacetate **S11** (152 mg, 0.290 mmol) and 2,6-di-*tert*-butyl-4-methylpyridinium triflate (21 mg, 58 μmol, 20 mol %) was added propionitrile (6.0 mL). The resulting mixture was stirred at RT for 5 min, until a clear solution was obtained. This clear solution was added to the solution of silylated N^6-benzoyladenine. The reaction mixture was stirred at 95 °C for 2.5 h, cooled to RT and the volatiles were removed *in vacuo*. Crude material was purified by silica gel chromatography (2,2,4-trimethylpentane/EtOAc, 0 → 100% then EtOAc/*i*-PrOH, 0 → 15%) to afford nucleoside **S12** (148 mg, 0.211 mmol, 73%) as a white amorphous solid.

R_f = 0.28 (EtOAc);

FTIR (thin film), cm^{-1}: ν_{max} 3330, 2950, 1744, 1703, 1609, 1581, 1510, 1487, 1454, 1408, 1373, 1330, 1239, 1214, 1177, 1095, 1047, 1028;

^{1}H NMR (600 MHz, $CDCl_3$): δ 9.28 (br. s, 1H), 8.74 (s, 1H), 8.11 (s, 1H), 8.01–7.97 (m, 2H), 7.59–7.53 (m, 1H), 7.49–7.44 (m, 2H), 7.33–7.24 (m, 5H), 6.12 (d, J = 5.3 Hz, 1H), 5.94 (t, J = 5.5 Hz, 1H), 5.45 (d, J = 3.5 Hz, 1H), 5.44 (t, J = 5.3 Hz, 1H), 5.07 (s, 2H), 4.34 (td, J = 8.0, 5.1 Hz, 1H), 4.15 (dt, J = 8.8, 4.9 Hz, 1H), 3.69 (s, 3H), 2.11 (s, 3H), 2.04 (s, 3H), 1.85–1.70 (m, 3H), 1.65–1.57 (m, 1H), 1.51–1.42 (m, 1H), 1.41–1.30 (m, 3H);

^{13}C NMR (126 MHz, $CDCl_3$): δ 172.9, 169.7, 169.5, 165.0, 155.9, 152.7, 151.8, 149.9, 141.9, 136.3, 133.6, 132.8, 128.8, 128.5, 128.2, 128.1, 128.0, 123.9, 86.5, 82.4, 73.3, 73.1, 67.0, 53.7, 52.4, 32.9, 32.5, 24.9, 24.9, 20.6, 20.4;

HRMS (ESI+): calcd. for $[C_{35}H_{38}N_6O_{10}Na]^+$ 725.2542, meas. 725.2573, Δ 4.3 ppm.

DESTHIA-SAH (**41**)

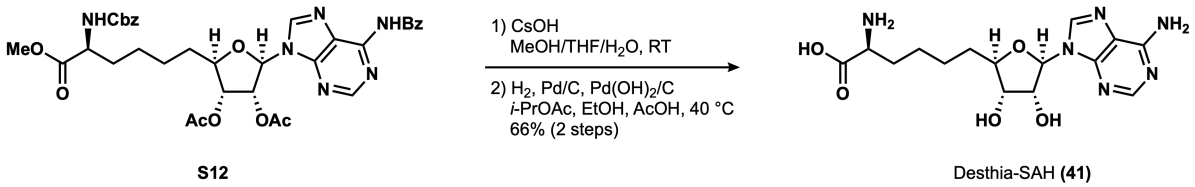

S12 Desthia-SAH **(41)**

To a solution of nucleoside **S12** (73 mg, 0.10 mmol) in a 4:2:1 mixture of MeOH, THF and water (35 mL) at RT was added $CsOH{\bullet}xH_2O$ (100 mg). The resulting mixture was stirred for 16 h and a 10% AcOH aq. solution was added dropwise until neutral pH was reached. Volatiles were removed *in vacuo*. Crude material was purified by preparative HPLC using a Kromasil® C18 column (10 μm particle size, 21.2 × 250 mm, room temperature, solvent A: 0.1% (v/v) TFA in water, solvent B: 0.1% (v/v) TFA in CH_3CN, gradient elution: 5% → 95% B over 80 min with flow rate: 10 mL/min, UV detection at 254 nm) to afford the partially deprotected carbamate.

To a solution of the carbamate intermediate in a 10:1 mixture of *i*-PrOAc and *t*-BuOH (25 mL) at RT, was added Pd/C (10%, 65 mg, 61 μmol). The reaction mixture was purged with hydrogen (3 ×) and stirred at RT under a hydrogen atmosphere (balloon) for 2 h. The reaction rate appeared sluggish so $Pd(OH)_2/C$ (20%, 105 mg, 150 μmol) was added as a slurry in a 1:1 mixture of *i*-PrOAc and AcOH (10 mL) and the resulting mixture was stirred at 50 °C for 2 h. The reaction remained slow, so EtOH (20 mL) was added. The temperature was lowered to 40 °C and the reaction media was stirred for 3 h, upon which complete cleavage of the Cbz protecting group was observed.[14] The flask headspace was purged with nitrogen under vigorous stirring. The contents were filtered over a pad of celite and the volatiles were removed *in vacuo*. Crude material was purified by preparative HPLC using a Kromasil® C18 column (10 μm particle size, 21.2 × 250 mm, room temperature, solvent A: 0.1% (v/v) TFA in water, solvent B: 0.1% (v/v) TFA in CH_3CN, gradient elution: 2.5% → 27.5% B over 80 min with flow rate: 10 mL/min, UV detection at 254 nm) to afford Desthia-SAH (**41**) (33 mg, 69 μmol, 66% over 2 steps) as the TFA salt, as a fluffy white powder.

^{1}H NMR (600 MHz, D_2O): δ 8.48 (s, 1H), 8.45 (s, 1H), 6.12 (d, J = 5.1 Hz, 1H), 4.82 (t, J = 5.2 Hz, 1H), 4.29 (t, J = 5.0 Hz, 1H), 4.21–4.16 (m, 1H), 4.00 (t, J = 6.2 Hz, 1H), 1.98 (app. ddt, J = 14.2, 10.9, 5.5 Hz,

[14] The authors note that the N-Cbz cleavage reaction rate increased markedly upon addition of EtOH.

1H), 1.94–1.86 (m, 1H), 1.88–1.77 (m, 2H), 1.59–1.39 (m, 4H);

^{13}C NMR (101 MHz, D_2O): δ 173.2, 150.3, 148.6, 144.9, 143.0, 119.2, 88.4, 85.1, 74.1, 73.4, 53.6, 32.5, 30.0, 24.7, 24.2;

HRMS (ESI+): calcd. for $[C_{15}H_{23}N_6O_5]^+$ 367.1724, meas. 367.1728, Δ 1.1 ppm.

3.5.2 (**42**) NS1-Alkyne

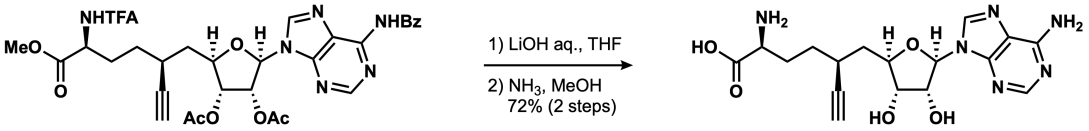

39 **42**

To a solution of alkyne **39** (42 mg, 61 μmol) in THF (1.0 mL) at RT, was added a 0.5 M LiOH aq. solution (1.0 mL). The resulting mixture was stirred for 1 h, cooled to 0 °C and a 10% AcOH aq. solution was added dropwise until pH 7 was reached. Volatiles were removed *in vacuo*. The residue was dissolved in a solution of ammonia in methanol (7 N, 3 mL) at RT. The resulting mixture was stirred for 16 h and the volatiles were removed *in vacuo*. Crude material was purified by preparative HPLC using a Kromasil® C18 column (10 μm particle size, 21.2 × 250 mm, room temperature, injection volume: 3.0 mL (water/CH_3CN, 98:2), solvent A: 0.1% (v/v) formic acid in water, solvent B: 0.1% (v/v) formic acid in CH_3CN, gradient elution: 2% B with flow rate: 0 → 10 mL/min over 5 min then 2% → 42% B over 30 min followed by 42% → 95% B over 5 min with flow rate: 10 mL/min, UV detection at 254 nm) to afford NS1-Alkyne (**42**) (22 mg, 44 μmol, 72% over 2 steps) as the TFA salt upon treatment with *d*-TFA (40 μL), as part of the sample preparation for NMR analysis.

^{1}H NMR (500 MHz, **CD_3CN** (350 μL)/D_2O (350 μL)/*d*-TFA (40 μL)): δ 8.87 (s, 2H), 6.50 (d, J = 5.0 Hz, 1H), 5.19 (t, J = 5.1 Hz, 1H), 4.68 (t, J = 4.8 Hz, 1H), 4.49 (dd, J = 6.7, 5.8 Hz, 1H), 3.08 (dddd, J = 13.7, 7.2, 5.8, 4.3 Hz, 1H), 3.02 (d, J = 2.4 Hz, 1H), 2.59 (dddd, J = 14.2, 11.6, 6.8, 4.7 Hz, 1H), 2.53–2.45

(m, 1H), 2.41 (td, J = 10.0, 5.2 Hz, 1H), 2.33 (ddd, J = 14.0, 10.9, 3.4 Hz, 1H), 2.19 (tt, J = 12.3, 5.0 Hz, 1H), 1.99 (dddd, J = 13.4, 11.9, 9.1, 4.6 Hz, 1H);

^{13}C NMR (101 MHz, **CD_3CN** (350 μL)/D_2O (350 μL)/*d*-TFA (40 μL)): δ 172.0, 150.9, 149.3, 145.2, 144.0, 120.0, 89.8, 86.1, 83.7, 74.8, 74.4, 73.1, 53.4, 38.8, 30.7, 28.8, 28.4;

HRMS (ESI+): calcd. for $[C_{17}H_{23}N_6O_5]^+$ 391.1724, meas. 391.1722, Δ 0.7 ppm.

3.5.3 (**43**) NS1-Phenyl

Nucleoside **S13**

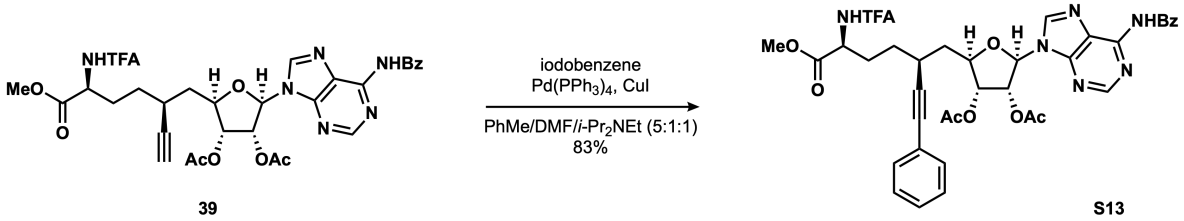

To a vial charged with nucleoside **39** (82 mg, 0.12 mmol) were added iodobenzamide (49 mg, 0.24 mmol, 2.0 equiv.), CuI (5 mg, 0.02 mmol, 20 mol %) and $Pd(PPh_3)_4$ (7 mg, 6 μmol, 5 mol %). The vial headspace was purged with nitrogen for 5 min and a 5:1:1 mixture of toluene, DMF and *i*-Pr_2NEt (degassed by sparging with nitrogen for 15 min, 3.5 mL) was added at RT. The resulting mixture was stirred at 70 °C for 3 h. The solution was allowed to cool to RT and volatiles were removed *in vacuo*. Crude material was purified by silica gel chromatography (EtOAc/*i*-PrOH, 0 $\rightarrow$ 5%) to afford alkyne **S13** (76 mg, 99 μmol, 83%) as a white amorphous solid.

$\mathbf{R_f}$ = 0.48 (EtOAc);

FTIR (thin-film), cm^{-1}: ν_{max} 3297, 3082, 2954, 1745, 1717, 1610, 1582, 1509, 1489, 1455, 1373, 1328, 1239, 1212, 1176, 1159, 1096, 1072, 1047, 1029;

^{1}H NMR (500 MHz, $CDCl_3$): δ 8.95 (s, 1H), 8.81 (s, 1H), 8.13 (s, 1H), 8.01 (d, J = 7.6 Hz, 2H), 7.61 (t, J = 7.2 Hz, 1H), 7.52 (t, J = 7.5 Hz, 2H), 7.40 (ddt, J = 5.3, 2.7, 1.4 Hz, 2H), 7.31 (tt, J = 3.8, 2.2 Hz, 3H), 6.92 (d, J = 5.8 Hz, 1H), 6.14 (d, J = 5.4 Hz, 1H), 6.09 (t, J = 5.4 Hz, 1H), 5.59 (t, J = 4.9 Hz, 1H) 4.66 (td, J = 7.7, 5.0 Hz, 1H), 4.53 (ddd, J = 10.8, 4.5, 2.9 Hz, 1H), 3.78 (s, 3H), 2.82 (ddt, J = 10.9, 9.1, 4.5 Hz, 1H), 2.16 (s, 3H), 2.19–2.09 (m, 1H), 2.07 (s, 3H), 2.06–1.92 (m, 2H), 1.70–1.60 (m, 2H), 1.58–1.46 (m, 1H);

^{13}C NMR (126 MHz, $CDCl_3$): δ 171.2, 169.8, 169.6, 164.8, 157.0 (q, $^2J_{C\text{-}F}$ = 38 Hz), 152.9, 151.7, 149.8, 142.4, 133.5, 132.9, 131.8, 128.4, 128.2, 128.0, 124.0, 123.2, 115.7 (q, $^1J_{C\text{-}F}$ = 288 Hz), 90.0, 87.1, 83.8, 81.0, 77.3, 73.7, 73.0, 53.1, 52.4, 38.8, 31.1, 30.0, 28.8, 20.7, 20.5;

^{19}F NMR (471 MHz, $CDCl_3$, BTF IStd): δ –76.7;

HRMS (ESI+): calcd. for $[C_{37}H_{36}F_3N_6O_9]^+$ 765.2490, meas. 765.2504, Δ 1.8 ppm.

NS1-Phenyl (**43**)

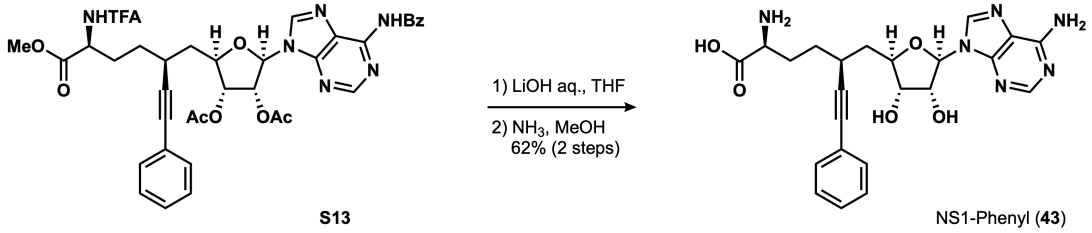

S13 NS1-Phenyl (**43**)

To a solution of alkyne **S13** (74 mg, 97 μmol) in THF (7.0 mL) at RT, was added a 0.5 M LiOH aq. solution (1.7 mL). The resulting mixture was stirred for 3 h, cooled to 0 °C and a 10% AcOH aq. solution was added dropwise until pH 7 was reached. Volatiles were removed *in vacuo*. The residue was dissolved in a solution of ammonia in methanol (7 N, 10 mL) at RT. The resulting mixture was stirred for 18 h and the volatiles were removed *in vacuo*. Crude material was purified by preparative HPLC using a Kromasil® C18 column (10 μm particle size, 21.2 × 250 mm, room temperature, injection volume: 3.0 mL (water/CH_3CN, 90:10), solvent

A: 0.1% (v/v) formic acid in water, solvent B: 0.1% (v/v) formic acid in CH_3CN, gradient elution: 5% B with flow rate: 0 → 10 mL/min over 5 min then 5% → 45% B over 45 min followed by 45% → 95% B over 5 min with flow rate: 10 mL/min, UV detection at 254 nm) to afford NS1-Phenyl (**43**) (35 mg, 60 μmol, 62% over 2 steps) as the TFA salt upon treatment with *d*-TFA (50 μL), as part of the sample preparation for NMR analysis.

^{1}H NMR (600 MHz, CD_3CN (350 μL)/**D_2O** (350 μL)/*d*-TFA (40 μL)): δ 8.84 (s, 1H), 8.82 (s, 1H), 7.84–7.80 (m, 2H), 7.78–7.74 (m, 3H), 6.47 (d, *J* = 5.1 Hz, 1H), 5.19 (t, *J* = 5.1 Hz, 1H), 4.83 (ddd, *J* = 10.5, 4.5, 3.2 Hz, 1H), 4.68 (t, *J* = 4.8 Hz, 1H), 4.48 (dd, *J* = 6.7, 5.7 Hz, 1H), 3.27 (ddt, *J* = 10.7, 9.2, 4.5 Hz, 1H), 2.63 (dddd, *J* = 14.3, 11.5, 6.8, 4.5 Hz, 1H), 2.56–2.44 (m, 2H), 2.38 (ddd, *J* = 13.9, 10.8, 3.3 Hz, 1H), 2.23 (tt, *J* = 12.6, 5.0 Hz, 1H), 2.03 (dddd, *J* = 13.4, 11.9, 9.2, 4.5 Hz, 1H);

^{13}C NMR (126 MHz, **CD_3CN** (350 μL)/D_2O (350 μL)/*d*-TFA (40 μL)): δ 172.0, 151.0, 149.4, 145.2, 144.0, 132.4, 129.5, 129.2, 123.9, 120.1, 91.7, 89.9, 84.2, 83.9, 74.8, 74.5, 53.5, 39.0, 30.9, 29.5, 28;

HRMS (ESI+): calcd. for $[C_{23}H_{26}N_6O_5Na]^+$ 489.1857, meas. 489.1841, Δ 3.2 ppm.

3.5.4 (**47**) Mini-NS1

Synthetic Scheme

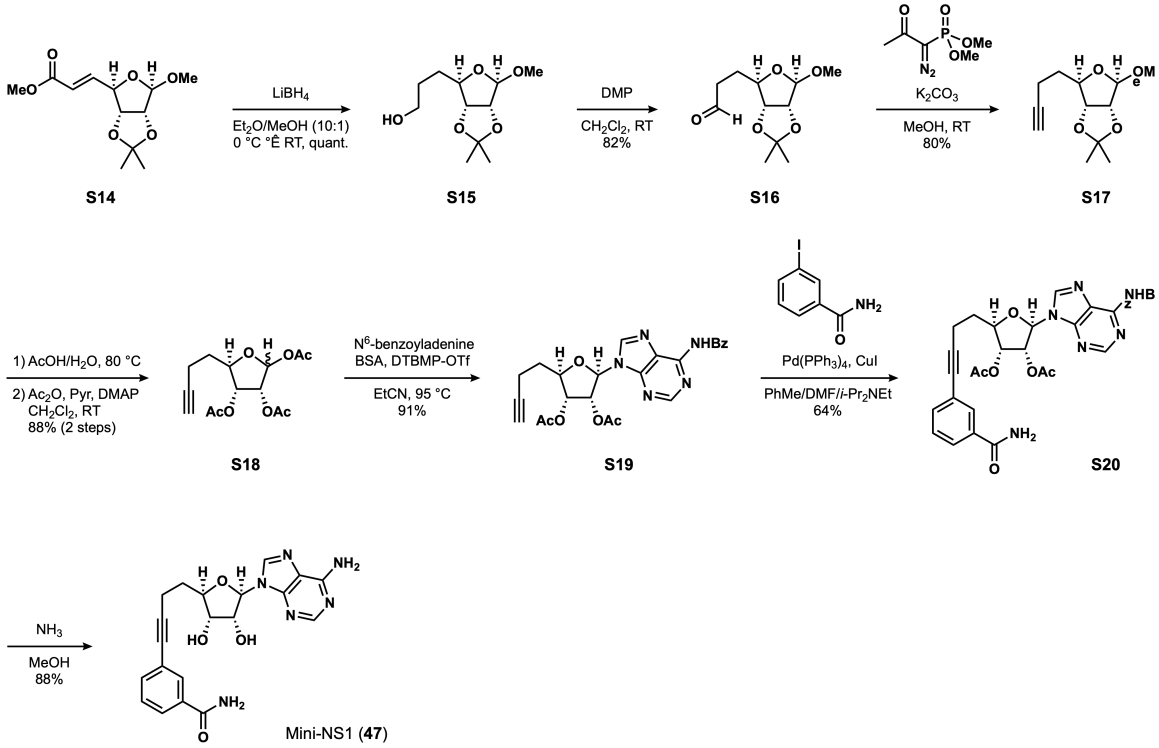

Alcohol **S15**[15]

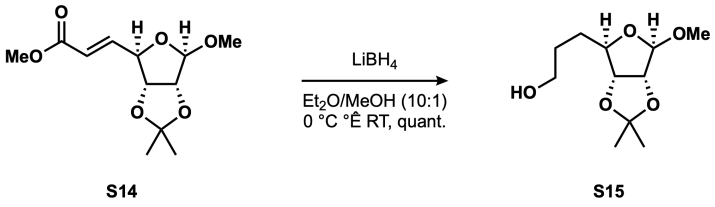

[15] Blanchard, P.; Kortbi, M. S. E.; Fourrey, J. L.; Lawrence, F.; Robert-Gero, M. *Nucleosides Nucleotides* **1996**, *15*, 1121–1135.

To a solution of known *α*,*β*-unsaturated methyl ester[16] **S14** (1.22 g, 4.72 mmol) in a 10:1 mixture of Et_2O and MeOH (22 mL) at 0 °C, was added a solution of $LiBH_4$ (2.0 M in THF, 9.45 mL, 18.9 mmol, 4.0 equiv.) dropwise. The resulting mixture was allowed to warm gradually to RT and stirred for 17 h, before the addition of a 1:1 mixture of a NH_4Cl sat. aq. solution and water (35 mL). The layers were separated and the aqueous phase was extracted with Et_2O (3 × 35 mL). The combined organic extracts were washed with brine (100 mL), dried over $MgSO_4$, filtered and concentrated to give alcohol **S15** (1.10 g, 4.72 mmol, quant.) as a colorless oil.

R_f = 0.24 (hexanes/EtOAc, 50:50);

FTIR (thin film), cm^{-1}: ν_{max} 3422, 2989, 2937, 1449, 1373, 1210, 1160, 1088, 1054, 1015;

^{1}H NMR (600 MHz, $CDCl_3$): δ 4.95 (s, 1H), 4.61 (d, J = 5.9 Hz, 1H), 4.54 (dd, J = 5.9, 1.0 Hz, 1H), 4.20–4.16 (m, 1H), 3.70–3.67 (m, 2H), 3.36 (s, 3H), 1.76–1.59 (m, 4H), 1.48 (s, 3H), 1.32 (s, 3H);

^{13}C NMR (151 MHz, $CDCl_3$): δ 112.4, 109.7, 87.2, 85.5, 84.3, 62.3, 55.1, 31.6, 29.6, 26.6, 25.1;

HRMS (ESI+): calcd. for $[C_{11}H_{20}O_5Na]^+$ 255.1203, meas. 255.1196, Δ 2.6 ppm.

Aldehyde **S16**[17]

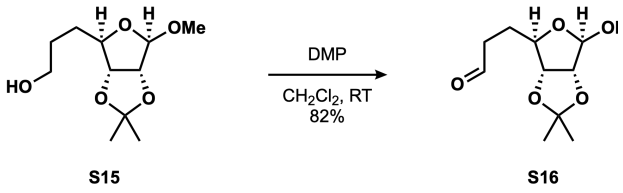

---

[16] Sarabia, F.; Martín-Ortiz, L.; López-Herrera, F. J. *Org. Lett.* **2003**, *5*, 3927–3930.

[17] Petakamsetty, R.; Ansari, A.; Ramapanicker, R. *Carbohydr. Res.* **2016**, *435*, 37–49.

To a solution of alcohol **S15** (400 mg, 1.72 mmol) in CH_2Cl_2 (11.5 mL) at RT, was added DMP (876 mg, 2.07 mmol, 1.2 equiv.) in one portion. The resulting mixture was stirred at RT for 1 h, before the addition of a 1:1 mixture of a $Na_2S_2O_3$ sat. aq. solution and a $NaHCO_3$ sat. aq. solution (10 mL). The biphasic mixture was stirred vigorously at RT for 10 min and the layers were separated. The aqueous phase was extracted with Et_2O (3 × 10 mL) and the combined organic extracts were washed with brine (40 mL), dried over $MgSO_4$, filtered and concentrated. Crude material was purified by silica gel chromatography (pentane/EtOAc, 2 → 50%) to afford aldehyde **S16** (324 mg, 1.41 mmol, 82%) as a colorless oil.

R_f = 0.32 (hexanes/EtOAc, 75:25);

FTIR (thin film), cm^{-1}: ν_{max} 2988, 2936, 2834, 2724, 1721, 1373, 1209, 1160, 1090, 1058;

^{1}H NMR (500 MHz, $CDCl_3$): δ 9.79 (t, J = 1.3 Hz, 1H), 4.93 (s, 1H), 4.59 (d, J = 5.9 Hz, 1H), 4.52 (dd, J = 5.9, 1.1 Hz, 1H), 4.14 (ddd, J = 9.2, 6.5, 1.1 Hz, 1H), 3.32 (s, 3H), 2.62 (dddd, J = 18.1, 7.9, 6.6, 1.3 Hz, 1H), 2.57 (dddd, J = 18.1, 8.2, 6.9, 1.3 Hz, 1H), 1.89–1.82 (m, 2H), 1.45 (s, 3H), 1.30 (s, 3H);

^{13}C NMR (151 MHz, $CDCl_3$): δ 201.4, 112.5, 109.9, 86.3, 85.6, 84.1, 55.3, 40.8, 27.5, 26.6, 25.1;

HRMS (ESI+): calcd. for $[C_{11}H_{18}O_5Na]^+$ 253.1046, meas. 253.1036, Δ 4.0 ppm.

ALKYNE **S17**[18]

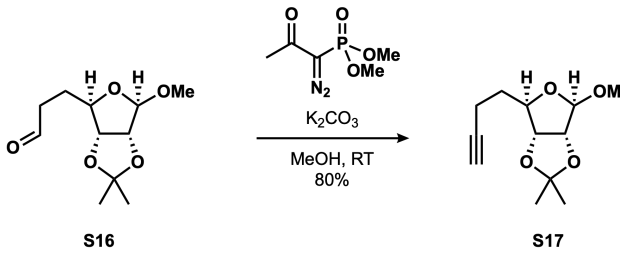

S16 **S17**

---

[18] Herrera, A. J.; Rondón, M.; Suárez, E. *J. Org. Chem.* **2008**, *73*, 3384–3391.

To a solution of aldehyde **S16** (324 mg, 1.41 mmol) in MeOH (6.0 mL) at RT, was added K_2CO_3 (583 mg, 4.22 mmol, 3.0 equiv.), followed by a solution of dimethyl-1-diazo-2-oxopropyl phosphonate (338 mg, 1.76 mmol, 1.25 equiv.) in MeOH (3.0 mL) under vigorous stirring. The resulting yellow suspension was stirred at RT for 3 h. The reaction was quenched by the addition of a NH_4Cl sat. aq. solution (15 mL) and Et_2O (25 mL) was added. The layers were separated and the aqueous phase was extracted with Et_2O (3×25 mL). The combined organic extracts were dried over $MgSO_4$, filtered and concentrated. Crude material was purified by silica gel chromatography (hexane/Et_2O, $2 \rightarrow 50\%$) to afford alkyne **S17** (254 mg, 1.12 mmol, 80%) as a colorless oil.

R_f = 0.50 (hexanes/EtOAc, 75:25);

^{1}H NMR (600 MHz, $CDCl_3$): δ 4.95 (s, 1H), 4.60 (d, J = 5.9 Hz, 1H), 4.56 (dd, J = 5.9, 1.0 Hz, 1H), 4.30 (ddd, J = 9.8, 5.8, 1.0 Hz, 1H), 3.34 (s, 3H), 2.36 (dddd, J = 16.8, 7.8, 5.9, 2.6 Hz, 1H), 2.31 (dddd, J = 16.8, 7.8, 7.3, 2.6 Hz, 1H), 1.98 (t, J = 2.6 Hz, 1H), 1.80 (dddd, J = 13.4, 9.8, 7.3, 5.9 Hz, 1H), 1.74 (app dtd, J = 13.4, 7.8, 5.8 Hz, 1H), 1.48 (s, 3H), 1.31 (s, 3H);

^{13}C NMR (151 MHz, $CDCl_3$): δ 112.5, 109.8, 85.9, 85.7, 84.1, 83.3, 69.1, 55.3, 33.9, 26.6, 25.1, 15.6;

HRMS (ESI+): calcd. for $[C_{12}H_{18}O_4Na]^+$ 249.1097, meas. 249.1118, Δ 8.4 ppm.

Triacetate **S18**

S17 **S18**

To a vial charged with acetonide **S17** (50 mg, 0.22 mmol) was added a 4:1 mixture of acetic acid and water (2.5 mL) at RT. The resulting mixture was stirred at 80 °C for 5 h. Volatiles were removed *in vacuo* and the

residue was dried by azeotropic distillation with benzene (2 × 1.0 mL). Crude material was used directly in the next step without further purification.

To a solution of the crude triol in CH_2Cl_2 (2.5 mL) at RT, were added pyridine (0.18 mL, 2.2 mmol, 10 equiv.), Ac_2O (0.21 mL, 2.2 mmol, 10 equiv.) and DMAP (19 mg, 0.15 mmol, 0.70 equiv.) sequentially. The resulting mixture was stirred at RT for 2 h and volatiles were removed *in vacuo*. Crude material was purified by silica gel chromatography (2,2,4-trimethylpentane/EtOAc, 2 → 60%) to afford triacetate **S18** (58 mg, 0.19 mmol, 88% over 2 steps) as a 1:1 mixture of diastereomers, as a colorless oil.

R_f = 0.42/0.50 (hexanes/EtOAc, 50:50);

FTIR (thin film), cm^{-1}: ν_{max} 3285, 2958, 2920, 2850, 2117, 1742, 1433, 1371, 1214, 1107, 1010;

^{1}H NMR (600 MHz, $CDCl_3$): δ 6.36 (d, *J* = 4.6 Hz, 1H), 6.12 (d, *J* = 1.0 Hz, 1H), 5.30 (dd, *J* = 4.8, 1.0 Hz, 1H), 5.21 (dd, *J* = 6.8, 4.6 Hz, 1H), 5.21 (dd, *J* = 7.0, 4.8 Hz, 1H), 5.10 (dd, *J* = 6.8, 3.6 Hz, 1H), 4.33 (ddd, *J* = 8.5, 4.9, 3.6 Hz, 1H), 4.27 (ddd, *J* = 8.5, 7.0, 4.6 Hz, 1H), 2.39–2.25 (m, 4H), 2.11 (s, 6H), 2.10 (s, 3H), 2.07 (s, 3H), 2.06 (s, 3H), 2.05 (s, 3H), 1.97 (t, *J* = 2.8 Hz, 1H), 1.96 (t, *J* = 2.6 Hz, 1H), 1.95–1.86 (m, 2H), 1.86–1.78 (m, 2H);

^{13}C NMR (126 MHz, $CDCl_3$): δ 170.2, 170.0, 169.8, 169.6, 169.5, 169.2, 98.3, 93.9, 83.0, 82.8, 82.1, 80.3, 74.7, 73.5, 72.1, 70.0, 69.4, 69.2, 33.2, 32.3, 21.2, 21.2, 20.8, 20.7, 20.6, 20.4, 14.9, 14.8;

HRMS (ESI+): calcd. for $[C_{14}H_{18}O_7Na]^+$ 321.0945, meas. 321.0952, Δ 2.3 ppm.

Nucleoside **S19**

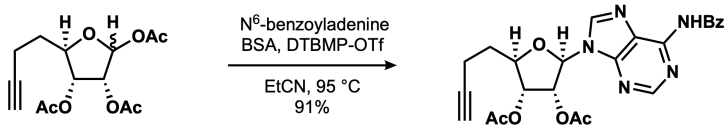

S18 **S19**

To a suspension of N^6-benzoyladenine (160 mg, 0.670 mmol, 4.0 equiv.) in propionitrile (dried over 4 Å M.S., 5.0 mL) at RT, was added *N,O*-bis(trimethylsilyl)acetamide (0.20 mL, 0.84 mmol, 5.0 equiv.). The resulting mixture was stirred at 80 °C for 10 min, upon which complete solubilization of N^6-benzoyladenine was observed. To a separate flask charged with triacetate **S18** (dried by azeotropic distillation with benzene (4×), 50 mg, 0.17 mmol) and 2,6-di-*tert*-butyl-4-methylpyridinium triflate (30 mg, 84 μmol, 50 mol %) was added propionitrile (5.0 mL). The resulting mixture was stirred at RT for 5 min, until a clear solution was obtained, and the solution of silylated N^6-benzoyladenine was added. The reaction mixture was stirred at 95 °C for 17 h, cooled to RT and the volatiles were removed *in vacuo*. Crude material was purified by silica gel chromatography (2,2,4-trimethylpentane/EtOAc, 0 → 100%) to afford nucleoside **S19** (73 mg, 0.15 mmol, 91%) as a colorless oil.

R_f = 0.31 (EtOAc);

FTIR (thin film), cm^{-1}: ν_{max} 3291, 3091, 2934, 1747, 1699, 1609, 1582, 1510, 1486, 1455, 1373, 1239, 1217, 1099, 1073, 1053;

^{1}H NMR (600 MHz, $CDCl_3$): δ 9.12 (s, 1H), 8.78 (s, 1H), 8.09 (s, 1H), 8.04–7.98 (m, 2H), 7.62–7.57 (m, 1H), 7.54–7.48 (m, 2H), 6.13 (d, *J* = 5.4 Hz, 1H), 6.04 (dd, *J* = 5.6, 5.4 Hz, 1H), 5.57 (dd, *J* = 5.6, 4.7 Hz, 1H), 4.37 (ddd, *J* = 9.2, 4.7, 4.3 Hz, 1H), 2.38 (dddd, *J* = 17.0, 7.0, 5.6, 2.6 Hz, 1H), 2.31 (dddd, *J* = 17.0, 8.5, 6.8, 2.6 Hz, 1H), 2.15 (s, 3H), 2.16–2.09 (m, 1H), 2.06 (s, 3H), 2.06–2.00 (m, 1H), 1.99 (t, *J* = 2.6 Hz, 1H);

^{13}C NMR (151 MHz, $CDCl_3$): δ 169.8, 169.6, 164.8, 153.0, 151.7, 149.9, 142.1, 133.6, 133.0, 129.0, 128.0, 124.0, 86.9, 82.8, 81.3, 73.3, 73.1, 69.6, 31.8, 20.7, 20.5, 14.8;

HRMS (ESI+): calcd. for $[C_{24}H_{24}N_5O_6]^+$ 478.1721, meas. 478.1728, Δ 1.5 ppm.

Benzamide **S20**

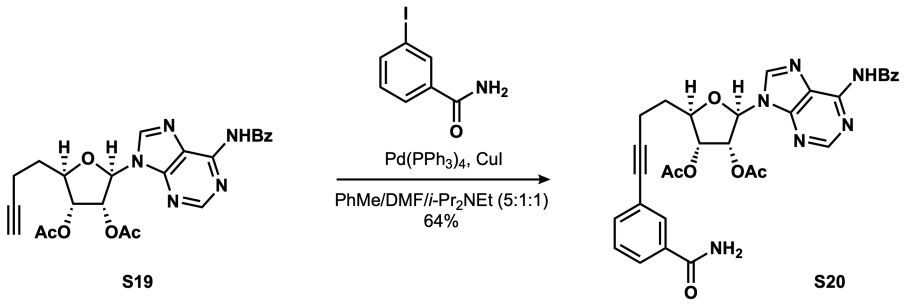

To a vial charged with alkyne **S19** (72 mg, 0.15 mmol) were added 3-iodobenzamide (75 mg, 0.30 mmol, 2.0 equiv.), CuI (7 mg, 38 μmol, 25 mol %) and $Pd(PPh_3)_4$ (9 mg, 8 μmol, 5 mol %). The vial headspace was purged with nitrogen for 5 min and a 5:1:1 mixture of toluene, DMF and *i*-Pr_2NEt (degassed by sparging with nitrogen for 15 min, 6.0 mL) was added at RT. The resulting mixture was stirred at 80 °C for 1 h. The solution was allowed to cool to RT and volatiles were removed *in vacuo*. Crude material was purified by silica gel chromatography (EtOAc/*i*-PrOH, 0 → 20%) to afford alkyne **S20** (58 mg, 97 μmol, 64%) as a colorless oil.

$\mathbf{R_f}$ = 0.24 (EtOAc/*i*-PrOH, 90:10);

FTIR (thin film), cm^{-1}: ν_{max} 3187, 2931, 1747, 1664, 1609, 1578, 1511, 1486, 1454, 1373, 1239, 1215, 1097, 1049;

^{1}H NMR (600 MHz, $CDCl_3$): δ 9.30 (s, 1H), 8.76 (s, 1H), 8.17 (s, 1H), 8.04–7.97 (m, 2H), 7.83 (app t, *J* = 1.5 Hz, 1H), 7.74 (app dt, *J* = 7.8, 1.5 Hz, 1H), 7.59–7.55 (m, 1H), 7.50–7.45 (m, 3H), 7.33 (app t, *J* = 7.8 Hz, 1H), 6.64 (br s, 1H), 6.17 (d, *J* = 5.6 Hz, 1H), 6.13 (br s, 1H), 6.11 (app t, *J* = 5.6 Hz, 1H), 5.71 (dd, *J* = 5.6, 4.3 Hz, 1H), 4.40 (ddd, *J* = 8.1, 4.9, 4.3 Hz, 1H), 2.61 (app dt, *J* = 17.2, 6.3 Hz, 1H), 2.53 (ddd, *J* = 17.2, 8.4, 6.1 Hz, 1H), 2.23–2.17 (m, 1H), 2.14 (s, 3H), 2.16–2.09 (m, 1H), 2.05 (s, 3H);

^{13}C NMR (101 MHz, $CDCl_3$): δ 170.0, 169.7, 168.9, 165.0, 152.9, 151.9, 149.9, 142.2, 134.7, 133.7, 133.5, 133.0, 130.6, 128.9, 128.7, 128.1, 127.1, 124.1, 124.0, 89.7, 86.7, 81.8, 80.8, 73.3, 73.0, 31.7, 20.8, 20.5, 15.6;

HRMS (ESI+): calcd. for $[C_{31}H_{29}N_6O_7]^+$ 597.2092, meas. 597.2097, Δ 0.8 ppm.

Mini-NS1 (**47**)

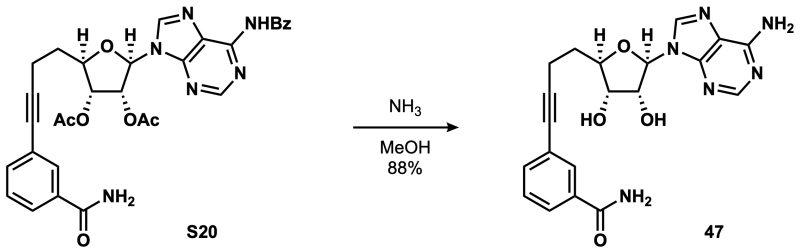

Performed by Dr. Ludovic Decultot. To a vial charged with benzamide **S20** (58 mg, 97 μmol) was added a solution of ammonia in methanol (7 N, 8.0 mL) at RT. The resulting mixture was stirred for 17 h and volatiles were removed *in vacuo*. Crude material was purified by preparative HPLC using a Kromasil® C18 column (10 μm particle size, 21.2 × 250 mm, room temperature, injection volume: 3.0 mL (water/CH_3CN, 85:15 + 30 μL TFA), solvent A: 0.1% (v/v) TFA in water, solvent B: 0.1% (v/v) TFA in CH_3CN, gradient elution: 10% B with flow rate: 0 → 10 mL/min over 5 min then 10% → 45% B over 35 min followed by 45% → 95% B over 5 min with flow rate: 10 mL/min, UV detection at 254 nm) to afford Mini-NS1 (**47**) (35 mg, 86 μmol, 88%) as a white fluffy solid.

^{1}H NMR (600 MHz, **CD_3CN** (400 μL)/D_2O (400 μL)): δ 8.36 (s, 1H), 8.31 (s, 1H), 7.70–7.69 (m, 1H), 7.71–7.67 (m, 1H), 7.46–7.43 (m, 1H), 7.38–7.35 (m, 1H), 5.98 (d, *J* = 5.1 Hz, 1H), 4.70 (dd, *J* = 5.1, 4.7 Hz, 1H), 4.22–4.18 (m, 2H), 2.53 (app dt, *J* = 17.3, 6.9 Hz, 1H), 2.49 (app dt, *J* = 17.3, 7.2 Hz, 1H), 2.03–1.96 (m, 2H);

^{13}C NMR (126 MHz, **CD_3CN** (400 μL)/D_2O (400 μL)): δ 171.3, 150.9, 149.4, 145.3, 143.8, 135.6, 134.2, 131.2, 129.9, 127.9, 124.6, 119.9, 91.6, 89.6, 84.8, 80.9, 74.8, 74.1, 32.6, 16.3;

HRMS (ESI+): calcd. for $[C_{20}H_{20}N_6O_4Na]^+$ 431.1438, meas. 431.1453, Δ 3.4 ppm.

3.5.5 (**48**) NS1-Cyclopropyl

Synthetic Scheme

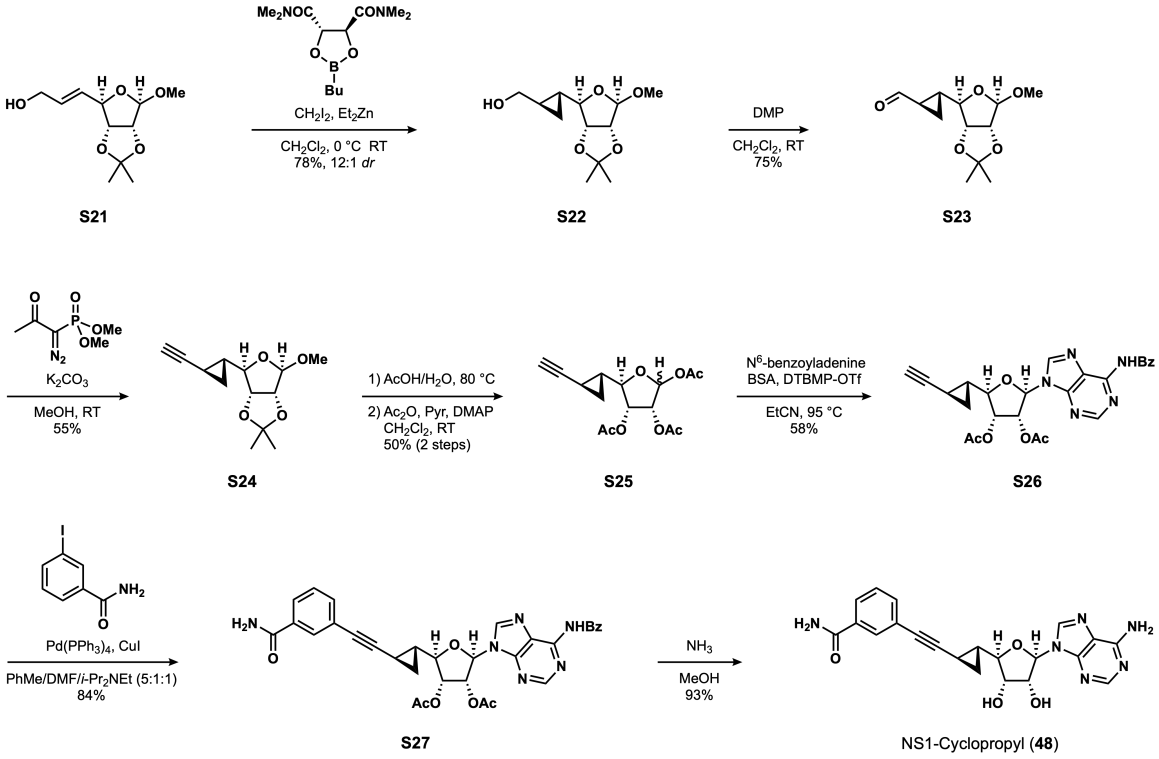

Alcohol **S22**

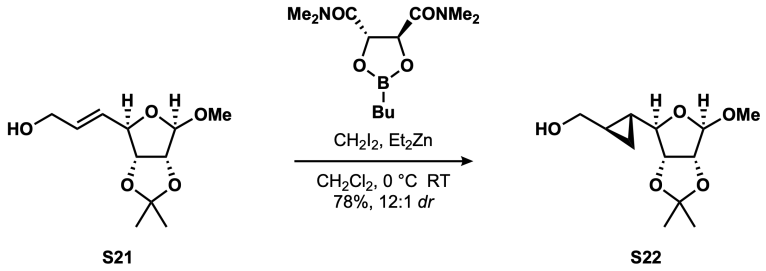

The following protocol was adapted from an early publication reporting the asymmetric cyclopropanation of allylic alcohols with dioxaborolane ligands[19]. To a stirred solution of diethylzinc in hexanes (1.0 M in hexanes, 4.46 mL, 4.46 mmol, 2.23 equiv.) was added CH_2Cl_2 (8.0 mL). The mixture was cooled to 0 °C and diiodomethane (0.72 mL, 8.9 mmol, 4.45 equiv.) was added dropwise over 5 min. The reaction mixture was stirred at 0 °C for 15 min (white precipitate was formed), and a precooled (0 °C) solution of butylboronic acid *N,N,N',N'*-tetramethyl-D-tartaric acid diamide ester[20] (360 mg, 2.28 mmol, 1.14 equiv.) and allylic alcohol **S21**[21] (457 mg, 2.00 mmol) in CH_2Cl_2 (12 mL) was rapidly added *via* syringe. The resulting mixture was stirred at RT for 1 h, cooled to 0 °C and a NH_4Cl sat. aq. solution (15 mL) was added slowly. The layers were separated and the aqueous phase was extracted with CH_2Cl_2 (3 × 30 mL). The combined organic extracts were passed through a phase separator (Biotage Isolute®), dried over $MgSO_4$, filtered and concentrated. Crude material was purified by silica gel chromatography (2,2,4-trimethylpentane/EtOAc, 0 → 100%) to afford cyclopropyl alcohol **S22** (382 mg, 1.56 mmol, 78%) as a 12:1 mixture of cyclopropyl diastereomers (major=desired), as a colorless oil.

R_f = 0.24 (cyclohexane/EtOAc, 50:50);

FTIR (thin film), cm^{-1}: ν_{max} 3446, 2991, 2935, 2251, 2041, 1458, 1382, 1373, 1274, 1210, 1194, 1159, 1105, 1089, 1053, 1030;

^{1}H NMR (600 MHz, $CDCl_3$): δ 4.95 (s, 1H), 4.74 (d, J = 5.9 Hz, 1H), 4.66 (d, J = 5.9 Hz, 1H), 3.51–3.43 (m, 3H), 3.38 (s, 3H), 1.45 (s, 3H), 1.31 (s, 3H), 1.21 (dddd, J = 12.0, 8.4, 6.9, 5.1 Hz, 1H), 0.94 (ddt, J = 10.4, 9.0, 4.7 Hz, 1H), 0.53 (ddt, J = 17.2, 8.4, 5.1 Hz, 2H);

^{13}C NMR (151 MHz, $CDCl_3$): δ 112.1, 109.1, 91.1, 85.3, 84.0, 65.5, 54.4, 26.3, 24.8, 20.8, 20.4, 8.1;

HRMS (ESI+): calcd. for $[C_{12}H_{20}O_5Na]^+$ 267.1203, meas. 267.1202, Δ 0.2 ppm.

---

[19] Charette, A. B.; Juteau, H.; Lebel, H.; Molinaro, C. *J. Am. Chem. Soc.* **1998**, *120*, 11943–11952.

[20] Synonym: (4*S*,5*S*)-2-butyl-*N,N,N',N'*-tetramethyl-1,3,2-dioxaborolane-4,5-dicarboxamide, CAS:161344-84-9.

[21] Sarabia, F.; Martín-Ortiz, L.; López-Herrera, F. J. *Org. Lett.* **2003**, *5*, 3927–3930.

Aldehyde **S23**

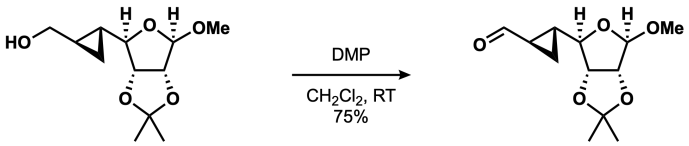

S22 **S23**

To a solution of cyclopropyl alcohol **S22** (245 mg, 1.00 mmol) in CH_2Cl_2 (20 mL) open to atmosphere at RT was added DMP (510 mg, 1.20 mmol, 1.2 equiv.) portionwise over 5 min. The reaction mixture was stirred for 2 h and was diluted with Et_2O (10 mL). The suspension was filtered and the volatiles were removed *in vacuo*. The crude residue was purified by silica gel chromatography (2,2,4-trimethylpentane/EtOAc, 0 → 50%) to yield aldehyde **S23** (182 mg, 0.751 mmol, 75%) as a clear oil. In our hands, aldehyde **S23** was best prepared, purified and used immediately in the next reaction.

$\mathbf{R_f}$ = 0.39 (cyclohexane/EtOAc, 67:33);

^{1}H NMR (600 MHz, $CDCl_3$): δ 9.16 (d, J = 4.9 Hz, 1H), 4.96 (s, 1H), 4.75 (d, J = 5.9 Hz, 1H), 4.66 (d, J = 5.8 Hz, 1H), 3.55 (d, J = 10.0 Hz, 1H), 3.28 (s, 3H), 2.02 (app dtd, J = 7.8, 4.9, 3.9 Hz, 1H), 1.79 (app tdd, J = 10.1, 8.9, 6.4, 4.0 Hz, 1H), 1.45 (s, 3H), 1.33 (dd, J = 8.9, 4.9 Hz, 1H), 1.31 (s, 3H), 1.07 (ddd, J = 8.3, 6.4, 4.9 Hz, 1H);

^{13}C NMR (151 MHz, $CDCl_3$): δ 199.9, 112.5, 109.2, 89.3, 85.4, 84.0, 54.6, 28.9, 26.4, 26.1, 25.0, 12.7;

Alkyne **S24**

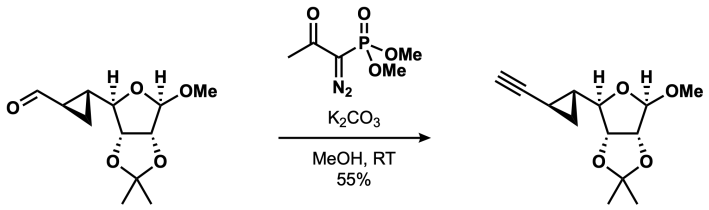

S23 **S24**

To a solution of aldehyde **S23** (182 mg, 0.751 mmol) in MeOH (4.0 mL) at RT was added K_2CO_3 (312 mg, 2.26 mmol, 3.0 equiv.) followed by a solution of dimethyl-1-diazo-2-oxopropyl phosphonate (180 mg, 0.939 mmol, 1.25 equiv.) in MeOH (3.0 mL) under vigorous stirring. The resulting yellow suspension was stirred at RT for 3 h. The reaction was quenched by the addition of a NH_4Cl sat. aq. solution (10 mL) and CH_2Cl_2 (15 mL) was added. The layers were separated and the aqueous phase was extracted with CH_2Cl_2 (3 × 15 mL). The combined organic extracts were dried over $MgSO_4$, filtered and concentrated. Crude material was purified by silica gel chromatography (cyclohexane/EtOAc, 0 → 50%) to afford alkyne **S30** (98 mg, 0.41 mmol, 55 %) as a colorless oil. Alkyne **S24** crystallized when stored as a neat oil at –20 °C for 1 week. A small molecule X-ray structure of **S24** was obtained, confirming its absolute configuration as shown in section 3.5.12.

R_f = 0.68 (cyclohexane/EtOAc, 67:33);

FTIR (thin film), cm^{-1}: ν_{max} 3283, 2989, 2935, 2834, 2116, 1458, 1407, 1382, 1373, 1307, 1273, 1233, 1209, 1194, 1159, 1104, 1090, 1056, 1034, 1023;

^{1}H NMR (600 MHz, $CDCl_3$): δ 4.99 (s, 1H), 4.73 (d, J = 5.9 Hz, 1H), 4.66 (d, J = 5.9 Hz, 1H), 3.42 (s, 3H), 3.39–3.34 (m, 1H), 1.80 (d, J = 2.0 Hz, 1H), 1.45 (s, 3H), 1.44–1.38 (m, 1H), 1.38–1.32 (m, 1H), 1.31 (s, 3H), 0.94 (app dt, J = 8.5, 5.0 Hz, 1H), 0.79–0.74 (m, 1H);

^{13}C NMR (151 MHz, $CDCl_3$): δ 112.4, 109.1, 90.5, 85.9, 85.6, 84.1, 64.8, 54.6, 26.5, 26.1, 25.0, 13.2, 6.1;

HRMS (ESI+): calcd. for $[C_{13}H_{19}O_4]^+$ 239.1278, meas. 239.1288, Δ 4.4 ppm.

Triacetate **S25**

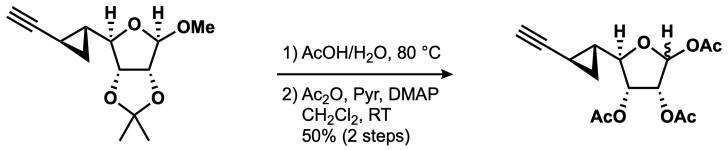

S24 **S25**

To a vial charged with acetonide **S24** (97 mg, 0.41 mmol) was added a 4:1 mixture of acetic acid and water (5.0 mL) at RT. The resulting mixture was stirred at 80 °C for 6 h. Volatiles were removed *in vacuo* and the residue was dried by azeotropic distillation with benzene (2 × 1.0 mL). Crude material was used directly in the next step without further purification.

To a solution of the crude triol in CH_2Cl_2 (5.0 mL) at RT, were added pyridine (0.99 mL, 12 mmol, 30 equiv.), Ac_2O (0.50 mL, 5.3 mmol, 13 equiv.) and DMAP (10 mg, 0.082 mmol, 0.20 equiv.) sequentially. The resulting mixture was stirred at RT for 2 h and volatiles were removed *in vacuo*. Crude material was purified by silica gel chromatography (2,2,4-trimethylpentane/EtOAc, 0 → 100%) to afford triacetate **S25** (63 mg, 0.20 mmol, 50% over 2 steps) as a 4:5 mixture of α and β anomers, as a colorless oil.

R_f = 0.60 (α-anomer) / 0.74 (β-anomer) (cyclohexane/EtOAc, 50:50);

FTIR (thin film), cm^{-1}: ν_{max} 3284, 2580, 1742, 1431, 1370, 1210, 1103, 1044, 1009;

^{1}H NMR (400 MHz, $CDCl_3$): δ α-anomer: 6.38 (dd, J = 3.9, 0.8 Hz, 1H), 5.26–5.19 (m, 2H), 3.85 (dd, J = 6.8, 2.9 Hz, 1H), 2.12 (s, 3H), 2.09 (s, 3H), 2.07 (s, 3H), 1.82 (d, J = 2.1 Hz, 1H), 1.42 (dddd, J = 8.8, 6.7, 6.0, 4.5 Hz, 1H), 1.31 (app. dtd, J = 9.5, 5.0, 2.1 Hz, 1H), 0.97 (app. dt, J = 8.7, 5.1 Hz, 1H), 0.91 (ddd, J = 8.9, 6.1, 4.8 Hz, 1H); β-anomer: 6.12 (d, J = 1.1 Hz, 1H), 5.33 (dd, J = 4.8, 1.1 Hz, 1H), 5.30 (dd, J = 6.6, 4.8 Hz, 1H), 3.75 (t, J = 6.8 Hz, 1H), 2.12 (s, 3H), 2.10 (s, 3H), 2.07 (s, 3H), 1.82 (d, J = 2.1 Hz, 1H), 1.39 (dddd, J = 8.8, 7.0, 6.0, 4.4 Hz, 1H), 1.37–1.26 (m, 1H), 0.95 (app. dt, J = 8.7, 5.0 Hz, 1H), 0.85 (ddd, J = 8.8, 6.0, 4.8 Hz, 1H);

^{13}C NMR (151 MHz, $CDCl_3$): δ α-anomer: 170.1, 169.7, 169.4, 93.9, 85.2, 84.5, 72.6, 70.0, 65.3, 23.7, 21.1, 20.8, 20.4, 11.7, 4.6; β-anomer: 169.8, 169.5, 169.3, 98.1, 82.8, 74.6, 73.8, 65.1, 55.5, 24.0, 21.2, 20.7, 20.6, 11.7, 4.4;

HRMS (ESI+): calcd. for $[C_{15}H_{18}O_7Na]^+$ 333.0945, meas. 333.0970, Δ 7.5 ppm.

Nucleoside **S26**

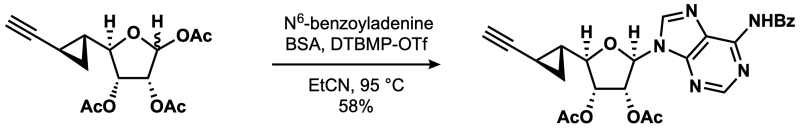

S25 **S26**

To a suspension of N^6-benzoyladenine (114 mg, 0.478 mmol, 2.15 equiv.) in propionitrile (dried over 4 Å M.S., 6.0 mL) at RT, was added *N,O*-bis(trimethylsilyl)acetamide (0.16 mL, 0.67 mmol, 3.00 equiv.). The resulting mixture was stirred at 80 °C for 10 min, upon which complete solubilization of N^6-benzoyladenine was observed. To a separate flask charged with triacetate **S25** (dried by azeotropic distillation with benzene (4×), 69 mg, 0.22 mmol) and 2,6-di-*tert*-butyl-4-methylpyridinium triflate (16 mg, 44 μmol, 20 mol %) was added propionitrile (6.0 mL). The resulting mixture was stirred at RT for 5 min, until a clear solution was obtained, and the solution of silylated N^6-benzoyladenine was added. The reaction mixture was stirred at 95 °C for 2.5 h, cooled to RT and the volatiles were removed *in vacuo*. Crude material was filtered through a short pad of silica gel (EtOAc/*i*-PrOH, 90:10) to afford alkyne **S26**, which was further purified by preparative HPLC using a Kromasil® C18 column (10 μm particle size, 21.2 × 250 mm, room temperature, injection volume: 2.5 mL (MeOH), solvent A: 0.1% (v/v) TFA in water, solvent B: 0.1% (v/v) TFA in CH_3CN, gradient elution: 5% B with flow rate: 0 → 10 mL/min over 5 min then 5% → 95% B over 40 min with flow rate: 10 mL/min, UV detection at 254 nm) to afford alkyne **S26** (63 mg, 0.13 mmol, 58%) as a white amorphous solid.

R_f = 0.19 (EtOAc);

FTIR (thin film), cm^{-1}: ν_{max} 3295, 3020, 2931, 1748, 1696, 1650, 1612, 1583, 1512, 1488, 1458, 1375, 1240, 1215, 1072, 1050;

^{1}H NMR (500 MHz, $CDCl_3$): δ 8.80 (s, 1H), 8.24 (s, 1H), 8.07–8.02 (m, 2H), 7.65–7.59 (m, 1H), 7.56–7.50 (m, 2H), 6.13 (d, J = 5.4 Hz, 1H), 6.07 (app t, J = 5.4 Hz, 1H), 5.66 (dd, J = 5.4, 4.3 Hz, 1H), 3.68 (dd, J = 8.3, 4.3 Hz, 1H), 2.15 (s, 3H), 2.08 (s, 3H), 1.83 (d, J = 2.1 Hz, 1H), 1.78–1.71 (m, 1H), 1.45–1.39 (m, 1H), 1.06 (app dt, J = 8.8, 5.2 Hz, 1H), 0.92 (ddd, J = 8.8, 5.8, 5.0 Hz, 1H);

^{13}C NMR (126 MHz, $CDCl_3$): δ 169.7, 169.5, 165.1, 152.0, 151.9, 149.7, 142.5, 133.2, 133.1, 129.0, 128.3, 123.7, 87.1, 85.2, 84.9, 73.6, 73.2, 65.5, 23.6, 20.7, 20.5, 12.1, 5.3;

HRMS (ESI+): calcd. for $[C_{25}H_{24}N_5O_6]^+$ 490.1721, meas. 490.1725, Δ 0.8 ppm.

Benzamide **S27**

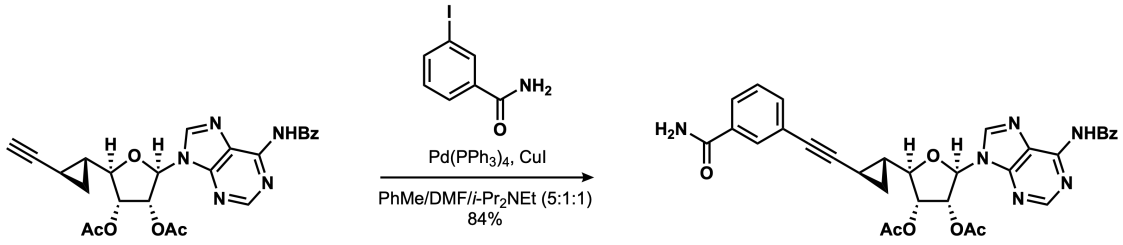

Performed by Dr. Ludovic Decultot. To a vial charged with alkyne **S26** (48 mg, 98 μmol) were added 3-iodobenzamide (61 mg, 0.25 mmol, 2.5 equiv.), CuI (5 mg, 0.03 mmol, 25 mol %) and $Pd(PPh_3)_4$ (6 mg, 5 μmol, 5 mol %). The vial headspace was purged with nitrogen for 10 min and a 5:1:1 mixture of toluene, DMF and i-Pr_2NEt (degassed by sparging with nitrogen for 15 min, 5.0 mL) was added at RT. The resulting mixture was stirred at 60 °C for 1.5 h. The solution was allowed to cool to RT and volatiles were removed *in*

vacuo. Crude material was filtered through a short pad of silica gel (EtOAc/*i*-PrOH, 75:25) to afford benzamide **S27**, which was further purified by preparative HPLC using a Kromasil® C18 column (10 μm particle size, 21.2 × 250 mm, room temperature, injection volume: 2.5 mL (MeOH), solvent A: 0.1% (v/v) TFA in water, solvent B: 0.1% (v/v) TFA in CH_3CN, gradient elution: 15% B with flow rate: 0 → 10 mL/min over 5 min then 15% → 95% B over 30 min with flow rate: 10 mL/min, UV detection at 254 nm) to afford benzamide **S27** (50 mg, 82 μmol, 84%) as a white amorphous solid.

R_f = 0.35 (EtOAc/*i*-PrOH, 95:5);

FTIR (thin film), cm^{-1}: ν_{max} 3351, 3199, 3067, 2934, 1748, 1664, 1611, 1583, 1514, 1457, 1375, 1241, 1215, 1072;

^{1}H NMR (500 MHz, $CDCl_3$): δ 8.80 (s, 1H), 8.35 (s, 1H), 8.03–7.99 (m, 2H), 7.76–7.74 (m, 1H), 7.74–7.71 (m, 1H), 7.62–7.57 (m, 1H), 7.52–7.46 (m, 3H), 7.33 (t, *J* = 7.7 Hz, 1H), 6.88 (br s, 1H), 6.80 (br s, 1H), 6.28 (dd, *J* = 5.8, 5.3 Hz, 1H), 6.17 (d, *J* = 5.8 Hz, 1H), 5.70 (dd, *J* = 5.3, 3.5 Hz, 1H), 3.69 (dd, *J* = 9.0, 3.5 Hz, 1H), 2.17 (s, 3H), 2.08 (s, 3H), 2.00–1.94 (m, 1H), 1.61–1.56 (m, 1H), 1.17 (app dt, *J* = 8.7, 5.2 Hz, 1H), 1.02 (app dt, *J* = 8.7, 5.4 Hz, 1H);

^{13}C NMR (126 MHz, $CDCl_3$): δ 170.2, 169.8, 169.6, 165.4, 151.9, 151.8, 149.6, 143.2, 135.4, 133.4, 132.8, 132.7, 130.7, 129.0, 128.9, 128.3, 127.2, 124.1, 123.6, 92.1, 87.5, 86.3, 76.3, 74.1, 72.9, 24.3, 20.8, 20.5, 13.0, 6.4;

HRMS (ESI+): calcd. for $[C_{32}H_{29}N_6O_7]^+$ 609.2092, meas. 609.2114, Δ 3.6 ppm.

NS1-Cyclopropyl (**48**)

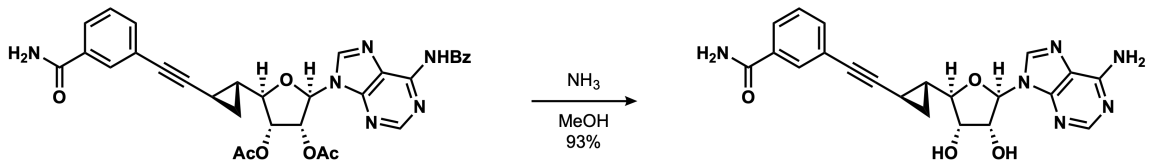

S27 **48**

Performed by Dr. Ludovic Decultot. To a vial charged with alkyne **S27** (50 mg, 82 μmol) was added a solution of ammonia in methanol (7 N, 6.0 mL) at RT. The resulting mixture was stirred for 17 h and volatiles were removed *in vacuo*. Crude material was purified by preparative HPLC using a Kromasil® C18 column (10 μm particle size, 21.2 × 250 mm, room temperature, injection volume: 3.0 mL (water/CH_3CN, 85:15 + 40 μL TFA), solvent A: 0.1% (v/v) TFA in water, solvent B: 0.1% (v/v) TFA in CH_3CN, gradient elution: 10% B with flow rate: 0 → 10 mL/min over 5 min then 10% → 45% B over 30 min followed by 45% → 95% B over 5 min with flow rate: 10 mL/min, UV detection at 254 nm) to afford NS1-Cyclopropyl (**48**) (32 mg, 76 μmol, 93%) as a white fluffy solid.

^{1}H NMR (500 MHz, **CD_3CN** (350 μL)/D_2O (350 μL)): δ 8.39 (s, 1H), 8.32 (s, 1H), 7.71 (td, J = 1.8, 0.6 Hz, 1H), 7.67 (ddd, J = 7.8, 1.8, 1.2 Hz, 1H), 7.44 (ddd, J = 7.8, 1.8, 1.2 Hz, 1H), 7.35 (td, J = 7.8, 0.6 Hz, 1H), 5.95 (d, J = 4.7 Hz, 1H), 4.73 (dd, J = 5.2, 4.7 Hz, 1H), 4.36 (dd, J = 5.2, 4.8 Hz, 1H), 3.45 (dd, J = 9.1, 4.8 Hz, 1H), 1.62 (dddd, J = 9.1, 8.8, 5.9, 4.4 Hz, 1H), 1.53 (ddd, J = 8.6, 5.4, 4.4 Hz, 1H), 1.05 (ddd, J = 8.8, 5.4, 4.8 Hz, 1H), 1.02 (ddd, J = 8.6, 5.9, 4.8 Hz, 1H);

^{13}C NMR (126 MHz, **CD_3CN** (350 μL)/D_2O (350 μL)): δ 171.2, 151.1, 149.3, 145.4, 143.8, 135.6, 134.3, 131.3, 129.8, 127.8, 124.5, 120.0, 93.6, 89.7, 88.5, 76.7, 74.9, 74.4, 25.2, 12.9, 6.4;

HRMS (ESI+): calcd. for $[C_{21}H_{21}N_6O_4]^+$ 421.1619, meas. 421.1627, Δ 1.9 ppm.

3.5.6 (**49**) NS1-Desadenine

Benzamide **S28**

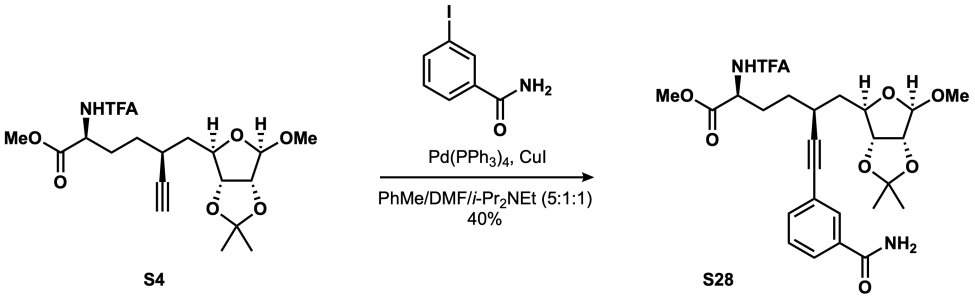

To a vial charged with alkyne **S4** (140 mg, 0.320 mmol) were added 3-iodobenzamide (197 mg, 0.799 mmol, 2.5 equiv.), CuI (15 mg, 80 μmol, 25 mol %) and $Pd(PPh_3)_4$ (19 mg, 16 μmol, 5 mol %). The vial headspace was purged with nitrogen for 5 min and a 5:1:1 mixture of toluene, DMF and *i*-Pr_2NEt (degassed by sparging with nitrogen for 15 min, 7.1 mL) was added at RT. The resulting mixture was stirred at 60 °C for 1 h. The solution was allowed to cool to RT and volatiles were removed *in vacuo*. Crude material was purified by silica gel chromatography (2,2,4-trimethylpentane/EtOAc, 0 $\rightarrow$ 100%) to afford alkyne **S28** (72 mg, 0.13 mmol, 40%) as a colorless solid.

$\mathbf{R_f}$ = 0.43 (EtOAc);

FTIR (thin-film), cm^{-1}: ν_{max} 3307, 3066, 2935, 2253, 1719, 1665, 1612, 1575, 1438, 1382, 1274, 1209, 1158;

^{1}H NMR (500 MHz, $CDCl_3$): δ 7.83 (td, *J* = 1.8, 0.6 Hz, 1H), 7.75 (ddd, *J* = 7.8, 1.9, 1.2 Hz, 1H), 7.51 (dt, *J* = 7.7, 1.4 Hz, 1H), 7.41–7.30 (m, 2H), 6.47 (br. s, 1H), 5.97 (br. s, 1H), 4.95 (s, 1H), 4.69 (td, *J* = 7.6, 5.2 Hz, 1H), 4.61 (s, 2H), 4.50 (dd, *J* = 10.8, 4.2 Hz, 1H), 3.80 (s, 3H), 3.34 (s, 3H), 2.87 (ddt, *J* = 10.6, 9.0, 4.4 Hz, 1H), 2.26–2.04 (m, 2H), 1.81–1.50 (m, 4H), 1.48 (s, 3H), 1.31 (s, 3H);

^{13}C NMR (126 MHz, $CDCl_3$): δ 171.5, 168.8, 157.2 (q, $^2J_{C\text{-}F}$ = 38 Hz), 134.9, 133.5, 130.8, 128.7, 127.2, 123.9, 115.8 (q, $^1J_{C\text{-}F}$ = 288 Hz), 112.5, 110.2, 91.7, 85.6, 85.3z, 84.5, 83.0, 55.4, 53.2, 52.7, 40.5, 30.9,

29.7, 29.4, 26.6, 25.0;

^{19}F NMR (376 MHz, $CDCl_3$, BTF IStd): δ –76.8;

HRMS (ESI+): calcd. for $[C_{26}H_{31}F_3N_2O_8Na]^+$ 579.1925, meas. 579.1928, Δ 0.5 ppm.

1,2-Diol **S29**

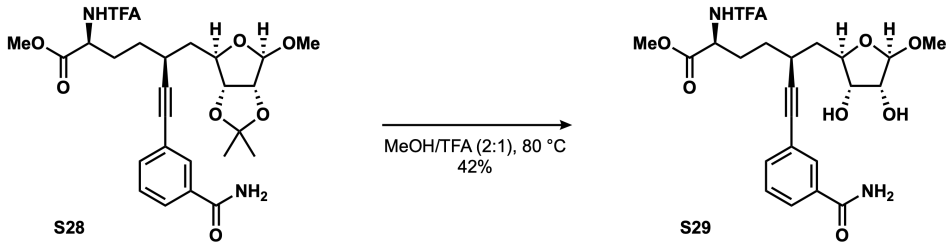

To a vial charged with acetonide **S28** (38 mg, 68 μmol) was added a 2:1 mixture of MeOH and TFA (6.0 mL) at RT. The vial was sealed tightly and the reaction mixture was stirred at 85 °C for 6 h. Volatiles were removed *in vacuo* and the residue was purified by silica gel chromatography (EtOAc/*i*-PrOH, 0 $\rightarrow$ 15% over 45 min) to afford, in order of elution, β-anomer **S29** (15 mg, 29 μmol, 42%) and the α-anomer counterpart (14 mg, 27 μmol, 40%) as off-white solids. Only β-anomer **S29** was used in the subsequent step.

R_f = 0.37 (β-anomer) (EtOAc/MeOH, 91:9);

FTIR (thin-film), cm^{-1}: ν_{max} 3349, 3076, 2921, 1719, 1665, 1613, 1598, 1573, 1438, 1383, 1250, 1211, 1180, 1161, 1127, 1103, 1063, 1029;

^{1}H NMR (600 MHz, $(CD_3)_2CO$): δ β-anomer: 8.82 (d, *J* = 8.1 Hz, 1H), 7.96 (t, *J* = 1.8 Hz, 1H), 7.88 (dt, *J* = 7.9, 1.4 Hz, 1H), 7.56 (dt, *J* = 7.7, 1.4 Hz, 1H), 7.54 (br. s, 1H), 7.44 (t, *J* = 7.7 Hz, 1H), 6.70 (br. s, 1H), 4.74 (s, 1H), 4.62 (ddd, *J* = 9.6, 8.0, 4.9 Hz, 1H), 4.23 (d, *J* = 4.1 Hz, 1H), 4.18 (ddd, *J* = 10.5, 6.5, 2.8 Hz, 1H), 4.12 (d, *J* = 7.2 Hz, 1H), 3.98 (td, *J* = 6.7, 4.8 Hz, 1H), 3.91 (t, *J* = 4.4 Hz, 1H), 3.74 (s, 3H),

3.29 (s, 3H), 2.98 (ddd, J = 15.3, 9.5, 4.7 Hz, 1H), 2.23 (dddd, J = 13.7, 10.9, 6.2, 4.8 Hz, 1H), 2.15 (ddt, J = 13.8, 9.6, 5.0 Hz, 1H), 1.91 (ddd, J = 13.4, 10.6, 2.9 Hz, 1H), 1.80 (dddd, J = 13.1, 10.0, 6.2, 4.9 Hz, 1H), 1.75–1.67 (m, 1H), 1.65 (ddd, J = 13.3, 10.6, 4.4 Hz, 1H);

^{13}C NMR (101 MHz, $(CD_3)_2CO$): δ β-anomer: 171.9, 168.3, 135.7, 135.1, 131.5, 129.4, 127.9, 124.9, 109.6, 93.3, 83.1, 82.0, 76.4, 76.2, 54.9, 53.6, 52.9, 42.1, 32.3;

^{19}F NMR (471 MHz, **$CDCl_3$** (500 μL)/$(CD_3)_2CO$ (50 μL), BTF IStd): δ β-anomer: –76.6;

HRMS (ESI+): calcd. for $[C_{23}H_{28}F_3N_2O_8]^+$ 517.1792, meas. 517.1788, Δ 0.8 ppm.

NS1-Desadenine (**49**)

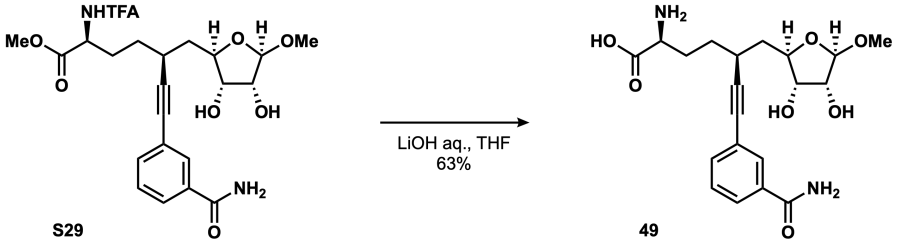

To a solution of 1,2-diol **S29** (23 mg, 44 μmol) in THF (2.0 mL) at RT, was added a 0.5 M LiOH aq. solution (2.0 mL). The reaction mixture was stirred at RT for 3 h and a 10% AcOH aq. solution was added slowly until pH 5 was obtained. Volatiles were removed *in vacuo* and the residue was purified by preparative HPLC using a Kromasil® C18 column (10 μm particle size, 21.2 × 250 mm, room temperature, injection volume: 3.0 mL (water/CH_3CN, 90:10), solvent A: 0.1% (v/v) TFA in water, solvent B: 0.1% (v/v) TFA in CH_3CN, gradient elution: 5% B with flow rate: 0 → 10 mL/min over 5 min then 5% → 55% B over 60 min followed by 55% → 95% B over 5 min with flow rate: 10 mL/min, UV detection at 254 nm) to afford NS1-Desadenine (**49**) (11 mg, 28 μmol, 63%) as the TFA salt.

^{1}H NMR (600 MHz, D_2O): δ 7.84 (t, J = 1.8 Hz, 1H), 7.74 (ddd, J = 7.9, 1.9, 1.0 Hz, 1H), 7.65 (ddt, J =

7.7, 1.6, 0.8 Hz, 1H), 7.47 (tt, *J* = 7.9, 0.6 Hz, 1H), 4.90 (d, *J* = 1.4 Hz, 1H), 4.31 (ddd, *J* = 10.2, 6.3, 3.0 Hz, 1H), 4.13 (dd, *J* = 6.3, 4.7 Hz, 1H), 4.11–4.06 (m, 2H), 3.40 (s, 3H), 2.97–2.89 (m, 1H), 2.25 (dddd, *J* = 14.2, 11.5, 6.7, 4.6 Hz, 1H), 2.16 (ddt, *J* = 14.4, 11.2, 5.5 Hz, 1H), 1.93 (ddd, *J* = 13.8, 10.9, 3.1 Hz, 1H), 1.85–1.80 (m, 1H), 1.77 (ddd, *J* = 13.7, 10.6, 4.5 Hz, 1H), 1.70–1.59 (m, 1H);

^{13}C NMR (101 MHz, D_2O): δ 172.6, 172.3, 135.3, 133.1, 130.5, 129.0, 127.2, 123.2, 108.2, 92.1, 82.7, 81.0, 74.6, 74.4, 55.2, 53.2, 39.5, 29.9, 29.1, 28.0;

HRMS (ESI+): calcd. for $[C_{20}H_{27}N_2O_7]^+$ 407.1813, meas. 407.1809, Δ 1.0 ppm.

3.5.7 (**55**) NS1-Urea

Synthetic Scheme

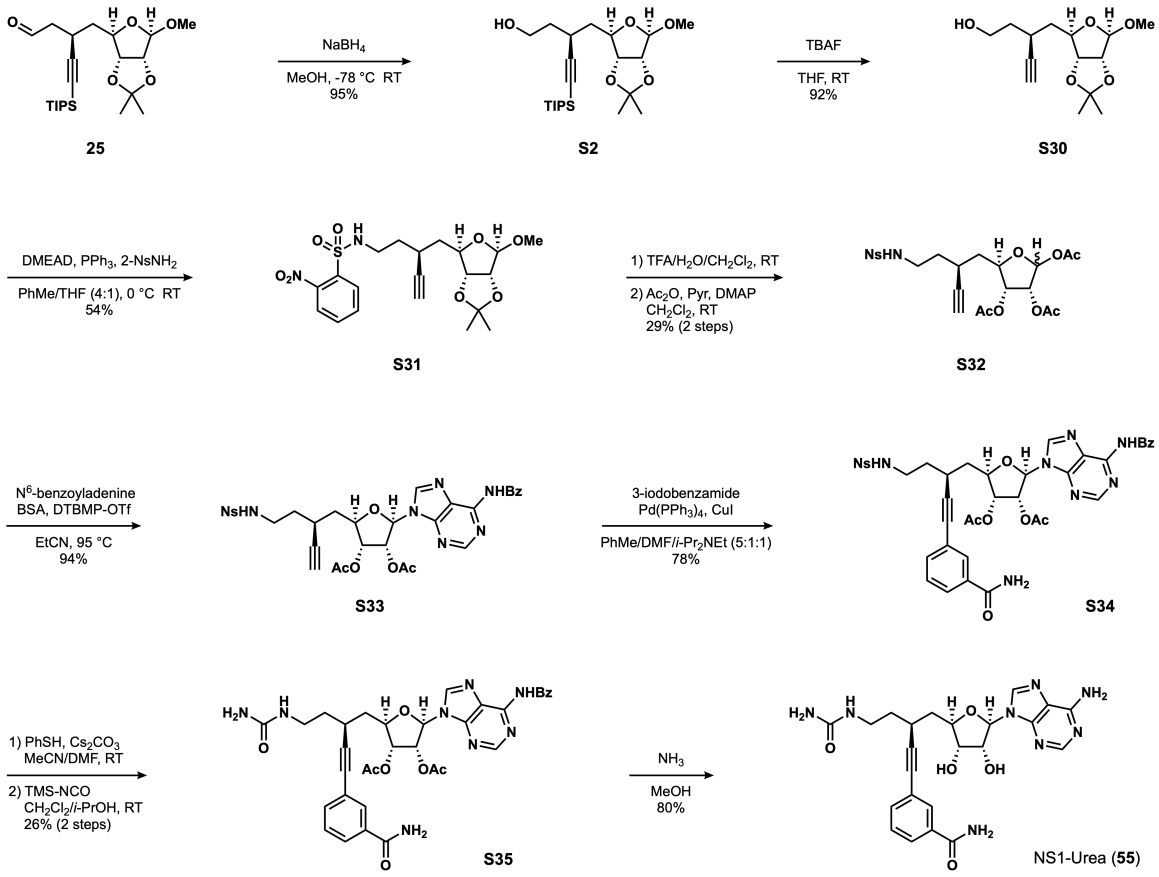

Alkyne **S30**

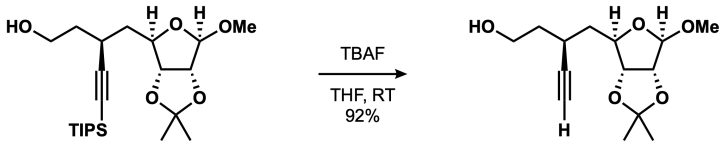

S2 **S30**

To a solution of TIPS-alkyne **S2** (3.81 g, 8.92 mmol) in THF (15 mL) was added TBAF (1.0 M in THF, 15.0 mL, 15.0 mmol, 1.7 equiv.) at RT. The reaction mixture was stirred for 3 h and the volatiles were removed in vacuo. The residue was partitioned between Et_2O (40 mL) and a NH_4Cl sat. aq. solution (40 mL). The layers were separated and the aqueous phase was extracted with Et_2O (4 × 40 mL). The combined organic extracts were washed with brine (120 mL), dried over $MgSO_4$, filtered and concentrated. Crude material was purified by silica gel chromatography (hexanes/EtOAc, 0 → 100%) to afford alkyne **S30** (2.22 g, 8.21 mmol, 92%) as a colorless oil. The pure material crystallized upon storage at –20 °C over three weeks. The crystals were of suitable quality to obtain X-ray crystallographic data which is reported in section 3.5.13.

R_f = 0.31 (cyclohexane/EtOAc, 50:50);

FTIR (thin-film), cm^{-1}: ν_{max} 3446, 3281, 2988, 2937, 2836, 1142, 1382, 1374, 1274, 1241, 1210, 1161, 1090, 1056;

^{1}H NMR (500 MHz MHz, $CDCl_3$): δ 4.94 (s, 1H), 4.60 (d, J = 6.0 Hz, 1H), 4.58 (dd, J = 6.0, 0.8 Hz, 1H), 4.50 (ddd, J = 11.2, 4.0, 0.8 Hz, 1H), 3.87–3.76 (m, 2H), 3.33 (s, 3H), 2.86–2.76 (m, 1H), 2.15 (d, J = 2.4 Hz, 1H), 1.79–1.66 (m, 3H), 1.62 (ddd, J = 13.3, 11.1, 4.0 Hz, 1H), 1.48 (s, 3H), 1.31 (s, 3H);

^{13}C NMR (126 MHz MHz, $CDCl_3$): δ 112.4, 110.1, 85.9, 85.7, 85.1, 84.5, 71.2, 60.8, 55.4, 40.5, 38.0, 26.6, 25.8, 25.1;

HRMS (ESI+): calcd. for $[C_{14}H_{23}O_5]^+$ 271.1540, meas. 271.1547, Δ 2.6 ppm.

Nosyl Amine **S31**

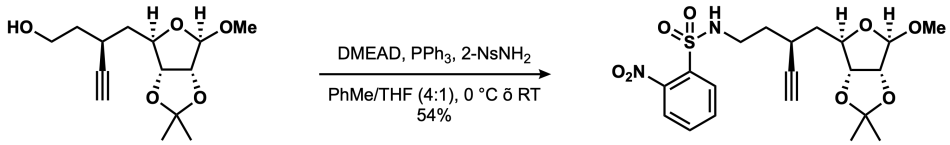

S30 **S31**

To a solution of alcohol **S30** (550 mg, 2.04 mmol), DMEAD[22] (1.19 g, 5.09 mmol, 2.5 equiv.) and PPh_3 (1.39 g, 5.29 mmol, 2.6 equiv.) in a 4:1 mixture of toluene and THF (110 mL) stirred at 0 °C over activated 4 Å M.S. (1.65 g), was added a solution of 2-$NsNH_2$ (1.44 g, 7.12 mmol, 3.5 equiv.) in THF (22 mL, prepared over 1.65 g of activated 4 Å M.S.) over 5 min. The reaction mixture was allowed to warm gradually to RT and was stirred for 72 h. The media was filtered and the volatiles were removed *in vacuo*. Crude material was purified by silica gel chromatography (hexanes/EtOAc, 0 → 100%) to afford nosyl amine **S31** (496 mg, 1.09 mmol, 54%) as a white amorphous solid and unreacted alcohol **S30** (81 mg, 0.30 mmol, 15%).

$\mathbf{R_f}$ = 0.27 (hexanes/EtOAc, 50:50);

FTIR (thin-film), cm^{-1}: ν_{max} 3289, 2989, 2936, 2836, 1540, 1442, 1415, 1363, 1343, 1300, 1274, 1241, 1210, 1192, 1162, 1087, 1056;

^{1}H NMR (600 MHz, $CDCl_3$): δ 8.16–8.11 (m, 1H), 7.89–7.83 (m, 1H), 7.78–7.70 (m, 2H), 5.50 (t, J = 6.1 Hz, 1H), 4.93 (s, 1H), 4.59 (d, J = 5.9 Hz, 1H), 4.54 (dd, J = 6.0, 0.9 Hz, 1H), 4.43 (ddd, J = 11.1, 3.9, 0.9 Hz, 1H), 3.32 (s, 3H), 3.30–3.26 (m, 2H), 2.71 (dddd, J = 14.6, 8.9, 4.5, 2.9 Hz, 1H), 2.13 (d, J = 2.4 Hz, 1H), 1.77 (dtd, J = 13.2, 7.5, 4.8 Hz, 1H), 1.71–1.63 (m, 2H), 1.58 (ddd, J = 13.3, 11.0, 4.0 Hz, 1H), 1.47 (s, 3H), 1.30 (s, 3H);

---

[22] Hagiya, K.; Muramoto, N.; Misaki, T.; Sugimura, T. *Tetrahedron* **2009**, *65*, 6109–6114.

^{13}C NMR (126 MHz, $CDCl_3$): δ 148.1, 133.7, 133.6, 132.9, 131.1, 125.5, 112.4, 110.1, 85.5, 84.8, 84.7, 84.4, 71.9, 55.4, 41.9, 40.3, 35.2, 26.5, 26.5, 25.0;

HRMS (ESI+): calcd. for $[C_{20}H_{26}N_2O_8S_1Na]^+$ 477.1302, meas. 477.1287, Δ 3.2 ppm.

Triacetate **S32**

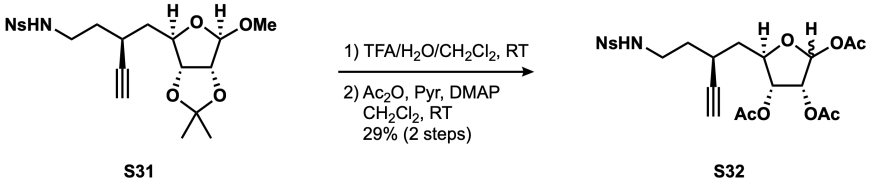

S31 **S32**

To a solution of acetonide **S31** (210 mg, 0.462 mmol) in CH_2Cl_2 (0.80 mL) at 0 °C, was added a 4:1 mixture of TFA and water (4.0 mL). The resulting mixture was stirred at RT for 15 h. Volatiles were removed *in vacuo* and the residue was dried by azeotropic distillation with benzene (2 × 1.0 mL). Crude material was used directly in the next step without further purification.

To a solution of the crude triol in CH_2Cl_2 (4.8 mL) at RT, were added pyridine (0.37 mL, 4.6 mmol, 10 equiv.), Ac_2O (0.44 mL, 4.6 mmol, 10 equiv.) and DMAP (11 mg, 92 μmol, 20 mol %) sequentially. The resulting mixture was stirred at RT for 1 h and volatiles were removed *in vacuo*. Crude material was purified by silica gel chromatography (2,2,4-trimethylpentane/EtOAc, 15 $\rightarrow$ 75%) to afford triacetate **S32** (70 mg, 0.13 mmol, 29% over 2 steps) as a 1.8:1 mixture of diastereomers, as a colorless oil.

R_f = 0.31/0.40 (hexanes/EtOAc, 40:60);

FTIR (thin film), cm^{-1}: ν_{max} 3288, 2925, 2853, 1747, 1541, 1424, 1368, 1222, 1167, 1124, 1082, 1058, 1012;

^{1}H NMR (600 MHz, $CDCl_3$): δ 8.16–8.11 (m, 2.8H), 7.89–7.84 (m, 2.8H), 7.79–7.71 (m, 5.6H), 6.32 (d, J = 4.6 Hz, 1.0H), 6.11 (d, J = 1.0 Hz, 1.8H), 5.55 (app t, J = 6.1 Hz, 1.0H), 5.52 (app t, J = 6.1 Hz, 1.8H),

5.29 (dd, J = 4.9, 1.0 Hz, 1.8H), 5.19 (dd, J = 6.7, 4.6 Hz, 1.0H), 5.16 (dd, J = 6.9, 4.9 Hz, 1.8H), 5.02 (dd, J = 6.7, 3.7 Hz, 1.0H), 4.40 (ddd, J = 10.3, 3.7, 3.3 Hz, 1.0H), 4.34 (ddd, J = 10.2, 6.9, 3.1 Hz, 1.8H), 3.33–3.22 (m, 5.6H), 2.70–2.61 (m, 2.8H), 2.14 (d, J = 2.4 Hz, 2.8H), 2.12 (s, 5.4H), 2.11 (s, 3.0H), 2.10 (s, 3.0H), 2.08 (s, 5.4H), 2.06 (s, 5.4H), 2.06 (s, 3.0H), 1.86–1.73 (m, 5.6H), 1.71–1.60 (m, 4.6H), 1.56 (ddd, J = 14.0, 10.3, 4.2 Hz, 1.0H);

^{13}C NMR (126 MHz, $CDCl_3$): δ 170.2, 170.0, 169.8, 169.6, 169.5, 169.2, 148.2, 133.8, 133.7, 133.7, 132.9, 132.9, 131.2, 131.2, 125.6, 125.6, 98.4, 93.8, 84.5, 84.3, 81.2, 79.6, 74.6, 73.8, 72.5, 72.1, 72.0, 69.9, 41.9, 40.1, 39.0, 35.2, 35.0, 26.6, 26.2, 21.2, 21.2, 20.8, 20.7, 20.7, 20.4;

HRMS (ESI+): calcd. for $[C_{22}H_{26}N_2O_{11}S_1Na]^+$ 549.1150, meas. 549.1138, Δ 2.1 ppm.

Nucleoside **S33**

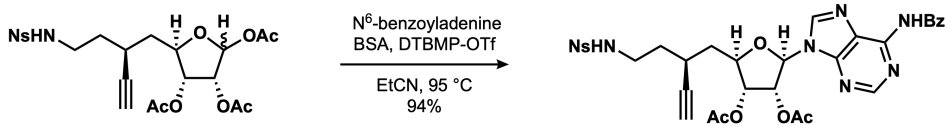

S32 **S33**

To a suspension of N^6-benzoyladenine (93 mg, 0.39 mmol, 2.15 equiv.) in propionitrile (dried over 4 Å M.S., 4.5 mL) at RT, was added *N,O*-bis(trimethylsilyl)acetamide (121 μL, 0.497 mmol, 2.75 equiv.). The resulting mixture was stirred at 80 °C for 10 min, upon which complete solubilization of N^6-benzoyladenine was observed. To a separate flask charged with triacetate **S32** (dried by azeotropic distillation with benzene (4×), 95 mg, 0.18 mmol) and 2,6-di-*tert*-butyl-4-methylpyridinium triflate (13 mg, 36 μmol, 20 mol %) was added propionitrile (4.5 mL). The resulting mixture was stirred at RT for 5 min, until a clear solution was obtained, and the solution of silylated N^6-benzoyladenine was added. The reaction mixture was stirred at 95 °C for 30 h, cooled to RT and the volatiles were removed *in vacuo*. Crude material was purified by silica gel chromatography (PhMe/MeCN, 0 → 50%) and lyophilized to afford nucleoside **S33** (120 mg, 0.170 mmol, 94%) as a white fluffy solid.

$\mathbf{R_f}$ = 0.36 (EtOAc);

FTIR (thin-film), cm^{-1}: ν_{max} 3295, 3097, 2945, 1746, 1699, 1610, 1582, 1540, 1509, 1485, 1455, 1423, 1365, 1338, 1298, 1240, 1218, 1164, 1074, 1047;

^{1}H NMR (600 MHz, $CDCl_3$): δ 9.09 (s, 1H), 8.76 (s, 1H), 8.10 (dd, J = 7.7, 1.6 Hz, 1H), 8.07 (s, 1H), 8.02 (dt, J = 7.1, 1.4 Hz, 2H), 7.80 (dd, J = 7.6, 1.6 Hz, 1H), 7.72 (td, J = 7.6, 1.6 Hz, 1H), 7.68 (td, J = 7.6, 1.6 Hz, 1H), 7.63–7.59 (m, 1H), 7.55–7.49 (m, 2H), 6.10 (d, J = 4.7 Hz, 2H), 5.55 (q, J = 6.2, 5.4 Hz, 2H), 4.46 (ddd, J = 11.0, 4.5, 2.8 Hz, 1H), 3.25 (dt, J = 7.5, 6.2 Hz, 2H), 2.62 (dddq, J = 11.2, 9.0, 4.6, 2.5 Hz, 1H), 2.17 (d, J = 2.4 Hz, 1H), 2.16 (s, 3H), 2.07–2.12 (m, 1H), 2.07 (s, 3H), 1.85 (ddd, J = 13.8, 11.2, 2.9 Hz, 1H), 1.82–1.73 (m, 2H), 1.69 (ddt, J = 13.5, 9.9, 6.3 Hz, 1H);

^{13}C NMR (126 MHz, $CDCl_3$): δ 169.9, 169.6, 164.8, 152.9, 151.6, 150.0, 148.1, 142.5, 133.8, 133.7, 133.6, 133.0, 133.0, 131.2, 129.0, 128.1, 125.5, 124.1, 87.2, 84.4, 80.8, 77.4, 73.7, 72.9, 72.2, 41.9, 38.3, 35.1, 26.1, 20.8, 20.6;

HRMS (ESI+): calcd. for $[C_{32}H_{32}N_7O_{10}S_1]^+$ 706.1926, meas. 706.1922, Δ 0.5 ppm.

Benzamide **S34**

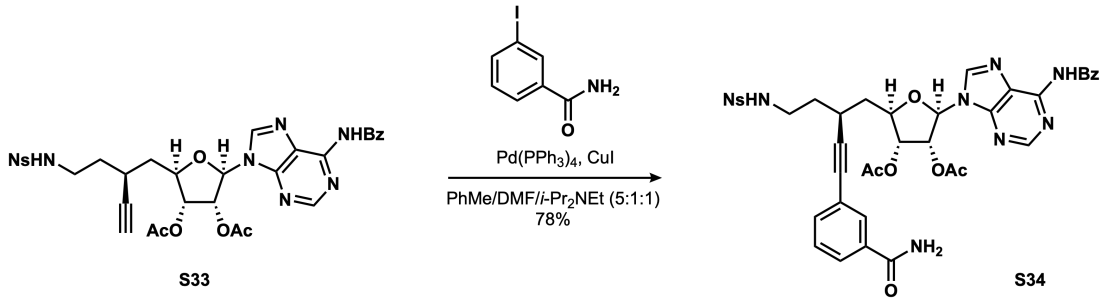

To a vial charged with alkyne **S33** (54 mg, 77 μmol) were added 3-iodobenzamide (29 mg, 0.12 mmol, 1.5 equiv.), CuI (3 mg, 0.02 mmol, 20 mol %) and $Pd(PPh_3)_4$ (4 mg, 4 μmol, 5 mol %). The vial headspace was purged with nitrogen for 10 min and a 5:1:1 mixture of toluene, DMF and *i*-Pr_2NEt (degassed by sparging with nitrogen for 15 min, 3.0 mL) was added at RT. The resulting mixture was stirred at 70 °C for 4 h. The solution was allowed to cool to RT and volatiles were removed *in vacuo*. Crude material was purified by silica gel chromatography (EtOAc/*i*-PrOH, 0 → 15%) to afford benzamide **S34** (50 mg, 60 μmol, 78%) as a white amorphous solid.

$\mathbf{R_f}$ = 0.16 (EtOAc/*i*-PrOH, 91:9);

FTIR (thin-film), cm^{-1}: ν_{max} 2926, 1746, 1667, 1610, 1579, 1540, 1511, 1484, 1455, 1366, 1339, 1298, 1241, 1215, 1163, 1073, 1047;

^{1}H NMR (500 MHz, $CDCl_3$): δ 9.13 (s, 1H), 8.76 (s, 1H), 8.11 (s, 1H), 8.10–8.07 (m, 1H), 8.05–8.00 (m, 2H), 7.87–7.86 (m, 1H), 7.80 (ddd, *J* = 7.8, 1.9, 1.2 Hz, 1H), 7.79–7.76 (m, 1H), 7.71–7.64 (m, 2H), 7.63–7.58 (m, 1H), 7.55–7.47 (m, 3H), 7.38 (td, *J* = 7.7, 0.6 Hz, 1H), 6.56 (br. s, 1H), 6.17 (t, *J* = 5.5 Hz, 1H), 6.13 (d, *J* = 5.8 Hz, 1H), 5.84 (br. s, 1H), 5.79 (t, *J* = 6.1 Hz, 1H), 5.64 (dd, *J* = 5.3, 4.0 Hz, 1H), 4.50 (dt, *J* = 10.3, 3.7 Hz, 1H), 3.38–3.29 (m, 1H), 3.32–3.23 (m, 1H), 2.87 (tt, *J* = 10.2, 4.2 Hz, 1H), 2.23–2.10 (m, 1H), 2.16 (s, 3H), 2.06 (s, 3H), 1.98 (ddd, *J* = 13.5, 11.1, 3.6 Hz, 1H), 1.92–1.73 (m, 2H);

^{13}C NMR (101 MHz, $CDCl_3$): δ 170.1, 169.7, 168.6, 164.9, 152.8, 151.7, 150.0, 148.1, 142.6, 134.7, 133.8, 133.6, 133.6, 133.5, 133.0, 133.0, 131.2, 130.9, 129.0, 128.8, 128.1, 127.5, 125.5, 124.3, 123.4, 91.1, 87.1, 83.5, 81.2, 77.4, 77.2, 76.9, 73.8, 72.7, 42.1, 38.5, 35.3, 27.0, 20.8, 20.6;

HRMS (ESI+): calcd. for $[C_{39}H_{37}N_8O_{11}S_1]^+$ 825.2297, meas. 825.2300, Δ 0.4 ppm.

Urea **S35**

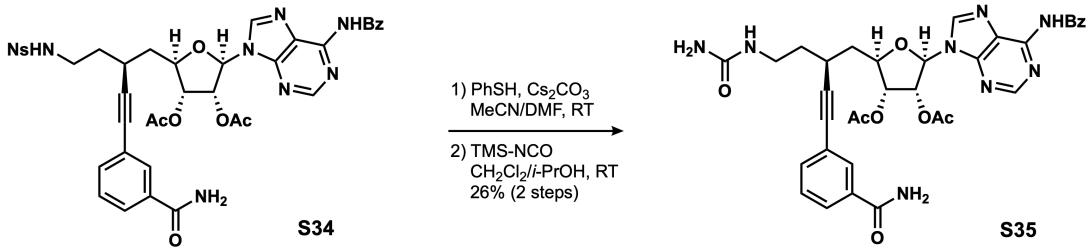

Performed by Dr. Ludovic Decultot. To a solution of nosyl amine **S34** (112 mg, 0.136 mmol) in a 2:1 mixture of MeCN and DMF (10.5 mL) at 0 °C, were added thiophenol (56 μL, 0.54 mmol, 4.0 equiv.) and Cs_2CO_3 (354 mg, 1.09 mmol, 8.0 equiv.) sequentially. The resulting mixture was stirred at RT for 1 h and was filtered twice through a nylon syringe filter (13 mm, 0.22 μm). Volatiles were removed *in vacuo*. The crude amine was used directly in the next step without further purification.

To a solution of the crude amine in a 1:1 mixture of CH_2Cl_2 and *i*-PrOH (13.5 mL) at RT, was added (trimethylsilyl)isocyanate (1.29 mL, 9.51 mmol, 70 equiv.). The resulting mixture was stirred at RT for 17 h and the volatiles were removed *in vacuo*. Crude material was purified by preparative HPLC using a Kromasil® C18 column (10 μm particle size, 21.2 × 250 mm, room temperature, injection volume: 4 mL (water/CH_3CN, 70:30 and 30 μL of DMSO), solvent A: 0.1% (v/v) formic acid in water, solvent B: 0.1% (v/v) formic acid in CH_3CN, gradient elution: 5% B with flow rate: 0 → 10 mL/min over 5 min then 5% → 95% B over 40 min with flow rate: 10 mL/min, UV detection at 254 nm) to afford urea **S35** (24 mg, 35 μmol, 26% over two steps) as a white fluffy solid.

^{1}H NMR (600 MHz, CD_3OD): δ 8.78 (s, 1H), 8.58 (s, 1H), 8.13–8.08 (m, 2H), 7.94 (t, J = 1.8 Hz, 1H), 7.83 (dt, J = 7.9, 1.6 Hz, 1H), 7.71–7.64 (m, 1H), 7.61–7.54 (m, 3H), 7.43 (t, J = 7.8 Hz, 1H), 6.35 (d, J = 5.3 Hz, 1H), 6.20 (t, J = 5.5 Hz, 1H), 5.68 (t, J = 5.2 Hz, 1H), 4.60 (ddd, J = 10.5, 4.8, 3.1 Hz, 1H), 3.40 (ddd, J = 13.1, 7.4, 5.3 Hz, 1H), 3.28 (dt, J = 13.5, 7.4 Hz, 1H), 2.91 (ddt, J = 11.0, 9.3, 4.5 Hz, 1H), 2.28 (ddd, J = 14.1, 10.5, 4.0 Hz, 1H), 2.18 (s, 3H), 2.07 (s, 3H), 2.03 (ddd, J = 14.0, 11.2, 3.2 Hz, 1H), 1.82 (dtd, J = 12.7, 7.6, 5.1 Hz, 1H), 1.74 (dddd, J = 13.0, 9.5, 7.3, 5.4 Hz, 1H);

^{13}C NMR (126 MHz, CD_3OD): δ 171.6, 171.4, 171.3, 168.2, 162.1, 153.5, 153.1, 151.4, 145.2, 135.7, 135.3, 134.9, 133.9, 131.8, 129.8, 129.7, 129.5, 128.1, 125.7, 125.2, 92.8, 88.5, 83.5, 82.1, 75.2, 74.2, 39.6,

36.9, 28.0, 20.5, 20.3;

HRMS (ESI+): calcd. for $[C_{34}H_{35}N_8O_8]^+$ 683.2572, meas. 683.2598, Δ 3.8 ppm.

NS1-Urea (**55**)

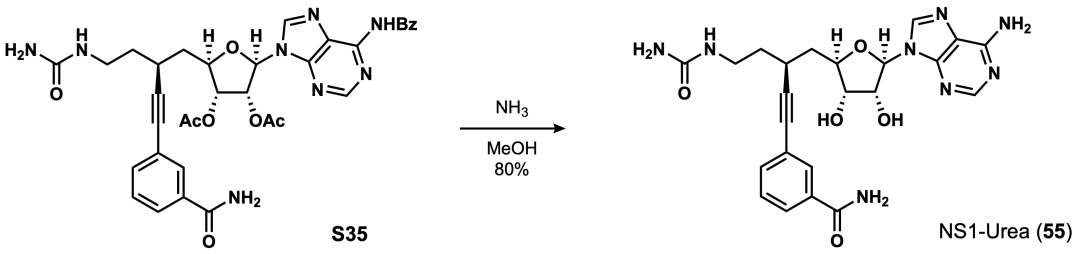

Performed by Dr. Ludovic Decultot. To a vial charged with nucleoside **S35** (31 mg, 45 μmol) was added a solution of ammonia in methanol (7 N, 5.0 mL) at RT. The resulting mixture was stirred for 17 h and the volatiles were removed *in vacuo*. Crude material was purified by preparative HPLC using a Kromasil® C18 column (10 μm particle size, 21.2 × 250 mm, room temperature, injection volume: 3.0 mL (water/CH_3CN, 90:10), solvent A: 0.1% (v/v) formic acid in water, solvent B: 0.1% (v/v) formic acid in CH_3CN, gradient elution: 5% B with flow rate: 0 → 10 mL/min over 5 min then 5% → 45% B over 35 min followed by 45% → 95% B over 5 min with flow rate: 10 mL/min, UV detection at 254 nm) to afford NS1-Urea (**55**) (18 mg, 36 μmol, 80%) as a white fluffy solid.

^{1}H NMR (600 MHz, CD_3CN (350 μL)/**D_2O** (350 μL)/*d*-TFA (40 μL)): δ 8.54 (s, 1H), 8.51 (s, 1H), 7.96 (t, *J* = 1.7 Hz, 1H), 7.90 (ddd, *J* = 7.8, 1.9, 1.1 Hz, 1H), 7.70 (dt, *J* = 7.7, 1.3 Hz, 1H), 7.58 (dd, *J* = 7.8, 0.6 Hz, 1H), 6.18 (d, *J* = 5.2 Hz, 1H), 4.93 (t, *J* = 5.2 Hz, 1H), 4.56 (dt, *J* = 10.6, 3.5 Hz, 1H), 4.40 (t, *J* = 4.7 Hz, 1H), 3.50 (ddd, *J* = 13.3, 7.7, 5.4 Hz, 1H), 3.43 (dt, *J* = 13.7, 7.5 Hz, 1H), 2.98 (tt, *J* = 9.7, 4.5 Hz, 1H), 2.19 (ddd, *J* = 14.4, 10.5, 4.2 Hz, 1H), 2.08 (ddd, *J* = 13.9, 10.9, 3.2 Hz, 1H), 2.00–1.91 (m, 1H), 1.86 (dddd, *J* = 13.2, 9.7, 7.4, 5.4 Hz, 1H);

^{13}C NMR (126 MHz, **CD_3CN** (350 μL)/D_2O (350 μL)/*d*-TFA (40 μL)): δ 171.6, 161.7, 151.0, 149.5,

145.2, 144.3, 135.9, 134.3, 131.5, 130.0, 128.2, 124.6, 120.1, 93.0, 90.1, 84.1, 83.2, 74.8, 74.6, 39.5, 39.0, 35.3, 27.6;

HRMS (ESI+): calcd. for $[C_{23}H_{26}N_8O_5Na]^+$ 517.1918, meas. 517.1912, Δ 1.2 ppm.

3.5.8 (**59**) NS1-Sulfonamide

Benzenesulfonamide **S36**

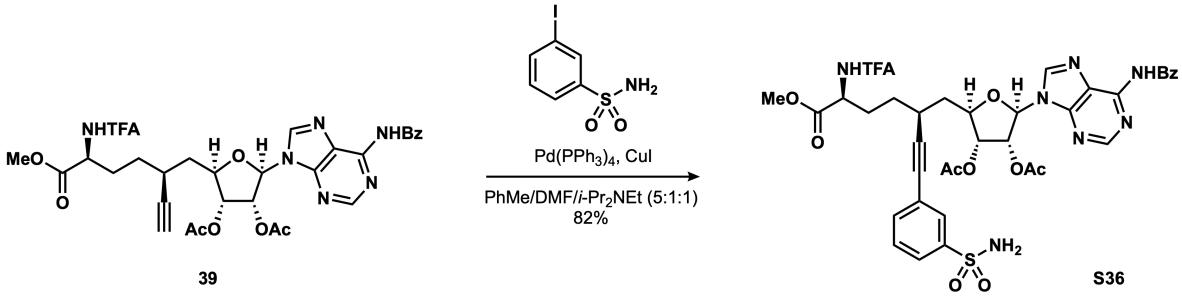

To a solution of alkyne **39** (41 mg, 59 μmol) and 3-iodobenzenesulfonamide (25 mg, 89 μmol, 1.5 equiv.) in a 5:1:1 mixture of toluene, DMF and *i*-Pr_2NEt (degassed by sparging with nitrogen for 15 min, 2.0 mL) at RT, were introduced CuI (3 mg, 0.01 mmol, 25 mol %) and $Pd(PPh_3)_4$ (3 mg, 3 μmol, 5 mol %) rapidly. The resulting mixture was stirred at 50 °C for 17 h. The solution was allowed to cool to RT and volatiles were removed *in vacuo*. Crude material was purified by silica gel chromatography (EtOAc/*i*-PrOH, 0 → 10%) to afford alkyne **S36** (41 mg, 49 μmol, 82%) as a colorless oil.

$\mathbf{R_f}$ = 0.29 (EtOAc/*i*-PrOH, 95:5);

FTIR (thin film), cm^{-1}: ν_{max} 3301, 3074, 2924, 1748, 1721, 1612, 1583, 1456, 1336, 1245, 1219, 1162, 1097;

^{1}H NMR (600 MHz, $CDCl_3$): δ 9.11 (s, 1H), 8.75 (s, 1H), 8.16 (s, 1H), 8.02–7.96 (m, 2H), 7.85 (app t, *J* = 1.2 Hz, 1H), 7.77 (app dt, *J* = 7.8, 1.2 Hz, 1H), 7.62–7.57 (m, 1H), 7.53–7.48 (m, 2H), 7.47 (app dt, *J*

= 7.8, 1.2 Hz, 1H), 7.37 (app t, J = 7.8 Hz, 1H), 7.27 (br d, J = 7.7 Hz, 1H), 6.15 (d, J = 5.7 Hz, 1H), 6.13 (dd, J = 5.7, 5.3 Hz, 1H), 5.63 (br s, 2H), 5.62 (dd, J = 5.3, 4.2 Hz, 1H), 4.65 (app td, J = 7.7, 5.5 Hz, 1H), 4.47 (ddd, J = 9.7, 4.2, 3.5 Hz, 1H), 3.77 (s, 3H), 2.86–2.81 (m, 1H), 2.21–2.14 (m, 1H), 2.16 (s, 3H), 2.10 (app ddt, J = 14.0, 11.1, 5.5 Hz, 1H), 2.06 (s, 3H), 2.05–1.98 (m, 2H), 1.69–1.60 (m, 1H), 1.60–1.52 (m, 1H);

^{13}C NMR (126 MHz, $CDCl_3$): δ 171.3, 170.1, 169.8, 165.0, 157.2 (q, $^2J_{C\text{-}F}$ = 38 Hz), 152.8, 151.8, 149.8, 142.7, 142.6, 135.2, 133.4, 133.1, 129.8, 129.1, 129.0, 128.1, 125.5, 124.4, 124.1, 115.7 (q, $^1J_{C\text{-}F}$ = 288 Hz), 92.7, 87.0, 82.2, 81.1, 73.6, 72.8, 53.3, 52.5, 38.1, 30.8, 29.8, 28.6, 20.8, 20.6;

^{19}F NMR (471 MHz, $CDCl_3$, BTF IStd): δ –76.6;

HRMS (ESI+): calcd. for $[C_{37}H_{37}F_3N_7O_{11}S_1]^+$ 844.2218, meas. 844.2198, Δ 2.4 ppm.

NS1-Sulfonamide (**59**)

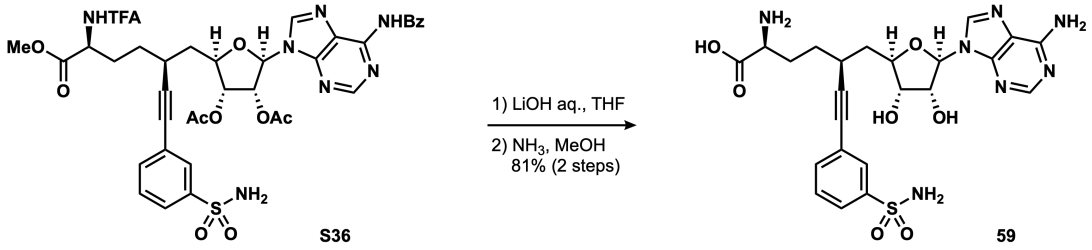

To a solution of alkyne **S36** (41 mg, 49 μmol) in THF (1.3 mL) at RT, was added a 0.5 M LiOH aq. solution (1.1 mL). The resulting mixture was stirred for 1 h, cooled to 0 °C and a 1 M HCl aq. solution (0.20 mL) was added. Volatiles were removed *in vacuo*. The residue was dissolved in a solution of ammonia in methanol (7 N, 5 mL) at RT. The resulting mixture was stirred for 18 h and volatiles were removed *in vacuo*. Crude material was purified by preparative HPLC using a Kromasil® C18 column (10 μm particle size, 21.2 × 250 mm, room temperature, injection volume: 4.0 mL (water/CH_3CN, 90:10), solvent A: 0.1% (v/v) formic acid in water, solvent B: 0.1% (v/v) formic acid in CH_3CN, gradient elution: 5% B with flow rate: 0 → 10

mL/min over 5 min then 5% → 45% B over 30 min followed by 45% → 95% B over 5 min with flow rate: 10 mL/min, UV detection at 254 nm) to afford NS1-Sulfonamide (**59**) (26 mg, 39 μmol, 81% over 2 steps) as the TFA salt upon treatment with *d*-TFA (40 μL), as part of the sample preparation for NMR analysis.

^{1}H NMR (600 MHz, **CD_3CN** (350 μL)/D_2O (350 μL)/*d*-TFA (40 μL)): δ 8.36 (s, 1H), 8.34 (s, 1H), 7.82 (dd, *J* = 1.9, 1.5 Hz, 1H), 7.77 (ddd, *J* = 7.8, 1.9, 1.2 Hz, 1H), 7.57 (ddd, *J* = 7.8, 1.5, 1.2 Hz, 1H), 7.48 (app t, *J* = 7.8 Hz, 1H), 6.00 (d, *J* = 5.1 Hz, 1H), 4.73 (dd, *J* = 5.2, 5.1 Hz, 1H), 4.36 (ddd, *J* = 10.3, 4.5, 3.3 Hz, 1H), 4.22 (dd, *J* = 5.2, 4.5 Hz, 1H), 4.01 (dd, *J* = 6.7, 5.8 Hz, 1H), 2.86–2.78 (m, 1H), 2.16 (dddd, *J* = 14.4, 11.7, 6.7, 4.5 Hz, 1H), 2.10–2.02 (m, 1H), 2.01 (ddd, *J* = 14.3, 10.3, 4.1 Hz, 1H), 1.96–1.90 (m, 1H), 1.77 (app ddt, *J* = 13.0, 11.7, 5.1 Hz, 1H), 1.58 (dddd, *J* = 13.0, 11.7, 9.6, 4.5 Hz, 1H);

^{13}C NMR (126 MHz, **CD_3CN** (350 μL)/D_2O (350 μL)/*d*-TFA (40 μL)): δ 172.1, 151.0, 149.4, 145.3, 144.1, 143.7, 136.4, 130.6, 129.6, 126.4, 125.2, 120.1, 93.8, 90.1, 83.9, 82.8, 74.9, 74.5, 53.6, 38.8, 30.9, 29.6, 28.7;

HRMS (ESI+): calcd. for $[C_{23}H_{28}N_7O_7S_1]^+$ 546.1765, meas. 546.1764, Δ 0.3 ppm.

3.5.9 (**60**) NS1-12'F

2-Fluoro-5-iodobenzamide (**S37**)

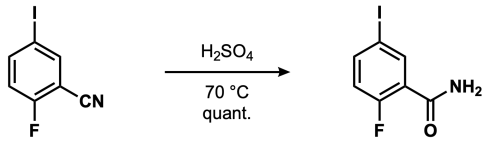

S37

Performed by undergraduate student Danny Huang under the supervision of Rocco L. Policarpo. To a vial charged with 2-fluoro-5-iodobenzonitrile (0.99 g, 4.0 mmol) was added H_2SO_4 (98%, 4.0 mL). The resulting mixture was stirred at 70 °C for 2 h, cooled to 0 °C, before the addition of a 1 N NaOH aq. solution (15 mL) and a $NaHCO_3$ sat. aq. solution (5 mL). The resulting white precipitate was filtered to yield 2-fluoro-

5-iodobenzamide (**S37**) as a pale orange, off-white powder (1.1 g, 4.0 mmol, quant.).

R_f = 0.43 (hexanes/EtOAc, 50:50);

FTIR (thin film), cm^{-1}: ν_{max} 3361, 3305, 3165, 1710, 1656, 1625, 1598, 1564, 1475, 1427, 1363, 1254, 1228;

^{1}H NMR (500 MHz, CD_3OD): δ 8.09 (1H, dd, J = 6.8, 2.4 Hz), 7.85 (1H, ddd, J = 8.7, 4.7, 2.4 Hz), 7.03 (1H, dd, J = 10.7, 8.7 Hz);

^{13}C NMR (101 MHz, CD_3OD): δ 166.9, 161.5 (d, $^1J_{C\text{-}F}$ = 251 Hz), 143.3 (d, $^3J_{C\text{-}F}$ = 8.7 Hz), 140.5 (d, $^3J_{C\text{-}F}$ = 2.6 Hz), 125.7 (d, $^2J_{C\text{-}F}$ = 15 Hz), 119.6 (d, $^2J_{C\text{-}F}$ = 25 Hz), 88.0 (d, $^4J_{C\text{-}F}$ = 3.7 Hz);

^{19}F NMR (471 MHz, CD_3OD, BTF IStd): δ –116.3;

HRMS (ESI+): calcd. for $[C_7H_5F_1I_1N_1O_1Na]^+$ 287.9292, meas. 287.9283, Δ 3.1 ppm.

Fluorobenzamide **S38**

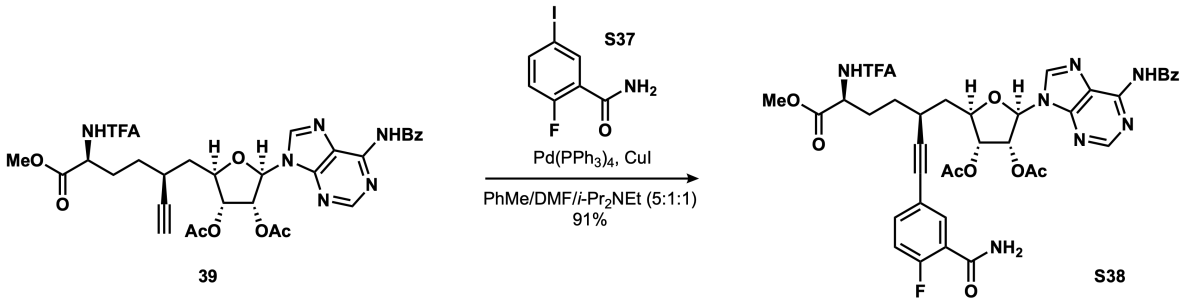

To a vial charged with nucleoside **39** (31 mg, 46 μmol) were added 2-fluoro-5-iodobenzamide (**S37**) (20 mg, 75 μmol, 1.65 equiv.), CuI (2 mg, 9 μmol, 20 mol %) and $Pd(PPh_3)_4$ (3 mg, 2 μmol, 5 mol %). The vial headspace was purged with nitrogen for 5 min and a 5:1:1 mixture of toluene, DMF and *i*-Pr_2NEt (degassed

by sparging with nitrogen for 15 min, 3.5 mL) was added at RT. The resulting mixture was stirred at 60 °C for 1 h. More 2-fluoro-5-iodobenzamide (10 mg, 38 μmol, 0.83 equiv.) in a 5:1:1 mixture of toluene, DMF and *i*-Pr_2NEt (2.0 mL) was added and the reaction mixture was stirred at 60 °C for another 3 h. The solution was allowed to cool to RT and volatiles were removed *in vacuo*. Crude material was purified by silica gel chromatography (EtOAc/*i*-PrOH, 0 → 10%) to afford alkyne **S38** (34 mg, 41 μmol, 91%) as a white amorphous solid.

FTIR (thin-film), cm^{-1}: ν_{max} 3256, 3082, 3060, 3026, 2924, 2853, 1748, 1719, 1672, 1611, 1583, 1513, 1491, 1453, 1366, 1245, 1216, 1183, 1159, 1110, 1074, 1048, 1029;

^{1}H NMR (600 MHz, $CDCl_3$): δ 9.02 (s, 1H), 8.80 (s, 1H), 8.14 (dd, *J* = 7.5, 2.3 Hz, 1H), 8.12 (s, 1H), 8.03 (d, *J* = 7.4 Hz, 2H), 7.69–7.59 (m, 1H), 7.55–7.44 (m, 3H), 7.09 (dd, *J* = 11.5, 8.5 Hz, 1H), 7.05 (br. d, *J* = 7.8 Hz, 1H), 6.68 (br. d, *J* = 10.9 Hz, 1H), 6.14 (d, *J* = 5.4 Hz, 1H), 6.11 (t, *J* = 5.4 Hz, 1H), 5.95 (br. s, 1H), 5.60 (t, *J* = 5.0 Hz, 1H), 4.65 (td, *J* = 7.7, 5.0 Hz, 1H), 4.50 (ddd, *J* = 10.7, 4.6, 3.0 Hz, 1H), 3.79 (s, 3H), 2.82 (ddt, *J* = 10.9, 9.1, 4.5 Hz, 1H), 2.17 (s, 3H), 2.18–2.08 (m, 2H), 2.08 (s, 3H), 2.04–1.92 (m, 2H), 1.64 (ddd, *J* = 18.6, 9.3, 5.4 Hz, 1H), 1.52 (dddd, *J* = 13.5, 11.0, 9.4, 4.6 Hz, 1H);

^{13}C NMR (101 MHz, $CDCl_3$): δ 171.3, 169.9, 169.7, 164.7, 164.1, 164.1, 161.6, 159.1, 157.3, 156.9, 156.5, 152.9, 151.7, 149.9, 142.4, 137.1, 137.0, 135.8, 135.8, 133.6, 133.0, 132.3, 132.2, 132.1, 132.1, 129.0, 128.7, 128.6, 128.0, 124.1, 120.5, 120.5, 120.4, 120.3, 117.2, 116.7, 116.4, 114.3, 91.1, 91.0, 87.2, 81.9, 80.9, 77.4, 73.7, 73.0, 53.3, 52.5, 38.6, 31.0, 30.0, 28.7, 23.6, 20.8, 20.6;

^{19}F NMR (471 MHz, $CDCl_3$, BTF IStd): δ –76.7, –113.0;

HRMS (ESI+): calcd. for $[C_{38}H_{35}F_4N_7O_{10}Na]^+$ 848.2272, meas. 848.2274, Δ 0.2 ppm.

NS1-12'F (**60**)

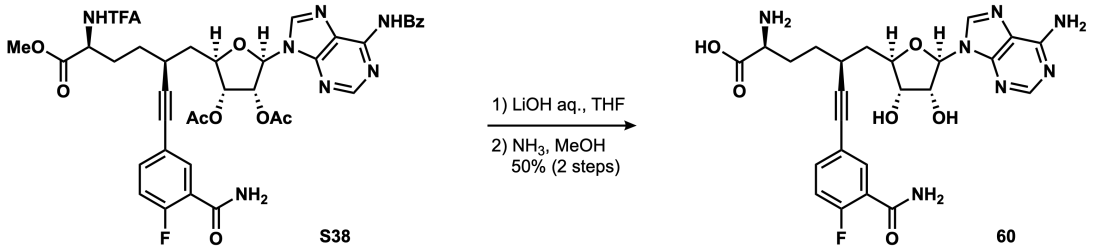

To a solution of alkyne **S38** (44 mg, 53 μmol) in THF (1 mL) at RT, was added a 0.5 M LiOH aq. solution (1 mL). The resulting mixture was stirred for 1 h, cooled to 0 °C and a 1 M HCl aq. solution (0.20 mL) was added. Volatiles were removed *in vacuo*. The residue was dissolved in a solution of ammonia in methanol (7 N, 5 mL) at RT. The resulting mixture was stirred for 18 h and the volatiles were removed *in vacuo*. Crude material was purified by preparative HPLC using a Kromasil® C18 column (10 μm particle size, 21.2 × 250 mm, room temperature, injection volume: 4.0 mL (water/CH_3CN, 90:10), solvent A: 0.1% (v/v) formic acid in water, solvent B: 0.1% (v/v) formic acid in CH_3CN, gradient elution: 5% B with flow rate: 0 → 10 mL/min over 5 min then 5% → 45% B over 30 min followed by 45% → 95% B over 5 min with flow rate: 10 mL/min, UV detection at 254 nm) to afford NS1-12'F (**60**) (17 mg, 26 μmol, 50% over 2 steps) as the TFA salt upon treatment with *d*-TFA (40 μL), as part of the sample preparation for NMR analysis.

^{1}H NMR (600 MHz, **CD_3CN** (350 μL)/D_2O (350 μL)/*d*-TFA (40 μL)): δ 8.36 (s, 1H), 8.34 (s, 1H), 7.76 (dd, J = 7.1, 2.3 Hz, 1H), 7.51 (ddd, J = 8.6, 4.8, 2.3 Hz, 1H), 7.15 (dd, J = 11.1, 8.6 Hz, 1H), 6.00 (d, J = 5.1 Hz, 1H), 4.72 (app t, J = 5.1 Hz, 1H), 4.35 (ddd, J = 10.3, 4.5, 3.3 Hz, 1H), 4.21 (dd, J = 5.1, 4.5 Hz, 1H), 4.01 (dd, J = 6.7, 5.8 Hz, 1H), 2.82–2.76 (m, 1H), 2.15 (dddd, J = 14.4, 11.7, 6.7, 4.5 Hz, 1H), 2.07–2.02 (m, 1H), 1.99 (ddd, J = 13.9, 10.3, 4.5 Hz, 1H), 1.91 (ddd, J = 13.9, 10.8, 3.3 Hz, 1H), 1.75 (app ddt, J = 12.9, 11.7, 5.0 Hz, 1H), 1.56 (dddd, J = 12.9, 11.9, 9.5, 4.5 Hz, 1H);

^{13}C NMR (126 MHz, **CD_3CN** (350 μL)/D_2O (350 μL)/*d*-TFA (40 μL)): δ 172.2, 167.5 (d, $^3J_{C\text{-}F}$ = 2.0 Hz), 160.7 (d, $^1J_{C\text{-}F}$ = 253 Hz), 151.0, 149.4, 145.3, 144.1, 137.7 (d, $^3J_{C\text{-}F}$ = 9.5 Hz), 134.8 (d, $^3J_{C\text{-}F}$ = 2.7 Hz), 122.4 (d, $^2J_{C\text{-}F}$ = 14 Hz), 120.9 (d, $^4J_{C\text{-}F}$ = 3.7 Hz), 120.1, 117.9 (d, $^2J_{C\text{-}F}$ = 25 Hz), 92.5, 90.0, 84.0, 82.4, 74.9, 74.5, 53.6, 38.9, 30.9, 29.6, 28.8;

^{19}F NMR (471 MHz, CD_3CN (350 μL)/D_2O (350 μL)/*d*-TFA (40 μL), HFB IStd): δ –113.6;

HRMS (ESI+): calcd. for $[C_{24}H_{26}F_1N_7O_6Na]^+$ 550.1821, meas. 550.1821, Δ 0.0 ppm.

3.5.10 (**62**) NS1-12'CF_3

5-Iodo-2-(trifluoromethyl)benzamide (**S39**)

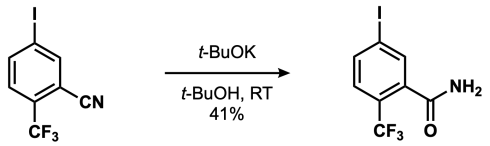

S39

Performed by undergraduate student Danny Huang under the supervision of Rocco L. Policarpo. To a vial charged with 5-iodo-2-(trifluoromethyl)benzonitrile (0.30 g, 1.0 mmol) and *t*-BuOK (0.67 g, 6.0 mmol, 6.0 equiv.) was added *t*-BuOH (5.0 mL) under a nitrogen atmosphere. The resulting mixture was stirred at 60 °C for 5 min, cooled to RT and stirred for 48 h. The reaction was quenched by the addition of water (10 mL). The resulting suspension was filtered to produce an orange solid. Crude material was purified by silica gel chromatography (hexanes/EtOAc, 0 → 100%) to yield 5-iodo-2-(trifluoromethyl)benzamide (**S39**) as a white solid (0.13 g, 0.41 mmol, 41%).

R_f = 0.46 (hexanes/EtOAc, 50:50);

FTIR (thin film), cm^{-1}: ν_{max} 3369, 3183, 1649, 1588, 1569, 1400, 1378, 1311, 1287;

^{1}H NMR (500 MHz, CD_3OD): δ 8.01 (1H, ddq, *J* = 8.3, 1.7, 0.9 Hz), 7.95–7.92 (1H, m), 7.50 (1H, br d, *J* = 8.3 Hz);

^{13}C NMR (126 MHz, CD_3OD): δ 171.3, 140.3, 138.6 (q, $^4J_{C\text{-}F}$ = 2.1 Hz), 138.3, 129.0 (q, $^3J_{C\text{-}F}$ = 4.8 Hz), 127.7 (q, $^2J_{C\text{-}F}$ = 32.6 Hz), 125.1 (q, $^1J_{C\text{-}F}$ = 273 Hz), 99.4 (q, $^5J_{C\text{-}F}$ = 1.4 Hz);

^{19}F NMR (471 MHz, CD_3OD, BTF IStd): δ –60.3;

HRMS (ESI+): calcd. for $[C_8H_5F_3I_1N_1O_1Na]^+$ 337.9260, meas. 337.9260, Δ 0.0 ppm.

(Trifluoromethyl)benzamide **S40**

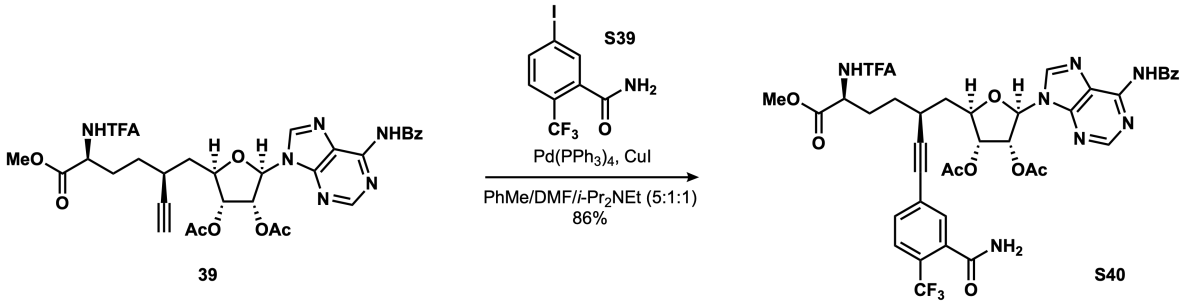

To a vial charged with alkyne **39** (82 mg, 0.12 mmol) were added 5-iodo-2-(trifluoromethyl)benzamide (**S39**) (62 mg, 0.20 mmol, 1.65 equiv.), CuI (5 mg, 24 μmol, 20 mol %) and $Pd(PPh_3)_4$ (7 mg, 6 μmol, 5 mol %). The vial headspace was purged with nitrogen for 5 min and a 5:1:1 mixture of toluene, DMF and *i*-Pr_2NEt (degassed by sparging with nitrogen for 15 min, 3.5 mL) was added at RT. The resulting mixture was stirred at 70 °C for 3 h. The solution was allowed to cool to RT and volatiles were removed *in vacuo*. Crude material was purified by silica gel chromatography (EtOAc/*i*-PrOH, 0 $\rightarrow$ 5%) to afford alkyne **S40** (90 mg, 0.10 mmol, 86%) as a white amorphous solid.

$\mathbf{R_f}$ = 0.48 (PhMe/MeCN, 50:50);

FTIR (thin-film), cm^{-1}: ν_{max} 3306, 2926, 2165, 1747, 1719, 1672, 1609, 1582, 1511, 1487, 1456, 1410, 1373, 1313, 1289, 1242, 1216, 1175, 1133, 1114, 1074, 1039;

^{1}H NMR (500 MHz, $CDCl_3$): δ 8.98 (s, 1H), 8.78 (s, 1H), 8.11 (s, 1H), 8.04–7.98 (m, 2H), 7.63–7.59 (m, 2H), 7.58 (dd, *J* = 1.6, 0.8 Hz, 1H), 7.57–7.49 (m, 2H), 7.48 (ddt, *J* = 8.2, 1.8, 0.9 Hz, 1H), 7.13 (d, *J* =

7.7 Hz, 1H), 6.20 (br. s, 1H), 6.16–6.12 (m, 2H), 6.05 (br. s, J = 2.7 Hz, 1H), 5.62 (td, J = 4.2, 0.8 Hz, 1H), 4.65 (td, J = 7.6, 5.2 Hz, 1H), 4.46 (dt, J = 10.3, 3.5 Hz, 1H), 2.86 (ddt, J = 10.6, 9.0, 4.5 Hz, 1H), 2.23–2.17 (m, 1H), 2.16 (s, 3H), 2.12 (ddd, J = 10.7, 8.4, 5.4 Hz, 1H), 2.07 (s, 3H), 2.04–1.96 (m, 2H), 1.66 (ddt, J = 13.1, 10.7, 5.4 Hz, 1H), 1.56 (ddd, J = 8.9, 6.3, 4.6 Hz, 1H);

^{13}C NMR (101 MHz, $CDCl_3$): δ 171.3, 170.0, 169.6, 169.3, 165.0, 157.2 (q, $^2J_{C\text{-}F}$ = 38 Hz), 152.7, 151.7, 149.9, 142.5, 135.2, 133.4, 133.0, 132.8, 132.2, 132.1, 131.7, 128.9, 128.6, 128.5, 128.1, 127.4, 126.6, 126.5, 126.3 (q, $^2J_{C\text{-}F}$ = 32 Hz), 124.7, 123.4 (q, $^1J_{C\text{-}F}$ = 274 Hz), 115.7 (q, $^1J_{C\text{-}F}$ = 287 Hz), 94.4, 87.0, 81.7, 81.0, 77.3, 73.6, 72.7, 53.1, 52.4, 38.1, 30.8, 29.7, 28.6, 20.7, 20.5;

^{19}F NMR (471 MHz, $CDCl_3$, BTF IStd): δ –60.0, –76.7;

HRMS (ESI+): calcd. for $[C_{39}H_{36}F_6N_7O_{10}]^+$ 876.2422, meas. 876.2426, Δ 0.4 ppm.

NS1-12'CF_3 (**62**)

To a solution of alkyne **S40** (51 mg, 58 μmol) in THF (5.0 mL) at RT, was added a 0.5 M LiOH aq. solution (1.5 mL). The resulting mixture was stirred for 3 h, cooled to 0 °C and a 10% AcOH aq. solution was added dropwise until pH 7 was reached. Volatiles were removed *in vacuo*. The residue was dissolved in a solution of ammonia in methanol (7 N, 8 mL) at RT. The resulting mixture was stirred for 18 h and the volatiles were removed *in vacuo*. Crude material was purified by preparative HPLC using a Kromasil® C18 column (10 μm particle size, 21.2 × 250 mm, room temperature, injection volume: 4.0 mL (water/CH_3CN, 90:10), solvent A: 0.1% (v/v) formic acid in water, solvent B: 0.1% (v/v) formic acid in CH_3CN, gradient elution: 5% B

with flow rate: 0 → 10 mL/min over 5 min then 5% → 35% B over 30 min followed by 35% → 95% B over 5 min with flow rate: 10 mL/min, UV detection at 254 nm) to afford NS1-12'CF_3 (**62**) (22 mg, 32 μmol, 55% over 2 steps) as the TFA salt upon treatment with *d*-TFA (50 μL), as part of the sample preparation for NMR analysis.

^{1}H NMR (600 MHz, CD_3CN (350 μL)/**D_2O** (350 μL)/*d*-TFA (40 μL)): δ 8.82 (s, 1H), 8.80 (s, 1H), 8.12 (d, J = 8.2 Hz, 1H), 8.01 (ddt, J = 8.2, 1.8, 1.0 Hz, 1H), 8.00 – 7.97 (m, 1H), 6.45 (d, J = 5.0 Hz, 1H), 5.16 (t, J = 5.1 Hz, 1H), 4.82 – 4.79 (m, 1H), 4.65 (t, J = 4.8 Hz, 1H), 4.46 (dd, J = 6.7, 5.8 Hz, 1H), 3.32 – 3.25 (m, 1H), 2.60 (dddd, J = 14.3, 11.5, 6.7, 4.5 Hz, 1H), 2.54 – 2.43 (m, 2H), 2.41 – 2.35 (m, 1H), 2.27 – 2.18 (m, 1H), 2.03 (dddd, J = 13.4, 11.8, 9.3, 4.5 Hz, 1H);

^{13}C NMR (126 MHz, **CD_3CN** (350 μL)/D_2O (350 μL)/*d*-TFA (40 μL)): δ 172.0, 171.9, 151.0, 149.4, 145.2, 144.0, 136.0, 133.8, 132.0, 128.3, 127.8, 127.8, 127.7, 126.6, 126.3, 125.5, 123.4, 120.0, 117.9, 115.6, 113.3, 95.7, 89.9, 83.8, 82.3, 74.8, 74.4, 53.5, 38.7, 30.7, 29.6, 28.7;

HRMS (ESI+): calcd. for $[C_{25}H_{26}F_3N_7O_6Na]^+$ 600.1789, meas. 600.1776, Δ 2.2 ppm.

3.5.11 (**66**) NS1-Methylenedioxy

Iodobenzamide **S42**

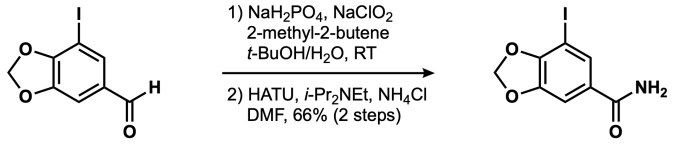

S41 **S42**

Performed by undergraduate student Danny Huang under the supervision of Rocco L. Policarpo. To a solution of known aldehyde[23] **S41** (500 mg, 1.81 mmol) in *t*-BuOH (20 mL) at RT, was added a solution of

[23] (a) Nammalwar, B.; Bunce, R. A.; Berlin, K. D.; Bourne, C. R.; Bourne, P. C.; Barrow, E. W.; Barrow, W. W. *Org. Prep. Proced. Int.* **2012**, *44*, 146–152; (b) Kim, Y.; Park, H.; Lee, J.; Tae, J.; Kim, H. J.; Min, S.-J.; Rhim, H.; Choo, H. *Eur. J.*

$NaClO_2$ (328 mg, 3.62 mmol, 2.0 equiv.) and NaH_2PO_4 (0.11 g, 0.91 mmol, 0.50 equiv.) in water (4 mL). The resulting pale yellow solution was cooled to 0 °C and 2-methyl-2-butene (4.0 mL, 38 mmol, 21 equiv.) was added dropwise. The reaction mixture was stirred at RT for 20 h, upon which more $NaClO_2$ (164 mg, 1.81 mmol, 1.0 equiv.) and NaH_2PO_4 (54 mg, 0.45 mmol, 0.25 equiv.) were added as a solution in water (2 mL). The resulting mixture was stirred at RT for 72 h and diluted with a 10% H_3PO_4 aq. solution (10 mL). Water (20 mL) and EtOAc (40 mL) were added. The layers were separated and the aqueous phase was extracted with EtOAc (2 × 40 mL). The combined organic extracts were washed with brine (80 mL), dried over Na_2SO_4, filtered and concentrated to give a white solid. Crude material was used directly in the next step without further purification.

To a flask charged with the crude carboxylic acid and HATU (758 mg, 1.99 mmol, 1.1 equiv.) were added DMF (20 mL) and *i*-Pr_2NEt (0.63 mL, 3.6 mmol, 2.0 equiv.) at RT. The resulting brown mixture was stirred for 30 min and NH_4Cl (116 mg, 2.18 mmol, 1.2 equiv.) was added. The flask headspace was flushed with nitrogen and the reaction mixture was stirred for 24 h, before the addition of EtOAc (30 mL) and water (20 mL). The layers were separated and the aqueous phase was extracted with EtOAc (3 × 30 mL). The combined organic extracts were washed with a 5% LiCl aq. solution (100 mL) and brine (2 × 100 mL), dried over Na_2SO_4, filtered and concentrated. Crude material was purified by silica gel chromatography (hexanes/EtOAc, 5 → 100%) to afford iodobenzamide **S42** (348 mg, 1.20 mmol, 66% over 2 steps) as a white solid.

R_f = 0.15 (hexanes/EtOAc, 50:50);

FTIR (thin film), cm^{-1}: ν_{max} 3355, 3187, 2924, 2854, 1658, 1592, 1479, 1424, 1254, 1044;

^{1}H NMR (500 MHz, CD_3OD): δ 7.77 (d, J = 1.6 Hz, 1H), 7.31 (d, J = 1.6 Hz, 1H), 6.11 (s, 2H);

^{13}C NMR (101 MHz, CD_3OD): δ 170.1, 153.9, 148.1, 132.3, 130.7, 108.7, 103.0, 70.6;

HRMS (ESI+): calcd. for $[C_8H_7I_1N_1O_3]^+$ 291.9465, meas. 291.9461, Δ 1.4 ppm.

Med. Chem. **2016**, *123*, 180–190.

Benzamide **S43**

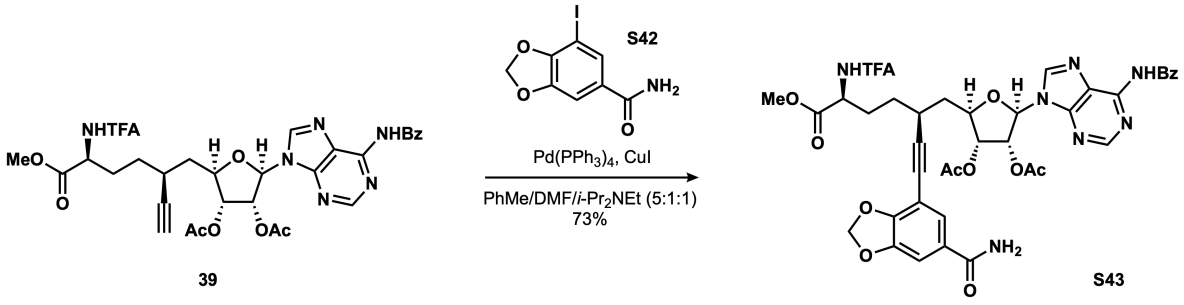

To a vial charged with alkyne **39** (30 mg, 44 μmol) were added iodobenzamide **S42** (32 mg, 0.11 mmol, 2.5 equiv.), CuI (2 mg, 0.01 mmol, 25 mol %) and $Pd(PPh_3)_4$ (3 mg, 2 μmol, 5 mol %). The vial headspace was purged with nitrogen for 5 min and a 5:1:1 mixture of toluene, DMF and *i*-Pr_2NEt (degassed by sparging with nitrogen for 15 min, 2.3 mL) was added at RT. The resulting mixture was stirred at 60 °C for 3 h. The solution was allowed to cool to RT and volatiles were removed *in vacuo*. Crude material was filtered through a short pad of silica gel (EtOAc/*i*-PrOH, 80:20) to afford alkyne **S43**, which was further purified by preparative HPLC using a Kromasil® C18 column (10 μm particle size, 21.2 × 250 mm, room temperature, injection volume: 2.0 mL (MeOH), solvent A: 0.1% (v/v) TFA in water, solvent B: 0.1% (v/v) TFA in CH_3CN, gradient elution: 15% B with flow rate: 0 → 10 mL/min over 5 min then 15% → 95% B over 30 min with flow rate: 10 mL/min, UV detection at 254 nm) to afford alkyne **S43** (27 mg, 32 μmol, 73%) as a white amorphous solid.

FTIR (thin film), cm^{-1}: ν_{max} 3351, 3222, 3077, 2937, 1746, 1717, 1659, 1593, 1424, 1243, 1203, 1045;

^{1}H NMR (500 MHz, CD_3OD): δ 8.80 (s, 1H), 8.70 (s, 1H), 8.12–8.06 (m, 2H), 7.70–7.65 (m, 1H), 7.60–7.55 (m, 2H), 7.45 (d, J = 1.7 Hz, 1H), 7.28 (d, J = 1.7 Hz, 1H), 6.34 (d, J = 5.0 Hz, 1H), 6.14 (dd, J = 5.7, 5.0 Hz, 1H), 6.10 (d, J = 1.1 Hz, 1H), 6.10 (d, J = 1.1 Hz, 1H), 5.65 (dd, J = 5.7, 5.1 Hz, 1H), 4.58 (ddd, J = 10.2, 5.1, 3.2 Hz, 1H), 4.52 (dd, J = 9.6, 5.0 Hz, 1H), 3.73 (s, 3H), 2.93–2.86 (m, 1H), 2.22 (ddd, J = 14.1, 10.2, 4.1 Hz, 1H), 2.15 (s, 3H), 2.17–2.10 (m, 1H), 2.06 (s, 3H), 2.07–1.98 (m, 2H), 1.72–1.58 (m, 2H);

^{13}C NMR (126 MHz, CD_3OD): δ 172.5, 171.6, 171.3, 170.7, 168.7, 159.1 (q, $^2J_{C\text{-}F}$ = 38 Hz), 153.0, 152.9, 152.2, 150.4, 149.4, 145.6, 134.4, 134.3, 129.8, 129.6, 128.9, 126.7, 124.3, 117.0 (q, $^1J_{C\text{-}F}$ = 288 Hz), 108.4, 105.6, 103.9, 96.7, 88.9, 82.2, 77.8, 74.9, 74.3, 53.7, 53.1, 39.3, 32.5, 29.9, 29.6, 20.5, 20.3;

^{19}F NMR (471 MHz, $CDCl_3$, BTF IStd): δ –76.7;

HRMS (ESI+): calcd. for $[C_{39}H_{37}F_3N_7O_{12}]^+$ 852.2447, meas. 852.2483, Δ 4.3 ppm.

NS1-Methylenedioxy (**66**)

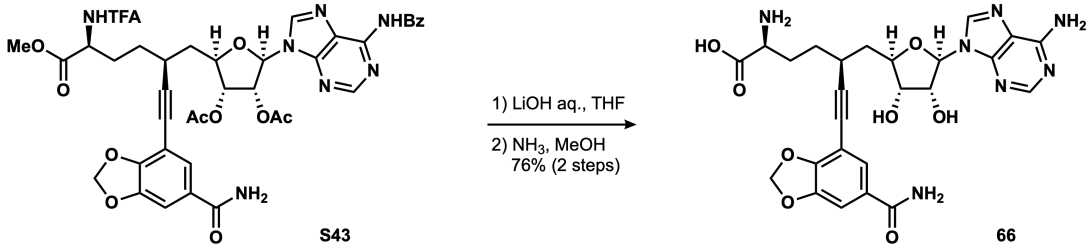

To a solution of alkyne **S43** (27 mg, 32 μmol) in THF (0.60 mL) at RT, was added a 0.5 M LiOH aq. solution (0.60 mL). The resulting mixture was stirred for 1 h, cooled to 0 °C and a 1 M HCl aq. solution (90 μL) was added. Volatiles were removed *in vacuo*. The residue was dissolved in a solution of ammonia in methanol (7 N, 4.5 mL) at RT. The resulting mixture was stirred for 18 h and volatiles were removed *in vacuo*. Crude material was purified by preparative HPLC using a Kromasil® C18 column (10 μm particle size, 21.2 × 250 mm, room temperature, injection volume: 3.0 mL (water/CH_3CN, 90:10), solvent A: 0.1% (v/v) TFA in water, solvent B: 0.1% (v/v) TFA in CH_3CN, gradient elution: 5% B with flow rate: 0 → 10 mL/min over 5 min then 5% → 40% B over 40 min followed by 40% → 95% B over 5 min with flow rate: 10 mL/min, UV detection at 254 nm) to afford NS1-Methylenedioxy (**66**) (16 mg, 24 μmol, 76% over 2 steps) as the TFA salt.

^{1}H NMR (600 MHz, **CD_3CN** (350 μL)/D_2O (350 μL)): δ 8.31 (s, 1H), 8.29 (s, 1H), 7.32 (d, J = 1.8 Hz,

1H), 7.19 (d, J = 1.8 Hz, 1H), 6.05 (d, J = 1.0 Hz, 1H), 6.04 (d, J = 1.0 Hz, 1H), 5.96 (d, J = 5.1 Hz, 1H), 4.71 (app t, J = 5.1 Hz, 1H), 4.32 (ddd, J = 10.4, 4.4, 3.2 Hz, 1H), 4.19 (dd, J = 5.1, 4.4 Hz, 1H), 3.88 (dd, J = 6.7, 5.8 Hz, 1H), 2.84–2.78 (m, 1H), 2.08 (dddd, J = 14.2, 11.7, 6.7, 4.7 Hz, 1H), 2.03–1.97 (m, 2H), 1.90 (ddd, J = 13.9, 10.7, 3.2 Hz, 1H), 1.72 (app ddt, J = 13.1, 11.7, 5.0 Hz, 1H), 1.55 (dddd, J = 13.1, 11.7, 9.2, 4.7 Hz, 1H);

^{13}C NMR (101 MHz, **CD_3CN** (350 μL)/D_2O (350 μL)/*d*-TFA (40 μL)): δ 172.4, 171.4, 152.8, 151.1, 149.5, 149.1, 145.4, 144.4, 127.8, 126.9, 120.1, 108.6, 105.4, 104.0, 97.2, 90.3, 84.1, 77.5, 74.9, 74.6, 53.8, 38.7, 30.9, 29.9, 28.9;

HRMS (ESI+): calcd. for $[C_{25}H_{28}N_7O_8]^+$ 554.1994, meas. 554.2004, Δ 1.8 ppm.

3.5.12 *X-Ray Crystal Structure*, NS1-Cyclopropyl: Cyclopropyl Alkyne **S24**

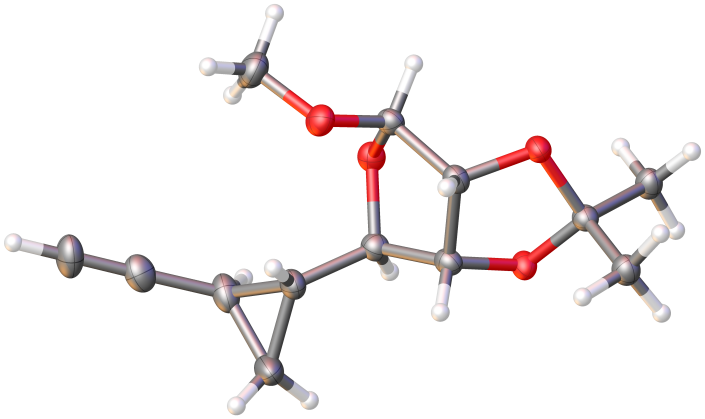

Table 3.5.1: Experimental Details

Crystal Data	
Chemical Formula	$C_{13}H_{18}O_4$
M_r	238.27
Crystal system, space group	Monoclinic, $F2_1$
Temperature (K)	100
a, b, c (Å)	5.7618 (1), 19.4824 (4), 11.8204 (2)

β (°)	90.0232 (11)
V(Å^3)	1326.88 (4)
Z	4
Radiation type	Cu $K\alpha$
μ (mm^{-1})	0.72
Crystal size (mm)	$0.14 \times 0.10 \times 0.06$
Data Collection	
Diffractometer	Bruker D8 goniometer with CCD area detector
Absorption correction	Multi-scan *SADABS*
T_{min}, T_{max}	0.797, 0.864
No. of measured, independent and observed $[I > 2\sigma(I)]$ reflections	26548, 4269, 4245
R_{int}	0.032
$(\sin\theta/\lambda)_{max}$(Å^{-1})	0.596
Refinement	
$R[F^2 > 2\sigma(F^2)], wR(F^2), S$	0.026, 0.064, 1.06
No. of reflections	4269
No. of parameters	314
No. of restraints	1
H atom parameters constrained	
$\Delta\rho_{max}, \Delta\rho_{min}$ (eÅ^{-3})	0.11, -0.15
Absolute structure	Flack x determined using 1834 quotients [(I+)-(I-)]/[(I+)+(I-)][24]
Absolute structure parameter	-0.02 (9)

Computer programs: SAINT 8.37A (Bruker-AXS, 2015), SHELXT2014 (Sheldrick, 2015), SHELXL2014 (Sheldrick, 2015), Bruker SHELXTL (Sheldrick, 2015).

Table 3.5.2: Geometric parameters (Å, °)

O1–C2	1.426 (3)	O5–C21	1.421 (3)
O1–C1	1.438 (3)	O5–C25	1.428 (3)
O2–C3	1.410 (3)	O6–C23	1.408 (3)
O2–C4	1.439 (3)	O6–C24	1.442 (3)
O3–C1	1.428 (3)	O7–C22	1.428 (3)
O3–C5	1.429 (3)	O7–C21	1.434 (4)
O4–C3	1.415 (3)	O8–C23	1.413 (3)
O4–C8	1.433 (4)	O8–C28	1.434 (4)
C1–C7	1.512 (4)	C21–C26	1.505 (4)
C1–C6	1.516 (4)	C21–C27	1.508 (4)
C2–C3	1.529 (4)	C22–C23	1.521 (4)

[24] Parsons, S.; Flack, H. D.; Wagner, T. *Acta Crystallogr., Sect. B* **2013**, *69*, 249–259.

Table 3.5.2 continued from previous page.

C2–C5	1.550 (4)	C22–C25	1.540 (4)
C2–H2	1	C22–H22	1
C3–H3	1	C23–H23	1
C4–C9	1.509 (4)	C24–C29	1.510 (4)
C4–C5	1.528 (4)	C24–C25	1.520 (4)
C4–H4	1	C24–H24	1
C5–H5	1	C25–H25	1
C6–H6A	0.98	C26–H26A	0.98
C6–H6B	0.98	C26–H26B	0.98
C6–H6C	0.98	C26–H26C	0.98
C7–H7A	0.98	C27–H27A	0.98
C7–H7B	0.98	C27–H27B	0.98
C7–H7C	0.98	C27–H27C	0.98
C8–H8A	0.98	C28–H28A	0.98
C8–H8B	0.98	C28–H28B	0.98
C8–H8C	0.98	C28–H28C	0.98
C9–C10	1.492 (4)	C29–C30	1.500 (4)
C9–C11	1.514 (4)	C29–C31	1.517 (4)
C9–H9	1	C29–H29	1
C10–C11	1.519 (5)	C30–C31	1.520 (4)
C10–H10A	0.99	C30–H30A	0.99
C10–H10B	0.99	C30–H30B	0.99
C11–C12	1.441 (5)	C31–C32	1.439 (4)
C11–H11	1	C31–H31	1
C12–C13	1.182 (5)	C32–C33	1.181 (4)
C13–H13	0.95	C33–H33	0.95
C2–O1–C1	107.74 (19)	C21–O5–C25	107.6 (2)
C3–O2–C4	107.8 (2)	C23–O6–C24	107.9 (2)
C1–O3–C5	107.19 (19)	C22–O7–C21	107.4 (2)
C3–O4–C8	112.1 (2)	C23–O8–C28	112.1 (2)
O3–C1–O1	103.8 (2)	O5–C21–O7	104.4 (2)
O3–C1–C7	108.9 (2)	O5–C21–C26	108.6 (2)
O1–C1–C7	109.1 (2)	O7–C21–C26	109.0 (2)
O3–C1–C6	111.3 (2)	O5–C21–C27	110.7 (2)
O1–C1–C6	111.1 (2)	O7–C21–C27	111.2 (3)
C7–C1–C6	112.2 (2)	C26–C21–C27	112.6 (2)
O1–C2–C3	110.1 (2)	O7–C22–C23	109.2 (2)
O1–C2–C5	104.7 (2)	O7–C22–C25	104.9 (2)
C3–C2–C5	103.9 (2)	C23–C22–C25	104.3 (2)
O1–C2–H2	112.5	O7–C22–H22	112.6
C3–C2–H2	112.5	C23–C22–H22	112.6
C5–C2–H2	112.5	C25–C22–H22	112.6
O2–C3–O4	111.9 (2)	O6–C23–O8	111.8 (2)
O2–C3–C2	106.2 (2)	O6–C23–C22	105.5 (2)

Table 3.5.2 continued from previous page.

O4–C3–C2	107.4 (2)	O8–C23–C22	107.3 (2)
O2–C3–H3	110.4	O6–C23–H23	110.7
O4–C3–H3	110.4	O8–C23–H23	110.7
C2–C3–H3	110.4	C22–C23–H23	110.7
O2–C4–C9	112.7 (2)	O6–C24–C29	112.5 (2)
O2–C4–C5	104.2 (2)	O6–C24–C25	104.1 (2)
C9–C4–C5	114.6 (2)	C29–C24–C25	114.5 (2)
O2–C4–H4	108.4	O6–C24–H24	108.5
C9–C4–H4	108.4	C29–C24–H24	108.5
C5–C4–H4	108.4	C25–C24–H24	108.5
O3–C5–C4	108.9 (2)	O5–C25–C24	108.5 (2)
O3–C5–C2	103.72 (19)	O5–C25–C22	104.1 (2)
C4–C5–C2	104.5 (2)	C24–C25–C22	104.8 (2)
O3–C5–H5	113	O5–C25–H25	112.9
C4–C5–H5	113	C24–C25–H25	112.9
C2–C5–H5	113	C22–C25–H25	112.9
C1–C6–H6A	109.5	C21–C26–H26A	109.5
C1–C6–H6B	109.5	C21–C26–H26B	109.5
H6A–C6–H6B	109.5	H26A–C26–H26B	109.5
C1–C6–H6C	109.5	C21–C26–H26C	109.5
H6A–C6–H6C	109.5	H26A–C26–H26C	109.5
H6B–C6–H6C	109.5	H26B–C26–H26C	109.5
C1–C7–H7A	109.5	C21–C27–H27A	109.5
C1–C7–H7B	109.5	C21–C27–H27B	109.5
H7A–C7–H7B	109.5	H27A–C27–H27B	109.5
C1–C7–H7C	109.5	C21–C27–H27C	109.5
H7A–C7–H7C	109.5	H27A–C27–H27C	109.5
H7B–C7–H7C	109.5	H27B–C27–H27C	109.5
O4–C8–H8A	109.5	O8–C28–H28A	109.5
O4–C8–H8B	109.5	O8–C28–H28B	109.5
H8A–C8–H8B	109.5	H28A–C28–H28B	109.5
O4–C8–H8C	109.5	O8–C28–H28C	109.5
H8A–C8–H8C	109.5	H28A–C28–H28C	109.5
H8B–C8–H8C	109.5	H28B–C28–H28C	109.5
C10–C9–C4	119.2 (3)	C30–C29–C24	118.2 (2)
C10–C9–C11	60.7 (2)	C30–C29–C31	60.49 (19)
C4–C9–C11	116.3 (3)	C24–C29–C31	115.2 (2)
C10–C9–H9	116.3	C30–C29–H29	117
C4–C9–H9	116.3	C24–C29–H29	117
C11–C9–H9	116.3	C31–C29–H29	117
C9–C10–C11	60.4 (2)	C29–C30–C31	60.32 (19)
C9–C10–H10A	117.7	C29–C30–H30A	117.7
C11–C10–H10A	117.7	C31–C30–H30A	117.7
C9–C10–H10B	117.7	C29–C30–H30B	117.7
C11–C10–H10B	117.7	C31–C30–H30B	117.7

Table 3.5.2 continued from previous page.

H10A–C10–H10B	114.9	H30A–C30–H30B	114.9
C12–C11–C9	119.9 (3)	C32–C31–C29	120.3 (3)
C12–C11–C10	121.5 (3)	C32–C31–C30	119.9 (3)
C9–C11–C10	58.9 (2)	C29–C31–C30	59.20 (19)
C12–C11–H11	115	C32–C31–H31	115.3
C9–C11–H11	115	C29–C31–H31	115.3
C10–C11–H11	115	C30–C31–H31	115.3
C13–C12–C11	179.2 (4)	C33–C32–C31	179.2 (4)
C12–C13–H13	180	C32–C33–H33	180
C5–O3–C1–O1	-36.5 (3)	C25–O5–C21–O7	-34.3 (3)
C5–O3–C1–C7	-152.6 (2)	C25–O5–C21–C26	-150.4 (2)
C5–O3–C1–C6	83.1 (3)	C25–O5–C21–C27	85.5 (3)
C2–O1–C1–O3	32.7 (3)	C22–O7–C21–O5	32.5 (3)
C2–O1–C1–C7	148.7 (2)	C22–O7–C21–C26	148.4 (2)
C2–O1–C1–C6	-87.1 (3)	C22–O7–C21–C27	-86.9 (3)
C1–O1–C2–C3	-127.7 (2)	C21–O7–C22–C23	-129.6 (2)
C1–O1–C2–C5	-16.6 (3)	C21–O7–C22–C25	-18.4 (3)
C4–O2–C3–O4	-81.8 (2)	C24–O6–C23–O8	-80.3 (2)
C4–O2–C3–C2	35.1 (3)	C24–O6–C23–C22	36.1 (3)
C8–O4–C3–O2	-61.9 (3)	C28–O8–C23–O6	-60.8 (3)
C8–O4–C3–C2	-178.2 (2)	C28–O8–C23–C22	-176.1 (2)
O1–C2–C3–O2	93.6 (2)	O7–C22–C23–O6	91.4 (2)
C5–C2–C3–O2	-18.1 (3)	C25–C22–C23–O6	-20.3 (3)
O1–C2–C3–O4	-146.4 (2)	O7–C22–C23–O8	-149.2 (2)
C5–C2–C3–O4	101.9 (2)	C25–C22–C23–O8	99.1 (2)
C3–O2–C4–C9	87.5 (3)	C23–O6–C24–C29	87.8 (3)
C3–O2–C4–C5	-37.3 (3)	C23–O6–C24–C25	-36.7 (3)
C1–O3–C5–C4	136.6 (2)	C21–O5–C25–C24	133.7 (2)
C1–O3–C5–C2	25.7 (3)	C21–O5–C25–C22	22.4 (3)
O2–C4–C5–O3	-86.3 (2)	O6–C24–C25–O5	-88.8 (2)
C9–C4–C5–O3	150.1 (2)	C29–C24–C25–O5	148.0 (2)
O2–C4–C5–C2	24.0 (3)	O6–C24–C25–C22	22.0 (3)
C9–C4–C5–C2	-99.6 (3)	C29–C24–C25–C22	-101.2 (2)
O1–C2–C5–O3	-5.4 (3)	O7–C22–C25–O5	-2.3 (3)
C3–C2–C5–O3	110.1 (2)	C23–C22–C25–O5	112.5 (2)
O1–C2–C5–C4	-119.4 (2)	O7–C22–C25–C24	-116.2 (2)
C3–C2–C5–C4	-3.9 (3)	C23–C22–C25–C24	-1.4 (3)
O2–C4–C9–C10	147.8 (3)	O6–C24–C29–C30	143.8 (3)
C5–C4–C9–C10	-93.2 (3)	C25–C24–C29–C30	-97.7 (3)
O2–C4–C9–C11	78.2 (3)	O6–C24–C29–C31	75.2 (3)
C5–C4–C9–C11	-162.8 (3)	C25–C24–C29–C31	-166.2 (2)
C4–C9–C10–C11	-105.6 (3)	C24–C29–C30–C31	-104.6 (3)
C10–C9–C11–C12	110.9 (4)	C30–C29–C31–C32	108.9 (3)
C4–C9–C11–C12	-138.8 (3)	C24–C29–C31–C32	-141.6 (3)

Table 3.5.2 continued from previous page.

C4–C9–C11–C10	110.3 (3)	C24–C29–C31–C30	109.5 (3)
C9–C10–C11–C12	-108.3 (3)	C29–C30–C31–C32	-109.5 (3)

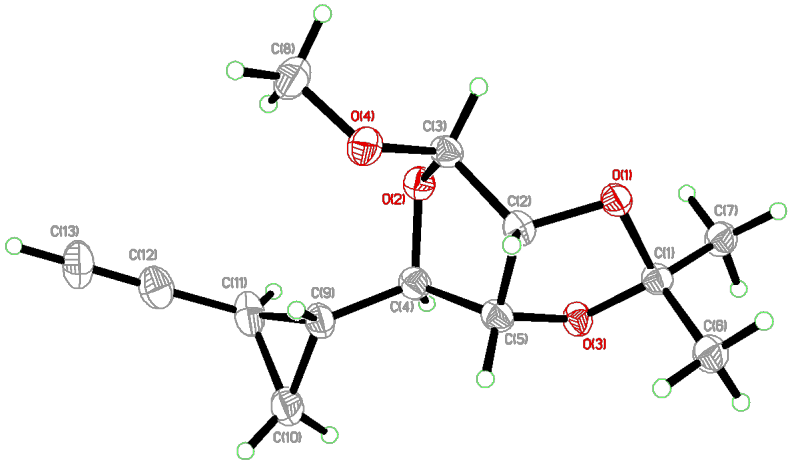

Figure 3.5.1: Perspective views showing 50% probability displacement.

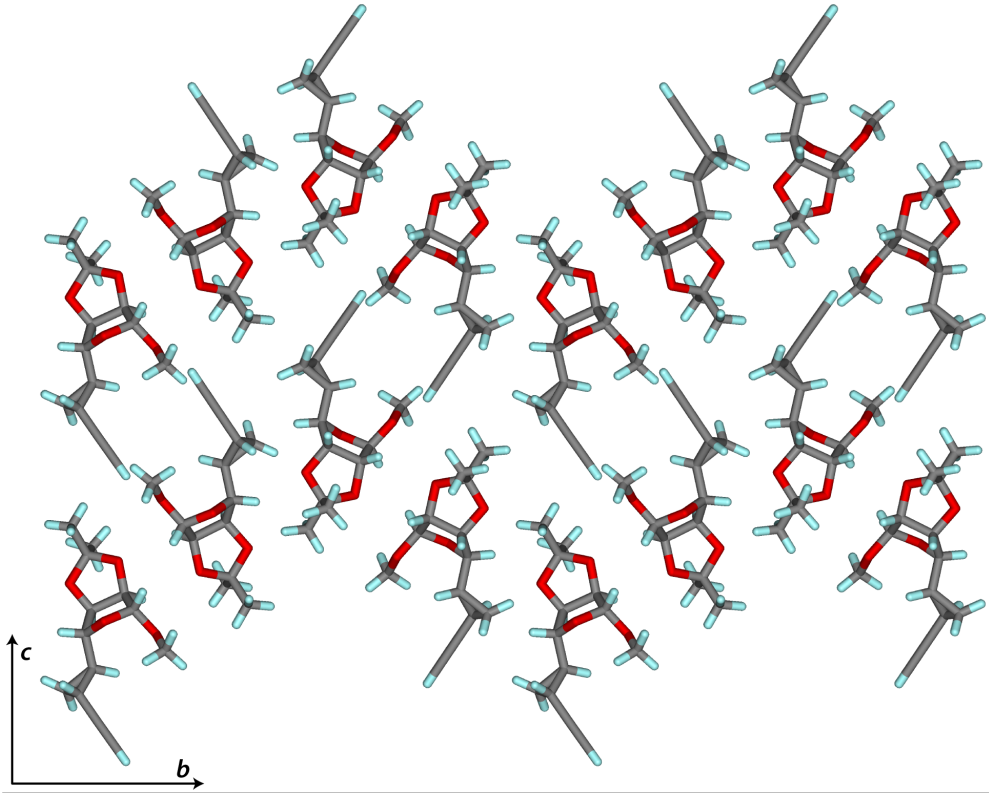

Figure 3.5.2: Three-dimensional supramolecular architecture viewed along the *a*-axis direction.

3.5.13 *X-Ray Crystal Structure*, NS1-Urea: Alkynyl Alcohol **S30**

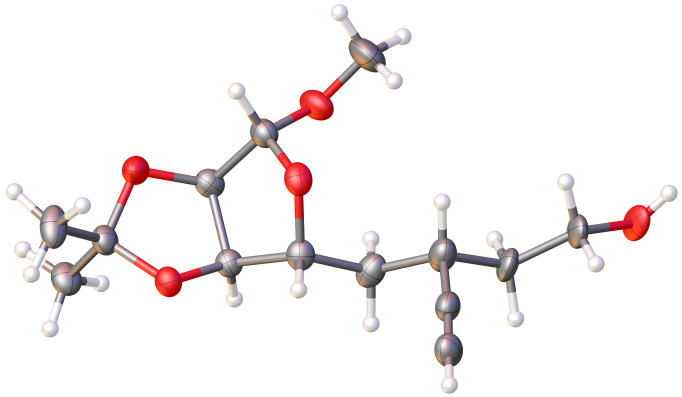

Table 3.5.3: Experimental Details

Crystal Data	
Chemical Formula	$C_{14}H_{22}O_5$
M_r	270.31
Crystal system, space group	Orthorhombic, $P2_12_12_1$
Temperature (K)	100
a, b, c (Å)	5.7488 (1), 9.3963 (2), 27.2172 (7)
V(Å^3)	1470.20 (6)
Z	4
Radiation type	Cu $K\alpha$
μ (mm^{-1})	0.76
Crystal size (mm)	$0.18 \times 0.12 \times 0.10$
Data Collection	
Diffractometer	Bruker D8 goniometer with CCD area detector
Absorption correction	Multi-scan *SADABS*
T_{min}, T_{max}	0.796, 0.864
No. of measured, independent and observed $[I > 2\sigma(I)]$ reflections	31333, 2577, 2531
R_{int}	0.035
$(\sin\theta/\lambda)_{max}$(Å^{-1})	0.596
Refinement	
$R[F^2 > 2\sigma(F^2)], wR(F^2), S$	0.040, 0.107, 1.09
No. of reflections	2577
No. of parameters	206
No. of restraints	252
H-atom treatment	H atom parameters constrained
$\Delta\rho_{max}, \Delta\rho_{min}$ (eÅ^{-3})	0.43, -0.23

Absolute structure	Flack x determined using 1012 quotients [(I+)-(I-)]/[(I+)+(I-)][25]
Absolute structure parameter	0.10 (4)

Computer programs: APEX3 v2016.9-0 (Bruker-AXS, 2016), SAINT 8.37A (Bruker-AXS, 2015), SHELXT2014 (Sheldrick, 2015), SHELXL2014 (Sheldrick, 2015), Bruker SHELXTL (Sheldrick, 2015).

Table 3.5.4: Geometric parameters (Å, °)

O1–C1	1.419 (3)	C8A–H8AA	0.99
O1–C5	1.438 (3)	C8A–H8AB	0.99
O2–C1	1.410 (3)	C9A–O5A	1.480 (9)
O2–C10	1.416 (4)	C9A–H9AA	0.99
O3–C2	1.424 (3)	C9A–H9AB	0.99
O3–C3	1.425 (3)	O5A–H5AA	0.84
O4–C3	1.428 (3)	C7B–C13	1.460 (4)
O4–C4	1.430 (3)	C7B–C8B	1.449 (15)
C1–C2	1.528 (4)	C7B–H7B	1
C1–H1	1	C8B–C9B	1.510 (19)
C2–C4	1.536 (3)	C8B–H8BA	0.99
C2–H2	1	C8B–H8BB	0.99
C3–C11	1.510 (4)	C9B–O5B	1.491 (11)
C3–C12	1.512 (4)	C9B–H9BA	0.99
C4–C5	1.527 (3)	C9B–H9BB	0.99
C4–H4	1	O5B–H5B	0.84
C5–C6	1.523 (3)	C7C–C13	1.460 (4)
C5–H5	1	C7C–C8C	1.606 (17)
C6–C7C	1.539 (4)	C7C–H7C	1
C6–C7	1.539 (4)	C8C–C9C	1.465 (18)
C6–C7A	1.539 (4)	C8C–H8CA	0.99
C6–C7B	1.539 (4)	C8C–H8CB	0.99
C6–H6A	0.99	C9C–O5C	1.497 (11)
C6–H6B	0.99	C9C–H9CA	0.99
C7–C13	1.460 (4)	C9C–H9CB	0.99
C7–C8	1.587 (11)	O5C–H5C	0.84
C7–H7	1	C10–H10A	0.98
C8–C9	1.505 (11)	C10–H10B	0.98
C8–H8A	0.99	C10–H10C	0.98
C8–H8B	0.99	C11–H11A	0.98
C9–O5	1.458 (8)	C11–H11B	0.98
C9–H9A	0.99	C11–H11C	0.98
C9–H9B	0.99	C12–H12A	0.98
O5–H5A	0.84	C12–H12B	0.98
C7A–C13	1.460 (4)	C12–H12C	0.98

[25] Parsons, S.; Flack, H. D.; Wagner, T. *Acta Crystallogr., Sect. B* **2013**, *69*, 249–259.

Table 3.5.4 continued from previous page.

C7A–C8A	1.596 (13)	C13–C14	1.185 (4)
C7A–H7AA	1	C14–H14	0.95
C8A–C9A	1.567 (14)		
C1–O1–C5	109.19 (19)	C9A–C8A–H8AB	110
C1–O2–C10	111.5 (2)	C7A–C8A–H8AB	110
C2–O3–C3	108.15 (19)	H8AA–C8A–H8AB	108.4
C3–O4–C4	107.27 (18)	O5A–C9A–C8A	104.6 (10)
O2–C1–O1	112.0 (2)	O5A–C9A–H9AA	110.8
O2–C1–C2	108.0 (2)	C8A–C9A–H9AA	110.8
O1–C1–C2	106.3 (2)	O5A–C9A–H9AB	110.8
O2–C1–H1	110.2	C8A–C9A–H9AB	110.8
O1–C1–H1	110.2	H9AA–C9A–H9AB	108.9
C2–C1–H1	110.2	C9A–O5A–H5AA	109.5
O3–C2–C1	109.7 (2)	C13–C7B–C8B	123.8 (9)
O3–C2–C4	105.43 (19)	C13–C7B–C6	109.8 (2)
C1–C2–C4	104.7 (2)	C8B–C7B–C6	120.8 (10)
O3–C2–H2	112.2	C13–C7B–H7B	97.9
C1–C2–H2	112.2	C8B–C7B–H7B	97.9
C4–C2–H2	112.2	C6–C7B–H7B	97.9
O3–C3–O4	103.81 (19)	C7B–C8B–C9B	101.5 (13)
O3–C3–C11	108.9 (2)	C7B–C8B–H8BA	111.5
O4–C3–C11	109.1 (2)	C9B–C8B–H8BA	111.5
O3–C3–C12	110.8 (2)	C7B–C8B–H8BB	111.5
O4–C3–C12	111.1 (2)	C9B–C8B–H8BB	111.5
C11–C3–C12	112.8 (2)	H8BA–C8B–H8BB	109.3
O4–C4–C5	109.61 (19)	O5B–C9B–C8B	98.8 (13)
O4–C4–C2	102.89 (19)	O5B–C9B–H9BA	112
C5–C4–C2	105.0 (2)	C8B–C9B–H9BA	112
O4–C4–H4	112.9	O5B–C9B–H9BB	112
C5–C4–H4	112.9	C8B–C9B–H9BB	112
C2–C4–H4	112.9	H9BA–C9B–H9BB	109.7
O1–C5–C6	111.8 (2)	C9B–O5B–H5B	109.5
O1–C5–C4	104.0 (2)	C13–C7C–C6	109.8 (2)
C6–C5–C4	113.4 (2)	C13–C7C–C8C	103.7 (13)
O1–C5–H5	109.2	C6–C7C–C8C	124.7 (11)
C6–C5–H5	109.2	C13–C7C–H7C	105.8
C4–C5–H5	109.2	C6–C7C–H7C	105.8
C5–C6–C7C	112.5 (2)	C8C–C7C–H7C	105.8
C5–C6–C7	112.5 (2)	C9C–C8C–C7C	133 (2)
C5–C6–C7A	112.5 (2)	C9C–C8C–H8CA	103.8
C5–C6–C7B	112.5 (2)	C7C–C8C–H8CA	103.8
C5–C6–H6A	109.1	C9C–C8C–H8CB	103.8
C7–C6–H6A	109.1	C7C–C8C–H8CB	103.8
C5–C6–H6B	109.1	H8CA–C8C–H8CB	105.4

Table 3.5.4 continued from previous page.

C7–C6–H6B	109.1	C8C–C9C–O5C	159 (3)
H6A–C6–H6B	107.8	C8C–C9C–H9CA	96.5
C13–C7–C6	109.8 (2)	O5C–C9C–H9CA	96.5
C13–C7–C8	113.5 (6)	C8C–C9C–H9CB	96.5
C6–C7–C8	104.0 (5)	O5C–C9C–H9CB	96.5
C13–C7–H7	109.8	H9CA–C9C–H9CB	103.4
C6–C7–H7	109.8	C9C–O5C–H5C	109.5
C8–C7–H7	109.8	O2–C10–H10A	109.5
C9–C8–C7	107.9 (8)	O2–C10–H10B	109.5
C9–C8–H8A	110.1	H10A–C10–H10B	109.5
C7–C8–H8A	110.1	O2–C10–H10C	109.5
C9–C8–H8B	110.1	H10A–C10–H10C	109.5
C7–C8–H8B	110.1	H10B–C10–H10C	109.5
H8A–C8–H8B	108.4	C3–C11–H11A	109.5
O5–C9–C8	112.2 (8)	C3–C11–H11B	109.5
O5–C9–H9A	109.2	H11A–C11–H11B	109.5
C8–C9–H9A	109.2	C3–C11–H11C	109.5
O5–C9–H9B	109.2	H11A–C11–H11C	109.5
C8–C9–H9B	109.2	H11B–C11–H11C	109.5
H9A–C9–H9B	107.9	C3–C12–H12A	109.5
C9–O5–H5A	109.5	C3–C12–H12B	109.5
C13–C7A–C6	109.8 (2)	H12A–C12–H12B	109.5
C13–C7A–C8A	112.1 (9)	C3–C12–H12C	109.5
C6–C7A–C8A	115.2 (6)	H12A–C12–H12C	109.5
C13–C7A–H7AA	106.4	H12B–C12–H12C	109.5
C6–C7A–H7AA	106.4	C14–C13–C7	176.6 (3)
C8A–C7A–H7AA	106.4	C14–C13–C7A	176.6 (3)
C9A–C8A–C7A	108.3 (10)	C14–C13–C7B	176.6 (3)
C9A–C8A–H8AA	110	C14–C13–C7C	176.6 (3)
C7A–C8A–H8AA	110	C13–C14–H14	180
C10–O2–C1–O1	-66.2 (3)	O1–C5–C6–C7C	57.3 (3)
C10–O2–C1–C2	177.1 (2)	C4–C5–C6–C7C	174.5 (2)
C5–O1–C1–O2	-88.6 (2)	O1–C5–C6–C7	57.3 (3)
C5–O1–C1–C2	29.2 (2)	C4–C5–C6–C7	174.5 (2)
C3–O3–C2–C1	-124.8 (2)	O1–C5–C6–C7A	57.3 (3)
C3–O3–C2–C4	-12.5 (3)	C4–C5–C6–C7A	174.5 (2)
O2–C1–C2–O3	-138.6 (2)	O1–C5–C6–C7B	57.3 (3)
O1–C1–C2–O3	101.1 (2)	C4–C5–C6–C7B	174.5 (2)
O2–C1–C2–C4	108.7 (2)	C5–C6–C7–C13	64.9 (3)
O1–C1–C2–C4	-11.6 (2)	C5–C6–C7–C8	-173.3 (6)
C2–O3–C3–O4	29.9 (3)	C13–C7–C8–C9	-75.3 (10)
C2–O3–C3–C11	146.0 (2)	C6–C7–C8–C9	165.5 (8)
C2–O3–C3–C12	-89.5 (3)	C7–C8–C9–O5	-167.4 (9)
C4–O4–C3–O3	-36.6 (2)	C5–C6–C7A–C13	64.9 (3)

Table 3.5.4 continued from previous page.

C4–O4–C3–C11	-152.5 (2)	C5–C6–C7A–C8A	-167.3 (11)
C4–O4–C3–C12	82.6 (2)	C13–C7A–C8A–C9A	-62.2 (17)
C3–O4–C4–C5	139.4 (2)	C6–C7A–C8A–C9A	171.2 (12)
C3–O4–C4–C2	28.2 (2)	C7A–C8A–C9A–O5A	-172.7 (13)
O3–C2–C4–O4	-9.4 (2)	C5–C6–C7B–C13	64.9 (3)
C1–C2–C4–O4	106.3 (2)	C5–C6–C7B–C8B	-140.7 (10)
O3–C2–C4–C5	-124.1 (2)	C13–C7B–C8B–C9B	80.0 (17)
C1–C2–C4–C5	-8.4 (2)	C6–C7B–C8B–C9B	-70.7 (17)
C1–O1–C5–C6	88.4 (2)	C7B–C8B–C9B–O5B	-178.6 (14)
C1–O1–C5–C4	-34.3 (2)	C5–C6–C7C–C13	64.9 (3)
O4–C4–C5–O1	-84.7 (2)	C5–C6–C7C–C8C	-171.4 (18)
C2–C4–C5–O1	25.2 (2)	C13–C7C–C8C–C9C	-69 (4)
O4–C4–C5–C6	153.6 (2)	C6–C7C–C8C–C9C	165 (3)
C2–C4–C5–C6	-96.5 (2)	C7C–C8C–C9C–O5C	162 (7)

Table 3.5.5: Hydrogen-bond parameters

D – H · · · A	D – H (Å)	H · · · A (Å)	D · · · A (Å)	D – H · · · A (°)
O5 – H5A · · · O5^{i}	0.84	2.33	3.132 (5)	159.9

Symmetry code(s): (i) x-1/2, -y+3/2, -z+1.

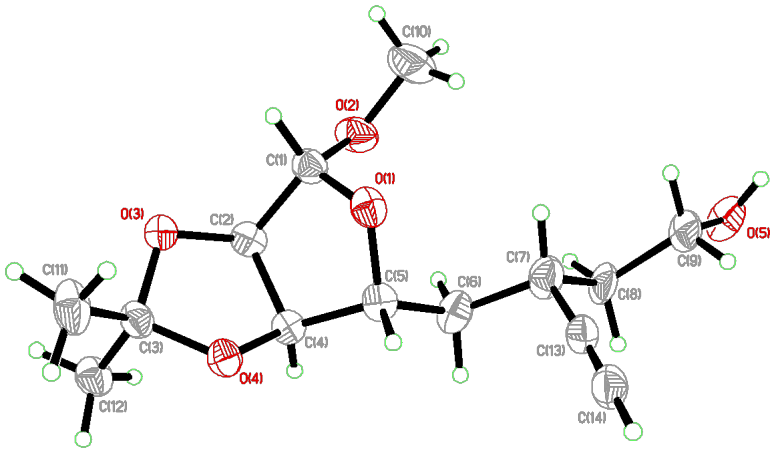

Figure 3.5.3: Perspective views showing 50% probability displacement.

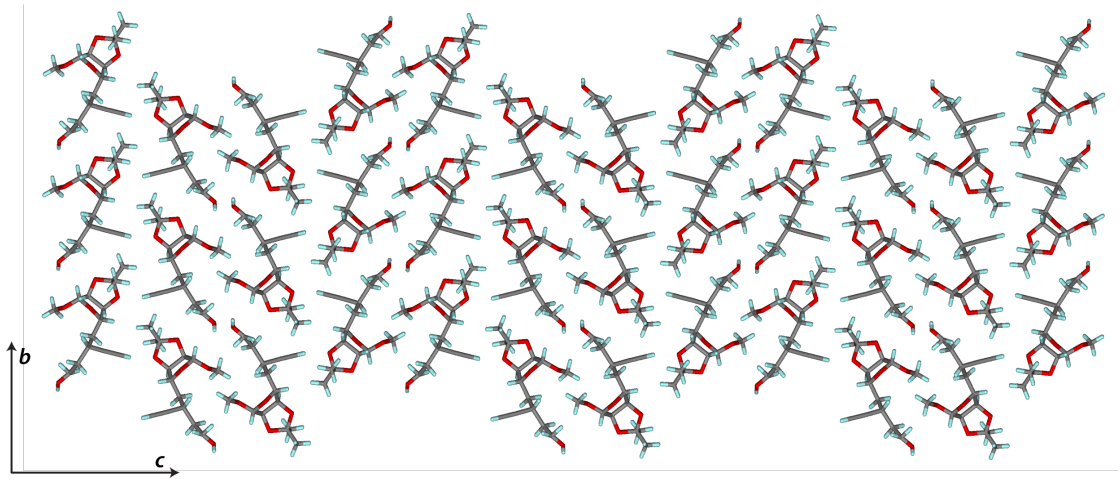

Figure 3.5.4: Three-dimensional supramolecular architecture viewed along the *a*-axis direction.

4

Selectivity and Cell-Based Evaluation

4.1 NS1 Selectivity

While several previously reported NNMT inhibitors were described as selective for NNMT, none of them have been tested against the closest homologues[1] of NNMT or other small-molecule methyltransferases[2,3]. We aimed to critically evaluate the selectivity profile of NS1 by testing it against the methyltransferases most like NNMT.

Sequence similarity analysis and generation of a sequence similarity network[4,5] (Figure 4.1.1, 6.2.1)

---

[1] Peng, Y.; Sartini, D.; Pozzi, V.; Wilk, D.; Emanuelli, M.; Yee, V. C. *Biochemistry* **2011**, *50*, 7800–7808.

[2] Fujioka, M *Int. J. Biochem.* **1992**, *24*, 1917–1924.

[3] Petrossian, T. C.; Clarke, S. G. *Mol. Cell. Proteomics* **2011**, *10*.

[4] Gerlt, J. A.; Bouvier, J. T.; Davidson, D. B.; Imker, H. J.; Sadkhin, B; Slater, D. R.; Whalen, K. L. *Biochim. Biophys. Acta.* **2015**, *1854*, 1019–1037.

[5] Zallot, R; Oberg, N. O.; Gerlt, J. A. *Curr. Opin. Chem. Biol.* **2018**, *47*, 77–85.

showed that NNMT, INMT (indolethylamine N-methyltransferase[6]), and PNMT (phenylethanolamine N-methyltransferase[7]) cluster tightly, with INMT and PNMT having 53% and 39% sequence identity to NNMT, respectively.

A complementary approach based on structural homology analysis via the DALI[8] server demonstrated that INMT and PNMT are also the closest structural homologues of NNMT (Figure 4.1.3, 4.1.4, Table 6.2.2).[9] In addition to the selectivity of NS1 amongst small-molecule methyltransferases, we tested NS1 against a few representative DNA, histone, and protein-arginine methyltransferases (Figure 4.1.5, Table 4.1.1). These studies revealed thiopurine S-methyltransferase (TPMT) to be the closest off-target of NS1, with an IC_{50} of $\sim$1 μM. This result might be explained by the flexibility of the TPMT active site[10] and the ability of TPMT to bind a variety of small molecule substrates and inhibitors[11]. INMT was the second closest off-target of NS1, with an IC_{50} of 3.4 μM (Figure 4.1.6).

---

[6] Thompson M.A., W. R.; Thompson M. A., W. R. *J. Biol. Chem.* **1998**, *273*, 34502–10.

[7] Axelrod, J *J. Biol. Chem.* **1962**, *237*, 1657–1660.

[8] Holm, L.; Laakso, L. M. *Nucleic Acids Res.* **2016**, *44*, W351–W355.

[9] Peng, Y.; Sartini, D.; Pozzi, V.; Wilk, D.; Emanuelli, M.; Yee, V. C. *Biochemistry* **2011**, *50*, 7800–7808.

[10] Peng, Y.; Feng, Q.; Wilk, D.; Adjei, A. A.; Salavaggione, O. E.; Weinshilboum, R. M.; Yee, V. C. *Biochemistry* **2008**, *47*, 6216–6225.

[11] Ames, M. M.; Selassie, C. D.; Woodson, L. C.; Van Loon, J. A.; Hansch, C; Weinshilboum, R. M. *J. Med. Chem.* **1986**, *29*, 354–358.

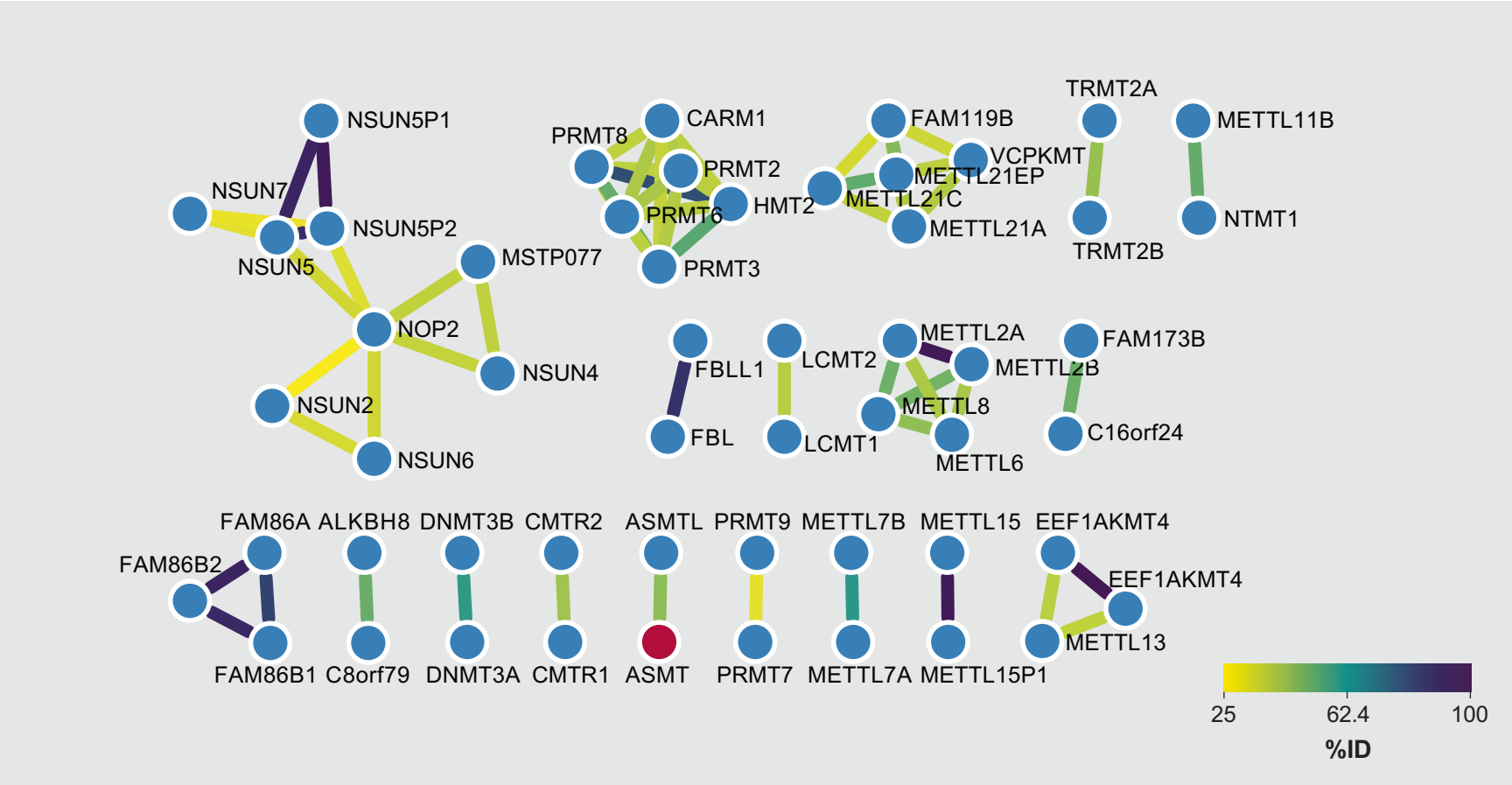

Figure 4.1.1: Sequence similarity network (SSN) of human methyltransferases. Node labels correspond to UniProt IDs and Protein Names found in Table 6.2.1. Red nodes correspond to small-molecule methyltransferases. Edges are color coded according to sequence similarity (%ID, legend at bottom right). A description of the SSN generation work flow is detailed in Section 4.3.1.

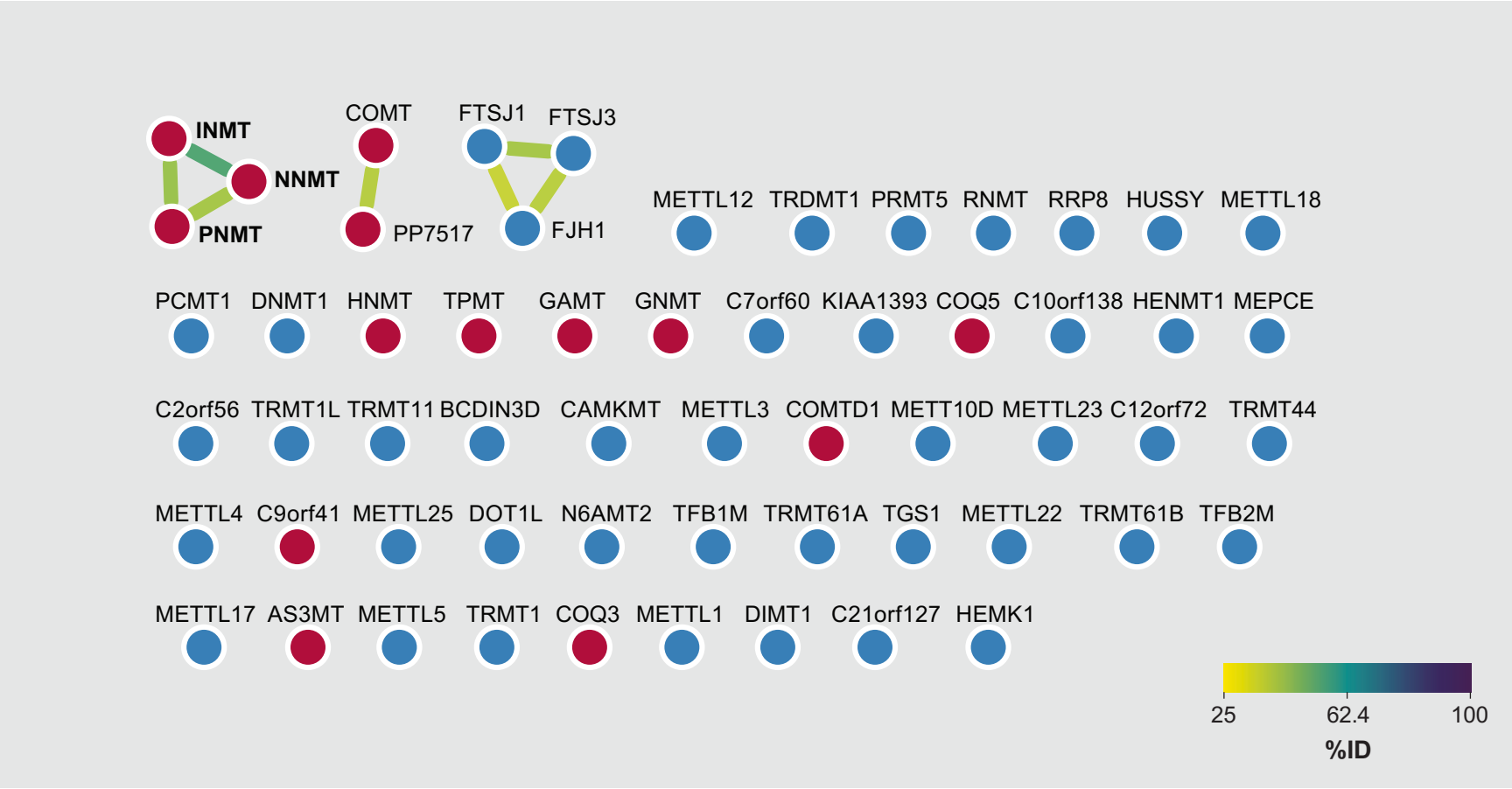

Figure 4.1.2: Sequence similarity network (SSN) of human methyltransferases. **The NNMT, INMT, PNMT cluster appears at top left**. Node labels correspond to UniProt IDs and Protein Names found in Table 6.2.1. Red nodes correspond to small-molecule methyltransferases. Edges are color coded according to sequence similarity (%ID, legend at bottom right). A description of the SSN generation workflow is detailed in Section 4.3.1.

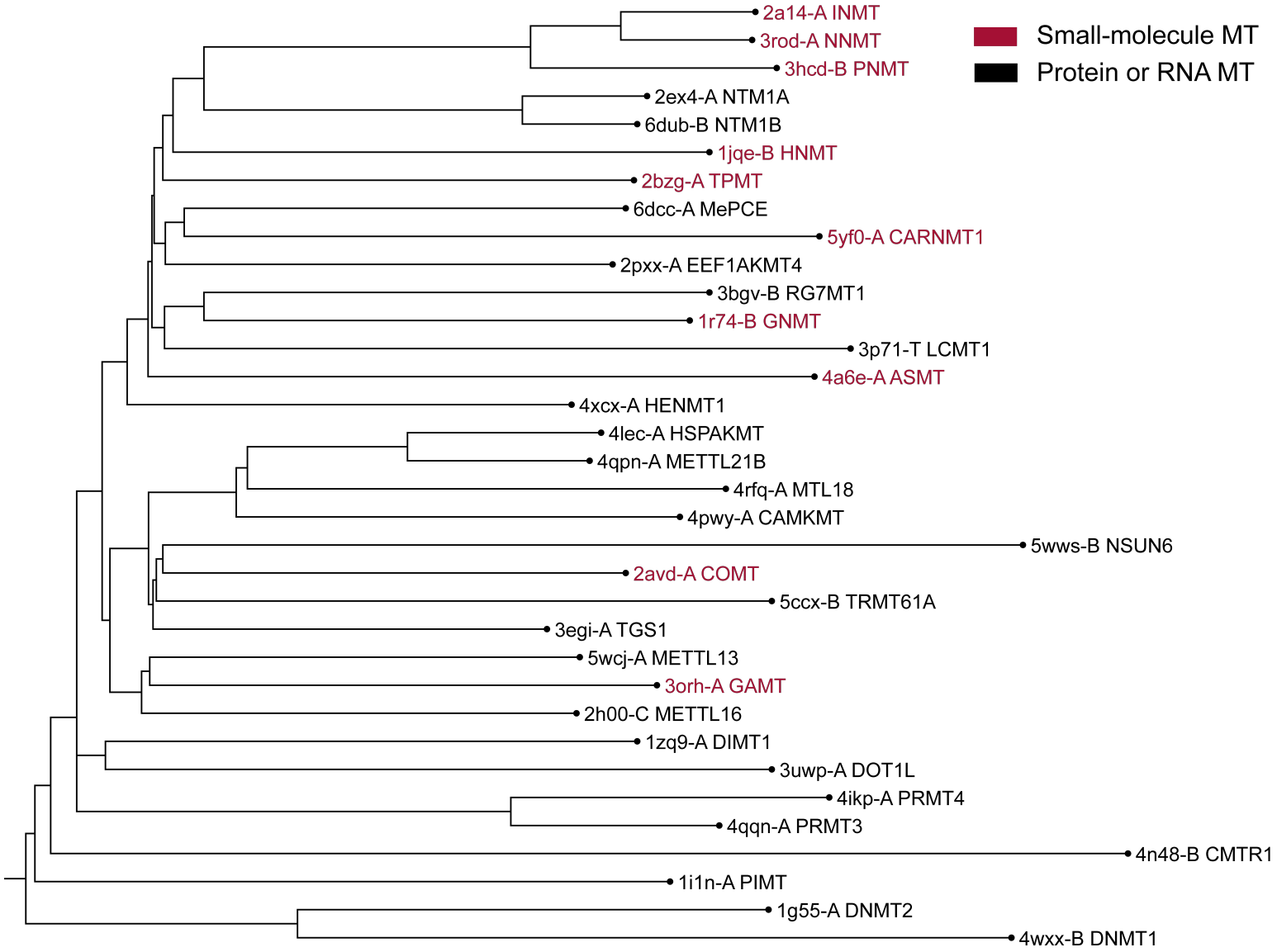

Figure 4.1.3: Structural similarity dendrogram. The dendrogram is derived by average linkage clustering of the structural similarity matrix (Dali Z-scores).

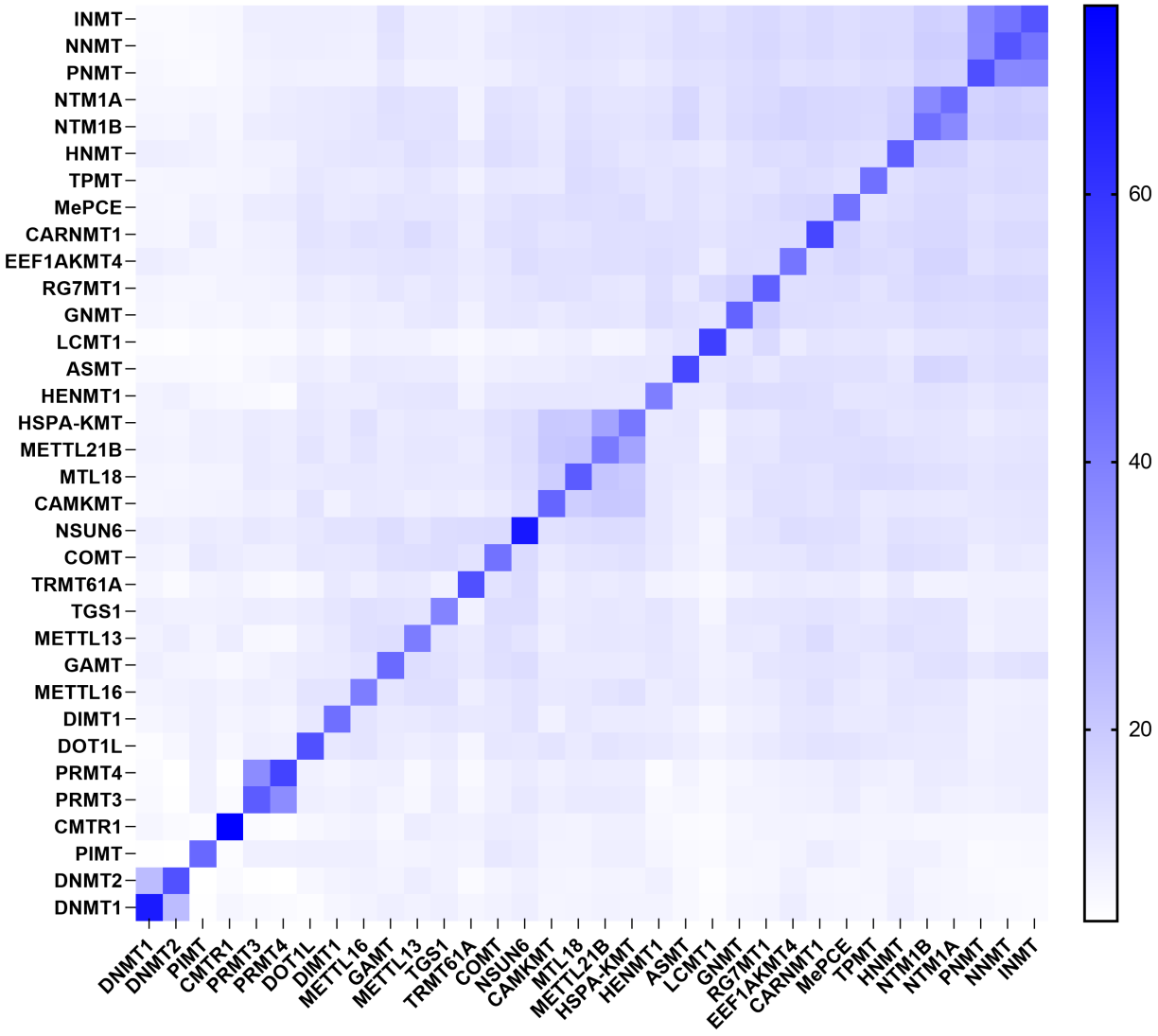

Figure 4.1.4: Heatmap of DALI Z-scores. Axes are labelled with protein abbreviations and correspond to those listed in Table 6.2.2. Note the NNMT/INMT/PNMT cluster (top right) indicating high structural similarity between these proteins.

small-molecule methyltransferase	inhibition at 10 μM (%)	inhibition at 1 μM (%)
TPMT[a]	76	51
INMT[b,*]	53	14
COMT[c]	43	0
PNMT[d]	26	0
GAMT[e]	26	0
GNMT[f]	23	4
HNMT[g]	2	6
protein or DNA methyltransferase	**IC_{50} (μM)**	
hDNMT3a[h]	7.6	
PRMT1[i]	>10	
ASH1L[j]	>10	
DOT1L[k]	>10	
EHMT1[l]	>10	
G9a[m]	>10	
SETDB1[n]	>10	

Figure 4.1.5: Methyltransferase selectivity profile of NS1. [a]thiopurine S-methyltransferase. [b]indolethylamine N-methyltransferase; *values interpolated from the full IC_{50} curve shown in Figure 4.1.6. [c]catechol O-methyltransferase. [d]phenylethanolamine N-methyltransferase. [e]guanidinoacetate N-methyltransferase. [f]glycine N-methyltransferase. [g]histamine N-methyltransferase. [h]DNA (cytosine-5)-methyltransferase 3A. [i]protein arginine N-methyltransferase 1. [j]histone-lysine N-methyltransferase ASH1L. [k]histone-lysine N-methyltransferase, H3 lysine-79 specific. [l]histone-lysine N-meth-yltransferase EHMT1. [m]histone-lysine N-methyltransferase EHMT2. [n]histone-lysine N-methyltransferase SETDB1.

Table 4.1.1: Assays performed in the course of this work to evaluate selectivity for NNMT.

Enzyme/Assay	Source	Substrate/Stimulus Tracer	Incubation	Measured Component	Detection Method	Reference
thiopurine S-methyltransferase (TPMT)	HR (E. coli)	6-mercaptopurine (8 µM), SAM (1.5 µM)	30 min, 22°C	SAH	MS	Krijt et al.[a]
indoleethylamine N-methyltransferase (INMT)	HR (E. coli)	tryptamine (1 mM), SAM (10 µM)	30 min, 22°C	luminescence	plate reader	this work
catechol O-methyltransferase (COMT)	HR (E. coli)	pyrocatechol (15 µM), SAM (10 µM)	15 min, 37°C	SAH	MS	Krijt et al.[a]
phenylethanolamine N-methyltransferase (PNMT)	HR (E. coli)	DL-normetanephrine (35 µM), SAM (6 µM)	45 min, 22°C	SAH	MS	Krijt et al.[a]
glycine N-methyltransferase (GNMT)	HR (E. coli)	glycine (100 µM), SAM (20 µM)	30 min, 22°C	SAH	MS	Krijt et al.[a]
guanidinoacetate N-methyltransferase (GAMT)	HR (E. coli)	guanidineacetic acid (4 µM), SAM (7 µM)	30 min, 22°C	SAH	MS	Krijt et al.[a]
histamine N-methyltransferase (HNMT)	HR (E. coli)	histamine (4 µM), SAM (4 µM)	15 min, 22°C	SAH	MS	Krijt et al.[a]
DNMT3a	HR (Sf9 cells)	poly(dI-dC)-poly(dI-dC) (0.6 mU/ml), [3H] SAM (100 nM)	10 min, 37°C	methylated poly(dI-dC)-Poly(dI-dC)	scint. counting	Aoki et al.[b]
PRMT1	HR (E. coli)	histone H4 full length (50 nM), [3H]SAM (700 nM)	20 min, 22°C	methylated histone H4 full length	scint. counting	Cheng et al.[c]
ASH1L	HR (E. coli)	polynucleosome (1.5 µg/ml), [3H] SAM (150nM)	15 min, 22°C	methylated polynucleosome	scint. counting	An et al.[d]
DOT1L	HR (E. coli)	polynucleosome (2.5 µg/ml), [3H]SAM (100 nM)	15 min, 22°C	methylated polynucleosome	scint. counting	Yost et al.[e]
EHMT1	HR (E. coli)	histone H3 full length (10 nM), [3H]SAM (25 nM)	120 min, 22°C	methylated histone H3 full length	scint. counting	Yost et al.[e]
G9a	HR (E. coli)	histone H3 full length (5 nM), [3H]SAM (25 nM)	120 min, 22°C	methylated histone H3 full length	scint. counting	Yost et al.[e]
SETDB1	HR (cellules Sf9)	histone H3 full length (30 nM), [3H]SAM (250 nM)	30 min, 22°C	methylated histone H3 full length	scint. counting	Schultz et al.[f]

[a] Krijt, J.; Dutá, A.; Kožich, V. *J. Chromatogr., B* **2009**, *877*, 2061–2066.

[b] Aoki, A. *Nucleic Acids Res.* **2001**, *29*, 3506–3512.

[c] Cheng, D.; Yadav, N.; King, R. W.; Swanson, M. S.; Weinstein, E. J.; Bedford, M. T. *J. Biol. Chem.* **2004**, *279*, 23892–23899.

[d] An, S.; Yeo, K. J.; Jeon, Y. H.; Song, J.-J. *J. Biol. Chem.* **2011**, *286*, 8369–8374.

[e] Yost, J. M.; Korboukh, I.; Liu, F.; Gao, C.; Jin, J. *Curr. Chem. Genomics* **2011**, *5*, 72–84.

[f] Schultz, D. C.; Ayyanathan, K.; Negorev, D.; Maul, G. G.; Rauscher, F. J. *Genes & Dev.* **2002**, *16*, 919–932.

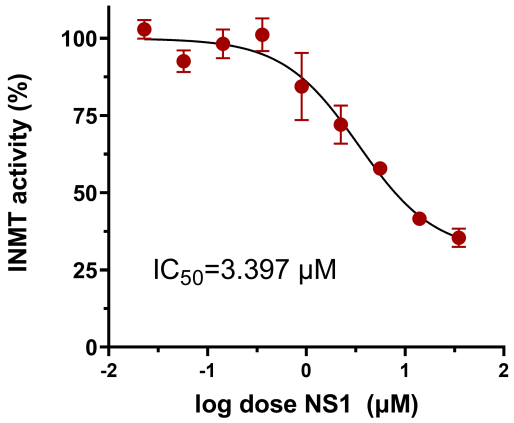

Figure 4.1.6: INMT IC_{50} assay performed using the Promega MTase-Glo™ assay. Full experimental details are reported in Section 4.3.2.

While in this case NS1 proved selective for NNMT, the introduction of different aryl groups on the NS1 scaffold could likely be used to target other methyltransferases selectively. In this work, cross coupling of compound **39** (Figure 2.5.1) with 3-iodobenzamide generated NS1; cross coupling of **39** with indole or thiopurine fragments could provide inhibitors of INMT and TPMT, respectively. In cases where off-target binding or inhibition is observed, aryl groups could be modified until a desired selectivity profile is achieved.

4.2 Thermal Stabilization and Cell-Based Evaluation

Along with biochemical profiling of NS1 and analogues, we found that NS1 binds and stabilizes NNMT in K562 cell lysate. The cellular thermal shift assay (CETSA[12]) revealed that NS1 and **55** shift the melting curve of NNMT by 8 and 5 °C, respectively (Figures 4.2.1, 4.2.3) and in a dose-dependent manner (Figures 4.2.2, 4.2.4). We also evaluated several compounds for cytotoxicity in U2OS cells. None of the compounds tested (NS1, **51**, **53**, **54**, **55**) were toxic to U2OS cells after 48 h at a 100 µM dose (Table 4.2.2).

[12] Martinez Molina, D.; Nordlund, P. *Annu. Rev. Pharmacol. Toxicol.* **2016**, *56*, 141–161.

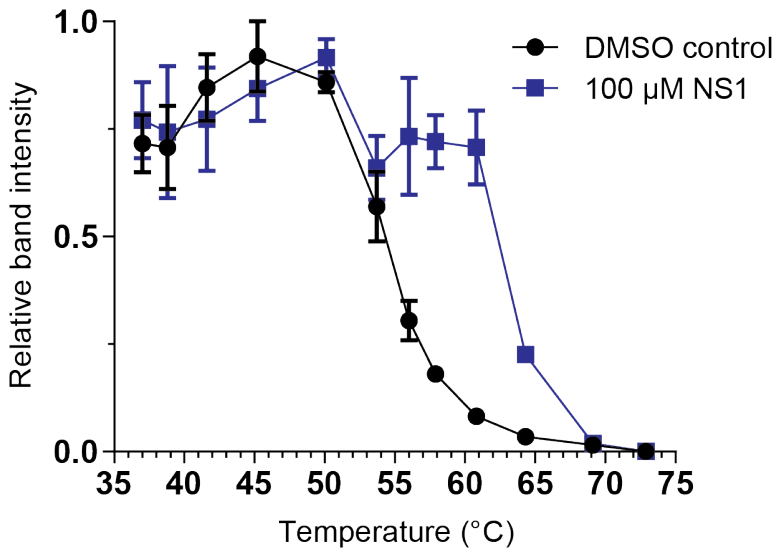

Figure 4.2.1: Cellular Thermal Shift Assay (CETSA) with NS1 (**33**), performed according to experimental protocols outlined in section 4.3.3.

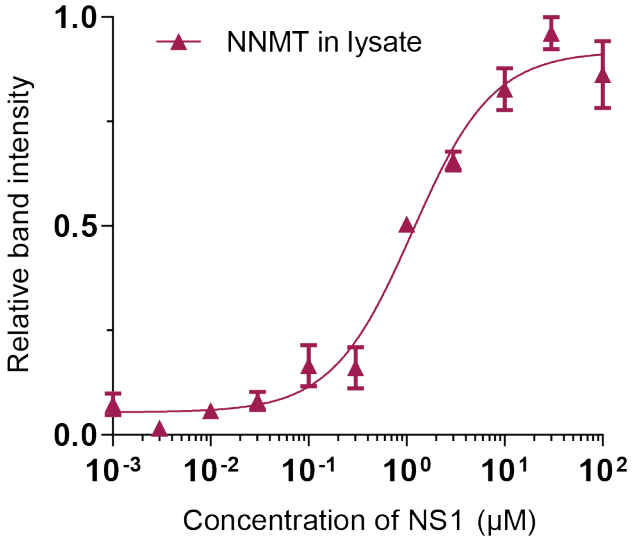

Figure 4.2.2: Isothermal Dose Reponse (ITDR) CETSA with with NS1 (**33**), performed according to experimental protocols outlined in section 4.3.3.

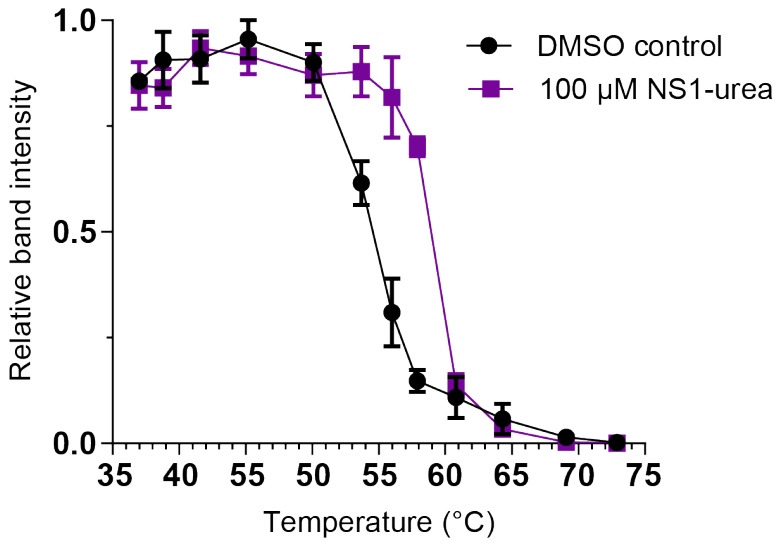

Figure 4.2.3: Cellular Thermal Shift Assay (CETSA) with **55** (NS1-Urea), performed according to experimental protocols outlined in section 4.3.3.

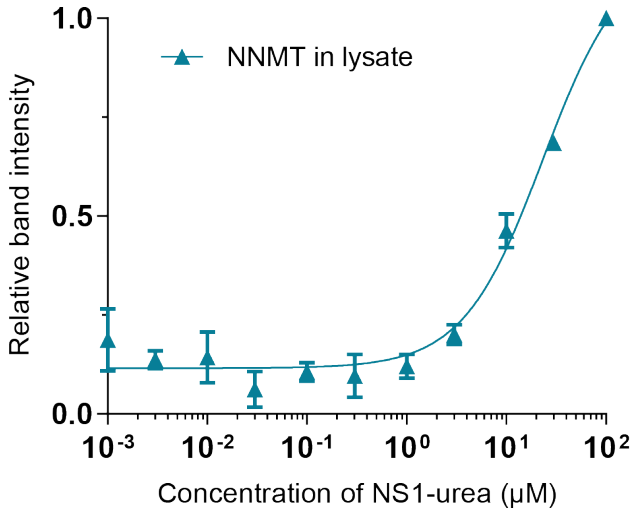

Figure 4.2.4: Isothermal Dose Reponse (ITDR) CETSA with **55** (NS1-Urea), performed according to experimental protocols outlined in section 4.3.3.

Table 4.2.1: Average % viability in a CellTiter-Glo cytotoxicity assay (U2OS cells, **24 h timepoint**). Experimental details are reported in Section 4.3.4.

Compound Identifier	Trivial Name	0.032 μM	0.1 μM	0.32 μM	1 μM	3.2 μM	10 μM	31.6 μM	100 μM
33	NS1	103	105	104	105	106	111	104	106
51	NS1-Amine	102	100	98	99	105	104	97	102
53	NS1-MethylEster	102	104	103	104	106	109	105	106
54	NS1-AminoAmide	99	97	98	100	101	105	101	104
55	NS1-Urea	103	103	100	103	104	107	103	105
Doxorubicin (Positive control)		At 3 μM	At 5 μM	At 10 μM					
		66	39	33					

Table 4.2.2: Average % viability in a CellTiter-Glo cytotoxicity assay (U2OS cells, **48 h timepoint**). Experimental details are reported in Section 4.3.4.

Compound Identifier	Trivial Name	0.032 μM	0.1 μM	0.32 μM	1 μM	3.2 μM	10 μM	31.6 μM	100 μM
33	NS1	103	105	104	103	103	103	102	106
51	NS1-Amine	102	104	104	103	103	102	103	102
53	NS1-MethylEster	102	104	104	102	102	103	102	104
54	NS1-AminoAmide	101	103	104	102	102	101	102	103
55	NS1-Urea	103	104	103	104	104	102	104	105
Doxorubicin (Positive control)		At 3 μM	At 5 μM	At 10 μM					
		26	25	16					

We tested the ability of NS1, **51**, **53**, **54**, and **55** to decrease MNAM levels in U2OS cells, but the effects were modest (Table 4.2.3). NS1-methyl ester (**53**), designed to be more cell permeable than NS1, performed best in this assay, decreasing MNAM levels by 30% at a 31.6 μM dose. A-B permeability testing (Caco-2, pH 6.5/7.4) showed that NS1 and analogues have limited permeability (most permeable out of those tested was NS1-amine **51**, 1.3 × 10-6 cm/s, Table S9). Ongoing work is aimed at developing more cell-penetrant alkynyl NNMT inhibitors that would be useful probes in cell-based studies.

Table 4.2.3: Cellular MNAM levels measured by LC-MS/MS after compound treatment. Experimental details are provided in Section 4.3.4. Compounds noted with ^{A} were ran on one plate and compounds noted with ^{B} were ran on a separate plate. ***N1*** and ***N2*** refer to independent experiments performed on different days. Each experiment was run with n=2 replicates. *JBSNF-0088 refers to 6-methoxynicotinamide, a known NNMT inhibitor, and was used a control inhibitor for assay validation.

		N1		***N2***	
Compound Identifier	**Compound Name**	**IC_{50} (μM)**	**% Inhibition at 31.6 μM**	**IC_{50} (μM)**	**% Inhibition at 31.6 μM**
P180810^{A}	JBSNF-0088* (control)	1.24		1.03	
33^{A}	NS1	>31.6	15	>31.6	21
53^{A}	NS1-MethylEster	>31.6	31	>31.6	29
P180810^{B}	JBSNF-0088* (control)	0.78		1.01	
51^{B}	NS1-Amine	NA		NA	
54^{B}	NS1-AminoAmide	>31.6	18	>31.6	17
55^{B}	NS1-Urea	NA		NA	

Table 4.2.4: A-B permeability assay (Caco-2, pH 6.5/7.4). Incubation: 0 and 60 min, 37°C. Detection, HPLC-MS/MS.[13]

Compound Identifier	Trivial Name	Conc. µM	Perm., 1st 10^{-6} cm/s	2nd	Mean	% Recovery 1st	2nd	Mean	Flags
51	NS1-Amine	10	1.16	1.52	1.3	76	78	77	
53	NS1-MethylEster	10	0.07	0.06	0.1	74	83	78	
55	NS1-Urea	10	0.18	0.2	<0.2	70	65	68	BLQ[2]
33	NS1	10	0.75	0.75	<0.7	90	100	95	BLQ
54	NS1-AminoAmide	10	0.07	0.07	<0.1	92	92	92	BLQ

Table 4.2.5: Reference compounds used in the validation of the Caco-2 assay.

Reference Compound	Conc. µM	Perm. 1st 10^{-6} cm/s	2nd	Mean	% Recovery 1stst	2nd	Mean
colchicine	10	0.17	0.22	0.2	72	85	78
labetalol	10	8.53	9.16	8.8	85	87	86
propranolol	10	22.25	25.12	23.7	66	68	67
ranitidine	10	0.56	0.46	0.5	97	96	97

[1] Hidalgo, I. J.; Raub, T. J.; Borchardt, R. T. *Gastroenterology*, **1989**, *96*, 736–749.

[2] *BLQ*: Below the Limit of Quantitation. Test compound was well detected in donor samples but not detected in receiver samples. The concentration of test compound in receiver sample was below the limit of quantitation.

4.3 Exerimental Details

Methyltransferase inhibition experiments used to generate data presented in Figure 4.1.5 were performed by a commercial vendor (Eurofins), with the exception of the INMT assay. No commcercial INMT assay was available; the INMT assay presented in this Dissertation was developed by Rocco L. Policarpo. Thermal stabilization (CETSA) experiments were performed by Vincent Chu of the Harvard Medical School Department of Cell Biology. Cytotoxicity assays and MNAM measurements were performed by Jubilant Biosystems Ltd. The design of this selectivity study and relevant bioinformatic analyses were performed by the author, Rocco L. Policarpo.

4.3.1 Sequence Similarity Analysis

To generate a data set for sequence similarity analysis, the UniProtKB[14,15] was queried with the following conditions: ec:2.1.1.– ipr029063 AND reviewed:yes AND organism: "Homo sapiens (Human) [9606]" AND proteome:up000005640. These conditions searched the UniProt database for human (organism: "Homo sapiens (Human) [9606]") methyltransferases (ec:2.1.1.–, *transferases*, *transferring one-carbon groups*, *methyltransferases*) that were Swiss-Prot reviewed (reviewed:yes) belonging to the InterPro Homologous Superfamily of SAM-dependent MTases (ipr029063) in the human proteome (proteome:up000005640).

This query returned 113 UniProt IDs which were submitted to the Enzyme Function Initiative Enzyme Similarity Tool[16,17,18] (EFI-EST, settings: *Computation Type*: Option D, *E-Value*: 5, *Fraction*: 1). A sequence similarity network (SSN) was generated using an *alignment score for output* value of 18. The SSN was processed in Cytoscape v3.7.1. Specifically, node labels were set to *Gene Name* and edges were colored via continuous mapping based on *%ID*. The node labels found in Figure 4.1.1 correlate to UniProt IDs and Protein Names in Table 6.2.1.

---

[14] https://www.uniprot.org/

[15] UniProt *Nucleic Acids Res.* **2018**, *47*, D506–D515.

[16] https://efi.igb.illinois.edu/efi-est/

[17] Gerlt, J. A.; Bouvier, J. T.; Davidson, D. B.; Imker, H. J.; Sadkhin, B.; Slater, D. R.; Whalen, K. L. *Biochim. Biophys. Acta, Proteins Proteomics* **2015**, *1854*, 1019 –1037.

[18] Zallot, R.; Oberg, N. O.; Gerlt, J. A. *Curr. Opin. Chem. Biol.* **2018**, *47*, 77 –85.

DALI Structural Similarity Analysis

The DALI server[19] (http://ekhidna2.biocenter.helsinki.fi/dali/) was queried using PDB search and entering identifier 3ROD (Chain A). The DALI structural alignment server returned 1792 hits with a DALI Z-score >2. Chain identifiers were removed from the DALI output (leaving a list of only PDB codes) and the list was then uploaded to the UniProt Retrieve/ID Mapping utility (https://www.uniprot.org/uploadlists/). 871 out of 914 PDB identifiers were successfully mapped to 453 UniProtKB IDs, with the remaining 43 (unmatched) set aside for manual curation. Of the remaining 43 unmatched PDB IDs, none corresponded to human proteins, so they were not included in further analysis.

The list of 453 UniProtKB IDs was filtered to show only methyltransferase enzymes from Homo Sapiens (query with operators: ec:2.1.1.– AND organism:"Homo sapiens (Human) [9606]") leaving 34 UniProtKB IDs remaining (Class EC 2.1.1.– represents enzymes from the methyltransferase family). In many cases multiple PDB IDs mapped to a single UniProtKB ID. These redundancies in the data set were removed by selecting the PDB ID (and chain) with the highest Dali Z-score for further analysis. The authors noted that the PDB code for a known human small-molecule methyltransferase (guanidinoacetate N-methyltransferase, GAMT, with structure 3orh available in the PDB) was missing, so 3orh (chain A) was manually added to the list. The list of PDB codes (and chain identifiers) was uploaded to the DALI server and an *all-against-all* query was submitted. The *all-against-all* output was used to generate the dendrogram presented in Figure 4.1.3 and the heatmap presented in Figure 4.1.4.

4.3.2 INMT Selectivity Study

wt-hINMT Preparation

The pET-28a plasmid containing N-terminally His_6-tagged hINMT (Addgene 25475; http://n2t.net/addgene:25475; RRID:Addgene_25475) was transformed into Agilent BL21-CodonPlus (DE3)-RIL Competent Cells (Agilent P/N: 230245) according to the manufacturer's protocol. Bacteria were subsequently grown up in terrific broth (containing 50 μg per mL kanamycin sulfate and 50 μg per mL chloramphenicol) at 37 °C, induced with IPTG (1 mM) when they reached an OD_{600} of ∼0.8, and incubated overnight at 32 °C.

---

[19] Holm, L.; Laakso, L. M. *Nucleic Acids Res.* **2016**, *44*, W351–W355.

The following day cell pellets were harvested by centrifugation. Five grams of cell pellet was then suspended in lysis buffer (15 mL, 20 mM Tris-HCl pH 8, 0.5 M NaCl, 40 mM imidazole, 1 mM DTT, 10% glycerol) supplemented with 1 tablet Roche cOmplete EDTA-free protease inhibitor cocktail, 10 mg lysozyme, and 1 mL DNase. The cell suspension was incubated on ice for 30 min and then sonicated on ice for 7 minutes (total sonication time) employing a duty cycle of 10/50 on/off at 20% power. The crude lysate was clarified by centrifugation and manually loaded onto a 5 mL GE FF HisTrap Crude Ni-NTA affinity chromatography column via syringe. The column was washed with 20 mL lysis buffer and then protein was eluted with 10 mL of elution buffer (20 mM Tris-HCl pH 8, 0.5 M NaCl, 400 mM imidazole, 1 mM DTT, 10% glycerol) while collecting 1.2 mL fractions. Eluted fractions were checked for the presence of protein via Bradford assay. Those containing purified INMT as evidenced by SDS-PAGE analysis were combined, concentrated, and desalted into storage buffer (20 mM Tris-HCl pH 8.0, 50 mM NaCl, 1 mM DTT, 5% glycerol) via GE HiTrap Desalting column. Fractions were combined, concentrated to 13.5 mg/mL, flash-frozen in liquid nitrogen and stored at –80 °C for future use.

The hINMT protein sequence is as follows:

```
MGSSHHHHHHSSGLVPRGSMKGGFTGGDEYQKHFLPRDYLATYYSFDGSPSPEAEMLKFNLECLH
KTFGPGGLQGDTLIDIGSGPTIYQVLAACDSFQDITLSDFTDRNREELEKWLKKEPGAYDWTPAV
KFACELEGNSGRWEEKEEKLRAAVKRVLKCDVHLGNPLAPAVLPLADCVLTLLAMECACCSLDAY
RAALCNLASLLKPGGHLVTTVTLRLPSYMVGKREFSCVALEKGEVEQAVLDAGFDIEQLLHSPQS
YSVTNAANNGVCCIVARKKPGP
```

INMT Inhibition Assay

A luminescence-based indolethylamine N-methyltransferase (INMT) assay was developed based on the Promega MTase-Glo™ Methyltransferase Assay (catalog #: V7601). The Promega MTase-Glo™ assay is a coupled luminescence-based assay that converts S-adenosylhomocysteine (SAH) to ADP which is then converted to light.[20] Full instructions and protocols outlining assay development and validation can be found in Promega application note #AN297 and technical manual TM453 (Revised 4/17).

[20] Hsiao, K.; Zegzouti, H.; Goueli, S. A. *Epigenomics* **2016**, *8*, 321–339.

INMT is capable of methylating a variety of tryptamine, harmine, and phenethylamine derivatives at variable rates, but the typical substrate is tryptamine. INMT is also known as thioether S-methyltransferase (TEMT) and is known to methylate a variety of thioethers and related compounds. From the UniProt[21] entry O95050[22] (INMT_HUMAN):

> Functions as thioether S-methyltransferase and is active with a variety of thioethers and the corresponding selenium and tellurium compounds, including 3-methylthiopropionaldehyde, dimethyl selenide, dimethyl telluride, 2-methylthioethylamine, 2-methylthioethanol, methyl-n-propyl sulfide and diethyl sulfide. Plays an important role in the detoxification of selenium compounds (By similarity). Catalyzes the N-methylation of tryptamine and structurally related compounds.

Our first goal was to choose substrate concentrations that were physiologically relevant (close to INMT substrate $K_m^{app.}$ values) and would also generate luminescence signal with adequate signal/noise ratio to study INMT inhibition. A literature search[23,24] revealed the apparent K_m of tryptamine to be ca. 0.3-2.9 mM, so we pursued INMT assay development using 1.0-2.0 mM tryptamine. A SAM concentration of 20-30 μM was employed in our experiments, again close to literature reported apparent K_m values of SAM.

Assay validation according to protocols outlined in the Promega technical manual led us to the final conditions for the hINMT IC_{50} assay: [hINMT]=150 nM, [tryptamine]=2 mM, [SAM]=30 μM, and reaction time=20 min. A detailed IC_{50} assay protocol is reported below.

Reagents and Materials:

- SpectraMax i3x Multi-Mode Microplate Reader (Molecular Devices)
- MTase-Glo™Methyltransferase Assay (Promega V7601)
- assay plate, 384 well, with lid (Corning 3570)

---

[21] UniProt *Nucleic Acids Res.* **2018**, *47*, D506–D515.

[22] https://www.uniprot.org/uniprot/O95050

[23] Thompson M.A., W. R.; Thompson M. A., W. R. *J. Biol. Chem.* **1998**, *273*, 34502–10.

[24] Chu, U. B.; Vorperian, S. K.; Satyshur, K.; Eickstaedt, K.; Cozzi, N. V.; Mavlyutov, T.; Hajipour, A. R.; Ruoho, A. E. *Biochemistry* **2014**, *53*, 2956–2965.

- PCR strip tubes, with caps (Axygen Scientific, PCR-0208-A, PCR-02CP-A)
- disposable pipetting reservoir (polystyrene, 25 mL, VWR 89094-662)
- molecular biology grade water (Corning 46-000-CM)
- 0.5 M EDTA, pH 8.0 (Boston BioProducts BM-150)
- 5M NaCl (Cell Signaling Technologies 7010S)
- 1M $MgCl_2$ (invitrogen AM9530G)
- albumin standard (2.0 mg/mL BSA in 0.9% NaCl solution containing NaN_3); (Thermo Scientific 23209)
- ethyl alcohol, 200 proof for molecular biology (Millipore Sigma E7023)
- DL-dithiothreitol BioUltra, for molecular biology (Millipore Sigma 43815)
- tryptamine (Millipore Sigma 193747)
- trifluoroacetic acid (VWR BDH15311.100)

Protocol (NS1 IC_{50} curve):

Reactions were performed in PCR strip tubes (with caps), and only transferred to a 384-well plate for final luminescence reading. Only every other well in a given row on the 384-well plate was used (the intermediate wells were left empty). The methyltransferase reaction mixture (including hINMT, tryptamine, SAM, and NS1) had a total volume of 20 µL. The experiment reported in Figure 4.1.6 was performed in duplicate.

To begin, 12 PCR tubes were aligned in an empty pipette tip box to allow for multichannel pipetting. From left to right, tubes 1–9 were experimental wells (NS1 at varying concentrations), 10 and 11 were positive controls (no NS1), and tube 12 was a negative control (no SAM).

1. 5 µL of 4× NS1 (prepared from a serial dilution to achieve the desired concentrations) was added to tubes 1–9, and 5 µL 1× reaction buffer added to tubes 10–12.
2. 5 µL of 4× SAM was added to tubes 1–11, and 5 µL 1× reaction buffer added to tube 12.

3. A master mix containing 2× hINMT and 2× tryptamine was prepared in a Falcon tube and poured into a multichannel pipette reagent reservoir.

4. Using a multichannel pipette, 10 µL of this master mix solution was transferred to all 12 tubes to initiate the INMT reaction.

5. The reactions were capped and incubated at RT for 20 min.

6. Reactions were quenched with 5 µL of 0.5% TFA and incubated for 5 min at RT to stop the methyltransferase reaction.

7. 5 µL of prepared 6× MTase-Glo™ Reagent was added and the reactions were capped and incubated for 30 min at RT.

8. 30 µL of MTase-Glo™ Detection Solution was added to the reactions and they were mixed by pipetting up-and-down.

9. 50 µL of each reaction was immediately transferred to a 384-well plate using a 12-channel (multichannel) pipette. Tubes 1–12 map to a 384-well plate as shown in Table 4.3.1 below.

10. The plate was centrifuged at 300 RPM for 2 min and immediately moved to the SpectraMax i3x Multi-Mode Microplate Reader.

11. Luminescence was read 5 min after transfer of the reaction mixtures from PCR tubes to the 384-well plate.

Table 4.3.1: Example 384-well plate layout showing final contents of each well. Row A shown here for illustrative purposes.

	1	3	5	7	9	11	13	15	17	19	21	23
A	35.0000 µM NS1	14.0000 µM NS1	5.6000 µM NS1	2.2400 µM NS1	0.8960 µM NS1	0.3584 µM NS1	0.1434 µM NS1	0.0573 µM NS1	0.0229 µM NS1	+ control (no NS1)	+ control (no NS1)	– control (no SAM)

Data analysis: Luminescence data were analyzed in Microsoft Excel and GraphPad Prism v8.0.2. To begin, background signal (value from A23) was subtracted from all wells. Positive control wells A19 and A21 (containing no inhibitor) were then averaged to provide a value representing signal derived from uninhibited hINMT reactions. Luminescence counts from wells containing inhibitor (A1–A17) were then each divided by the control value to generate values representing % enzyme activity (relative to control). A

plot of log(NS1) vs. % hINMT activity was then fitted via nonlinear regression in Prism using the model log(inhibitor) vs. response–variable slope (four parameters) to generate the IC_{50} value.

4.3.3 Cellular Thermal Shift Assay (CETSA)

K562 Cell Culture

The human chronic myeloid leukemia cell line K562 (ATCC CCL-243) was cultured in RPMI 1640 with Glutamax (Gibco) supplemented with 10% fetal bovine serum (Atlanta Biologicals), and 100 IU penicillin and 100 mg/mL streptomycin (Corning). Cells were cultured in T175 flasks with 50 mL of media per flask (Corning) in a 37 °C incubator with 5% CO_2 until the cells reached a density of 2×10^6 cells/mL.

Preparation of K562 Cell Lysate

K562 cells were cultured as described above. Cells were washed with PBS and then resuspended in an appropriate volume of PBS supplemented with cOmplete protease inhibitor cocktail (Roche) to obtain a final cell count of 3.0×10^7 to 3.6×10^7 cells/mL. The suspension was transferred to microcentrifuge tubes and subjected to three rounds of freeze-thaw using liquid nitrogen and a room temperature water bath. The cell lysate was clarified by centrifuging at 17,000g for 20 minutes at 4 °C, and the supernatant was transferred to a new microcentrifuge tube. Lysate protein concentration was determined by BCA assay and the lysate was diluted to a protein concentration of 3 mg/mL with PBS supplemented with protease inhibitor cocktail. Aliquots were snap frozen in liquid nitrogen and stored at –80 °C.

CETSA with K562 Lysate

The CETSA assay was adapted from previously published protocols.[25,26] K562 lysate prepared as described above was incubated at room temperature with DMSO, 100 μM of NS1 (**33**), or 100 μM of NS1-Urea (**55**) for 30 minutes.

A Bio-Rad C1000 Touch Thermal Cycler was preheated to the following temperatures using the gradient setting: 37 °C, 38.8 °C, 41.6 °C, 45.2 °C, 50.1 °C, 53.7 °C, 56 °C, 57.9 °C, 60.8 °C, 64.3 °C, 69.1 °C, 72.9 °C.

---

[25] Molina, D. M.; Jafari, R.; Ignatushchenko, M.; Seki, T.; Larsson, E. A.; Dan, C.; Sreekumar, L.; Cao, Y.; Nordlund, P. *Science* **2013**, *341*, 84–87.

[26] Jafari, R.; Almqvist, H.; Axelsson, H.; Ignatushchenko, M.; Lundbäck, T.; Nordlund, P.; Martinez Molina, D. *Nature Protocols* **2014**, *9*, 2100–2122.

DMSO-treated and compound-treated lysate were aliquotted into twelve PCR tubes, and each tube was heated at one of the temperatures listed above for 3 minutes. The samples were cooled at room temperature for 3 minutes, then snap frozen in liquid nitrogen. When thawed, the samples were centrifuged at 17,000g for 20 minutes at 4 °C. The supernatant was transferred to a new tube, mixed with NuPAGE LDS sample buffer (Novex) and β-mercaptoethanol (2.5%). The samples were heated at 70 °C for 10 minutes and analyzed by SDS-PAGE and western blot using an anti-NNMT mouse antibody (Abcam, ab119758, 1:1000 dilution), an anti-actin HRP-conjugated mouse antibody (Abcam, ab49900, 1:250000 dilution), and an anti-mouse HRP-conjugated IgG (Promega, W402B, 1:5000 dilution).

Isothermal Dose Response (ITDR) CETSA with K562 Lysate

K562 lysate prepared as described above was incubated at room temperature with DMSO or various concentrations of NS1 or NS1-Urea for 30 minutes.

A Bio-Rad C1000 Touch thermal cycler was preheated to 57 °C. Samples were aliquotted into PCR tubes, and each tube was heated at 57 °C in the thermal cycler for 3 minutes. The samples were cooled at room temperature for 3 minutes and then snap frozen in liquid nitrogen. When thawed, the samples were centrifuged at 17,000g for 20 minutes at 4 °C. The supernatant was prepared for western blot analysis as described in the CETSA procedure above.

4.3.4 Cell-Based Assays: Cytotoxicity and MNAM Measurement

Cytotoxicity Assay in U2OS Cells

Principle: The CellTiter-Glo Luminescent Cell Viability Assay is a homogeneous method to determine the number of viable cells in culture based on quantification of the ATP present, which signals the presence of metabolically active cells. Addition of the CellTiter-Glo reagent results in cell lysis and generation of a luminescent signal proportional to the amount of ATP present. The amount of ATP is directly proportional to the number of cells present in culture.

Cell Culture: U2OS were maintained in DMEM-F12 glutamax complete growth media supplemented with 10% heat-inactivated fetal bovine serum (HI FBS).

CT-Glo Reagent Preparation: CellTiter-Glo Buffer & CellTiter-Glo Substrate were thawed at room temperature prior to use. An appropriate volume (10 mL) of CellTiter-Glo Buffer was transferred into the amber bottle containing CellTiter-Glo Substrate to reconstitute the lyophilized enzyme/substrate mixture. The contents were gently vortexed to obtain a homogeneous solution.

Experimental Protocol: U2OS cells were seeded at 10000 cells/150 µL/well in 96 well cell culture plate and incubated overnight at 37 °C and 5% CO_2. The next day, media was changed (150 µL), various concentrations of compounds (50 µL from 4X stock) were tested in duplicates, at eight concentrations, in semi log dilution pattern, with starting concentration being 100 µM. Final concentration of DMSO in the assay was 1 %. 10 µM, 5 µM and 3 µM of doxorubicin hydrochloride was used as positive control in the assay. The plates were incubated for 24h and 48h at 37°C with 5% CO_2. After 24 h and 48 h of incubation, CellTiter-Glo Reagent (Promega) preparation was added to the cell culture medium present in each well in a 1:1 ratio by volume (e.g., add 50 µL of reagent to 50 µL of medium containing cells). The plate was gently vortexed for 10 minutes on an orbital shaker to induce cell lysis. The contents of the plate were transferred to an opaque half area 96 well plate. The plate was incubated at RT for 10 min to stabilize the luminescent signal. Luminescence output was read on a Tecan Spark plate reader.

Data Analysis: The % cell viability was calculated relative to DMSO control.

MNAM Measurement in U2OS cells via LC-MS/MS

Reagents and Materials:

- Acetonitrile (Millipore Sigma 1000292500)
- D4 MNAM (BioOrganics SRK(I)-257-3226)
- MNAM (BioOrganics BST(I)-256-3271)
- DPBS (Invitrogen 14190-136)
- Top Seal-A Plus (Perkin Elmer 6050185)
- 96-well plate sterile TC treated (Eppendorf 0030730119)

- 96 well plate transfer plate (Costar 3364)
- Reference compound 6-methoxy nicotinamide/(*alternate name:* JBSNF-0088) (Arbor chemical corporation Limited, P180810)

Cell line: U2OS (Source: ATCC). Cells are maintained in DMEM-F12 growth media containing 10% HI FBS and 1% Pen-Strep (filter sterilized) in 37 C incubator with 5 % CO_2.

Extraction buffer preparation: 100% acetonitrile (containing 20 ng/ml of D4 MNAM as internal standard) is used to extract MNAM from the cells.

Stepwise protocol:

1. Cells are kept in cell culture flask until seeding into microwell plate.
2. Remove cell medium, wash with DPBS (-/-).
3. Detach cells with TrypLE Express (4mL) into 150 cm^2 flask (incubate at 37 °C for 5 min).
4. Stop reaction by addition of 5 mL culture medium.
5. Count cells with Vi-CELL cell counter.
6. Seed cells into 96-well microplate (100 µL/well = 10000 cells/well)
7. Incubate for 24 h at 37 °C, 5% CO_2, 95% humidity with lid on.
8. Replace medium by addition of 100 µL of medium/compound mixture as per the plate layout.
9. Incubate for 24 h at 37 °C, 5 % CO_2, 95 % humidity with lid on.
10. Remove medium/compound mixture and wash 2 times with 150 µL of DPBS(-/-).
11. Remove DPBS and add 100 µL acetonitrile containing internal standard D4 MNAM 10 ng/ml final concentration.
12. Incubate for 20 min at RT with mild haking.
13. Add 100 µL of autoclaved water and mix gently.

14. Centrifuge the plate at 5000g for 10 min.

15. Transfer 150 µL into 96-well microplate (Costar 3364).

16. Readout in LC-MS/MS according to methods previously reported by Kannt et al.[27]

[27] Kannt, A. et al. *Sci. Rep.* **2018**, *8*, 3660–3660.

5

Conclusion

In this work, I designed and synthesized the most potent and selective NNMT inhibitors reported to date. A modular, scalable synthesis of alkynyl nucleosides enabled the production and testing of a variety of alkynyl bisubstrate inhibitors, leading to the discovery of NS1 as a selective, picomolar NNMT inhibitor. Alkynyl bisubstrate inhibition could be a generalizable strategy; covalent tethering of alkynyl nucleosides to substrate mimics of other small molecule methyltransferases could provide a method for selective inhibition of these enzymes (Figures 5.0.1). The stereodefined alkyne present in the NS1 scaffold could be used for click chemistry or other functionalization, enabling the development of bisubstrate probes or inhibitors of protein arginine/lysine methyltransferases.[1,2].

---

[1] Zhang, G.; Richardson, S. L.; Mao, Y.; Huang, R. *Org. Biomol. Chem.* **2015**, *13*, 4149–4154.

[2] Srinivasan, R.; Li, J.; Ng, S. L.; Kalesh, K. A.; Yao, S. Q. *Nature Protocols* **2007**, *2*, 2655–2664.

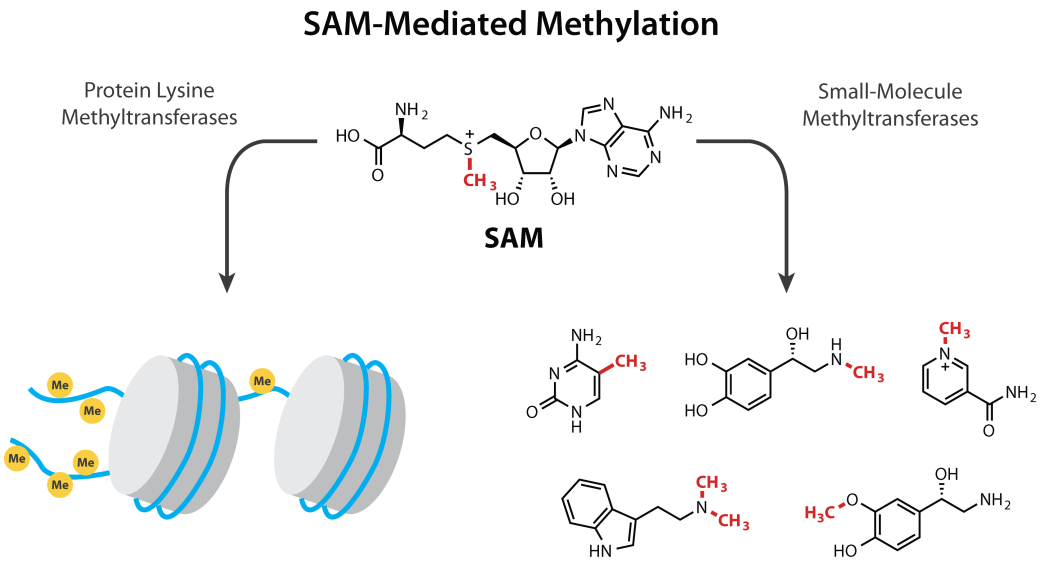

Figure 5.0.1: SAM is used to methylate a variety of proteins and small molecules. Alkynyl-SAM compounds presented in this work could be use to make bisubstrate inhibitors of other small-molecule methyltransferases.

Finally, this work demonstrates the value of alkynes in small-molecule ligand design in the context of methyltransferase inhibition. Alkynes provide unique rigidity, geometry, and spatial occupancy not captured by common fragment linkers. Current state-of-the-art bisubstrate inhibitor designs often rely upon reductive amination, alkylation, and amide-bond forming reactions to link fragments together. These reactions are generally fast and easy to implement, but often produce highly flexible structures characterized by relatively weak overall binding affinity. This report demonstrates that C6' alkynyl nucleosides–while more synthetically complex–can be used to generate potent bisubstrate methyltransferase inhibitors.

6

Appendix

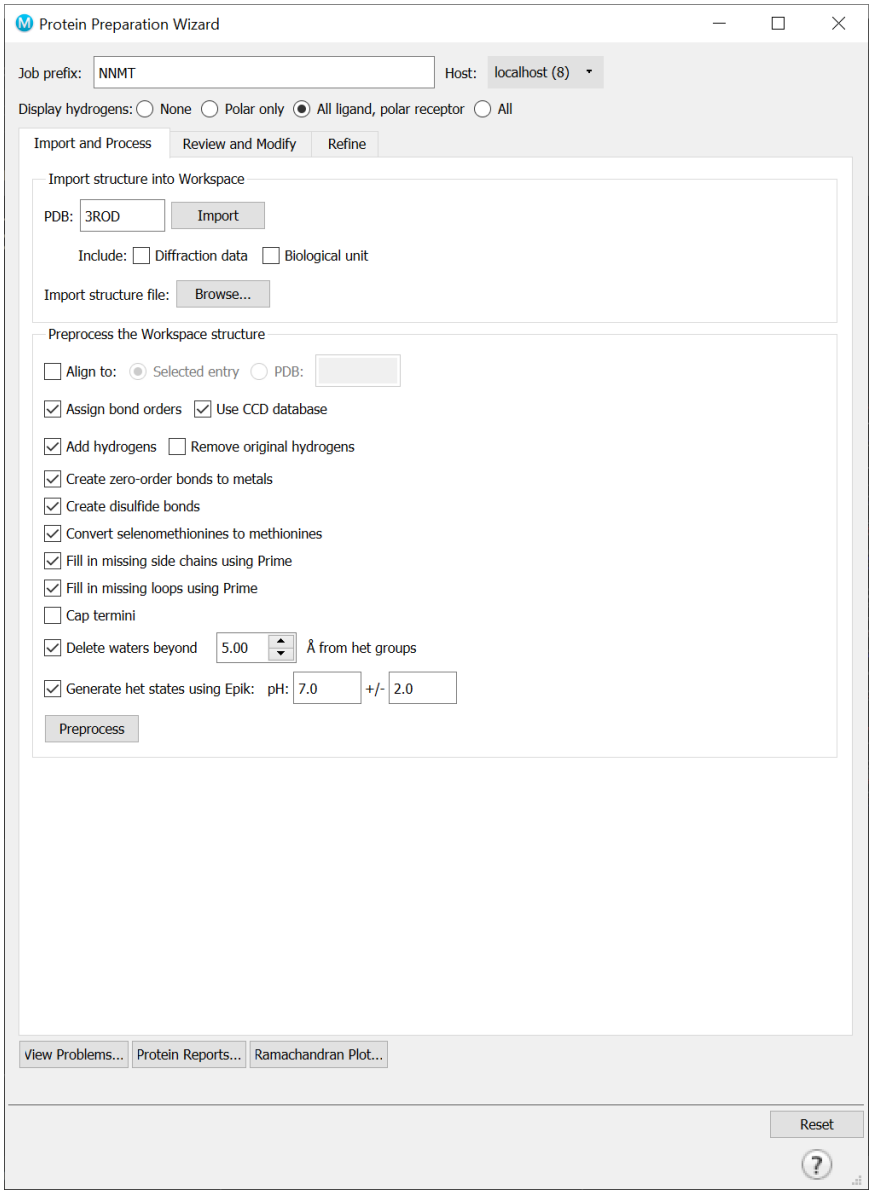

Figure 6.1.1: *Import and Process* parameters in the Protein Preparation Wizard.

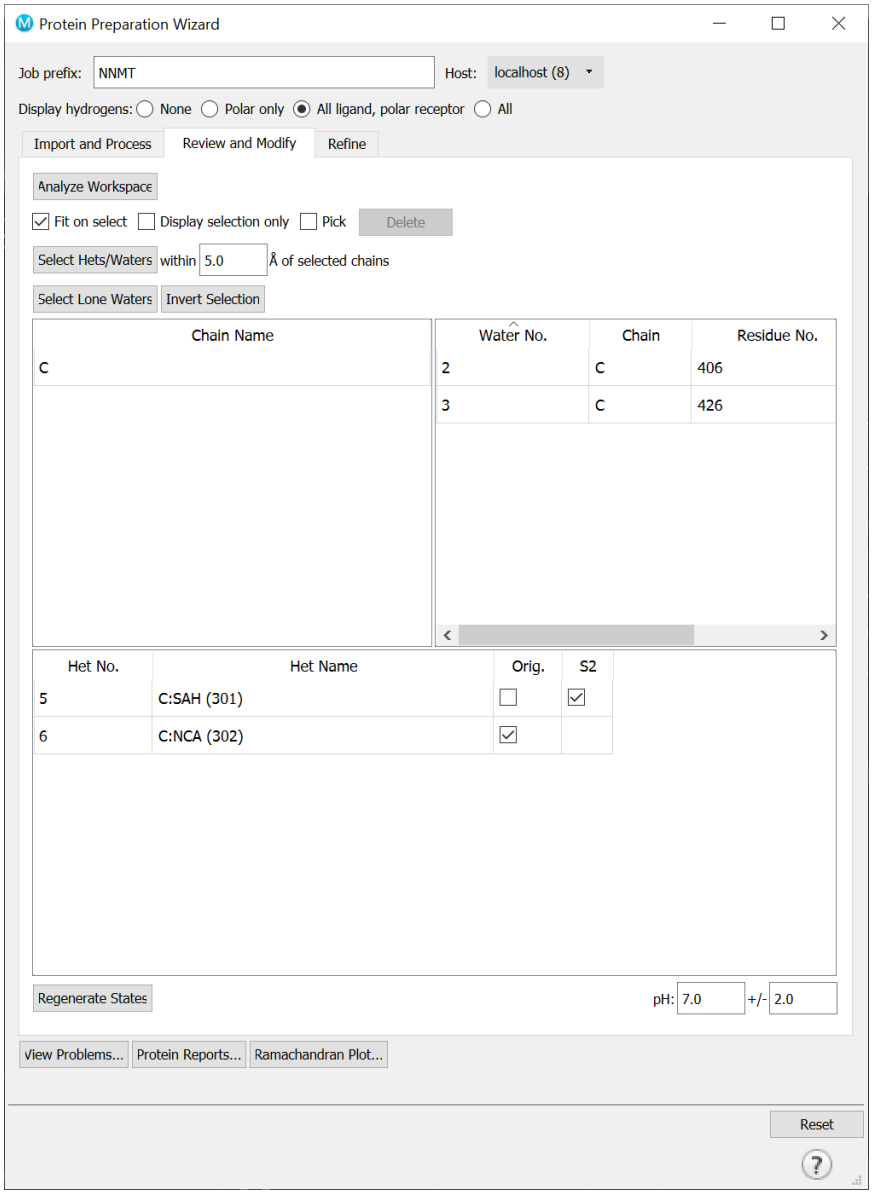

Figure 6.1.2: *Review and Modify* parameters in the Protein Preparation Wizard.

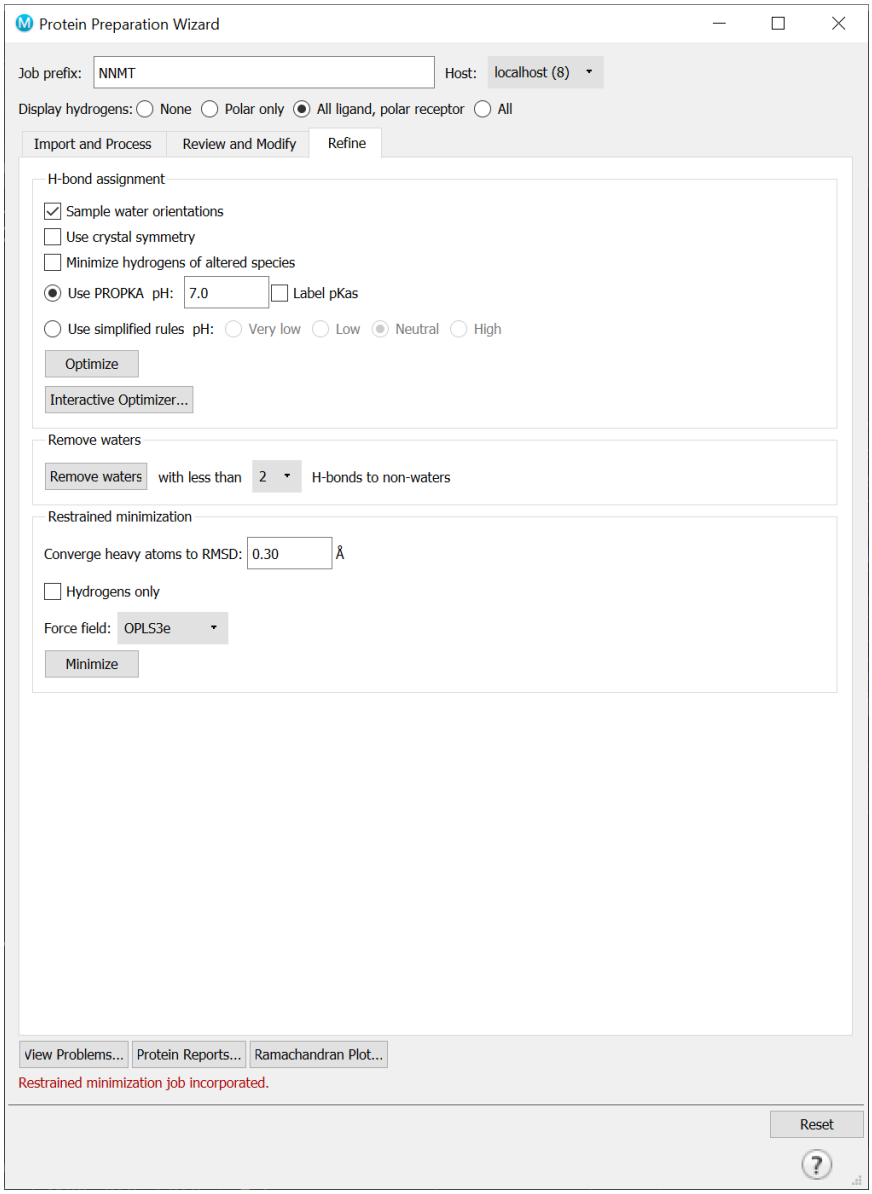

Figure 6.1.3: *Refine* parameters in the Protein Preparation Wizard.

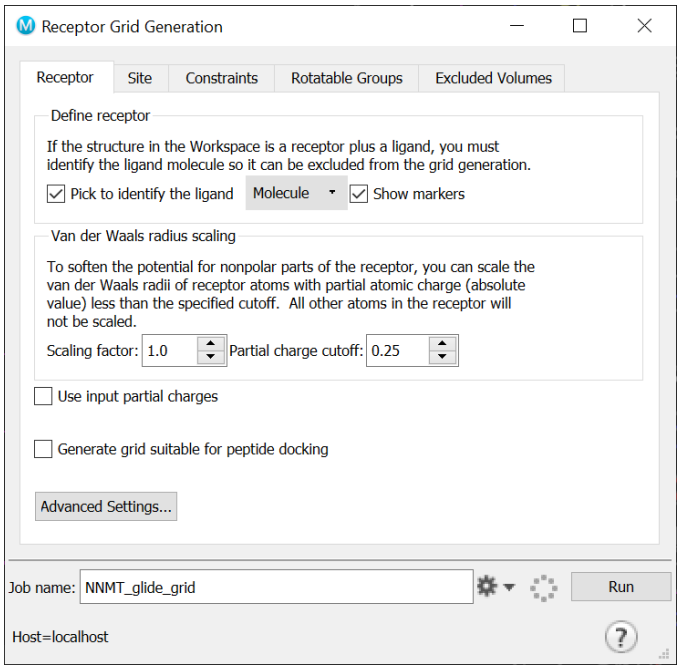

Figure 6.1.4: Parameters set in the Receptor Grid Generation.

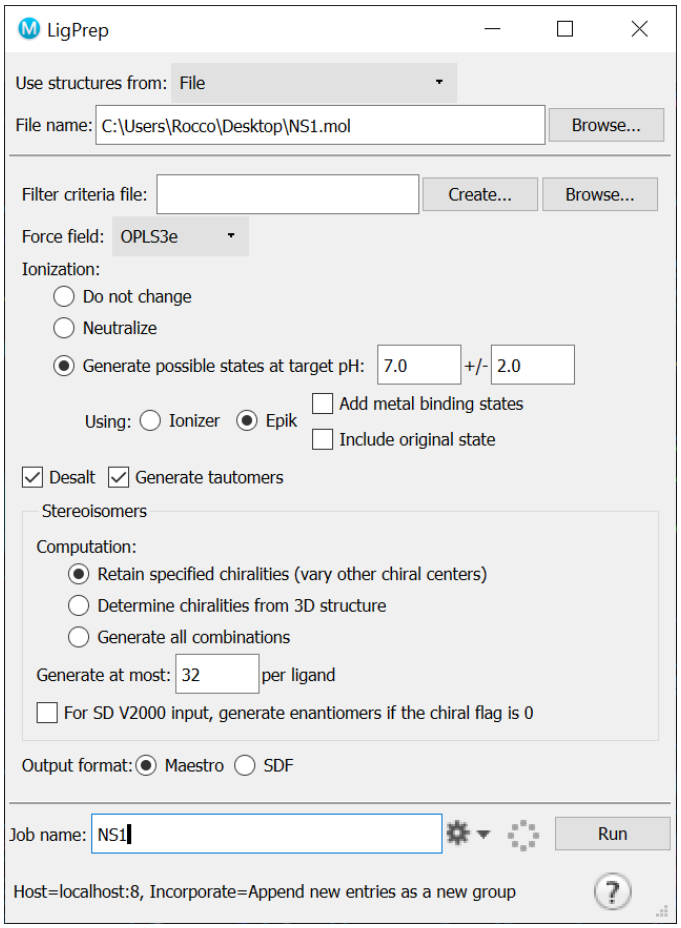

Figure 6.1.5: Parameters set during ligand preparation in LigPrep.

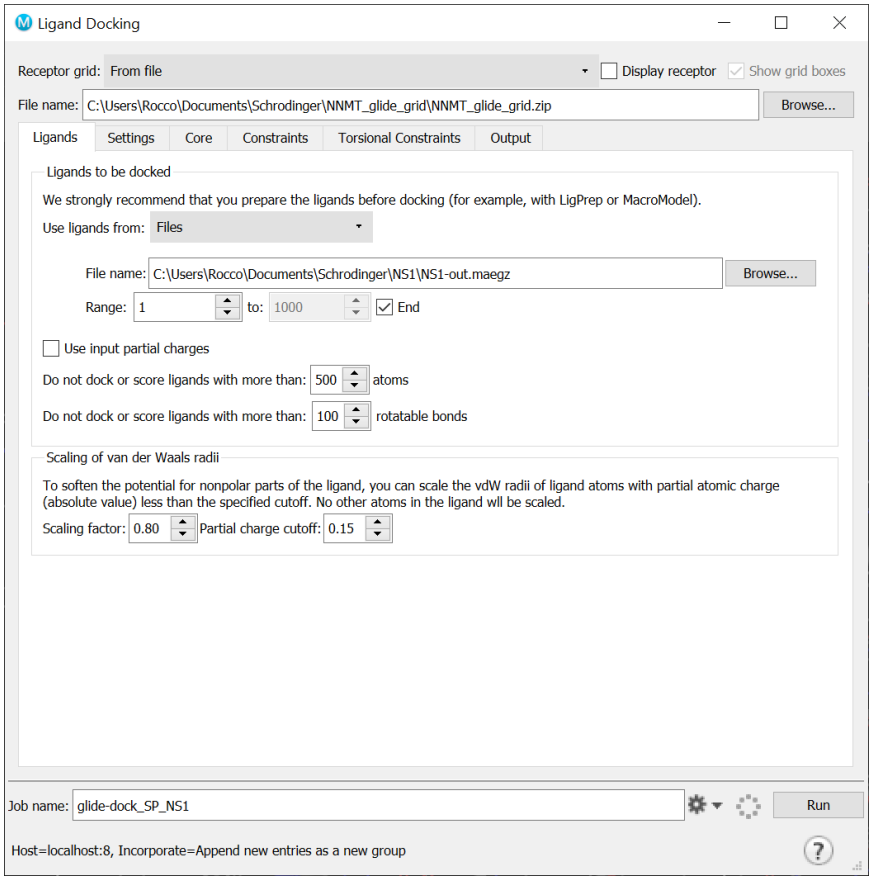

Figure 6.1.6: Parameters set in Ligand Docking (Ligands tab).

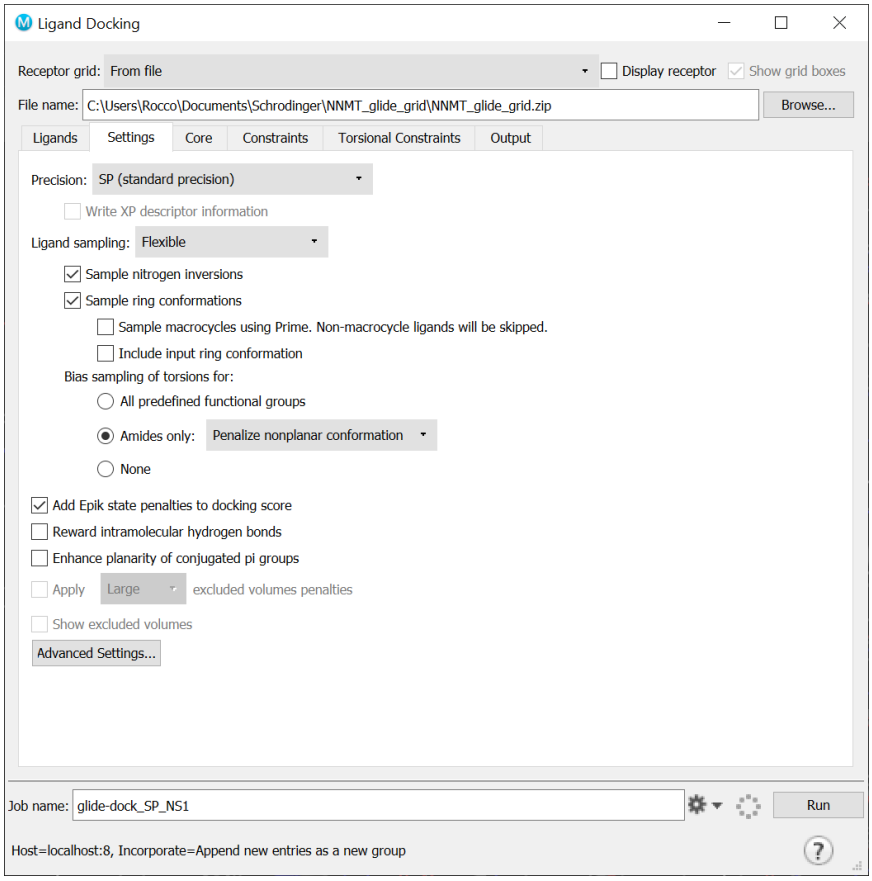

Figure 6.1.7: Parameters set in Ligand Docking (Settings tab).

Table 6.2.1: Human methyltransferases used to construct a sequence similarity network (SSN). A description of the SSN generation workflow is provided in Section 4.3.1.

SSN Node Label	UniProt Entry ID	UniProt Entry Name	Gene Names	Protein Name
ALKBH8	Q96BT7	ALKB8_HUMAN	ALKBH8 ABH8	Alkylated DNA repair protein alkB homolog 8
AS3MT	Q9HBK9	AS3MT_HUMAN	AS3MT CYT19	Arsenite methyltransferase
ASMT	P46597	ASMT_HUMAN	ASMT	Acetylserotonin O-methyltransferase
ASMTL	O95671	ASML_HUMAN	ASMTL	N-acetylserotonin O-methyltransferase-like protein Short-ASMTL
BCDIN3D	Q7Z5W3	BN3D2_HUMAN	BCDIN3D	Pre-miRNA 5'-monophosphate methyltransferase
C10orf138	Q5JPI9	EFMT2_HUMAN	EEF1AKMT2 C10orf138 METTL10	EEF1A lysine methyltransferase 2
C12orf72	Q8IXQ9	ETKMT_HUMAN	ETFBKMT C12orf72 METTL20	Electron transfer flavoprotein beta subunit lysine methyltransferase
C16orf24	Q9BQD7	F173A_HUMAN	FAM173A C16orf24 RJD7	Protein N-lysine methyltransferase FAM173A
C21orf127	Q9Y5N5	N6MT1_HUMAN	N6AMT1 C21orf127 HEMK2 PRED28	Methyltransferase N6AMT1
C2orf56	Q7L592	NDUF7_HUMAN	NDUFAF7 C2orf56 PRO1853	Protein arginine methyltransferase NDUFAF7, mitochondrial
C7orf60	Q1RMZ1	SAMTR_HUMAN	BMT2 C7orf60 SAMTOR	S-adenosylmethionine sensor upstream of mTORC1
C8orf79	Q9P272	TRM9B_HUMAN	TRMT9B C8orf79 KIAA1456 TRM9L	Probable tRNA methyltransferase 9B
C9orf41	Q8N4J0	CARME_HUMAN	CARNMT1 C9orf41	Carnosine N-methyltransferase
CAMKMT	Q7Z624	CMKMT_HUMAN	CAMKMT C2orf34 CLNMT	Calmodulin-lysine N-methyltransferase ShortCLNMT ShortCaM KMT
CARM1	Q86X55	CARM1_HUMAN	CARM1 PRMT4	Histone-arginine methyltransferase CARM1
CMTR1	Q8N1G2	CMTR1_HUMAN	CMTR1 FTSJD2 KIAA0082 MTR1	Cap-specific mRNA (nucleoside-2'-O-)-methyltransferase 1
CMTR2	Q8IYT2	CMTR2_HUMAN	CMTR2 AFT FTSJD1	Cap-specific mRNA (nucleoside-2'-O-)-methyltransferase 2
COMT	P21964	COMT_HUMAN	COMT	Catechol O-methyltransferase
COMTD1	Q86VU5	CMTD1_HUMAN	COMTD1 UNQ766/PRO1558	Catechol O-methyltransferase domain-containing protein 1
COQ3	Q9NZJ6	COQ3_HUMAN	COQ3 UG0215E05	Ubiquinone biosynthesis O-methyltransferase, mitochondrial
COQ5	Q5HYK3	COQ5_HUMAN	COQ5	2-methoxy-6-polyprenyl-1,4-benzoquinol methylase, mitochondrial
DIMT1	Q9UNQ2	DIM1_HUMAN	DIMT1 DIMT1L HUSSY-05	Probable dimethyladenosine transferase
DNMT1	P26358	DNMT1_HUMAN	DNMT1 AIM CXXC9 DNMT	DNA (cytosine-5)-methyltransferase 1 ShortDnmt1
DNMT3A	Q9Y6K1	DNM3A_HUMAN	DNMT3A	DNA (cytosine-5)-methyltransferase 3A ShortDnmt3a
DNMT3B	Q9UBC3	DNM3B_HUMAN	DNMT3B	DNA (cytosine-5)-methyltransferase 3B ShortDnmt3b
DOT1L	Q8TEK3	DOT1L_HUMAN	DOT1L KIAA1814 KMT4	Histone-lysine N-methyltransferase, H3 lysine-79 specific
EEF1AKMT4	P0DPD7	EFMT4_HUMAN	EEF1AKMT4	EEF1A lysine methyltransferase 4

Table 6.2.1 continued from previous page

EEF1AKMT4	P0DPD8	EFCE2_HUMAN	EEF1AKMT4-ECE2	EEF1AKMT4-ECE2 readthrough transcript protein
FAM119B	Q96AZ1	EFMT3_HUMAN	EEF1AKMT3 FAM119B HCA557A METTL21B	EEF1A lysine methyltransferase 3
FAM173B	Q6P4H8	F173B_HUMAN	FAM173B	Protein N-lysine methyltransferase FAM173B
FAM86A	Q96G04	EF2KT_HUMAN	EEF2KMT FAM86A SB153	Protein-lysine N-methyltransferase EEF2KMT
FAM86B1	Q8N7N1	F86B1_HUMAN	FAM86B1	Putative protein N-methyltransferase FAM86B1
FAM86B2	P0C5J1	F86B2_HUMAN	FAM86B2	Putative protein N-methyltransferase FAM86B2
FBL	P22087	FBRL_HUMAN	FBL FIB1 FLRN	rRNA 2'-O-methyltransferase fibrillarin
FBLL1	A6NHQ2	FBLL1_HUMAN	FBLL1	rRNA/tRNA 2'-O-methyltransferase fibrillarin-like protein 1
FJH1	Q9UI43	MRM2_HUMAN	MRM2 FJH1 FTSJ2	rRNA methyltransferase 2, mitochondrial
FTSJ1	Q9UET6	TRM7_HUMAN	FTSJ1 JM23	Putative tRNA (cytidine(32)/guanosine(34)-2'-O)-methyltransferase
FTSJ3	Q8IY81	SPB1_HUMAN	FTSJ3 SB92	pre-rRNA processing protein FTSJ3
GAMT	Q14353	GAMT_HUMAN	GAMT	Guanidinoacetate N-methyltransferase
GNMT	Q14749	GNMT_HUMAN	GNMT	Glycine N-methyltransferase
HEMK1	Q9Y5R4	HEMK1_HUMAN	HEMK1 HEMK	HemK methyltransferase family member 1
HENMT1	Q5T8I9	HENMT_HUMAN	HENMT1 C1orf59	Small RNA 2'-O-methyltransferase
HMT2	Q99873	ANM1_HUMAN	PRMT1 HMT2 HRMT1L2 IR1B4	Protein arginine N-methyltransferase 1
HNMT	P50135	HNMT_HUMAN	HNMT	Histamine N-methyltransferase ShortHMT
HUSSY	O43709	BUD23_HUMAN	BUD23 MERM1 WBSCR22 HUSSY-03 PP3381	Probable 18S rRNA (guanine-N(7))-methyltransferase
INMT	O95050	INMT_HUMAN	INMT	Indolethylamine N-methyltransferase ShortIndolamine N-methyltransferase
KIAA1393	Q32P41	TRM5_HUMAN	TRMT5 KIAA1393 TRM5	tRNA (guanine(37)-N1)-methyltransferase
LCMT1	Q9UIC8	LCMT1_HUMAN	LCMT1 LCMT CGI-68	Leucine carboxyl methyltransferase 1
LCMT2	O60294	TYW4_HUMAN	LCMT2 KIAA0547 TYW4	tRNA wybutosine-synthesizing protein 4 ShorttRNA yW-synthesizing protein 4
MEPCE	Q7L2J0	MEPCE_HUMAN	MEPCE BCDIN3	7SK snRNA methylphosphate capping enzyme ShortMePCE
METT10D	Q86W50	MET16_HUMAN	METTL16 METT10D	RNA N6-adenosine-methyltransferase METTL16
METTL1	Q9UBP6	TRMB_HUMAN	METTL1 C12orf1	tRNA (guanine-N(7)-)-methyltransferase
METTL11B	Q5VVY1	NTM1B_HUMAN	METTL11B C1orf184 NRMT2	Alpha N-terminal protein methyltransferase 1B
METTL12	A8MUP2	CSKMT_HUMAN	CSKMT METTL12	Citrate synthase-lysine N-methyltransferase CSKMT, mitochondrial
METTL13	Q8N6R0	EFNMT_HUMAN	EEF1AKNMT KIAA0859 METTL13 CGI-01	Methyltransferase-like protein 13
METTL15	A6NJ78	MET15_HUMAN	METTL15 METT5D1	Probable methyltransferase-like protein 15
METTL15P1	P0C7V9	ME15P_HUMAN	METTL15P1 METT5D2	Putative methyltransferase-like protein 15P1
METTL17	Q9H7H0	MET17_HUMAN	METTL17 METT11D1	Methyltransferase-like protein 17, mitochondrial

Table 6.2.1 continued from previous page

METTL18	O95568	MET18_HUMAN	METTL18 ASTP2 C1orf156	Histidine protein methyltransferase 1 homolog
METTL21A	Q8WXB1	MT21A_HUMAN	METTL21A FAM119A HCA557B	Protein N-lysine methyltransferase METTL21A
METTL21C	Q5VZV1	MT21C_HUMAN	METTL21C C13orf39	Protein-lysine methyltransferase METTL21C
METTL21EP	A6NDL7	MT21E_HUMAN	METTL21EP METTL21CP1	Putative methyltransferase-like protein 21E pseudogene
METTL22	Q9BUU2	MET22_HUMAN	METTL22 C16orf68 LP8272	Methyltransferase-like protein 22
METTL23	Q86XA0	MET23_HUMAN	METTL23 C17orf95	Methyltransferase-like protein 23
METTL25	Q8N6Q8	MET25_HUMAN	METTL25 C12orf26	Methyltransferase-like protein 25
METTL2A	Q96IZ6	MET2A_HUMAN	METTL2A METTL2 HSPC266	Methyltransferase-like protein 2A
METTL2B	Q6P1Q9	MET2B_HUMAN	METTL2B	Methyltransferase-like protein 2B
METTL3	Q86U44	MTA70_HUMAN	METTL3 MTA70	N6-adenosine-methyltransferase catalytic subunit
METTL4	Q8N3J2	METL4_HUMAN	METTL4	Methyltransferase-like protein 4
METTL5	Q9NRN9	METL5_HUMAN	METTL5 DC3 HSPC133	Methyltransferase-like protein 5
METTL6	Q8TCB7	METL6_HUMAN	METTL6	Methyltransferase-like protein 6
METTL7A	Q9H8H3	MET7A_HUMAN	METTL7A PRO0066 UNQ1902/PRO4348	Methyltransferase-like protein 7A
METTL7B	Q6UX53	MET7B_HUMAN	METTL7B UNQ594/PRO1180	Methyltransferase-like protein 7B
METTL8	Q9H825	METL8_HUMAN	METTL8	Methyltransferase-like protein 8
MSTP077	Q9H649	NSUN3_HUMAN	NSUN3 MSTP077 UG0651E06	tRNA (cytosine(34)-C(5))-methyltransferase, mitochondrial
N6AMT2	Q8WVE0	EFMT1_HUMAN	EEF1AKMT1 N6AMT2	EEF1A lysine methyltransferase 1
NNMT	P40261	NNMT_HUMAN	NNMT	Nicotinamide N-methyltransferase
NOP2	P46087	NOP2_HUMAN	NOP2 NOL1 NSUN1	Probable 28S rRNA (cytosine(4447)-C(5))-methyltransferase
NSUN2	Q08J23	NSUN2_HUMAN	NSUN2 SAKI TRM4	tRNA (cytosine(34)-C(5))-methyltransferase
NSUN4	Q96CB9	NSUN4_HUMAN	NSUN4	5-methylcytosine rRNA methyltransferase NSUN4
NSUN5	Q96P11	NSUN5_HUMAN	NSUN5 NSUN5A WBSCR20 WBSCR20A	Probable 28S rRNA (cytosine-C(5))-methyltransferase
NSUN5P1	Q3KNT7	NSN5B_HUMAN	NSUN5P1 NSUN5B WBSCR20B	Putative NOL1/NOP2/Sun domain family member 5B
NSUN5P2	Q63ZY6	NSN5C_HUMAN	NSUN5P2 NSUN5C WBSCR20B WBSCR20C	Putative methyltransferase NSUN5C
NSUN6	Q8TEA1	NSUN6_HUMAN	NSUN6 NOPD1	Putative methyltransferase NSUN6
NSUN7	Q8NE18	NSUN7_HUMAN	NSUN7	Putative methyltransferase NSUN7
NTMT1	Q9BV86	NTM1A_HUMAN	NTMT1 C9orf32 METTL11A NRMT NRMT1 AD-003	N-terminal Xaa-Pro-Lys N-methyltransferase 1
PCMT1	P22061	PIMT_HUMAN	PCMT1	Protein-L-isoaspartate(D-aspartate) O-methyltransferase ShortPIMT
PNMT	P11086	PNMT_HUMAN	PNMT PENT	Phenylethanolamine N-methyltransferase ShortPNMTase
PP7517	Q8WZ04	TOMT_HUMAN	LRTOMT COMT2 TOMT PP7517	Transmembrane O-methyltransferase
PRMT2	P55345	ANM2_HUMAN	PRMT2 HMT1 HRMT1L1	Protein arginine N-methyltransferase 2
PRMT3	O60678	ANM3_HUMAN	PRMT3 HRMT1L3	Protein arginine N-methyltransferase 3

Table 6.2.1 continued from previous page

PRMT5	O14744	ANM5_HUMAN	PRMT5 HRMT1L5 IBP72 JBP1 SKB1	Protein arginine N-methyltransferase 5
PRMT6	Q96LA8	ANM6_HUMAN	PRMT6 HRMT1L6	Protein arginine N-methyltransferase 6
PRMT7	Q9NVM4	ANM7_HUMAN	PRMT7 KIAA1933	Protein arginine N-methyltransferase 7
PRMT8	Q9NR22	ANM8_HUMAN	PRMT8 HRMT1L3 HRMT1L4	Protein arginine N-methyltransferase 8
PRMT9	Q6P2P2	ANM9_HUMAN	PRMT9 PRMT10	Protein arginine N-methyltransferase 9
RNMT	O43148	MCES_HUMAN	RNMT KIAA0398	mRNA cap guanine-N7 methyltransferase
RRP8	O43159	RRP8_HUMAN	RRP8 KIAA0409 NML hucep-1	Ribosomal RNA-processing protein 8
TFB1M	Q8WVM0	TFB1M_HUMAN	TFB1M CGI-75	Dimethyladenosine transferase 1, mitochondrial
TFB2M	Q9H5Q4	TFB2M_HUMAN	TFB2M NS5ATP5	Dimethyladenosine transferase 2, mitochondrial
TGS1	Q96RS0	TGS1_HUMAN	TGS1 HCA137 NCOA6IP PIMT	Trimethylguanosine synthase
TPMT	P51580	TPMT_HUMAN	TPMT	Thiopurine S-methyltransferase
TRDMT1	O14717	TRDMT_HUMAN	TRDMT1 DNMT2	tRNA (cytosine(38)-C(5))-methyltransferase
TRMT1	Q9NXH9	TRM1_HUMAN	TRMT1	tRNA (guanine(26)-N(2))-dimethyltransferase
TRMT11	Q7Z4G4	TRM11_HUMAN	TRMT11 C6orf75 MDS024	tRNA (guanine(10)-N2)-methyltransferase homolog
TRMT1L	Q7Z2T5	TRM1L_HUMAN	TRMT1L C1orf25 TRM1L MSTP070	TRMT1-like protein
TRMT2A	Q8IZ69	TRM2A_HUMAN	TRMT2A HTF9C	tRNA (uracil-5-)-methyltransferase homolog A
TRMT2B	Q96GJ1	TRM2_HUMAN	TRMT2B CXorf34	tRNA (uracil(54)-C(5))-methyltransferase homolog
TRMT44	Q8IYL2	TRM44_HUMAN	TRMT44 C4orf23 METTL19	Probable tRNA (uracil-O(2)-)-methyltransferase
TRMT61A	Q96FX7	TRM61_HUMAN	TRMT61A C14orf172 TRM61	tRNA (adenine(58)-N(1))-methyltransferase catalytic subunit TRMT61A
TRMT61B	Q9BVS5	TR61B_HUMAN	TRMT61B	tRNA (adenine(58)-N(1))-methyltransferase, mitochondrial
VCPKMT	Q9H867	MT21D_HUMAN	VCPKMT C14orf138 METTL21D	Protein-lysine methyltransferase METTL21D

Table 6.2.2: DALI output used to rank human methyltransferases by structural similarity (sorted by Z-score). A detailed description of the DALI structural alignment workflow is given in Section 4.3.1

Number	PDB ID	Z	rmsd	lali	nres	%id	Abbrev.	Full Name	Substrate	UniProt ID
1	3rod-A	51.2	0	260	260	100	NNMT	nicotinamide N-methyltransferase	SM	P40261
30	2a14-A	43.2	1.1	258	258	52	INMT	indolethylamine N-methyltransferase	SM	O95050
35	3hcd-B	37.6	1.5	252	269	39	PNMT	phenylethanolamine N-methyltransferase	SM	P11086
115	6dub-B	18.7	2.9	197	218	15	NTM1B	alpha N-terminal protein methyltransferase 1B	protein	Q5VVY1
117	2ex4-A	18.5	2.9	197	222	18	NTM1A	N-terminal Xaa-pro-lys N-methyltransferase 1	protein	Q9BV86
285	3bgv-B	15.9	3.2	192	271	13	RG7MT1	mRNA cap guanine-N7 methyltransferase	RNA	O43148
349	2bzg-A	15.5	2.8	190	230	12	TPMT	thiopurine S-methyltransferase	SM	P51580
385	5yf0-A	15.4	3.1	192	337	14	CARNMT1	carnosine N-methyltransferase	SM	Q8N4J0
422	1jqe-B	15.2	3.0	188	281	12	HNMT	histamine N-methyltransferase	SM	P50135
498	1r74-B	14.9	2.7	183	279	16	GNMT	glycine N-methyltransferase	SM	Q14749
517	2pxx-A	14.8	2.9	173	214	14	EEF1AKMT4	EEF1A lysine methyltransferase 4	Protein	P0DPD7
625	4a6e-A	14.4	3.1	188	346	14	ASMT	acetylserotonin O-methyltransferase	SM	P46597
633	6dcc-A	14.4	3.1	179	222	17	MePCE	7SK snRNA methylphosphate capping enzyme	RNA	Q7L2J0
666	3p71-T	14.2	3.5	205	315	8	LCMT1	leucine carboxyl methyltransferase 1	protein	Q9UIC8
886	4xcx-A	13.1	3.2	169	217	12	HENMT1	Small RNA 2'-O-methyltransferase	RNA	Q5T8I9
897	4rfq-A	13.0	3.5	182	269	17	MTL18	histidine protein methyltransferase 1 homolog	protein	O95568
–	3orh-A	13.0	3.3	192	231	17	GAMT	guanidinoacetate N-methyltransferase	SM	Q14353
977	4qpn-A	12.5	2.8	162	203	17	METTL21B	EEF1A lysine methyltransferase 3	protein	Q96AZ1
991	4pwy-A	12.4	3.3	174	251	15	CLNMT	calmodulin-lysine N-methyltransferase	Protein	Q7Z624
1078	4lec-A	12.0	3.1	163	203	13	HSPA-KMT	protein N-lysine methyltransferase METTL21A	protein	Q8WXB1
1090	5wws-B	12.0	3.6	166	458	14	NSUN6	putative methyltransferase NSUN6	RNA	Q8TEA1
1160	2avd-A	11.4	3.6	163	220	10	COMT	catechol O-methyltransferase domain-containing protein 1	SM	Q86VU5
1230	3egi-A	10.4	3.0	156	195	10	TGS1	trimethylguanosine synthase	RNA	Q96RS0
1233	5wcj-A	10.3	3.2	155	222	14	METTL13	methyltransferase-like protein 13	protein	Q8N6R0
1246	3uwp-A	10.1	3.2	166	341	11	DOT1L	histone-lysine N-methyltransferase, H3 lysine-79 specific	protein	Q8TEK3
1266	4ikp-A	10.0	2.9	157	335	13	PRMT4	histone-arginine methyltransferase CARM1	protein	Q86X55
1270	1zq9-A	9.9	2.8	156	279	13	DIMT1	probable dimethyladenosine transferase	RNA	Q9UNQ2
1315	2h00-C	9.7	3.3	161	204	14	METTL16	RNA N6-adenosine-methyltransferase METTL16	RNA	Q86W50
1342	4qqn-A	9.6	2.9	149	299	15	PRMT3	protein arginine N-methyltransferase 3	protein	O60678
1351	5ccx-B	9.5	3.4	155	371	11	TRMT61A	tRNA (adenine(58)-N(1))-methyltransferase catalytic subunit TRMT61A	RNA	Q96FX7
1558	4n48-B	7.7	4.0	164	406	6	CMTR1	cap-specific mRNA (nucleoside-2'-O-)-methyltransferase 1	RNA	Q8N1G2
1588	4wxx-B	7.3	3.5	142	1178	10	DNMT1	DNA (cytosine-5)-methyltransferase 1	DNA	P26358
1589	1i1n-A	7.2	3.3	137	225	15	PIMT	protein-L-isoaspartate(D-aspartate) O-methyltransferase	protein	P22061
1601	1g55-A	7.0	4.5	132	314	11	TRDMT1	tRNA (cytosine(38)-C(5))-methyltransferase	RNA	O14717

The remainder of this page is intentionally left blank.

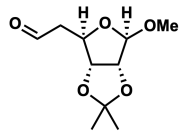

23, ^{1}H, 500 MHz, $CDCl_3$

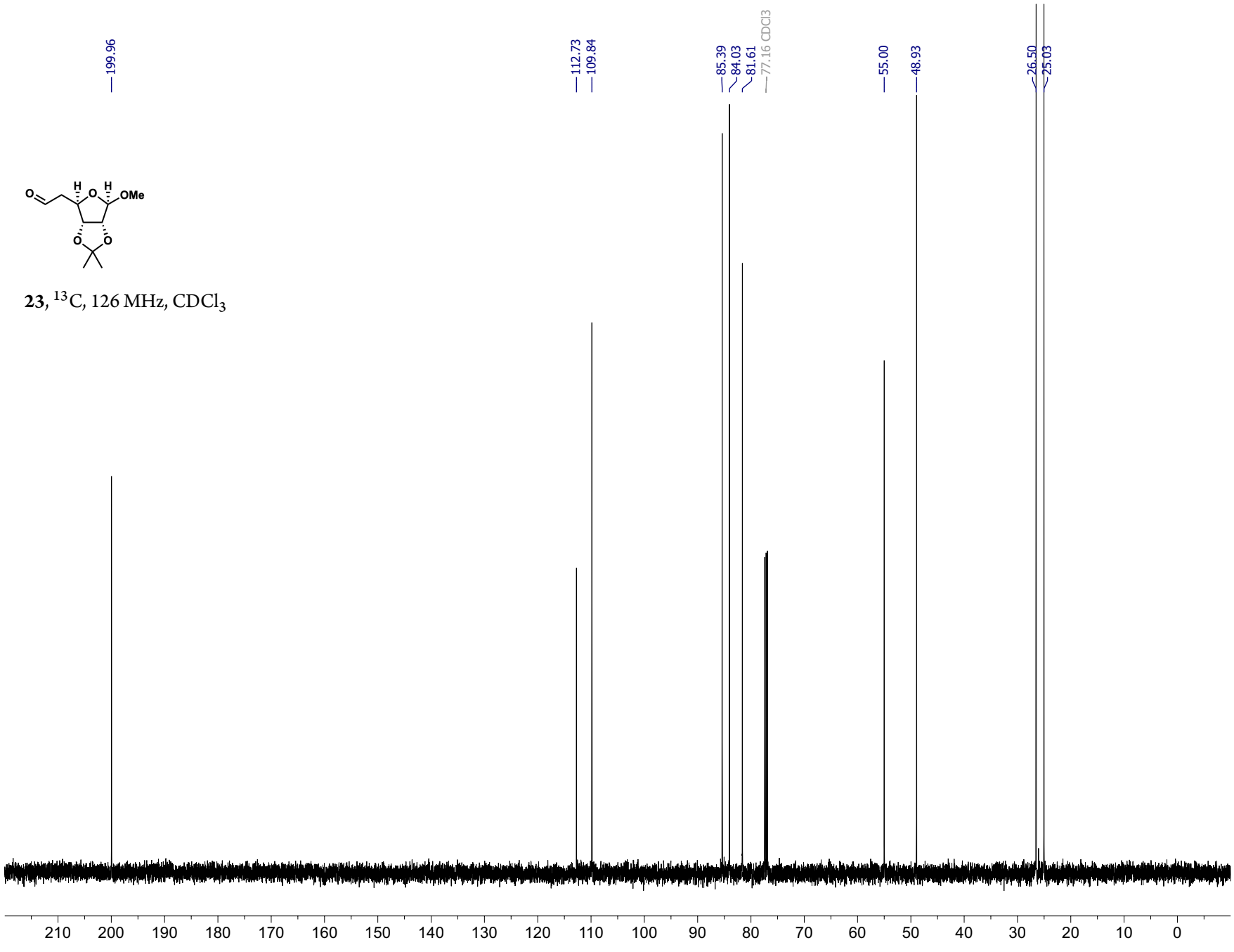

23, ^{13}C, 126 MHz, $CDCl_3$

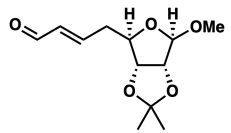

24, ^{1}H, 500 MHz, $CDCl_3$

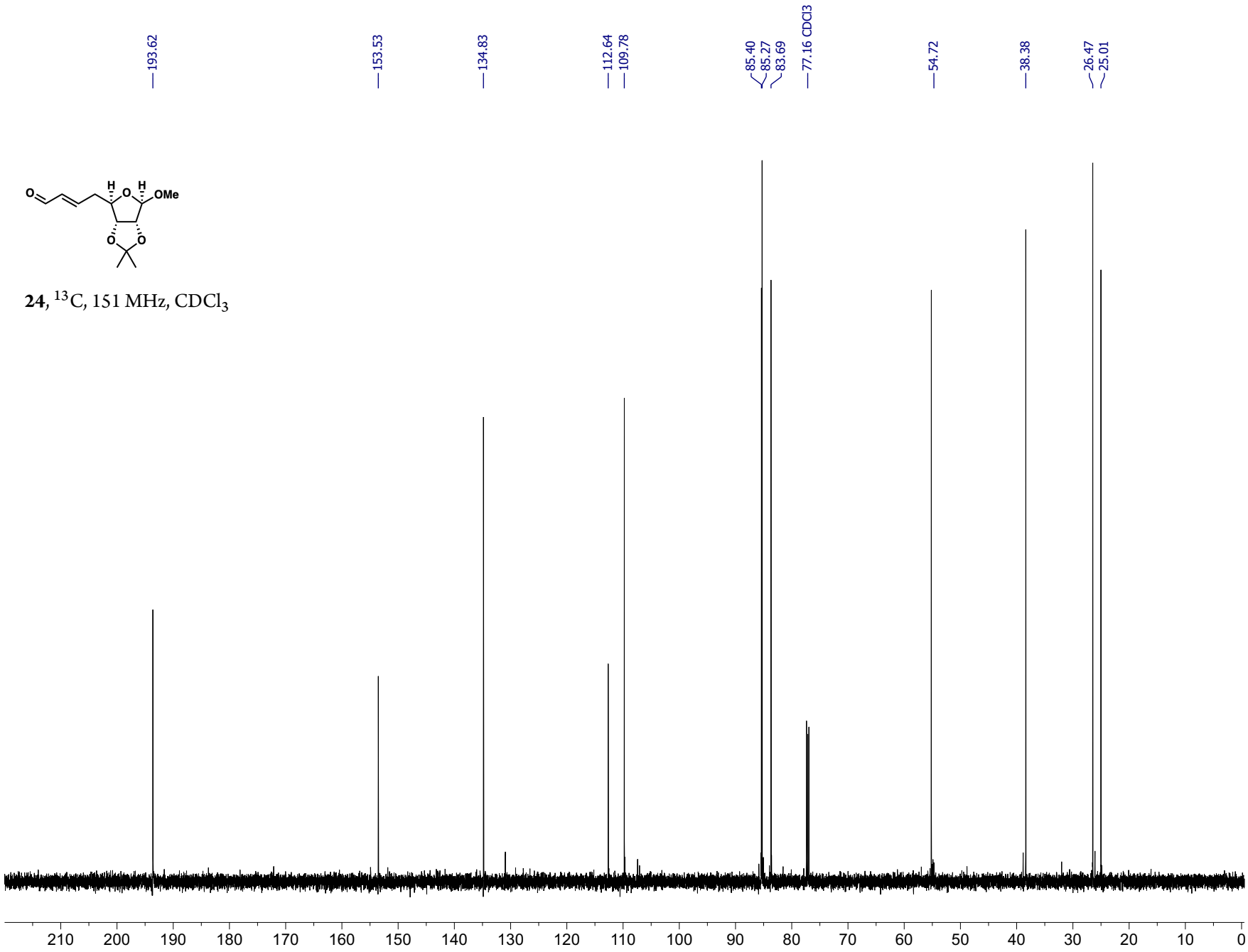

24, ^{13}C, 151 MHz, $CDCl_3$

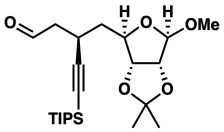

25, ^{1}H, 600 MHz, $CDCl_3$

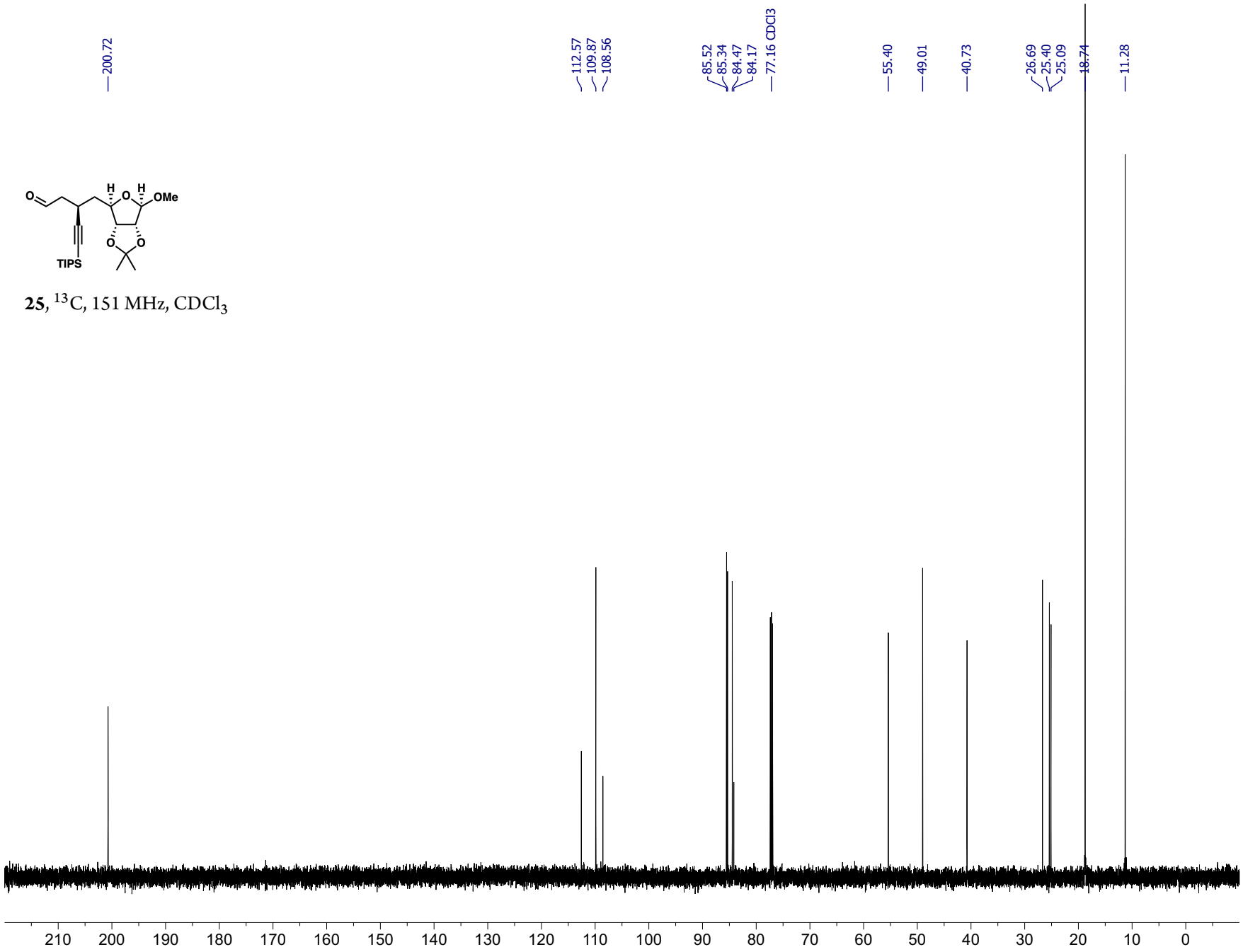

25, ^{13}C, 151 MHz, $CDCl_3$

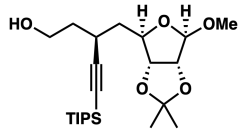

S2, ^{1}H, 600 MHz, $CDCl_3$

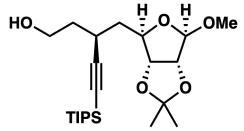

S2, ^{13}C, 151 MHz, $CDCl_3$

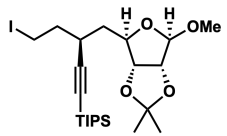

26, ^{1}H, 600 MHz, $CDCl_3$

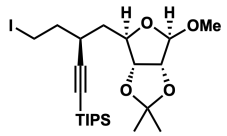

26, ^{13}C, 151 MHz, $CDCl_3$

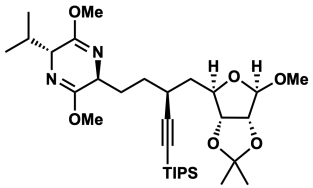

28, ^{1}H, 600 MHz, $CDCl_3$

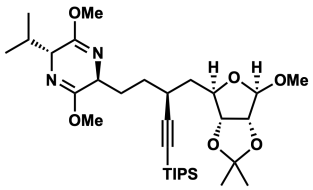

28, ^{13}C, 151 MHz, $CDCl_3$

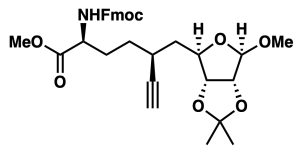

29, ^{1}H, 500 MHz, $CDCl_3$

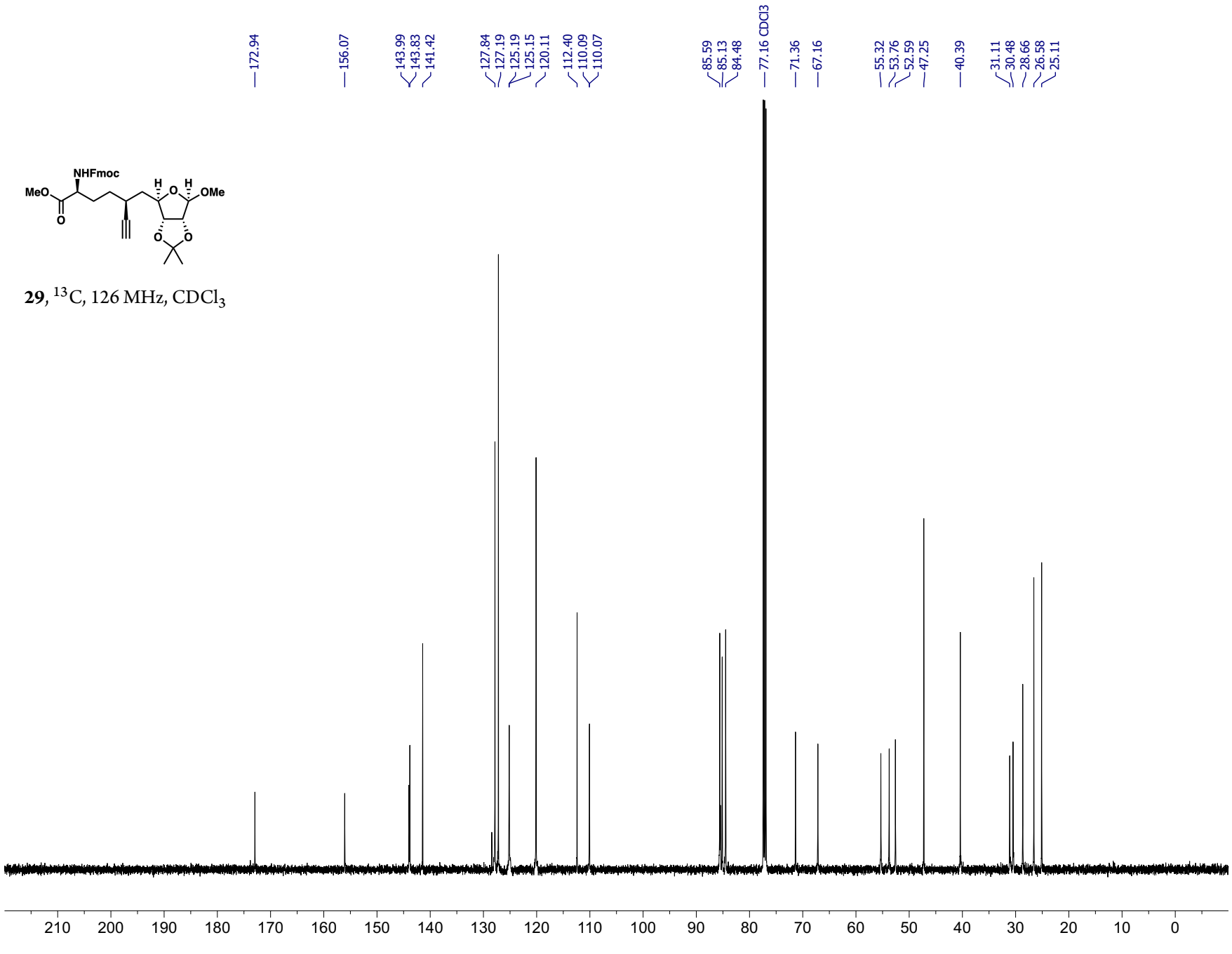

29, ^{13}C, 126 MHz, $CDCl_3$

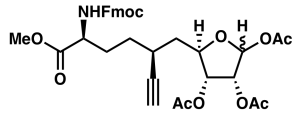

30, ^{1}H, 500 MHz, $CDCl_3$

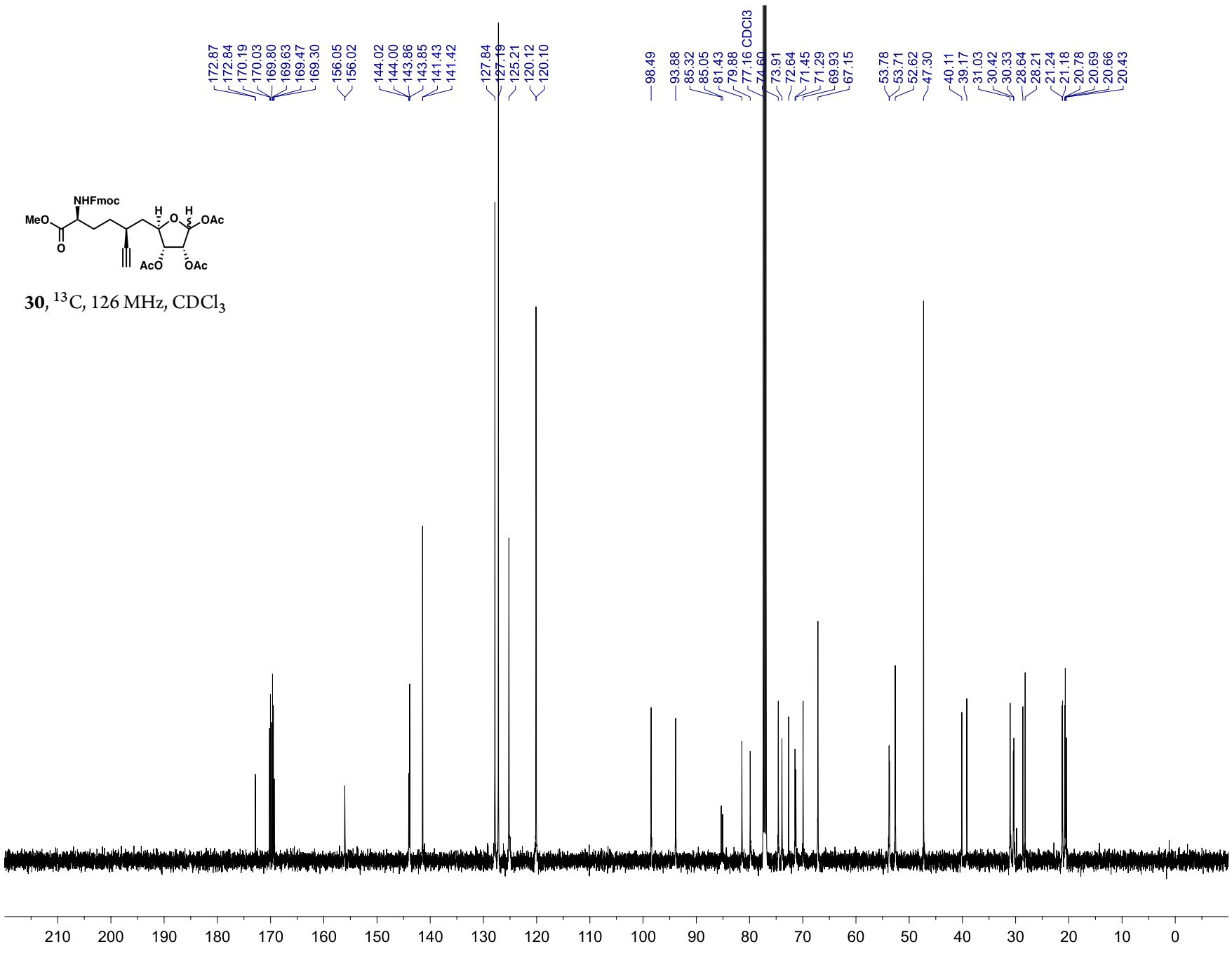

30, ^{13}C, 126 MHz, $CDCl_3$

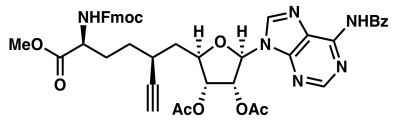

31, ^{1}H, 500 MHz, $CDCl_3$

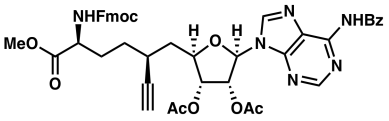

31, ^{13}C, 126 MHz, $CDCl_3$

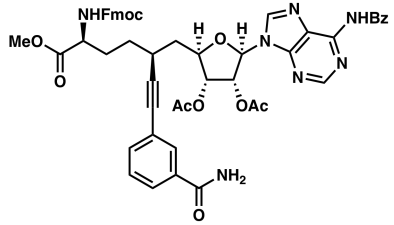

32, ^{1}H, 500 MHz, $CDCl_3$

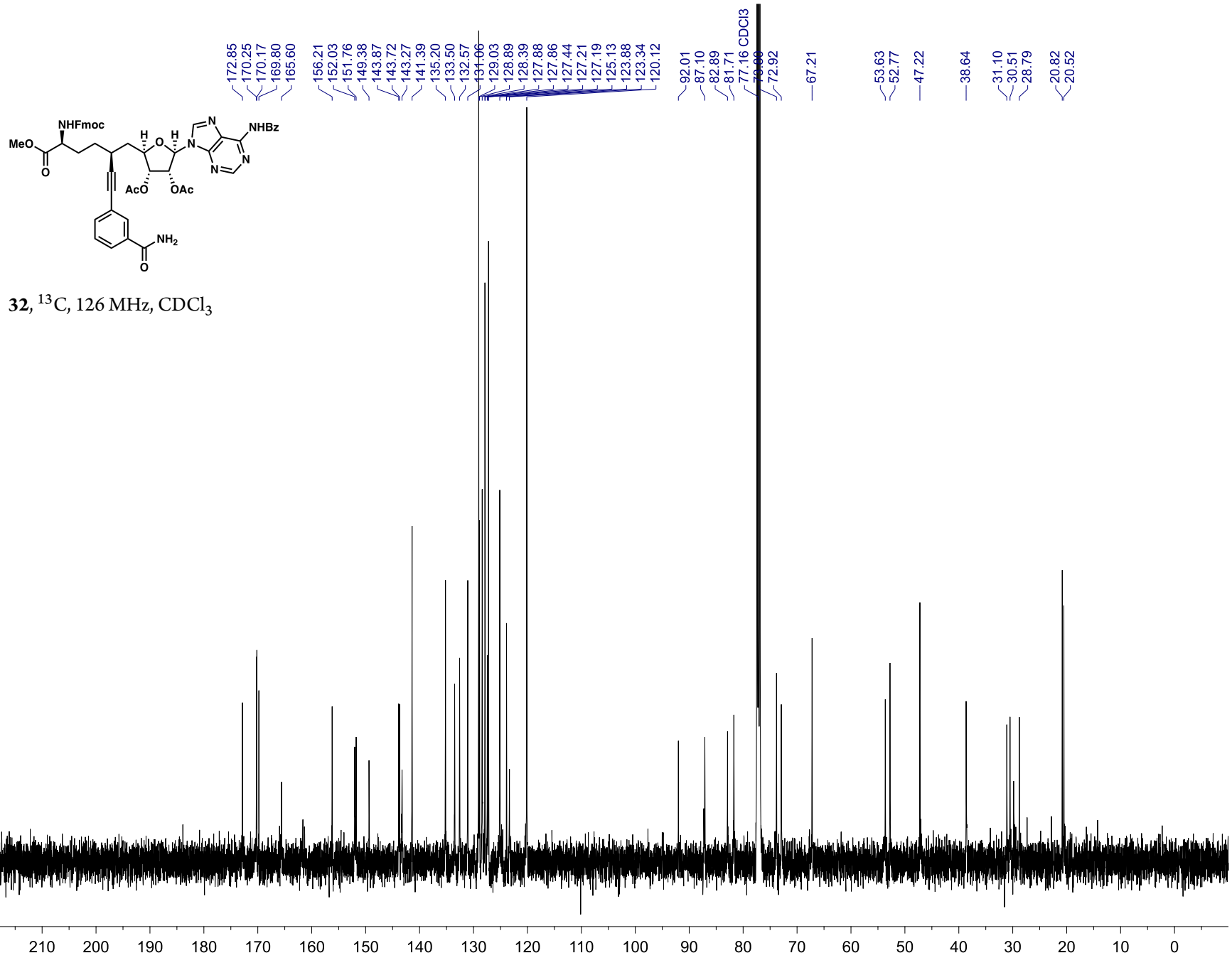

32, ^{13}C, 126 MHz, $CDCl_3$

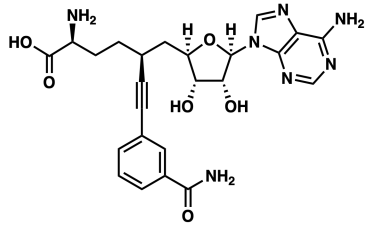

33, ^{1}H, 600 MHz, **CD$_3$CN**/D$_2$O/*d*−TFA

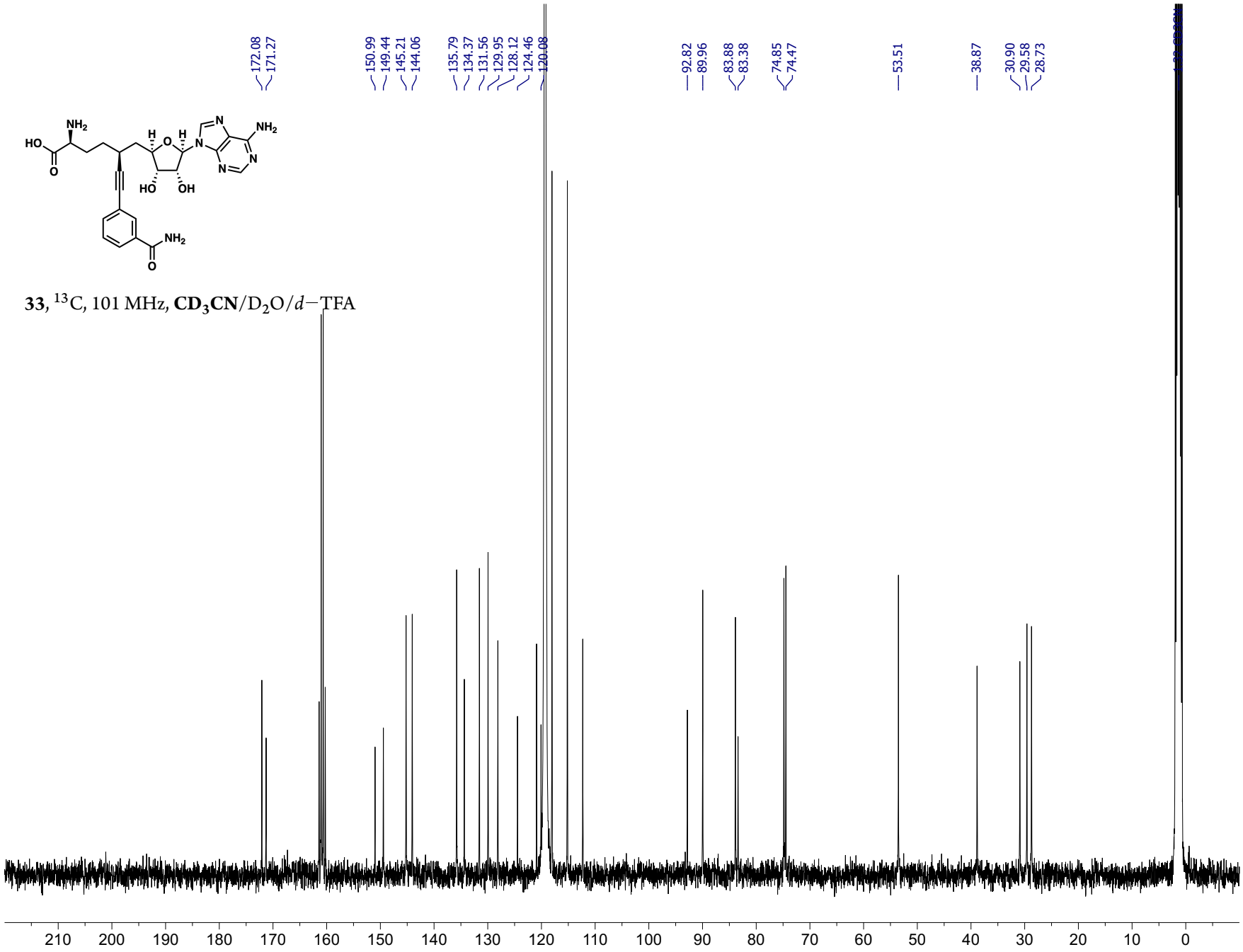

33, ^{13}C, 101 MHz, $\mathbf{CD_3CN}/D_2O/d-$TFA

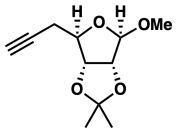

34, ^{1}H, 600 MHz, $CDCl_3$

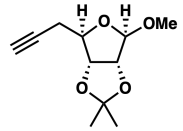

34, ^{13}C, 151 MHz, $CDCl_3$

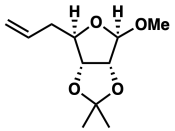

35, ^{1}H, 600 MHz, $CDCl_3$

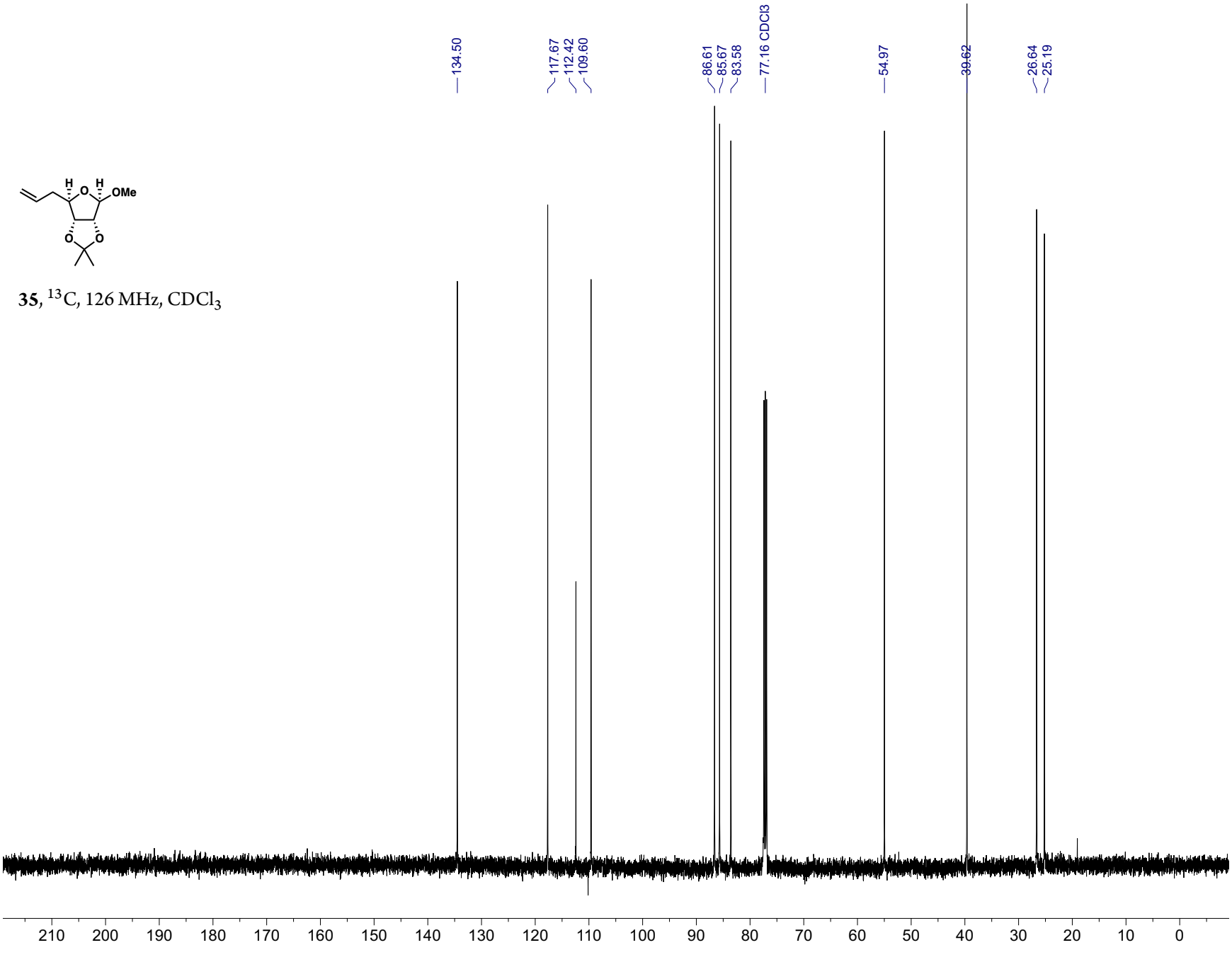

35, ^{13}C, 126 MHz, $CDCl_3$

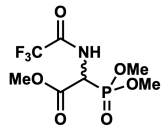

36, ^{1}H, 600 MHz, $CDCl_3$

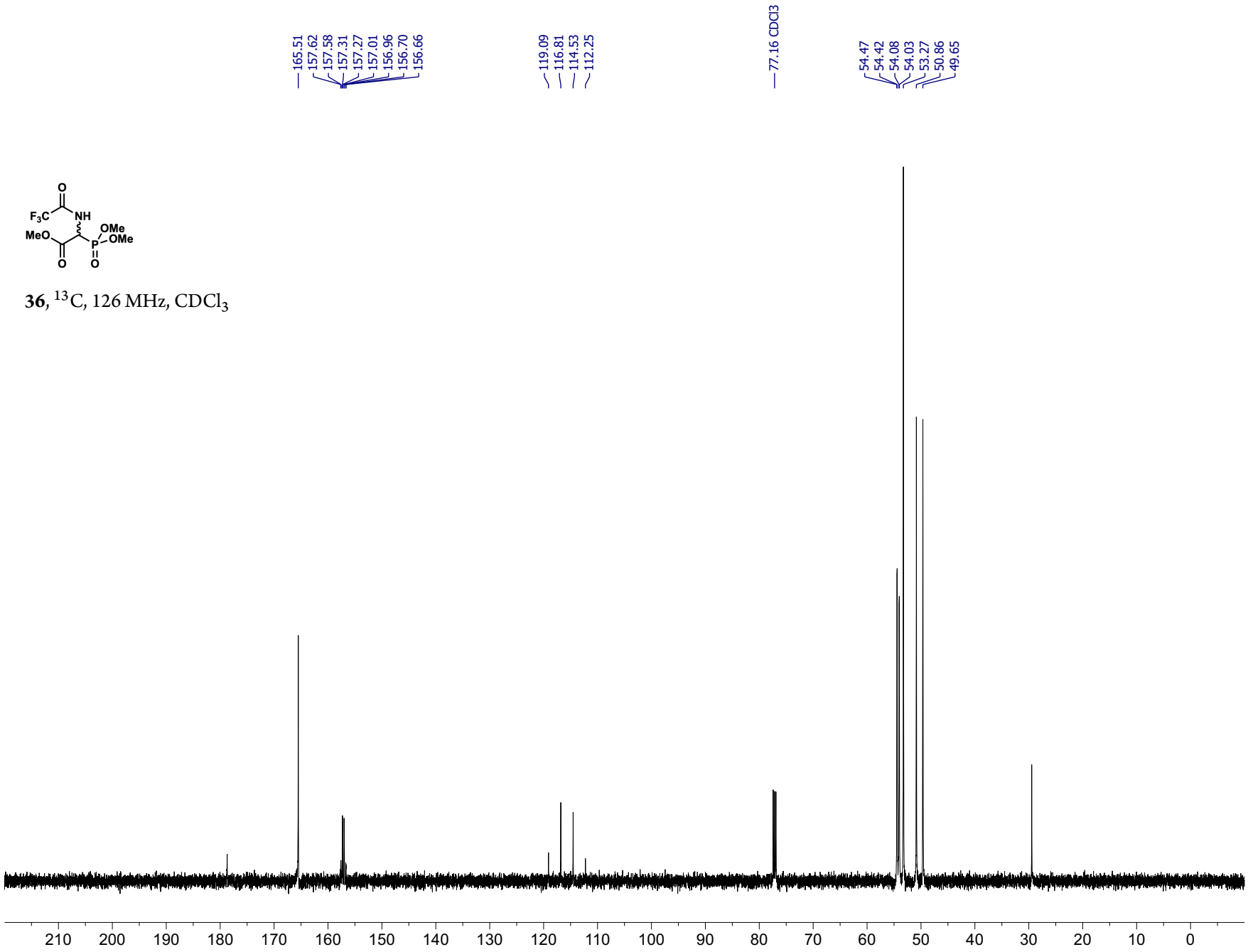

36, ^{13}C, 126 MHz, $CDCl_3$

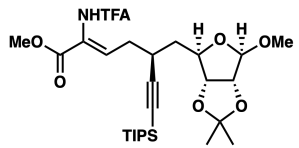

37, ^{1}H, 600 MHz, $CDCl_3$

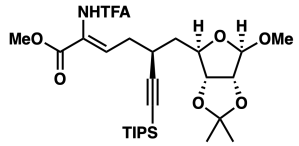

37, ^{13}C, 126 MHz, $CDCl_3$

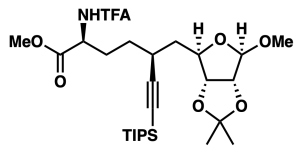

38, ^{1}H, 600 MHz, $CDCl_3$

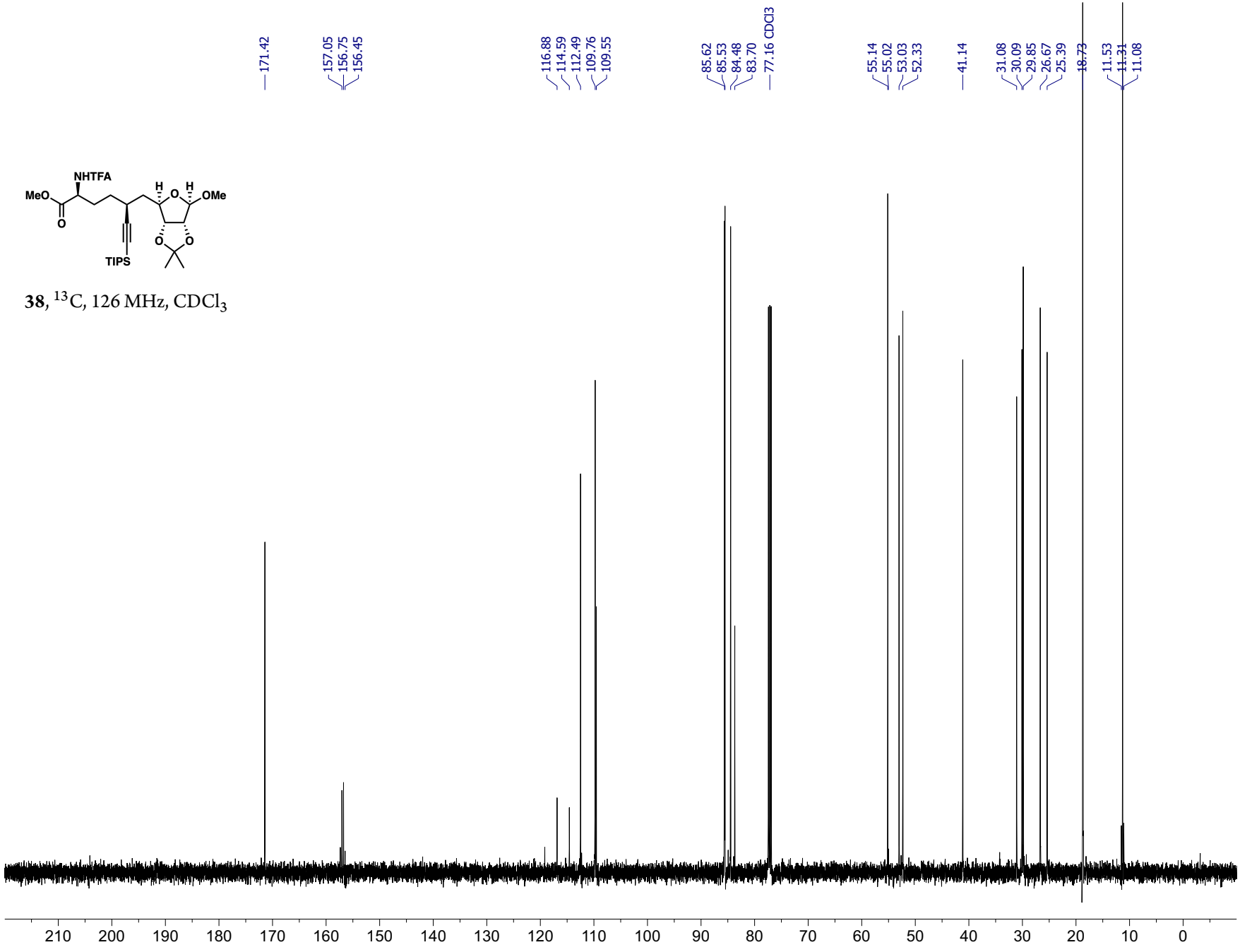

38, ^{13}C, 126 MHz, $CDCl_3$

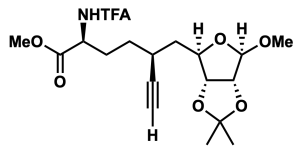

S4, ^{1}H, 600 MHz, $CDCl_3$

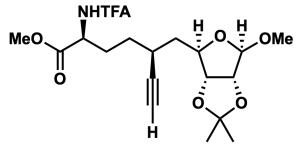

S4, ^{13}C, 126 MHz, $CDCl_3$

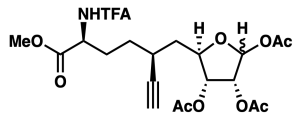

S5, ^{1}H, 600 MHz, $CDCl_3$

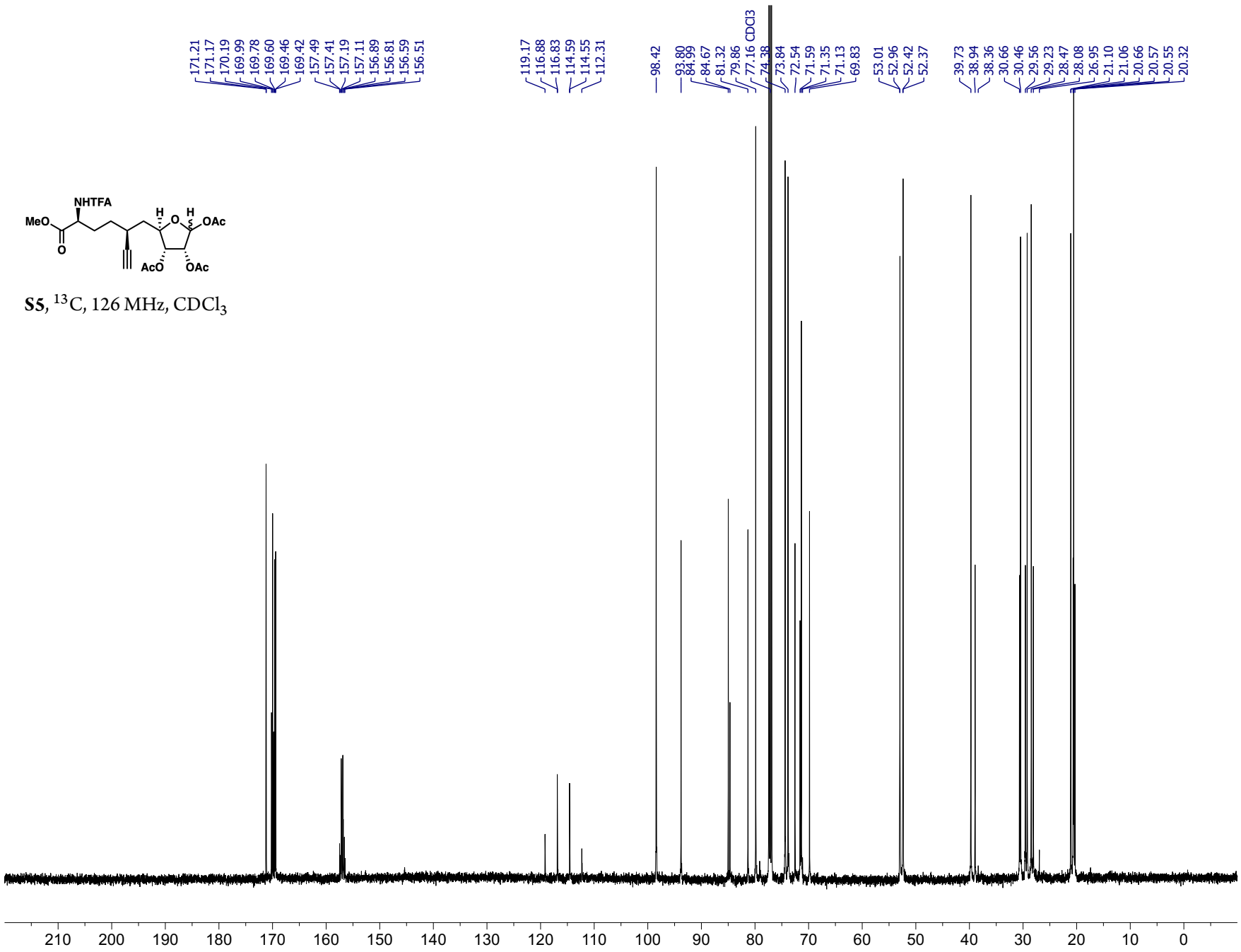

S5, ^{13}C, 126 MHz, $CDCl_3$

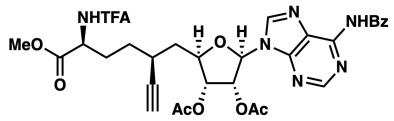

39, ^{1}H, 500 MHz, $CDCl_3$

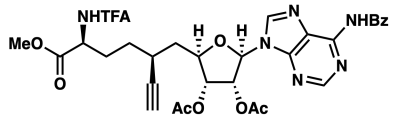

39, ^{13}C, 126 MHz, $CDCl_3$

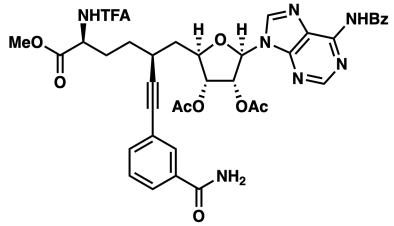

40, ^{1}H, 600 MHz, CD_2Cl_2

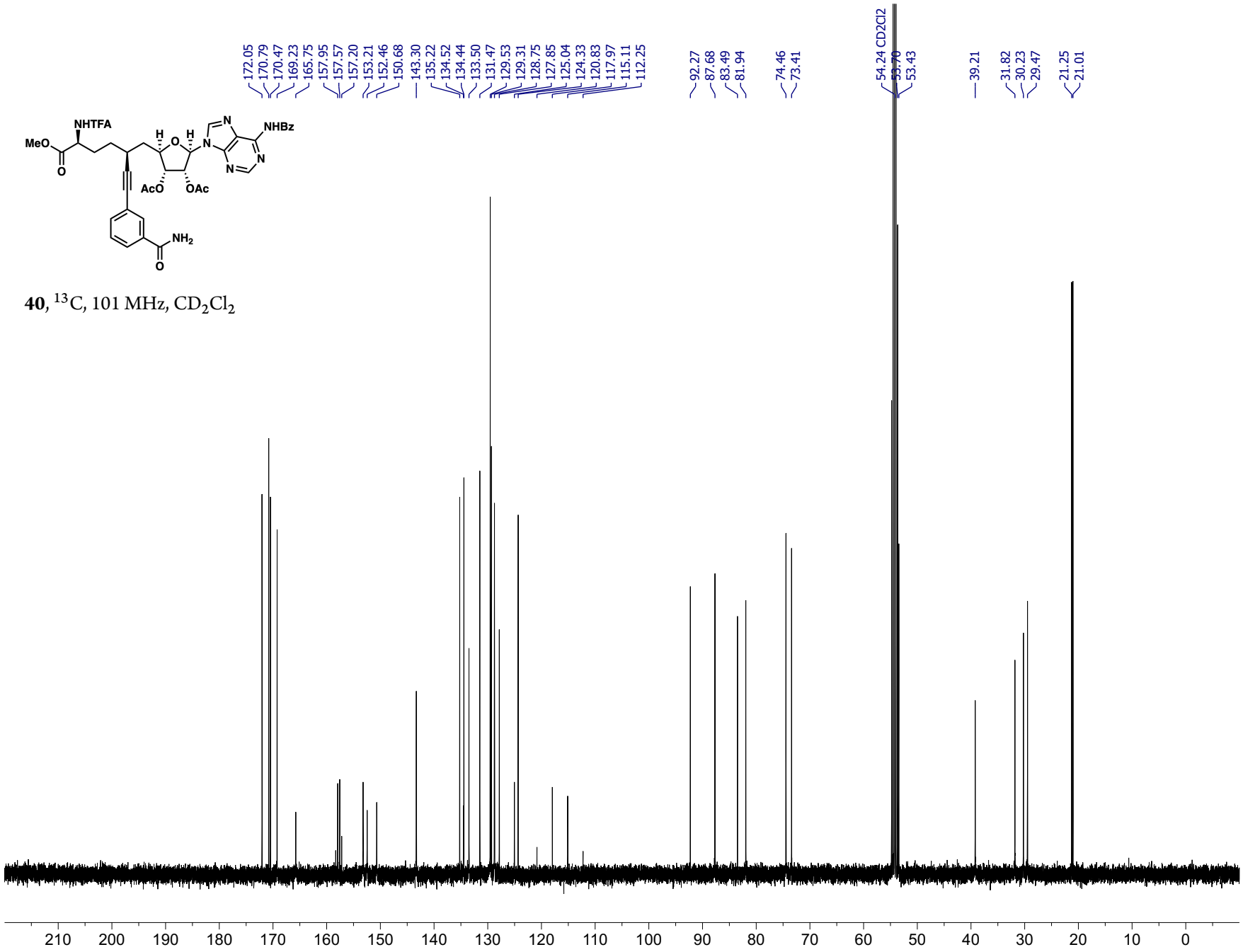

40, ^{13}C, 101 MHz, CD_2Cl_2

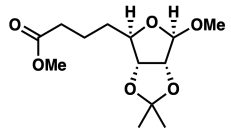

S7, ^{1}H, 600 MHz, $CDCl_3$

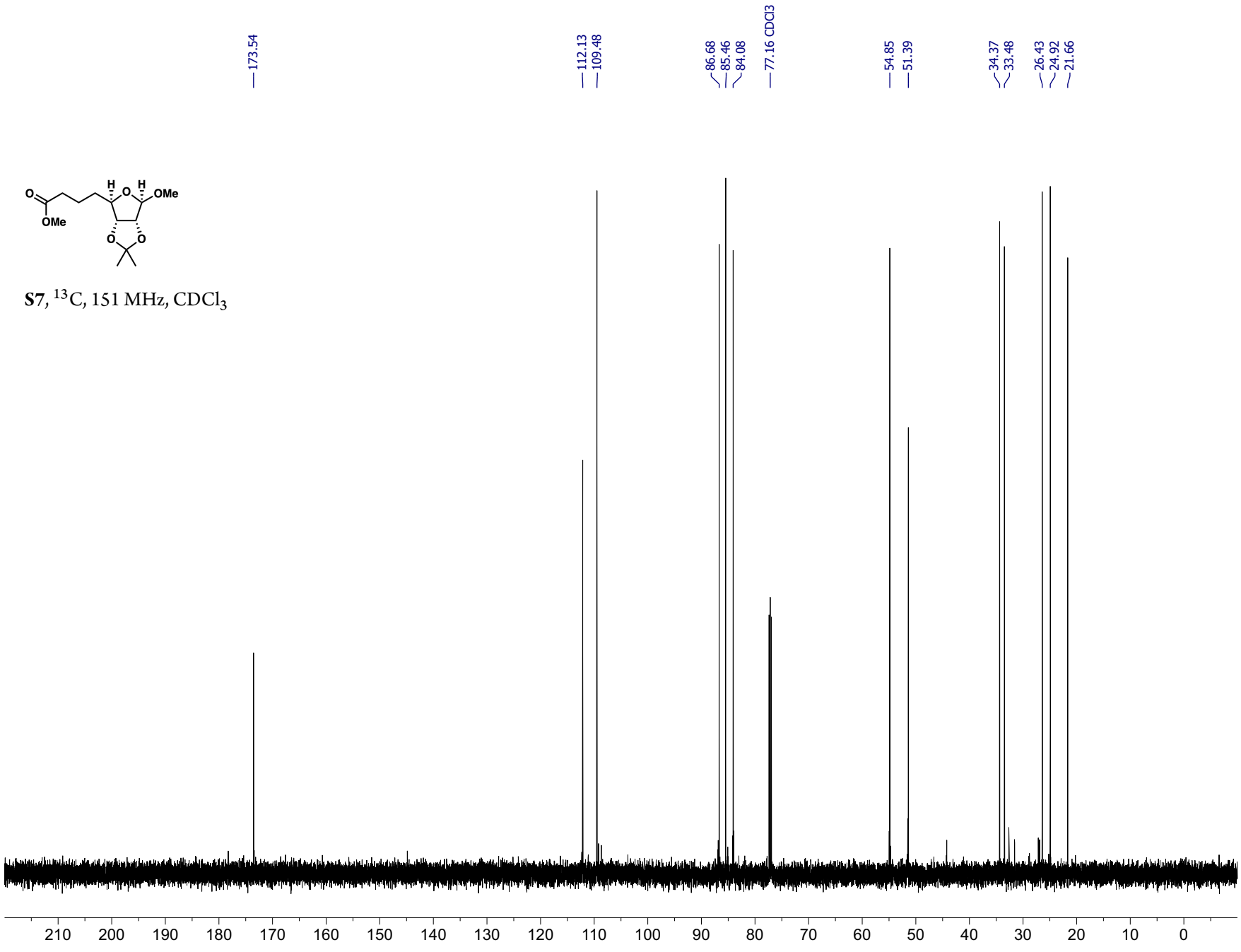

S7, ^{13}C, 151 MHz, $CDCl_3$

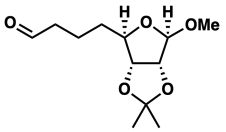

S8, ^{1}H, 600 MHz, $CDCl_3$

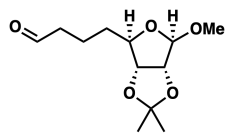

S8, ^{13}C, 151 MHz, $CDCl_3$

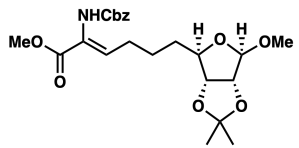

S9, ^{1}H, 600 MHz, $CDCl_3$

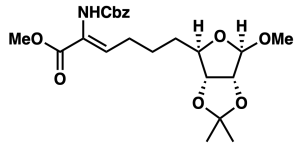

S9, ^{13}C, 151 MHz, $CDCl_3$

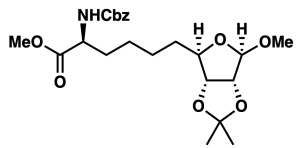

S10, ^{1}H, 600 MHz, $CDCl_3$

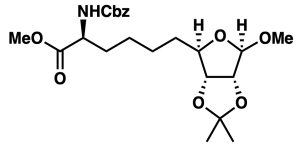

S10, ^{13}C, 151 MHz, $CDCl_3$

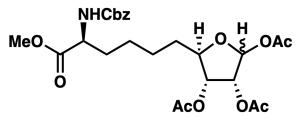

S11, ^{1}H, 600 MHz, $CDCl_3$

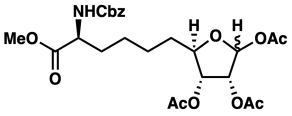

S11, ^{13}C, 126 MHz, $CDCl_3$

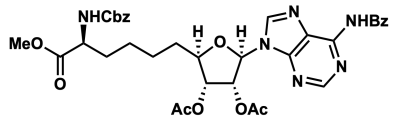

S12, ^{1}H, 600 MHz, $CDCl_3$

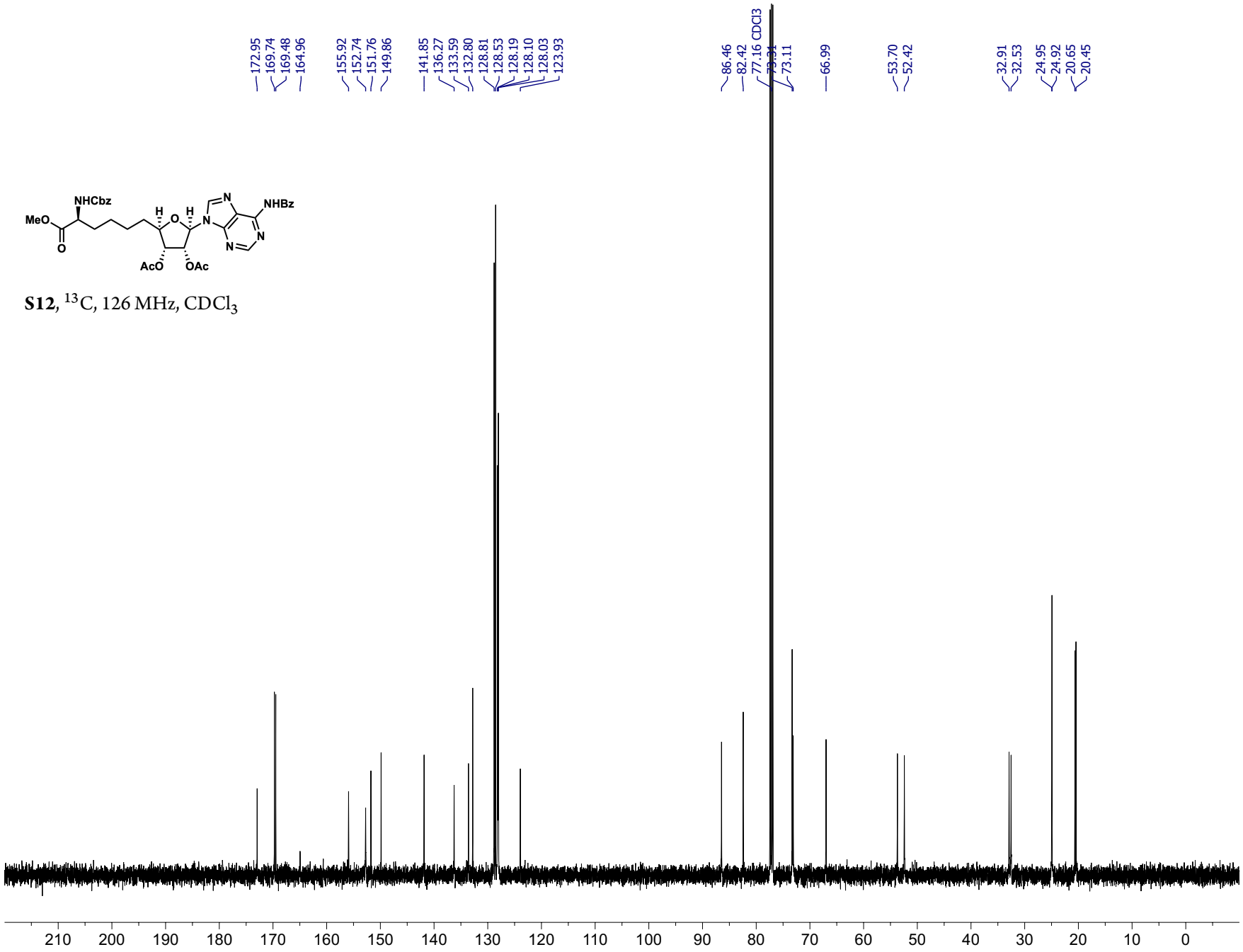

S12, ^{13}C, 126 MHz, $CDCl_3$

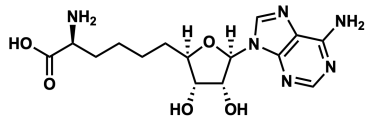

41, ^{1}H, 600 MHz, D_2O

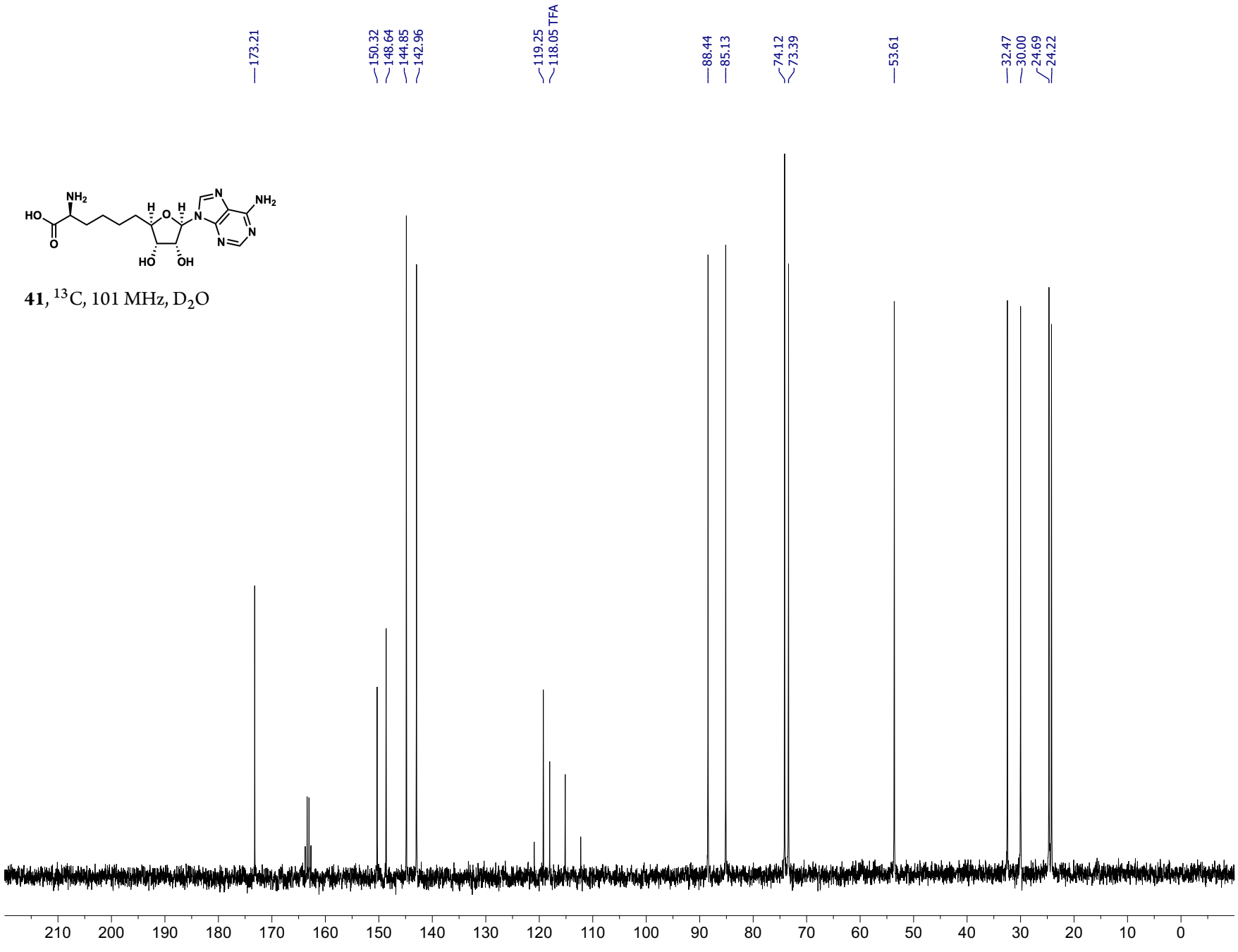

41, ^{13}C, 101 MHz, D_2O

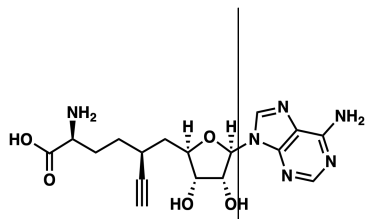

42, ^{1}H, 500 MHz, $CD_3CN/\mathbf{D_2O}/d-$TFA

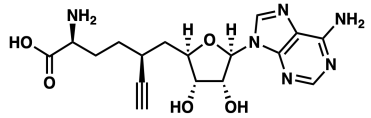

42, ^{13}C, 126 MHz, $\mathbf{CD_3CN}/D_2O/d-$TFA

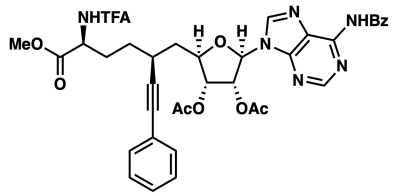

S13, ^{1}H, 500 MHz, $CDCl_3$

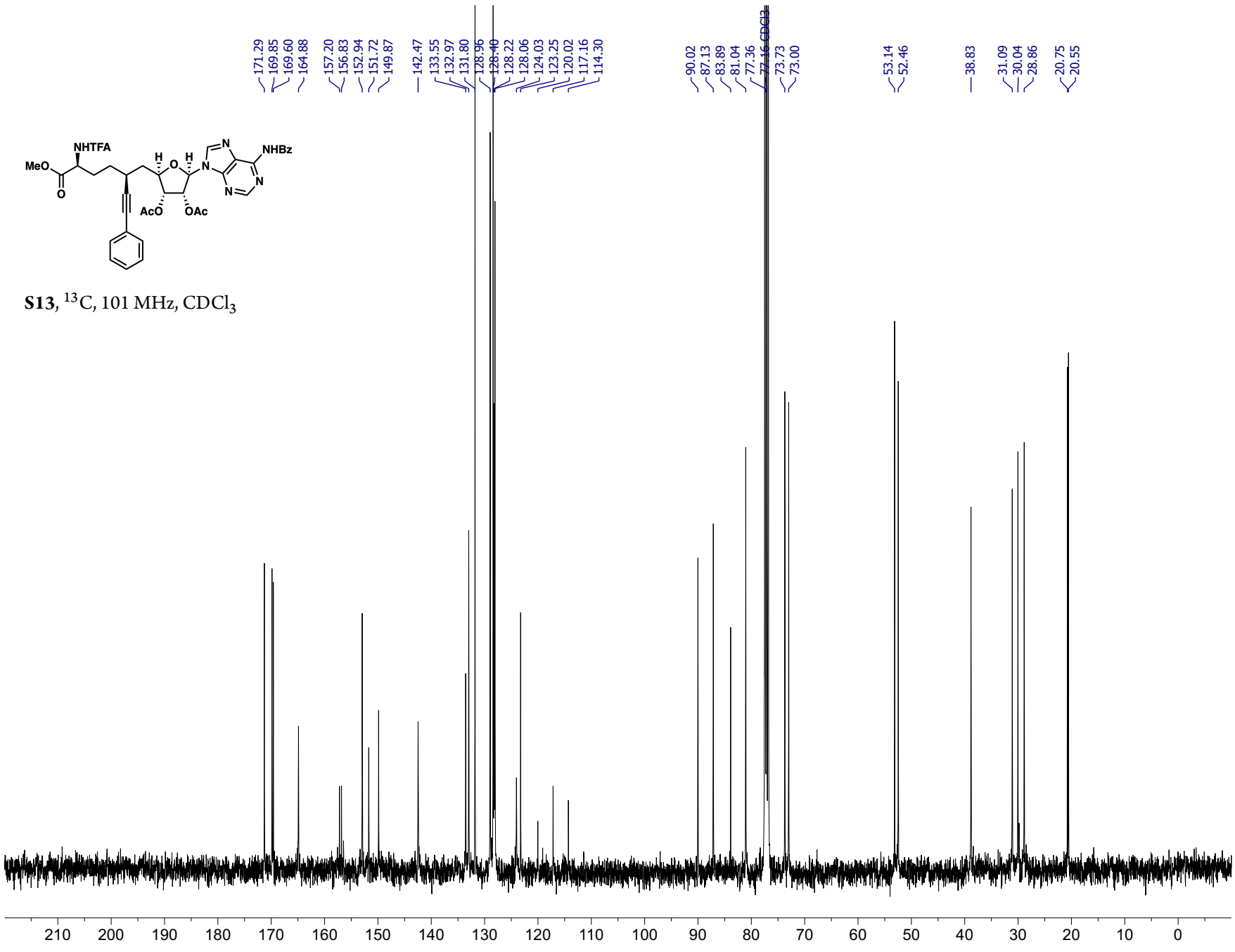

S13, ^{13}C, 101 MHz, $CDCl_3$

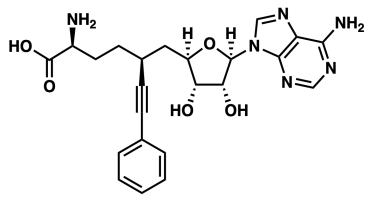

43, ^{1}H, 600 MHz, CD_3CN/$\mathbf{D_2O}$/*d*−TFA

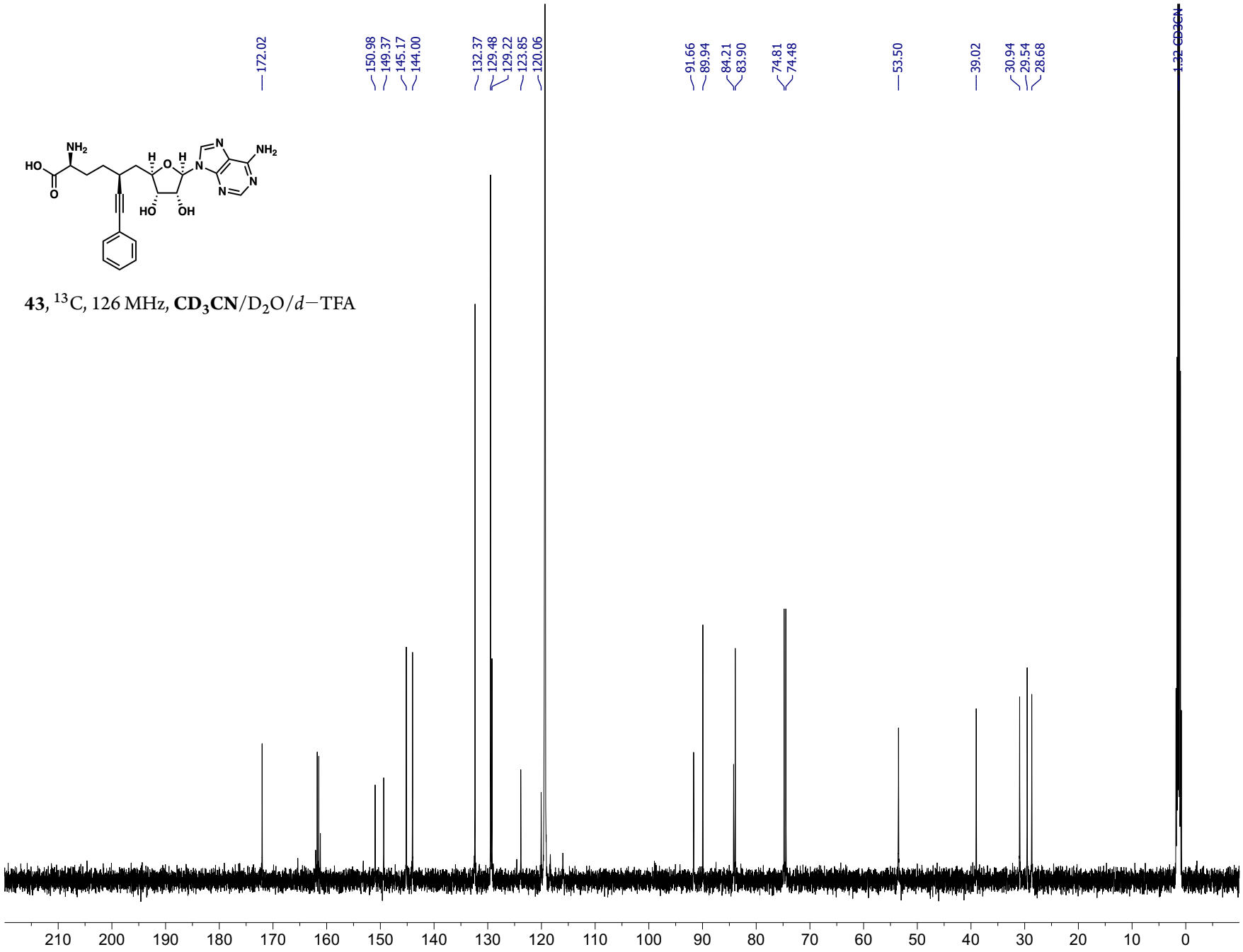

43, ^{13}C, 126 MHz, $\mathbf{CD_3CN}/D_2O/d-$TFA

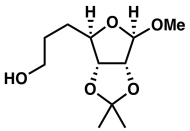

S15, ^{1}H, 600 MHz, $CDCl_3$

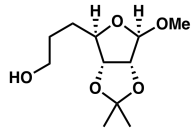

S15, ^{13}C, 151 MHz, $CDCl_3$

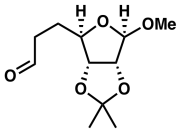

S16, ^{1}H, 500 MHz, $CDCl_3$

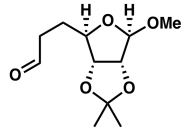

S16, ^{13}C, 151 MHz, $CDCl_3$

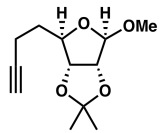

S17, ^{1}H, 600 MHz, $CDCl_3$

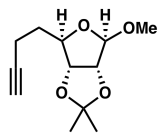

S17, ^{13}C, 151 MHz, $CDCl_3$

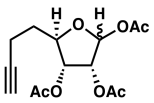

S18, ^{1}H, 600 MHz, $CDCl_3$

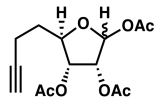

S18, ^{13}C, 126 MHz, $CDCl_3$

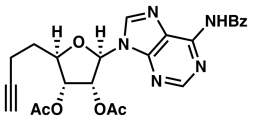

S19, ^{1}H, 600 MHz, $CDCl_3$

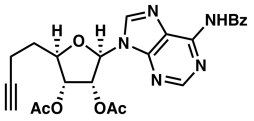

S19, ^{13}C, 151 MHz, $CDCl_3$

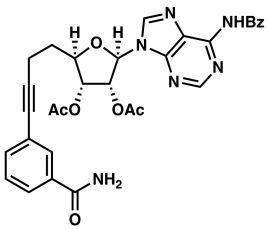

S20, ^{1}H, 600 MHz, $CDCl_3$

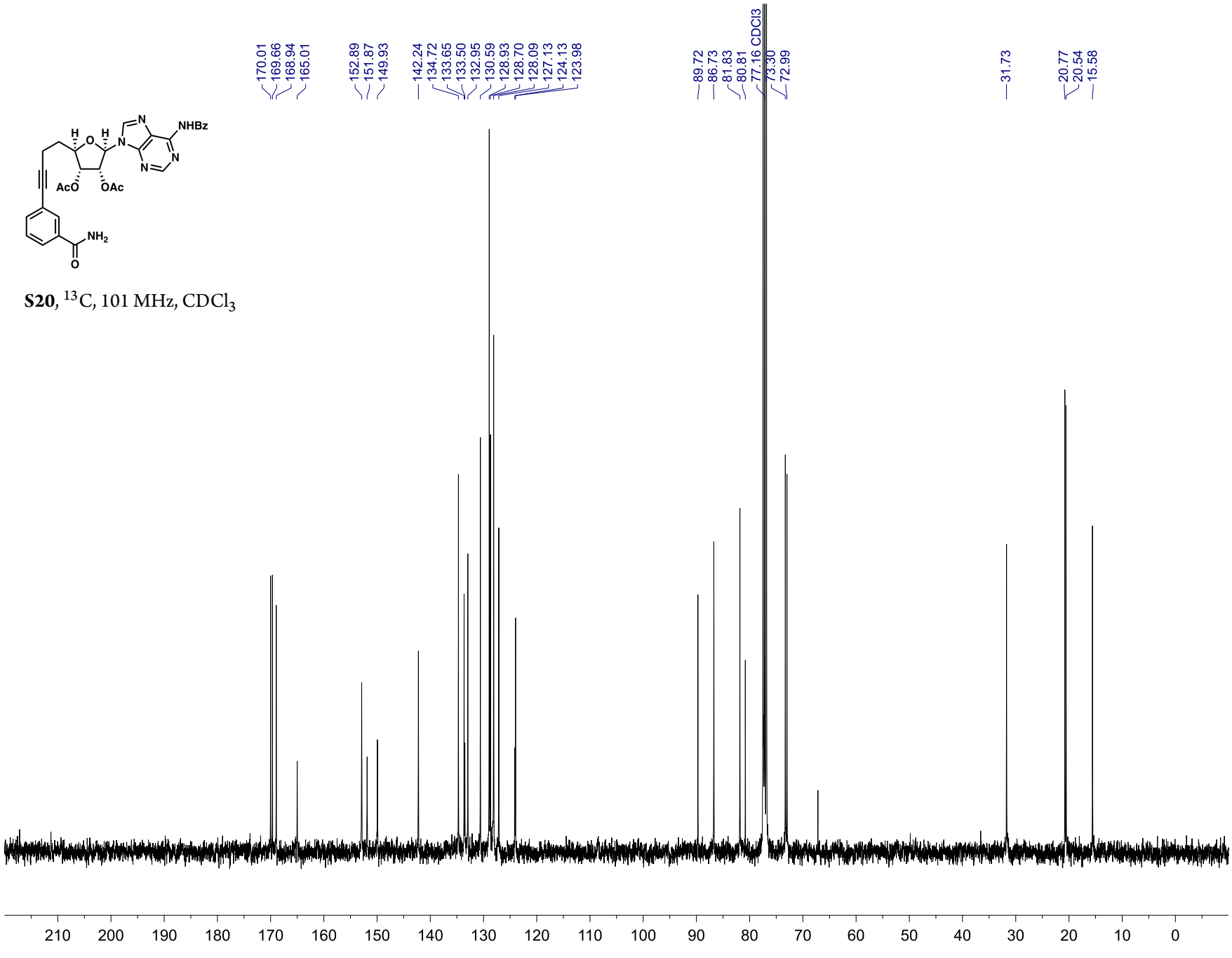

S20, ^{13}C, 101 MHz, $CDCl_3$

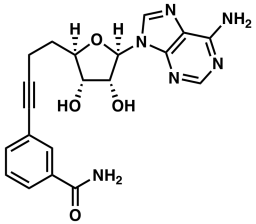

47, ^{1}H, 600 MHz, **CD_3CN**/D_2O

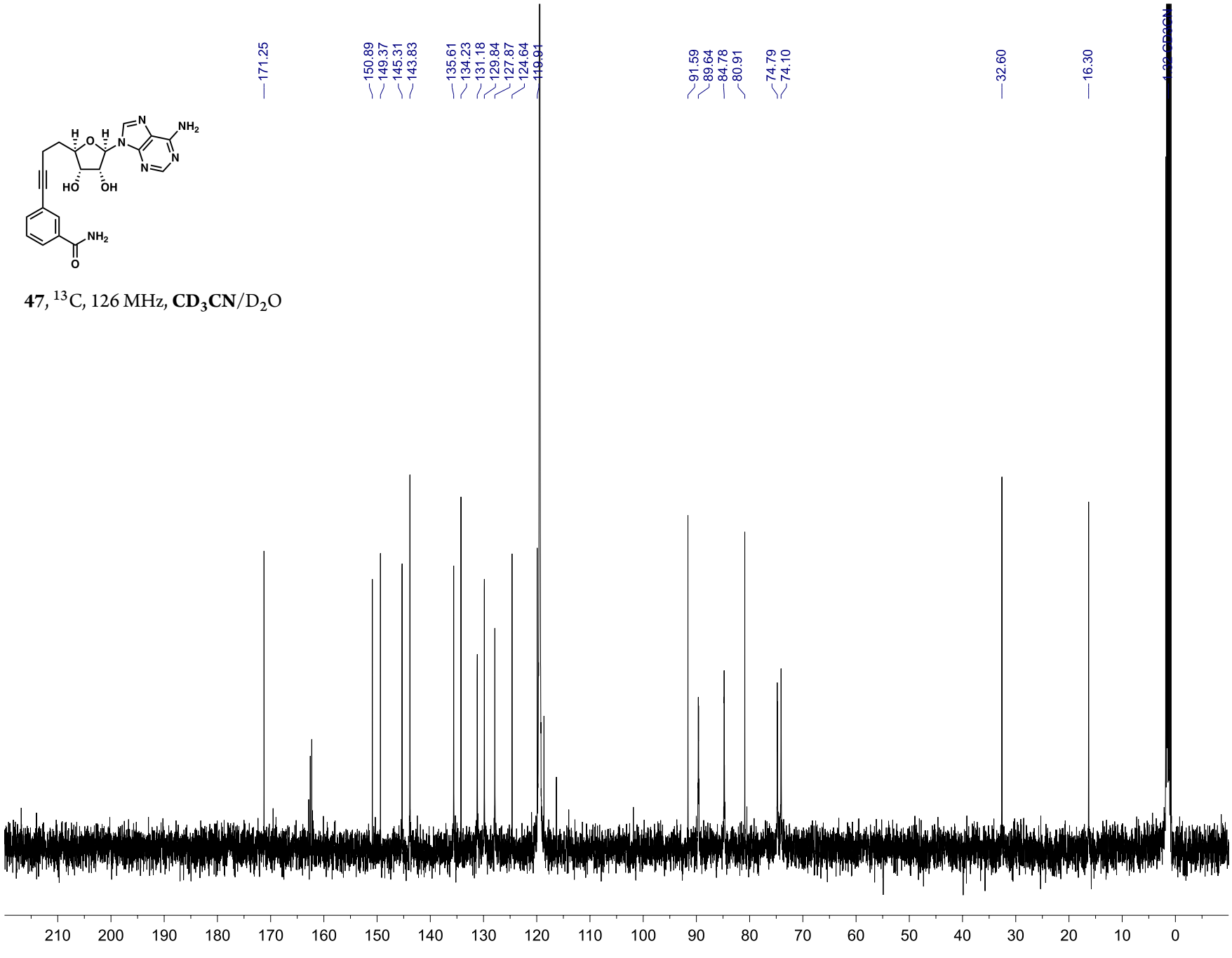

47, ^{13}C, 126 MHz, $\mathbf{CD_3CN}/D_2O$

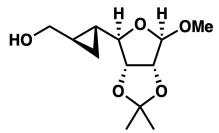

S22, ^{1}H, 600 MHz, $CDCl_3$

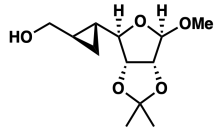

S22, ^{13}C, 151 MHz, $CDCl_3$

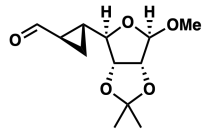

S23, ^{1}H, 600 MHz, $CDCl_3$

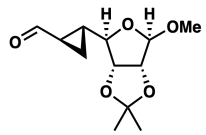

S23, ^{13}C, 151 MHz, $CDCl_3$

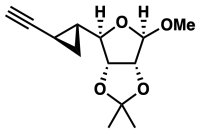

S24, ^{1}H, 600 MHz, $CDCl_3$

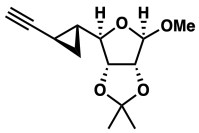

S24, ^{13}C, 151 MHz, $CDCl_3$

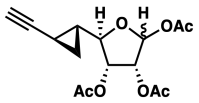

S25, ^{1}H, 600 MHz, $CDCl_3$

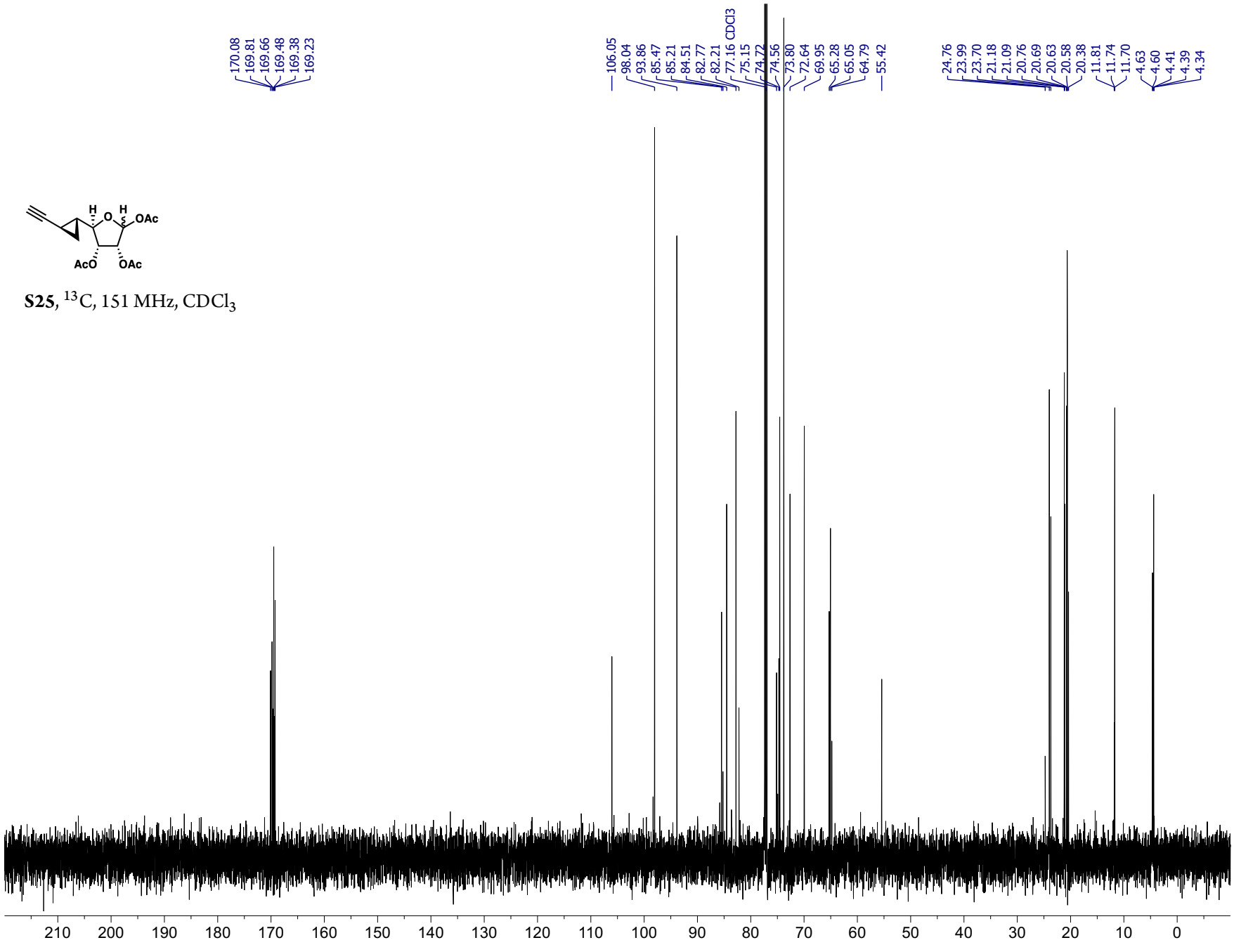

S25, ^{13}C, 151 MHz, $CDCl_3$

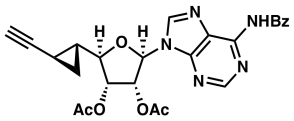

S26, ^{1}H, 500 MHz, $CDCl_3$

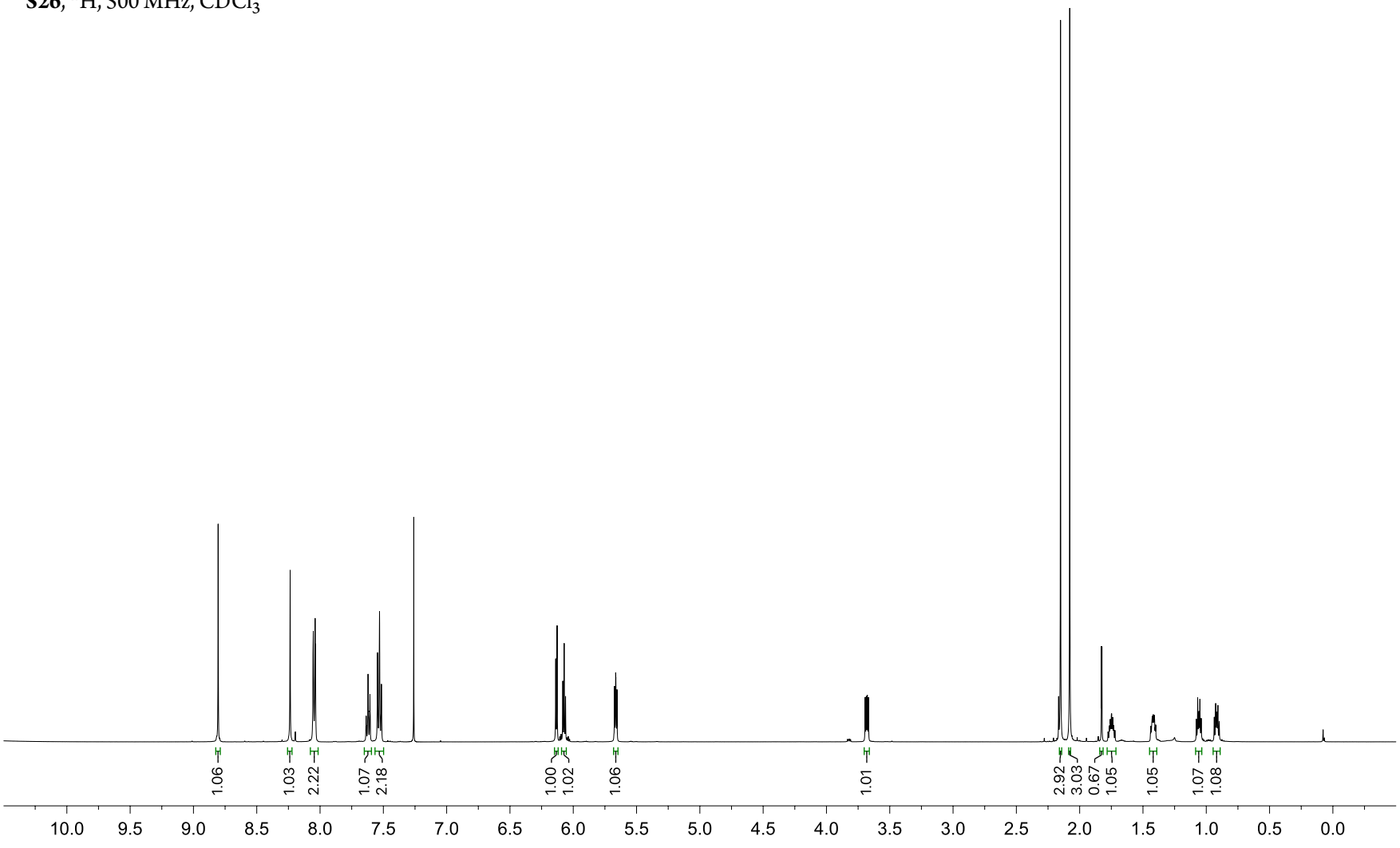

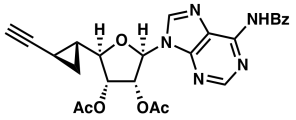

S26, ^{13}C, 126 MHz, $CDCl_3$

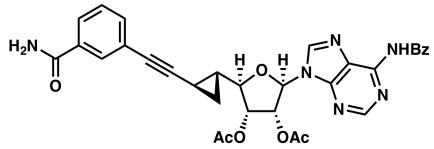

7.26 CDCl3

S27, ^{1}H, 500 MHz, $CDCl_3$

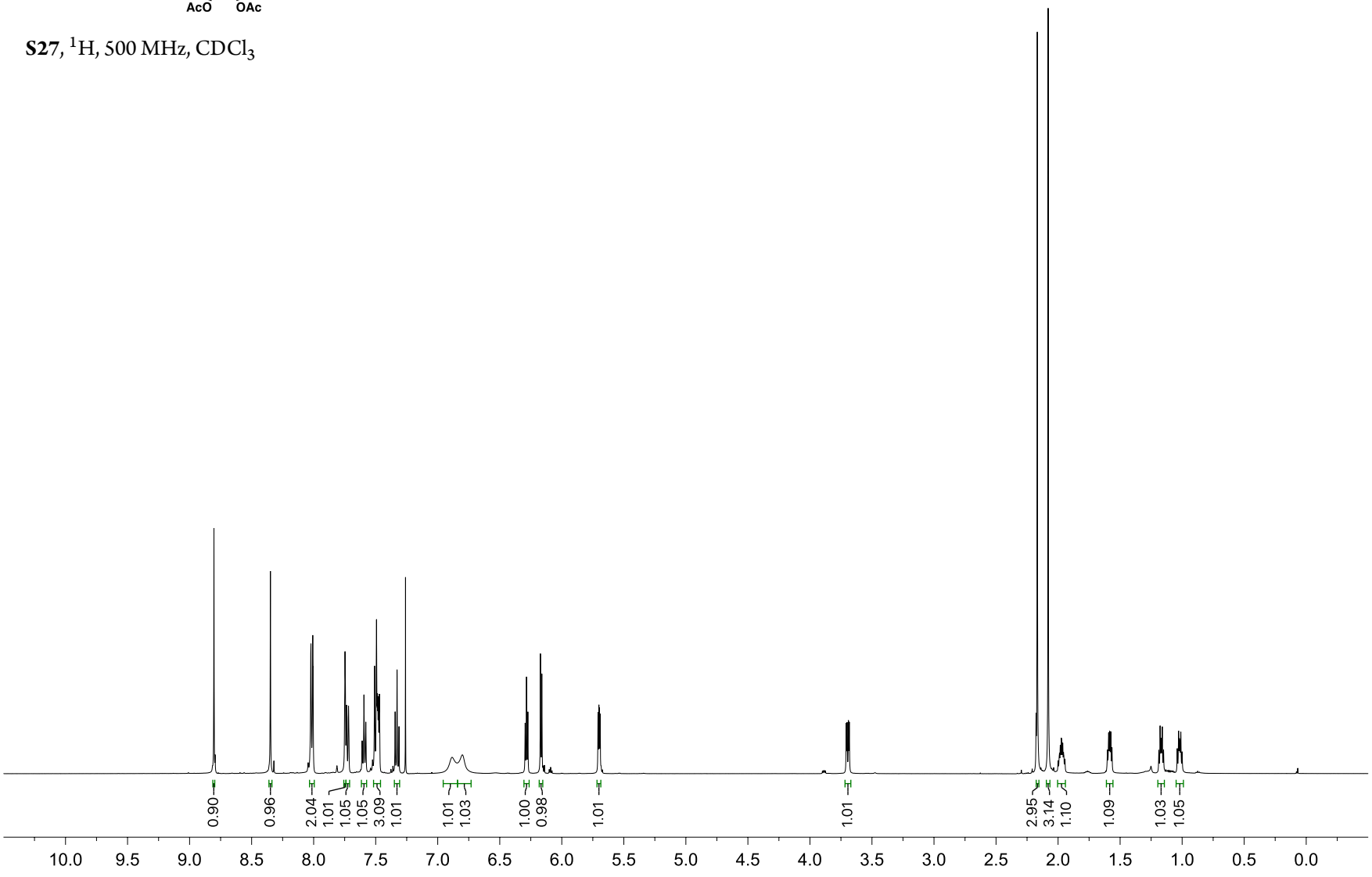

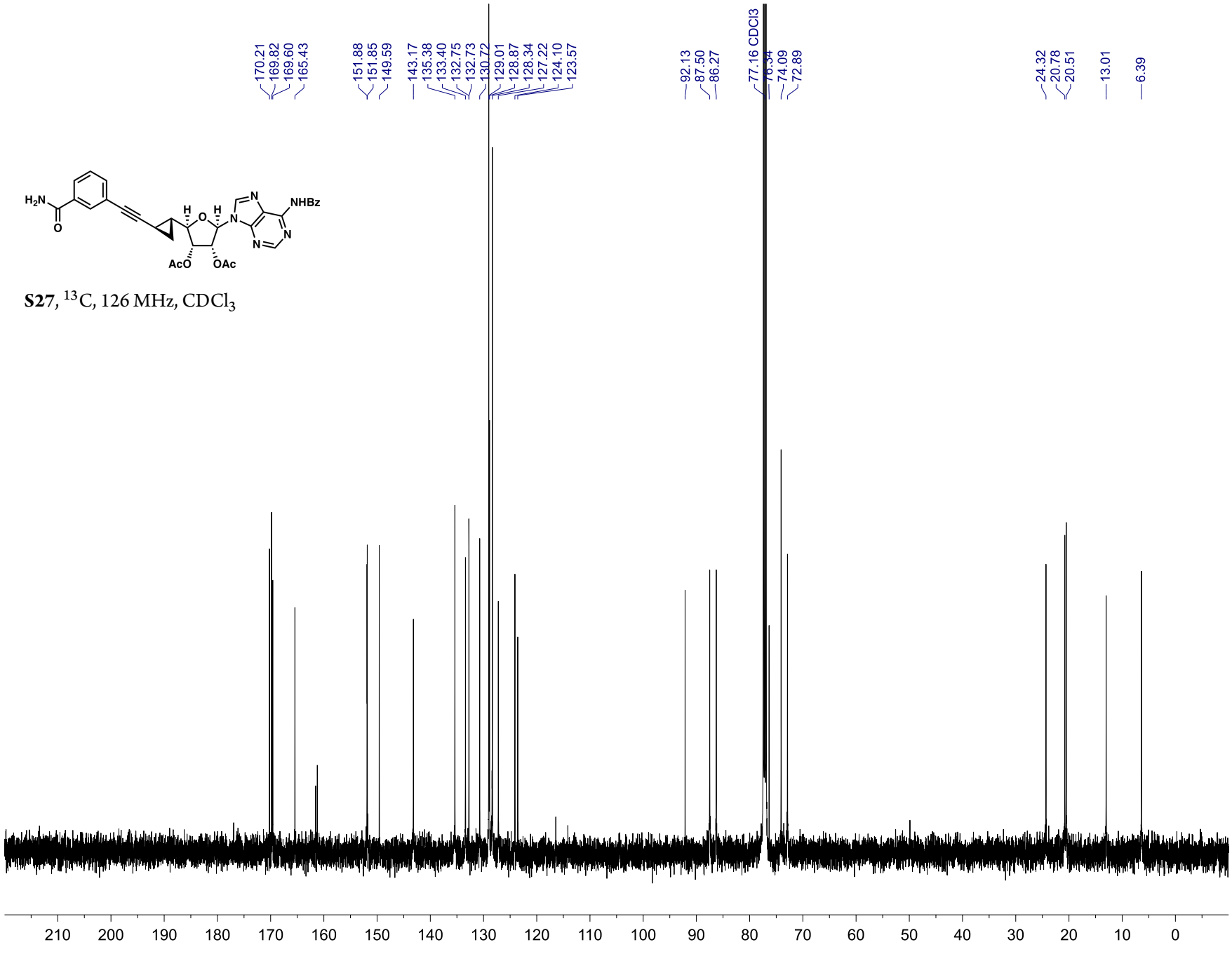

S27, ^{13}C, 126 MHz, $CDCl_3$

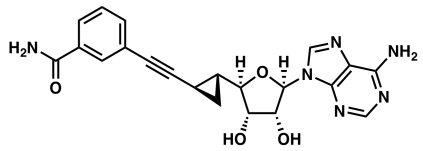

48, ^{1}H, 500 MHz, **CD_3CN**/D_2O

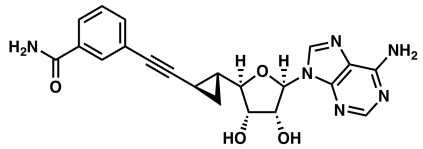

48, ^{13}C, 126 MHz, $\mathbf{CD_3CN}/D_2O$

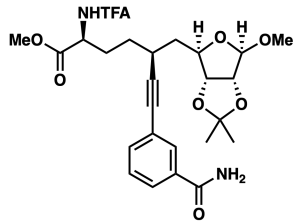

S28, ^{1}H, 500 MHz, $CDCl_3$

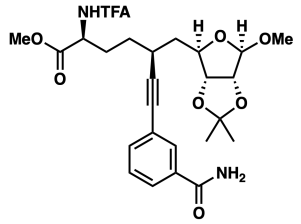

S28, ^{13}C, 126 MHz, $CDCl_3$

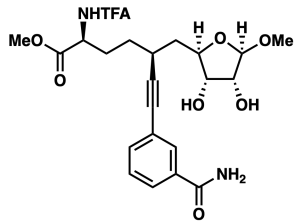

S29, ^{1}H, 600 MHz, $(CD_3)_2CO$

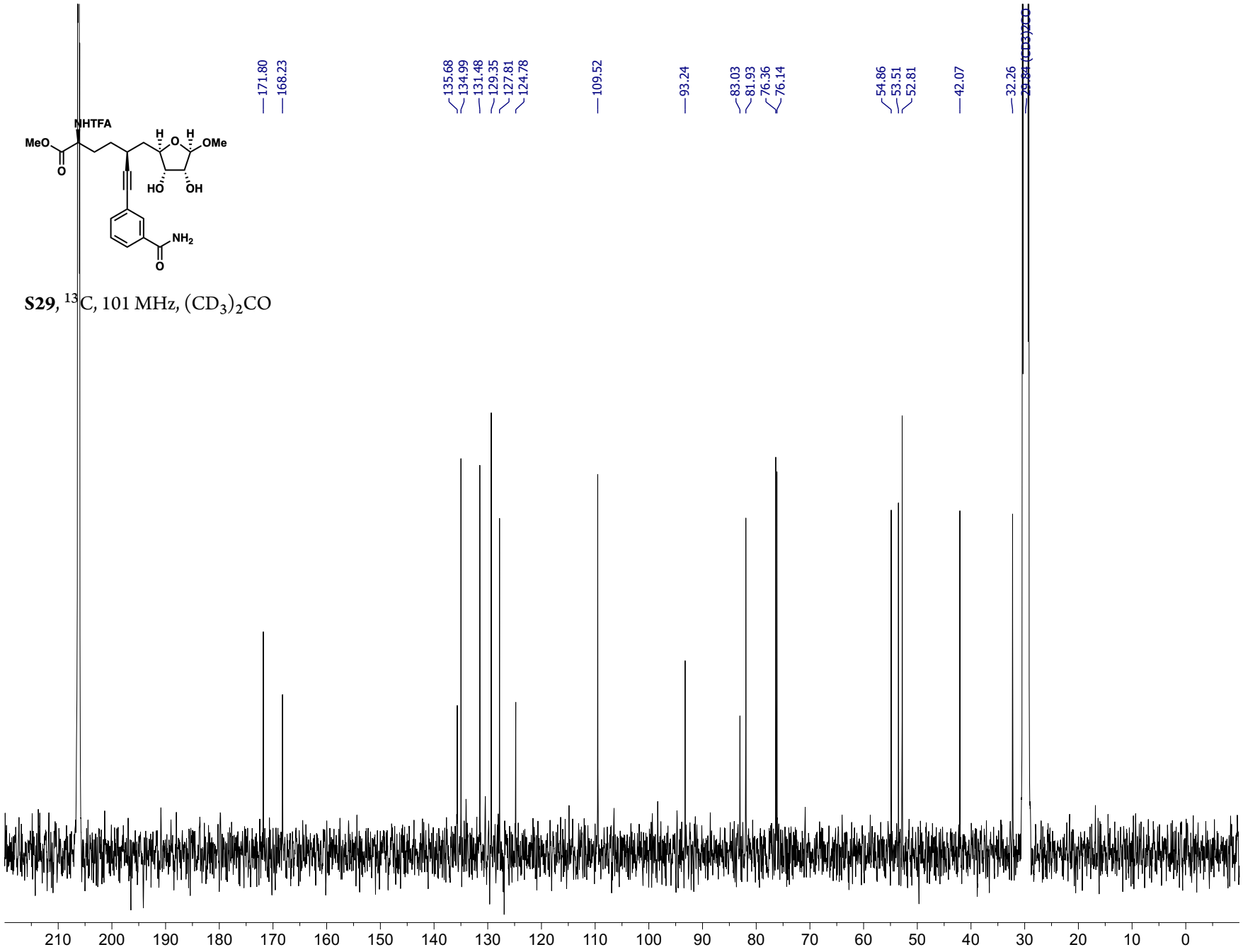

S29, ^{13}C, 101 MHz, $(CD_3)_2CO$

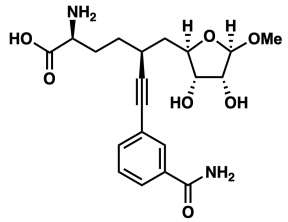

49, ^{1}H, 600 MHz, D_2O

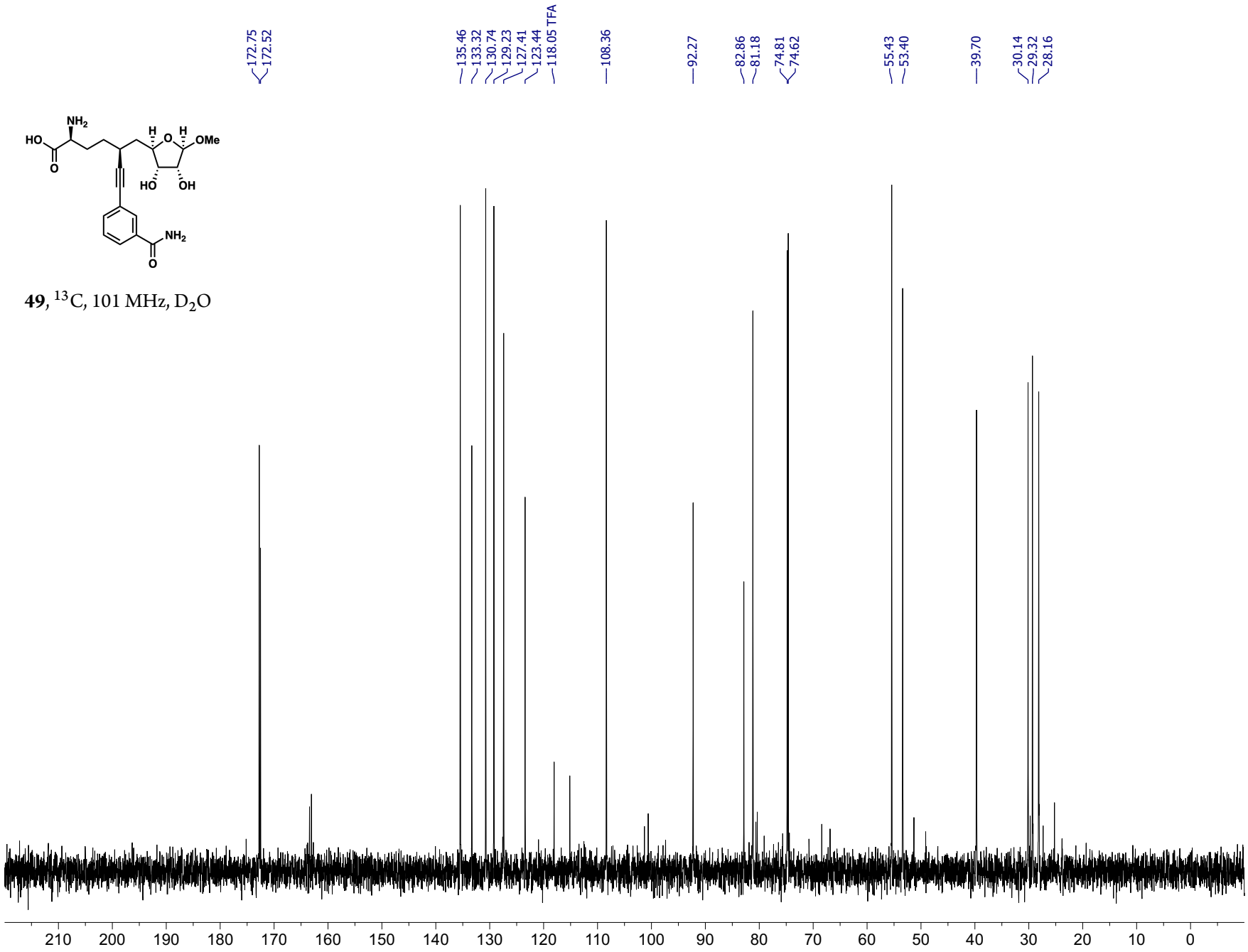

49, ^{13}C, 101 MHz, D_2O

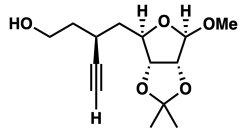

S30, ^{1}H, 500 MHz, $CDCl_3$

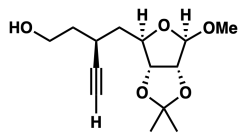

S30, ^{13}C, 126 MHz, $CDCl_3$

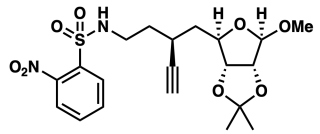

S31, ^{1}H, 600 MHz, $CDCl_3$

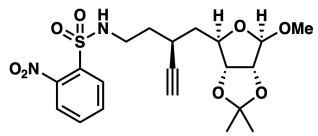

S31, ^{13}C, 151 MHz, $CDCl_3$

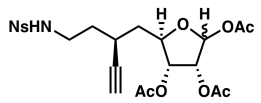

S32, ^{1}H, 600 MHz, $CDCl_3$

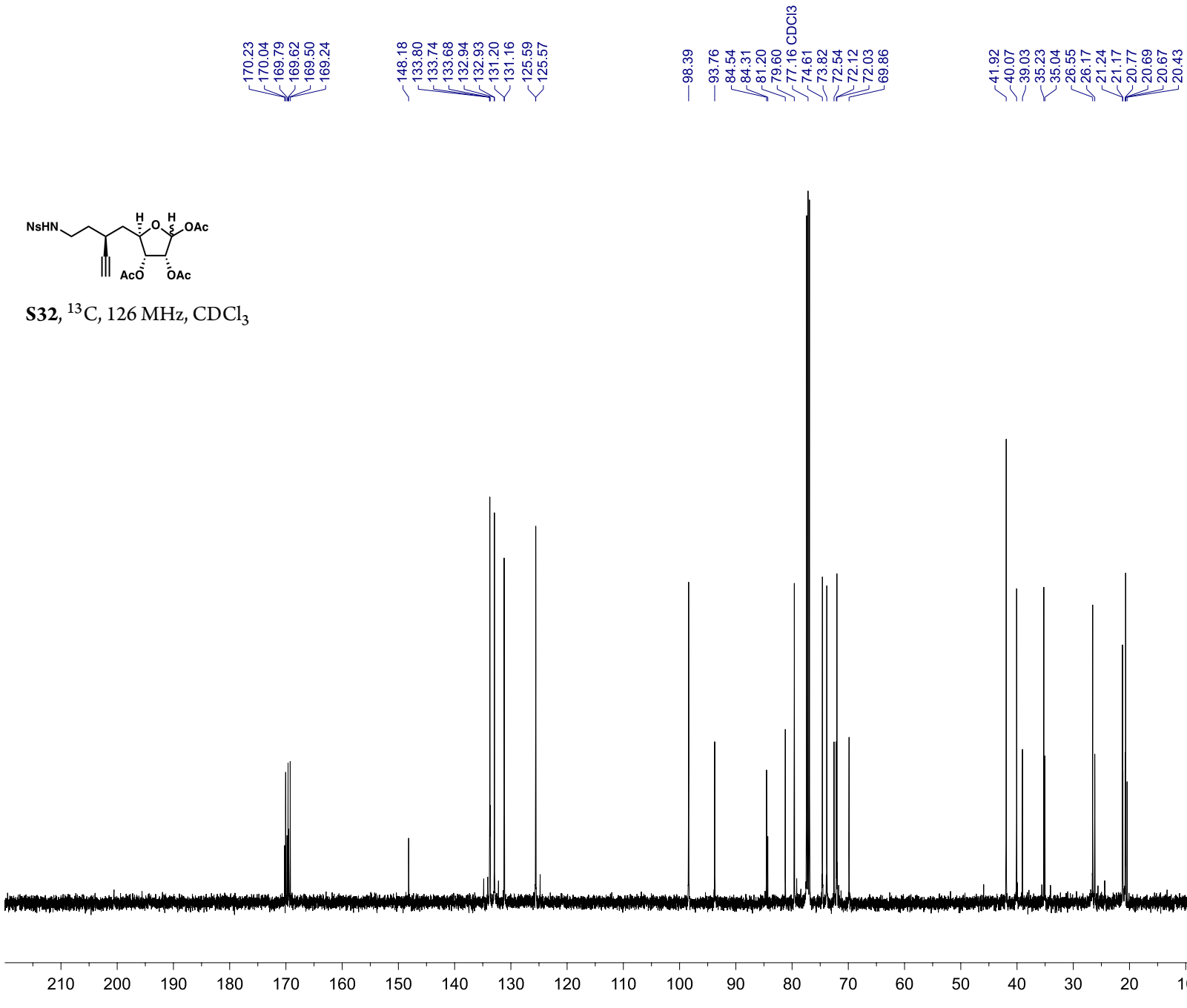

S32, ^{13}C, 126 MHz, $CDCl_3$

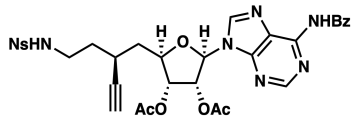

S33, ^{1}H, 600 MHz, $CDCl_3$

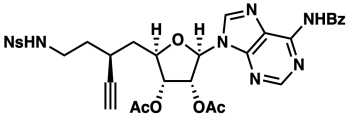

S33, ^{13}C, 101 MHz, $CDCl_3$

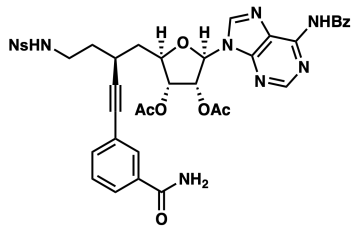

S34, ^{1}H, 500 MHz, $CDCl_3$

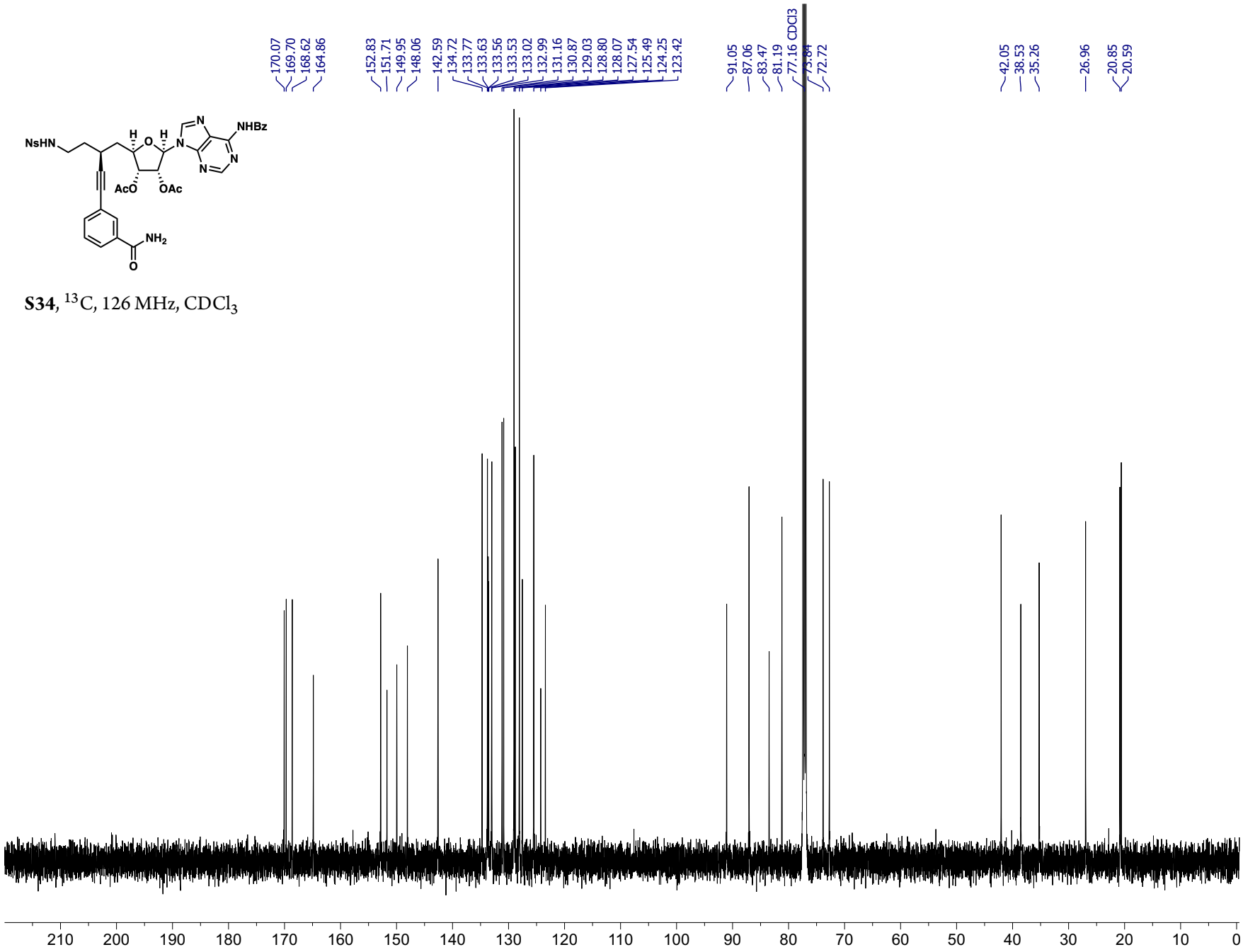

S34, ^{13}C, 126 MHz, $CDCl_3$

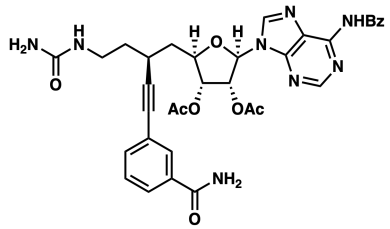

S35, ^{1}H, 600 MHz, CD_3OD

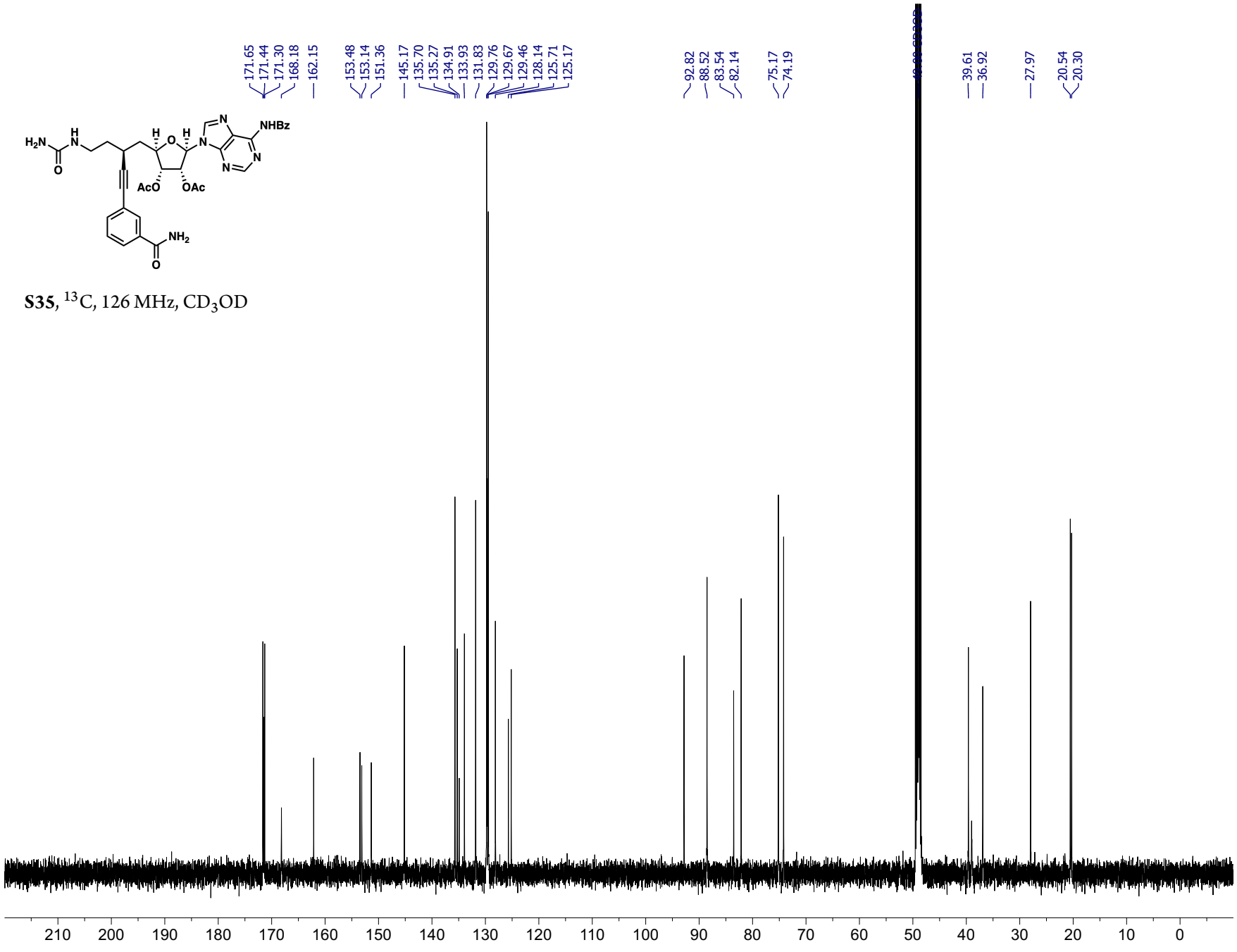

S35, ^{13}C, 126 MHz, CD_3OD

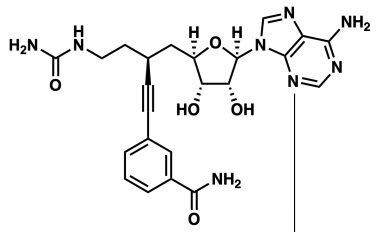

55, ^{1}H, 600 MHz, CD_3CN/**D_2O**/*d*−TFA

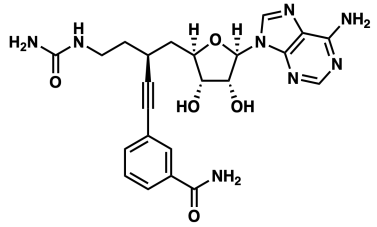

55, ^{13}C, 126 MHz, **CD_3CN**/D_2O/*d*−TFA

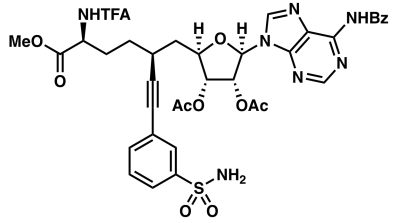

S36, ^{1}H, 600 MHz, $CDCl_3$

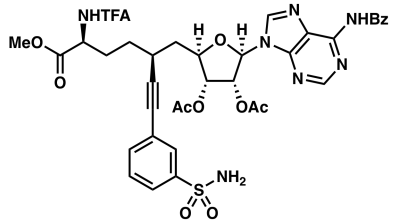

S36, ^{13}C, 126 MHz, $CDCl_3$

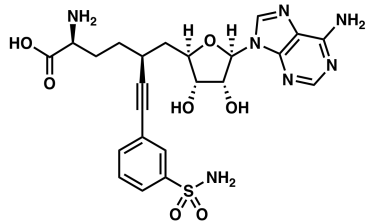

59, ^{1}H, 600 MHz, **CD$_3$CN**/D$_2$O/*d*−TFA

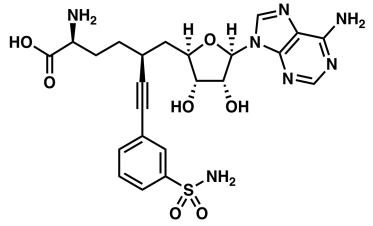

59, ^{13}C, 126 MHz, **CD_3CN**/D_2O/*d*−TFA

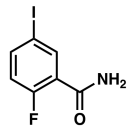

S37, ^{1}H, 500 MHz, CD_3OD

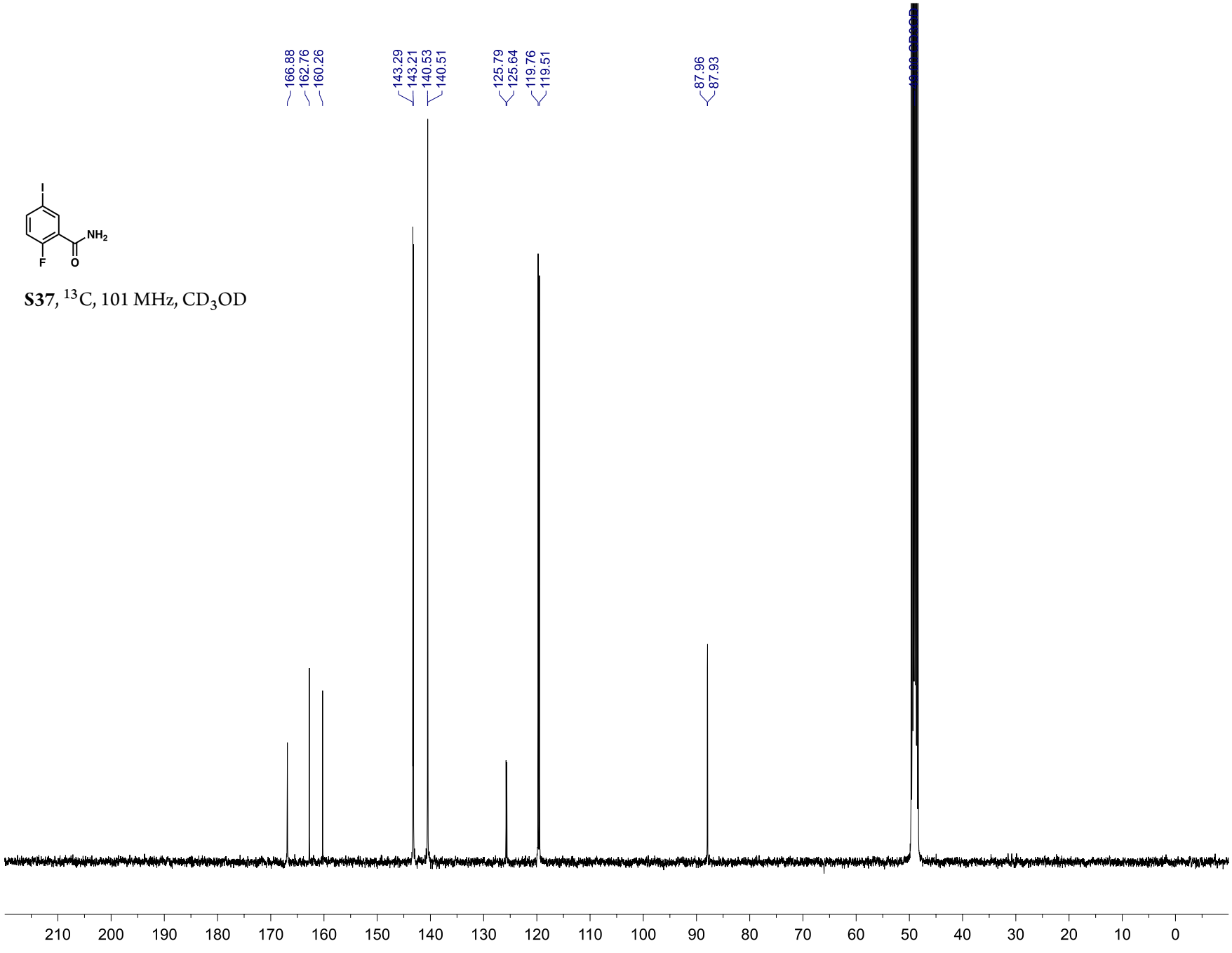

S37, ^{13}C, 101 MHz, CD_3OD

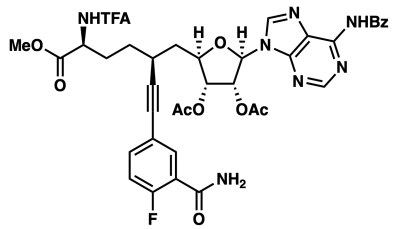

S38, ^{1}H, 600 MHz, $CDCl_3$

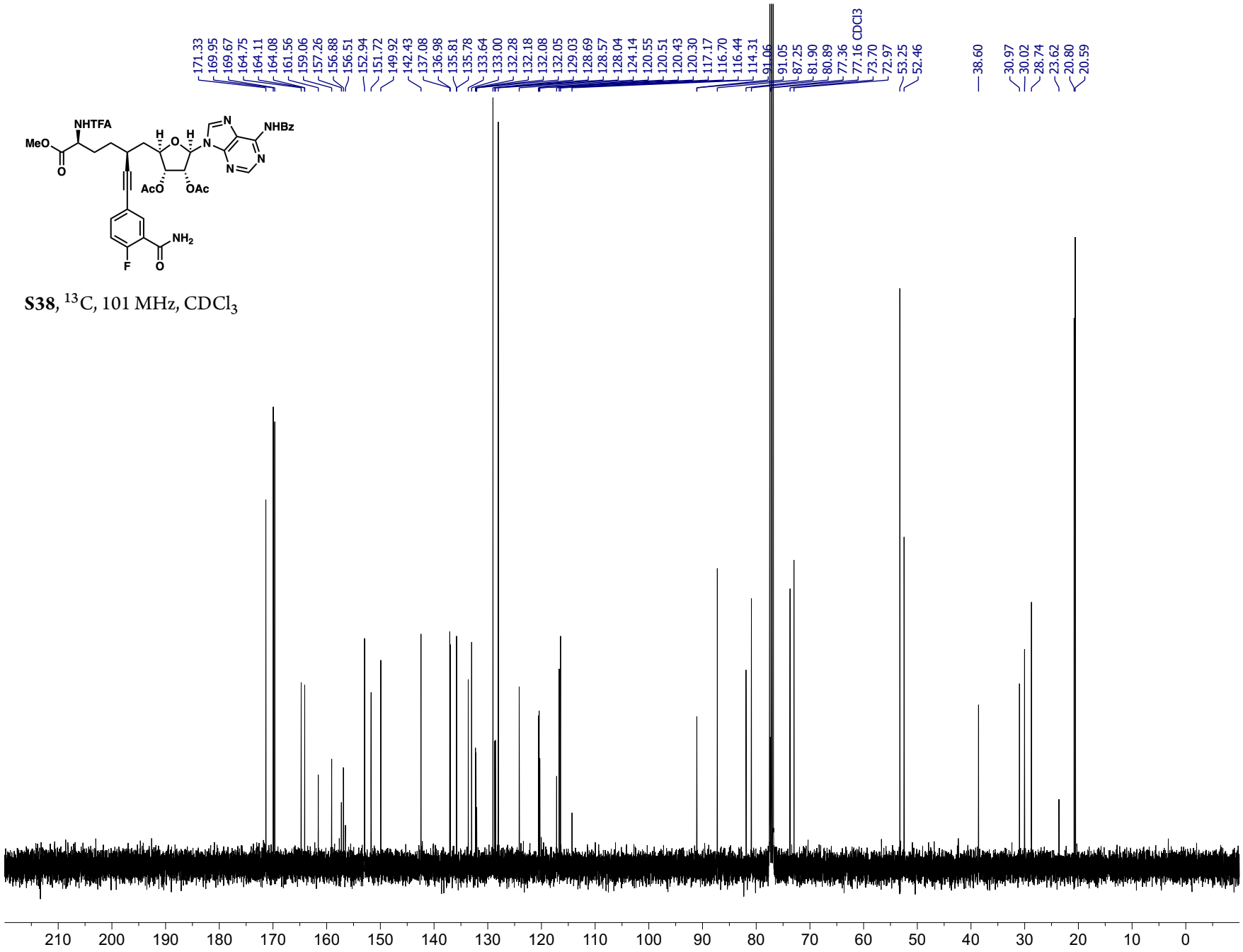

S38, ^{13}C, 101 MHz, $CDCl_3$

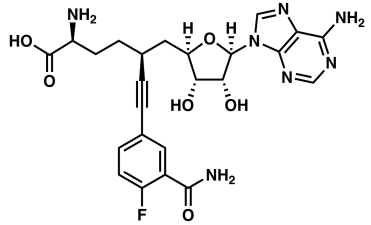

60, ^{1}H, 600 MHz, **CD_3CN**/D_2O/*d*−TFA

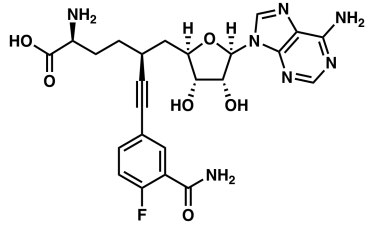

60, ^{13}C, 126 MHz, **CD_3CN**/D_2O/*d*−TFA

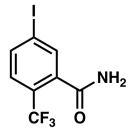

S39, ^{1}H, 500 MHz, CD_3OD

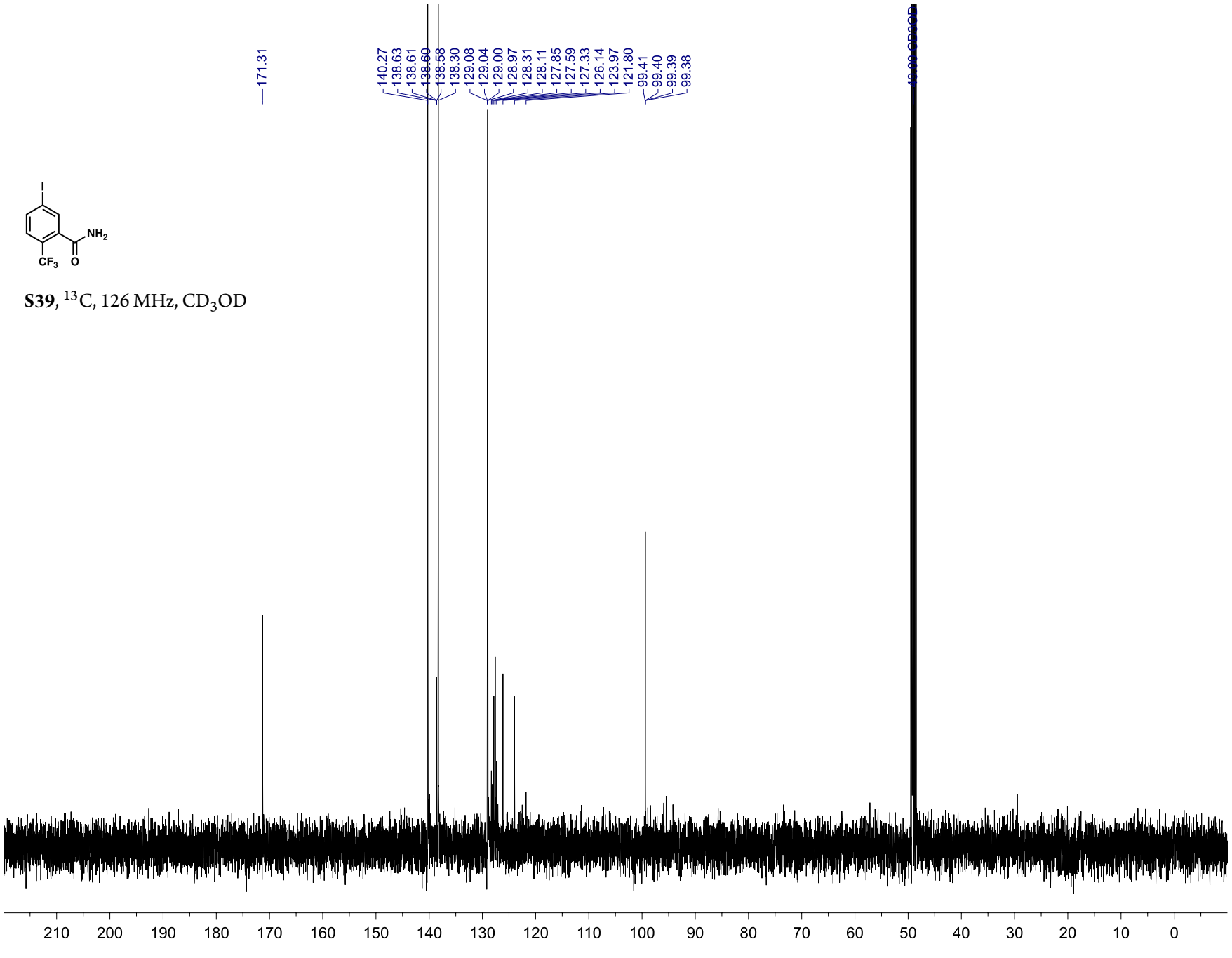

S39, ^{13}C, 126 MHz, CD_3OD

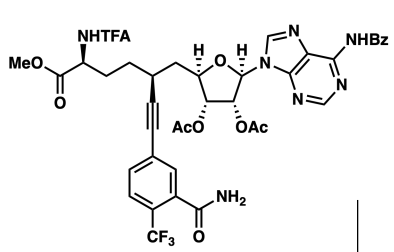

S40, ^{1}H, 500 MHz, $CDCl_3$

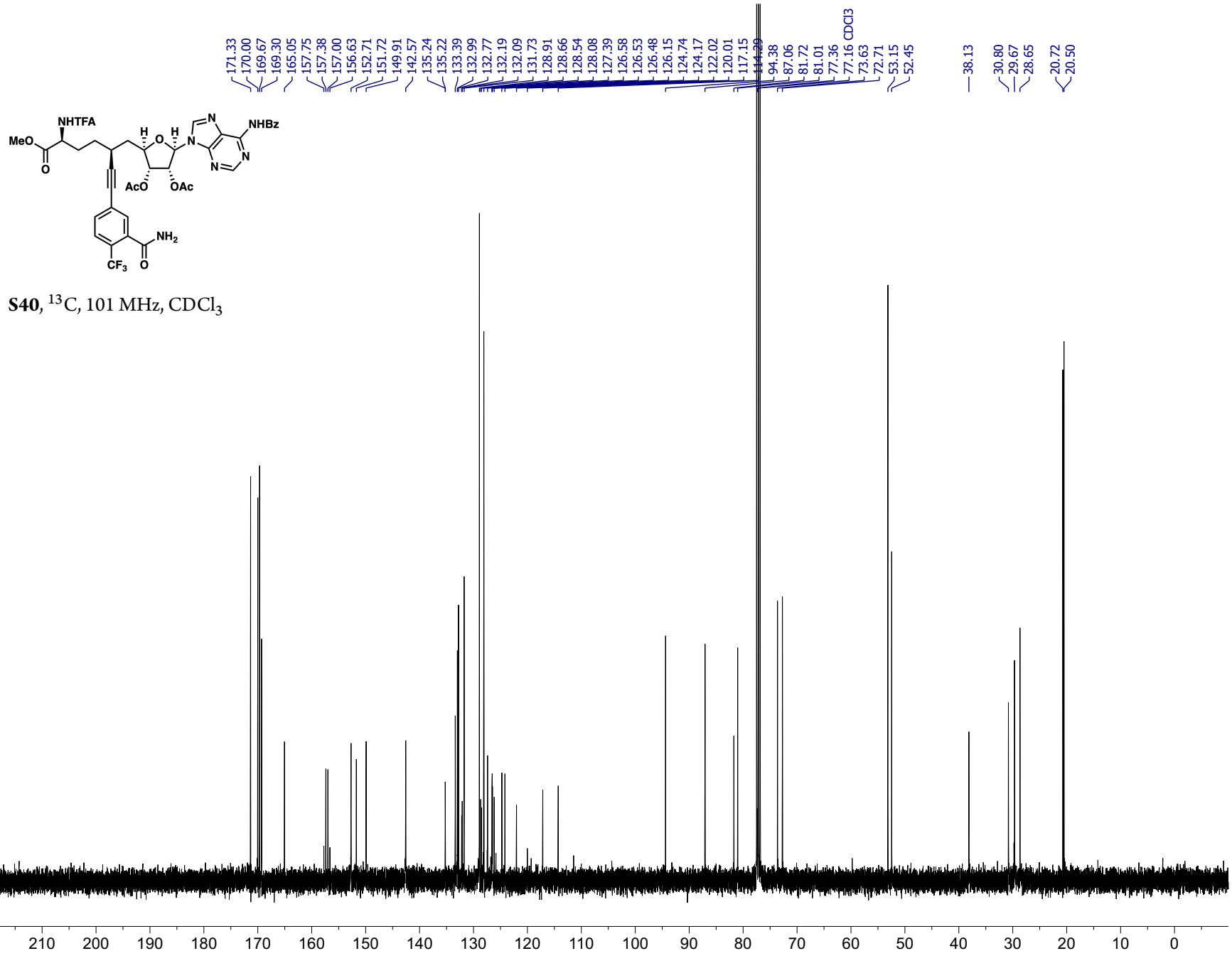

S40, ^{13}C, 101 MHz, $CDCl_3$

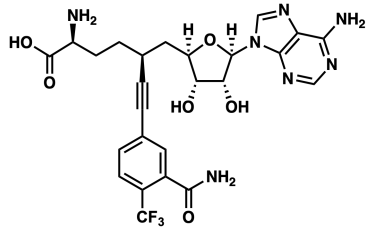

62, ^{1}H, 600 MHz, $CD_3CN/\mathbf{D_2O}/d-$TFA

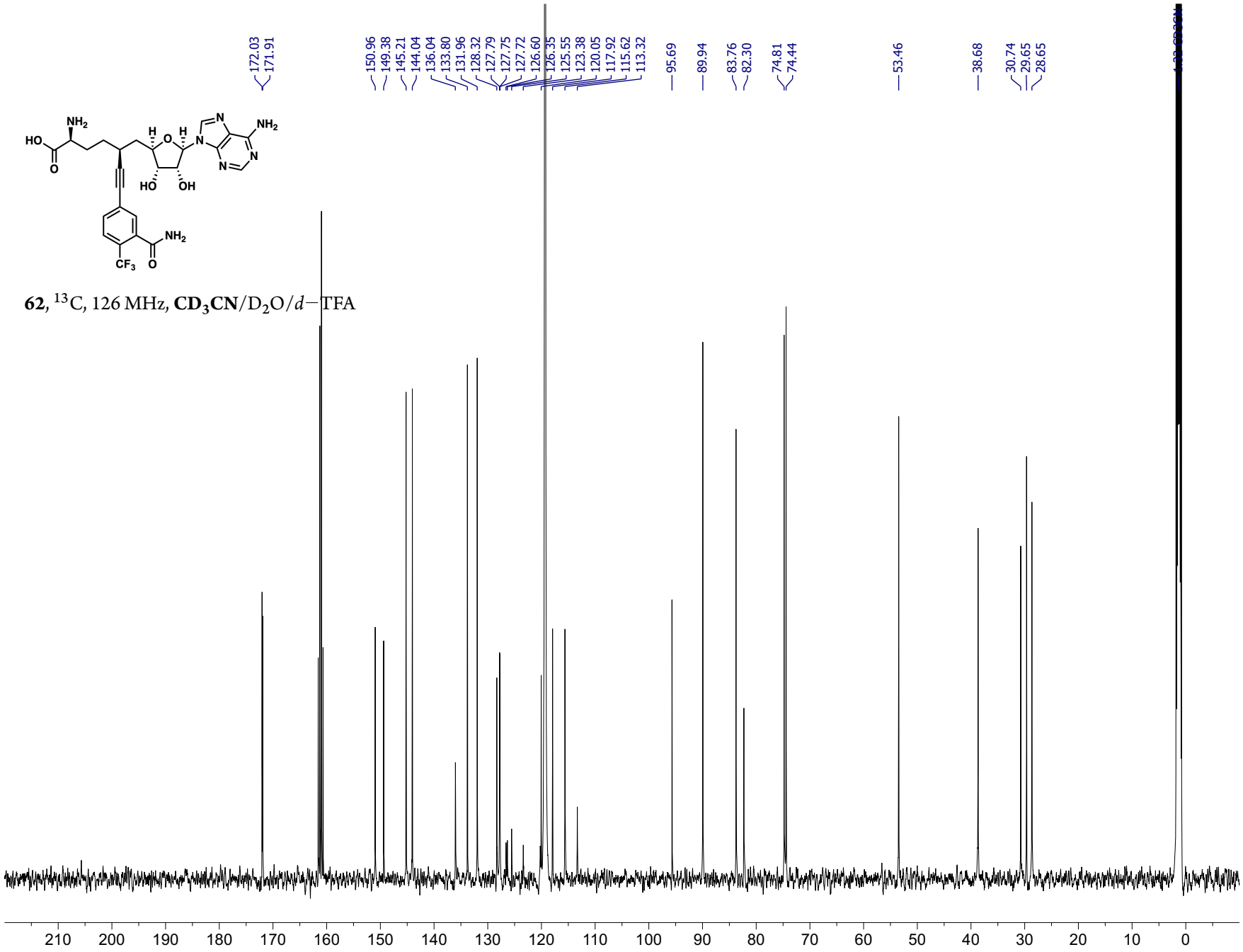

62, ^{13}C, 126 MHz, $\mathbf{CD_3CN}/D_2O/d-$TFA

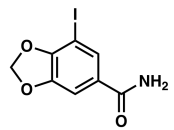

S42, ^{1}H, 500 MHz, CD_3OD

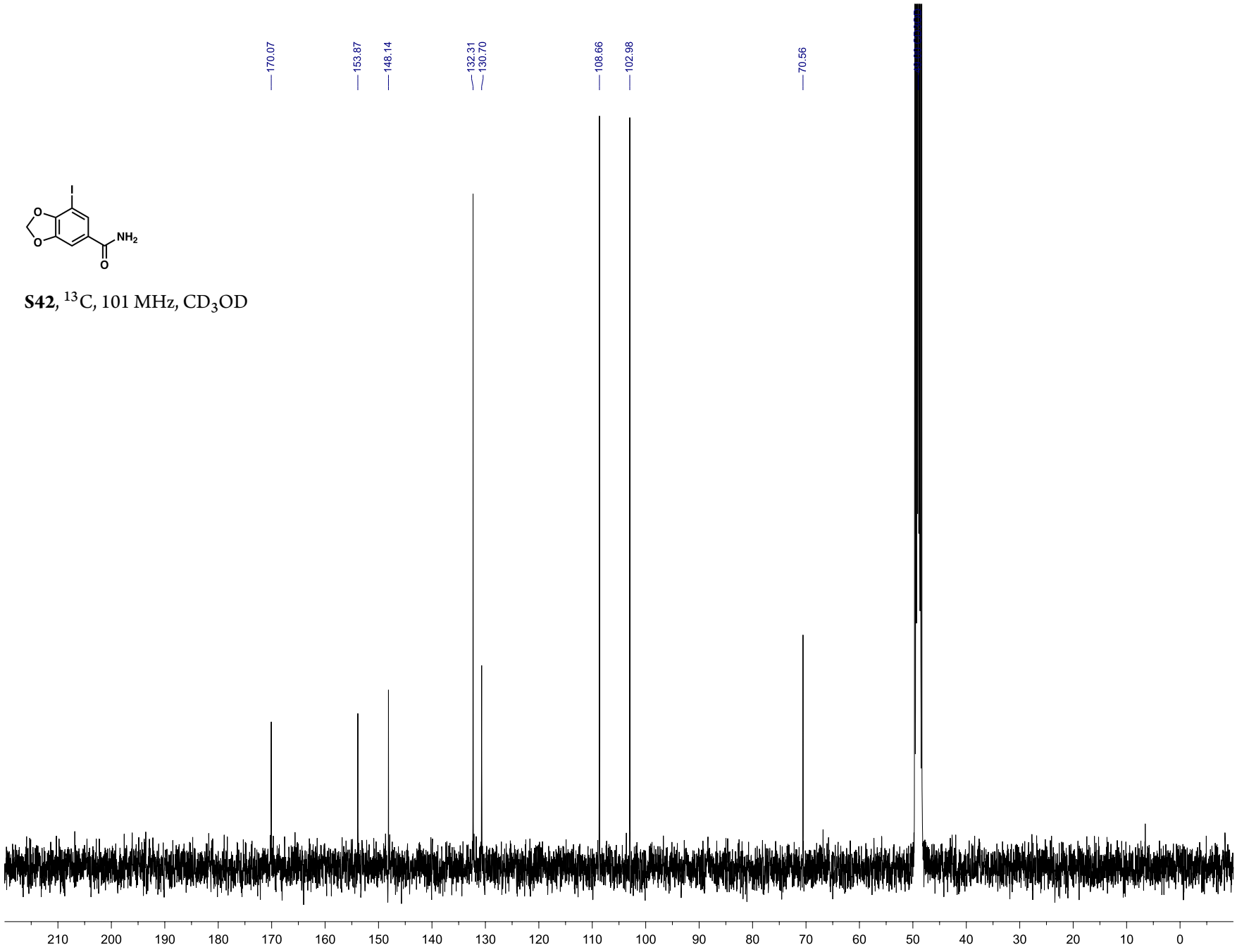

S42, ^{13}C, 101 MHz, CD_3OD

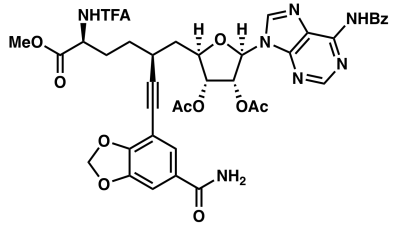

S43, ^{1}H, 500 MHz, CD_3OD

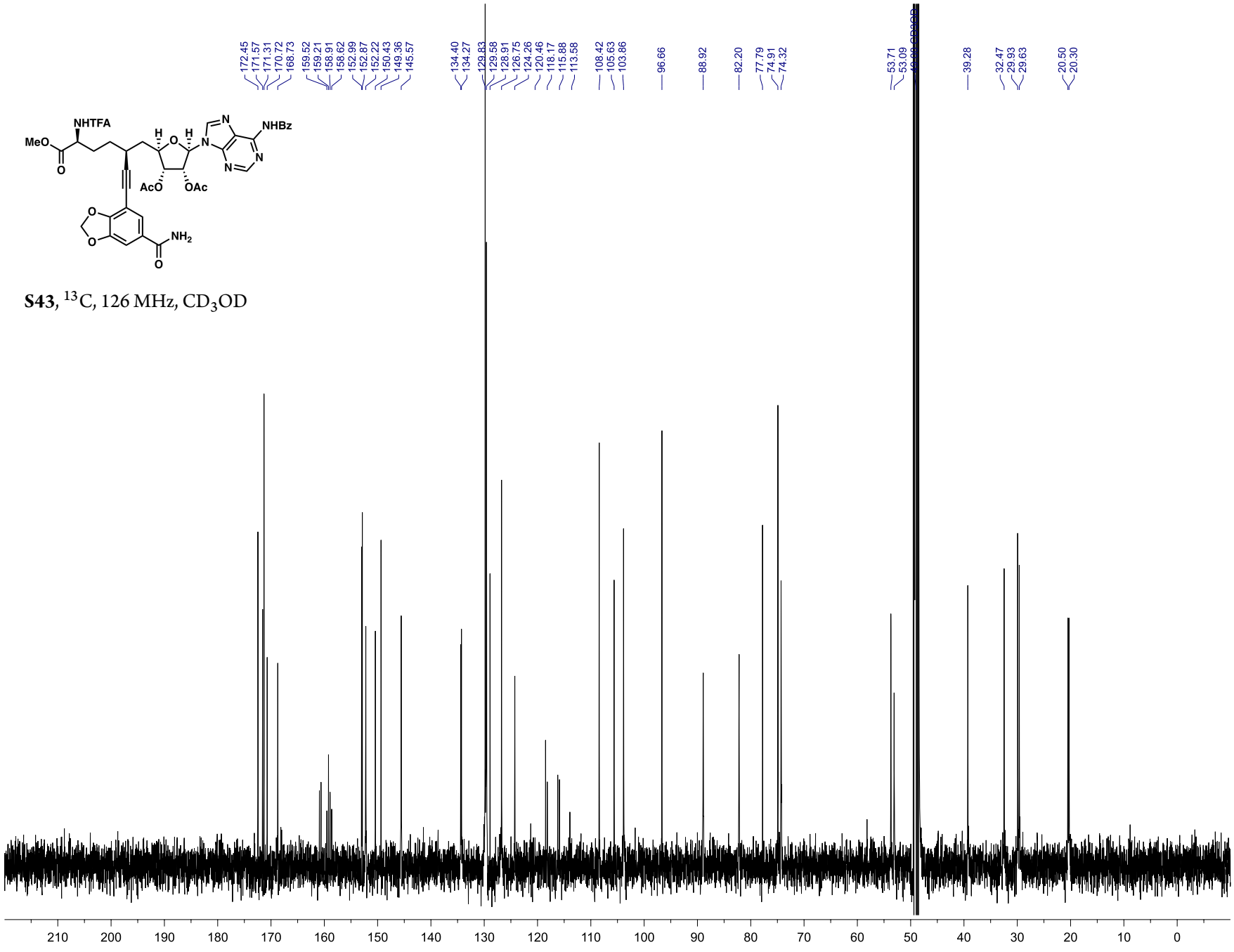

S43, ^{13}C, 126 MHz, CD_3OD

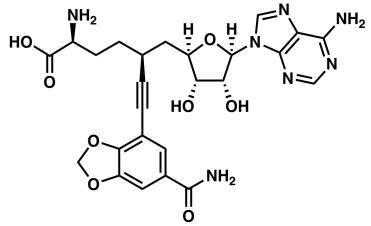

66, ^{1}H, 600 MHz, **CD_3CN**/D_2O

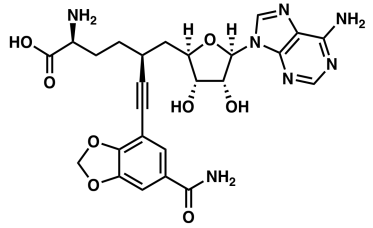

66, ^{13}C, 101 MHz, $\mathbf{CD_3CN}/D_2O/d$—TFA

Colophon

This thesis was typeset using LaTeX, originally developed by Leslie Lamport and based on Donald Knuth's TeX. The body text is set in 11 point Arno Pro, designed by Robert Slimbach in the style of book types from the Aldine Press in Venice, and issued by Adobe in 2007. A template, which can be used to format a PhD thesis with this look and feel, has been released under the permissive MIT (X11) license, and can be found online at github.com/suchow/ or from the author at suchow@post.harvard.edu.